Republic of Iraq
Ministry of Higher Education & Scientific Research
University of Babylon
College of Science
Department of Applied Geology

Total Petroleum System Analysis for Gotnia Basin/ Gharraf Oil Field Extended From Upper Jurassic-Upper Cretaceous, Southern Iraq

A Thesis

Submitted to the Council of the College of Science, University of Babylon, as a Partial Fulfillment of the Requirements for the Degree of Master of Science in Applied Geology.

By

Ali Kareem Neamah Mushatet

(B.Sc. 2012)

Supervised by

Prof. Dr. Amer Jassim Al-Khafaji

Prof. Dr. Fadhil Nomas Al-Sadooni

2021 A.C. **1443 A.H.**

بسم الله الرحمن الرحيم

﴿يَرفَعِ اللَّهُ الَّذِينَ ءَامَنُوا مِنكُم وَالَّذِينَ أُوتُوا العِلمَ دَرَجَاتٍ وَاللَّهُ بِمَا تَعمَلُونَ خَبِيرٌ﴾

صدق الله العلي العظيم

سورة المجادلة (الآية ١١)

ألإهداء

الى أشرف الخلق رسول الله محمد (صلى الله عليه واله)

الـــى امي والمرحوم أبي برا واحسانا

الـــى زوجتي الغالية حبا واخلاصا

الـــى اطفالي احبائي (غدير و مصطفى) تشجيعا والهاما

الـــى اساتذتي المشرفين تقديرا وعرفانا

علي كريم

Acknowledgements

“In the name of Allah, The Most Merciful, The Most Compassionate.”

First of all, I would like to thank Allah Almighty very much for his great blessing and success for me to complete this study.

My thanks, gratitude and appreciation to my supervisors; Prof. Dr. Amer J. Al-Khafaji and Prof. Dr. Fadhil N. Al-Sadooni for their guidance and encouragement throughout this study.

I would like to thank the Department of Geology at the University of Babylon.

My thanks and appreciation to all staff of the Reservoirs and Fields Development in the Ministry of Oil.

My thanks and appreciation to all staff of the Oil Exploration Company.

My thanks and appreciation to all staff of the Petroleum Research and Development Center.

My thanks, gratitude and appreciation to all my friends whose supported and helped me.

Finally, many thanks, gratitude and love to my family who gave me all the support and encouragement to complete this study.

Ali Kareem

Summery

Five vertical wells were selected in this study are Ga-1, Ga-2, Ga-3, Ga-5 and Ga-A1P. The necessary samples, well logs, maps, seismic section, and other data were obtained from the official sources represented by the Oil Exploration Company (OEC) and the Reservoirs Department of the Ministry of Oil, as well as from previous studies. The reliable software are Petrel, IP, Didger, and PetroMod were installed and used to handle these data. The petrophysical properties of the main reservoirs, Yamama and Mishrif, were studied based on the interpretation of the available well logs using Interactive Petrophysics V3.5 software, as well as 3D geological models were built for them to determine the distribution of the petrophysical properties; permeability, porosity, and water saturation in these two reservoirs. The lithology of Mishrif and Yamama formations were determined as mainly limestone with a minor percentage of dolomite by using several cross plots. Geochemical analyzes of potential source rocks (TOC content and pyrolysis), were based on reports obtained from the Oil Exploration Company in Baghdad and from other published studies. One crude oil sample took from Mishrif reservoir Gharraf oil field Well Ga-1, sent to GeoMark Institute in the USA, and geochemical analysis performed on it and analysis data of bulk properties, biomarkers, and carbon isotope was received and used in determine the potential generated source rocks type, depositional environment, redox conditions, thermal maturity level, and age of the generated source rocks. As for the study of building basin models, the data was processed using the PetroMod software.

Mishrif Formation consists of two main units separated by a shale layer, the lower main unit has good reservoir properties and subdivided into nine reservoir units are: M1, M1.2, M2, L1, L1.2, L2, L2.2, L2.3, and L2.4. Units L1.2 and L2 have good petrophysical properties; Øeff = 18-22%, Sw = 16-38%, and K = 80-343md. They are considered as the best reservoir units for oil. They

contain economical quantity of oil reserves 584 million cubic meters. Units M1, M1.2, and M2 have less petrophysical properties and less quantity of oil reserves 229 million cubic meters, while lower units L2.2, L2.3, and L2.4 are almost fully saturated with reservoir water Sw=68-87% with small quantity of oil reserve 125 million cubic meters. Total Petroleum reserve is 938 million cubic meters (5900.02 million barrels) for Mishrif reservoir.

Yamama Formation consists of three reservoir units are from upper to lower respectively YA, YB1, and YB2. Unit YA has good petrophysical properties; Øeff = 11%, Sw = 26%, and K = 119md, and considered as the best reservoir unit for oil of Yamama Formation. It contains economical quantity of oil in the studied wells Ga-1, Ga-2 and Ga-3. Petroleum reserve is 477 million cubic meters (3000.33 million barrels) for Yamama reservoir.

The organic geochemistry results of the potential source rocks analysis to determine the oil prone source rocks in Gharraf and adjacent Nasiriyah oil fields indicate that the Sulaiy source was good to excellent hydrocarbon generating potential, oil-prone II/III kerogen type, and was mature. Therefore, it is possible that it generated hydrocarbons and contributed to the charging of oil to Cretaceous reservoirs. Other source rocks (Yamama, Zubair, and Nahr Umr) were immature; therefore, they did not generate oil, despite its good hydrocarbon source rocks potential and did not contribute to filling Cretaceous reservoirs with hydrocarbons. The Mishrif oils have a specific gravity of 27.2˚ API and high sulfur content of 4.2 wt %. This suggests that the Mishrif oils were generated from source rock have kerogen Type II/S at early peak oil stage of maturity level. The concentration of short-chain n-alkanes is higher than the long-chain n-alkanes, as well as high ratio of C_{22}/C_{21} tricyclic terpane and C_{31}R/H hopane and low ratios of C_{24}/C_{23} and C_{26}/C_{25} tricyclic terpane, indicated that they originated from marine carbonate-rich source rocks with little terrigenous input. The stable carbon isotope ratios include C15+ Saturate -

27.23‰ and C15+ Aromatic -27.53‰ hydrocarbons were also indicated that Mishrif oils derived from predominately marine organic matter. The gas chromatography analysis shows normal alkane and acyclic isoprenoid distributions. In additional the Pr/n-C_{17}, Ph/n-C_{18}, GA/C31R, and C35S/C34S biomarker ratios indicated that the source rocks deposited under anoxic environmental conditions. The biomarker maturity parameters such as C_{29}20S/R, C_{27}Ts/Tm, C_{29}Ts/Tm, and TAS3 (CR) are indicative of a low maturity stage of the probable source rock.

In petroleum systems (TPS) with carbonate source units, the C_{28}/C_{29} regular sterane ratio of 0.66, along with the corresponding triaromatic steranes $C_{27}R/C_{28}R$ suggests that the Mishrif oils were generated from Middle Jurassic Sargelu Formation to Upper Jurassic - Lower Cretaceous Sulaiy Formation carbonate source rocks. The saturated fraction of the analyzed oils has a value of stable carbon isotope ration is -27.23 ‰, which confirms. The results of the basin model show that these formations attained a peak oil-generation window at different times, releasing differing amounts of oil. Since the Upper Cretaceous until the present, the organic-rich of the Sargelu, Najmah and Sulaiy source rocks has begun to discharge enormous quantity of oil, equating to a transformation ratio (TR) of 100% percent, according to the basin model results. These generated oils migrated to shallow Cretaceous stratigraphic reservoir intervals through the vertical pathway of faults, where they are today recovered for use in the oil industry.

List of Contents

List of Figures

List of Tables

Chapter One

Introduction

1.1. Preface

The Gharraf oilfield is one of the important oil fields in southern Iraq. The studied Gharraf oil field is located in the south of Iraq in Thi Qar governorate about 5 kilometers (km) northwest of Al-Refaei city and 85 km to the north of Nasiriya city. The Gharraf oil field structure is an NW-SE trending anticline with an area of 24 km length and 5 km width, (OEC, 1995). The field was discovered in 1984. The first three wells (Ga-1, Ga-2, and Ga-3) were drilled in the Gharraf oil field during the years 1984, 1987, 1988.

The oil reserves in the field are about 1 billion barrels of oil, (Al-Sakini, 1992). The oil found according to Oil Exploration Company reports ranged in specific gravity from 15 to 36 °API, in multiple Cretaceous reservoirs. Petronas, Japex, and North Oil Companies start developing the field and production in 2011. The production volume at the end of March 2019 is approximately 90,000 barrels per day at average. The importance of the Gharraf oil field, because it contains important economic quantities of crude oil.

Although it was discovered in 1984, the production actually started in 2011, and therefore the completion of this study that includes the total petroleum system for this field has become necessary (OEC, 1995). The term of the total petroleum system (TPS) was first used by (Perrodon 1983). Hunt, (1995) formalized the criteria for petroleum system essential element and processes. The petroleum system is also including all genetically related oil and gas which occur in oil shows, seeps, and accumulations (Hunt, 1995).

Iraq is considered to be one of the Middle East's most oil-rich countries and have three petroleum systems, including Paleozoic (TPS202301), Jurassic (TPS202302) and Cretaceous-Tertiary (TPS203001), (Verma *et al.*, 2004), as shown in the Figure (1-1(A)). The Gharraf oil field petroleum system is part of the Cretaceous-Tertiary (TPS203001) total petroleum system.

Iraq's oil and gas fields are extended into large geographical areas, where giant oil fields are concentrated to the east while giant gas fields are to the west side of Iraq, with the exception of the Diala zone, which the gas and oil fields located to the northeast (Al-Ameri, 2013).

The reservoirs are distributed in stratigraphic successions of the Middle and Upper Jurassic strata in North Iraq, Upper Jurassic with Lower Cretaceous in North-East and Central Iraq, Lowermost Cretaceous in Basra Governorates of South Iraq, Middle Triassic in North West Iraq, and Lower Paleozoic in West Iraq (Aqrawi *et al.*, 2010).

In the south Mesopotamian Basin, the Cretaceous succession (Sulaiy, Yamama, Zubair, and Nahr Umr formations) have excellent to good hydrocarbon potential, and they are at high to moderate levels of thermal maturity, except Nahr Umr Formation (Al-Ameri *et al.*, 2009; Abeed *et al.*, 2011). The Middle to Upper Jurassic Sargelu and Najmah formations are at a stage of thermal maturity beyond peak oil generation (Pitman *et al.*, 2004). Pitman *et al.*, (2004) and Verma *et al.*, (2004) reported that 24 percent of Iraq's reserves are in Cenozoic reservoirs, 76 percent in Cretaceous reservoirs, and just about 0.1 percent in older reservoirs. Al-Khirsan and Al-Siddiki, (1989), reported that 24 B. brl. of oil reserves in the Cenozoic, 76 B. brl. in the Cretaceous, and some of 100 M. brl. in the Jurassic and Triassic, noted a similar division of reserves (Aqrawi *et al.*, 2010), see Table (1-1). This study concentrates on the TPS (Total Petroleum System) of the Upper Jurassic to Cretaceous stratigraphic sequence formations of the Gharraf oil field, which includes several oil reservoirs.

Table (1-1): Reserves percentages per reservoir age based on (Al-Sakini, 1992)

Reservoir age	Percentage of reserves
Tertiary	16.3 %
Late Cretaceous	13.8 %
Middle Cretaceous	39.5 %
Early Cretaceous	29.7 %
Older reservoirs	0.70 %

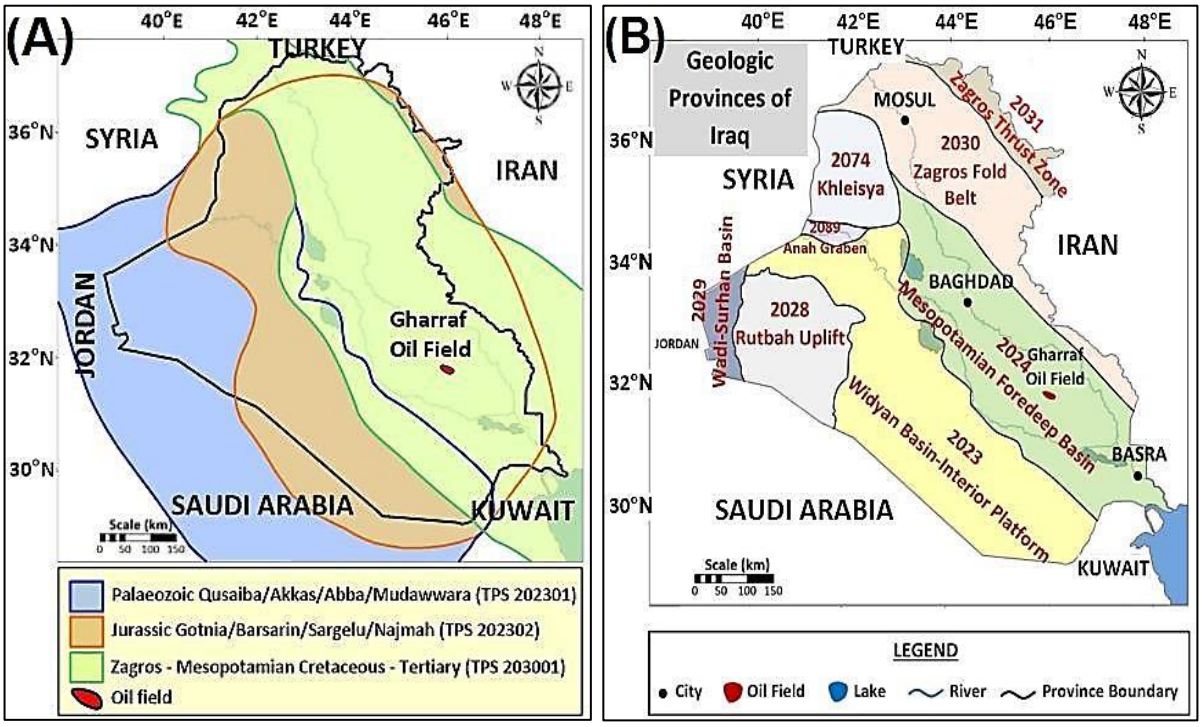

Figure (1-1): (A) Map showing the extent of Total Petroleum Systems in Iraq. Modified from (Verma *et al.*, 2004). (B) Map showing Geologic Provinces of Iraq and the location of Gharraf oil field. Modified from (Roberts *et al.*, 2005;Al-Khafaji, 2015).

1.2. A Brief Overview About The Study Area

1.2.1. Geographic situation

The Gharraf oil field is located in Dhi Qar Governorate, south of Iraq, around 265 km southeast of Baghdad, 85 km north of Nasiriya city. The coordinate range of the study area is (31 ° 48 '22" - 31 ° 44' 48 " N), and (45° 53' 15"- 46° 12' 13" E), see Figure (1-2). Five vertical wells were studied which are: Ga-1, Ga-2, Ga-3, Ga-5 and Ga-A1P. Location coordinates for the wells studied illustrated in Table (1-2).

Table (1-2): Location coordinates of the studied wells according to South Oil Company wells final reports.

Well No.	Geographic Coordinates			
	(DMS)		(UTM)	
	Longitude	Latitude	Easting (X)	Northing (Y)
Ga-1	46° 04′ 45″ E	31° 45′ 42″ N	602200	3514516
Ga-2	45° 59′ 08″ E	31° 47′ 15″ N	593300	3517300
Ga-3	46° 01′ 36″ E	31° 47′ 27″ N	597200	3517700
Ga-5	45° 56′ 25″ E	31° 49′ 05″ N	589001	3520662
Ga-A1P	46° 05′ 05″ E	31° 45′ 41″ N	602712	3514499

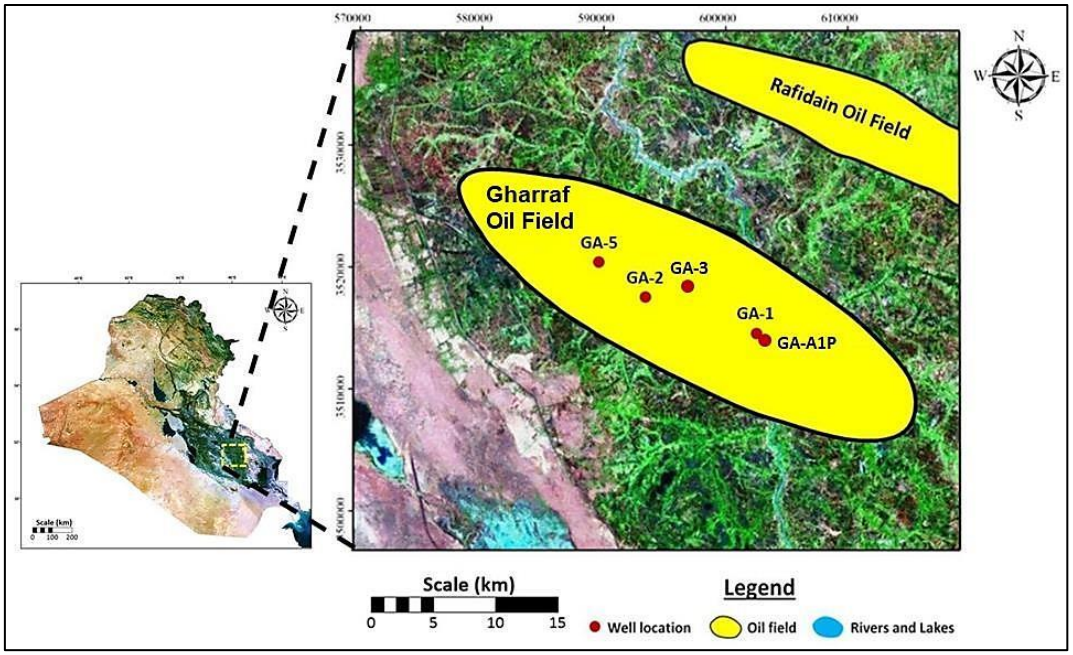

Figure (1-2): Satellite image of Iraq illustrating the location of the Gharraf oil field, indicated by the locations of the studied wells.

1.2.2. Geological setting

The Gharraf oilfield is an anticlinal structure, and it is a stratigraphic trap in the western side of the field and the eastern side of the field is a structural trap. The field structure main axis is trending NW-SE, (Figure 1-4). The Gharraf structure forms and development of a series of anticlinal structures which then developed on the south of the flank of the Zagros Mountain front flexure. The trend of the Gharraf anticline is parallel to the main Zagros trend. According to the longitudinal tectonic classification of Iraq for (Jassim & Goff, 2006), the Gharraf oil field is situated in the stable shelf's Mesopotamian basin. It is specifically located in the Euphrates subzone, see Figure (1-3). The Euphrates subzone characterized by short structures of longitudinal anticlines trending from the northwest to the southeast. The area dimensions of the Gharraf oil field is 5 km width and 24 km length according to (OEC, 1995).

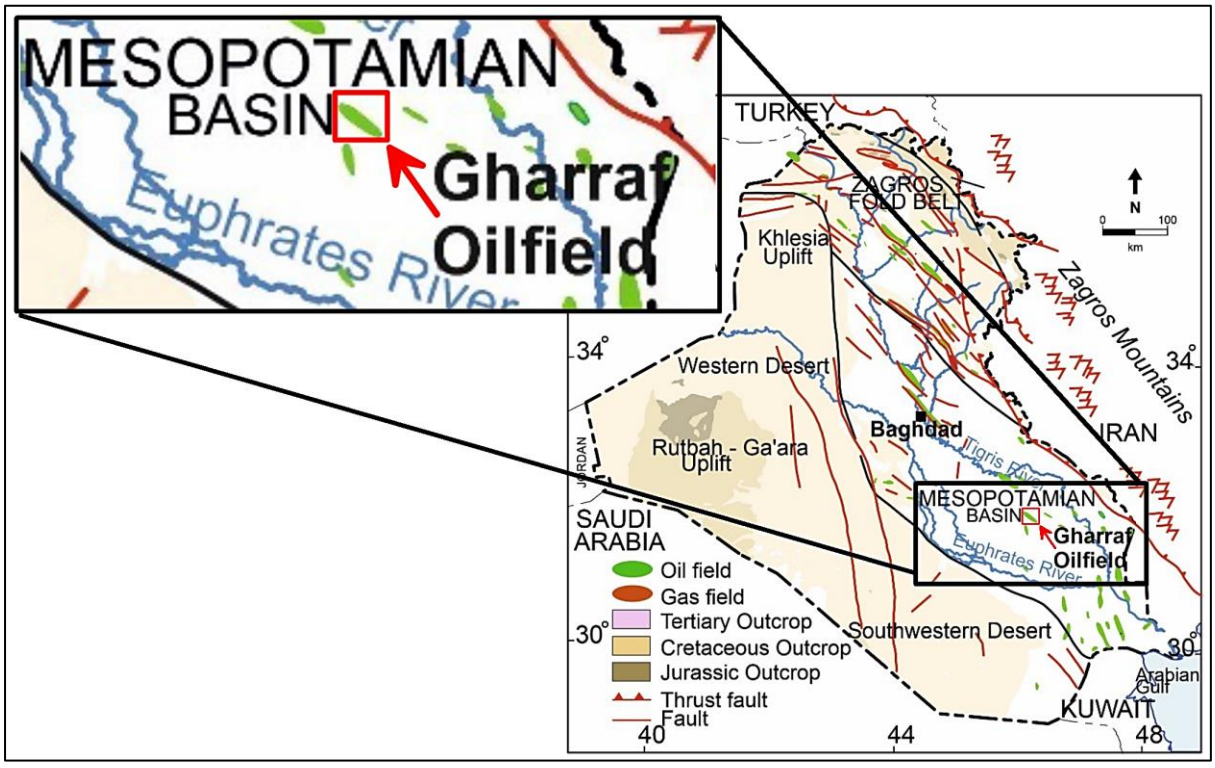

Figure (1-3): Geologic map of Iraq and the location of the structure of the Gharraf oil field. Modified from (Al-Ameri *et al.*, 2009).

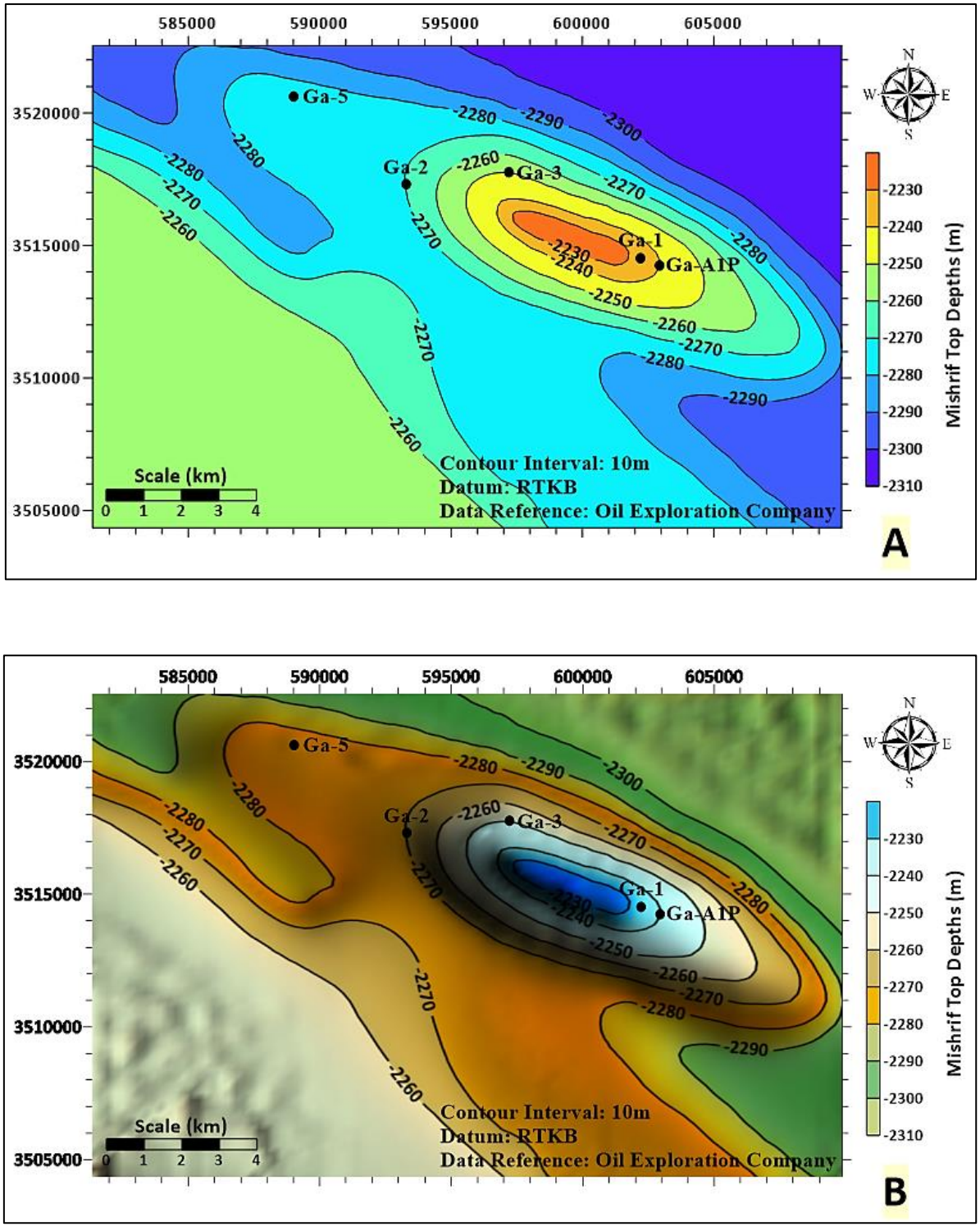

Figure (1-4): (A) 2D and (B) 3D Structural contour map of the Gharraf oil field for the top of the lower main unit of Mishrif Formation, specifying the location of the studied wells, the source of data is the Oil Exploration Company final well drilling reports.

1.3. Stratigraphic Sequence

Because of the abundance of reservoir intervals, the Cretaceous succession has been widely investigated. It is Iraq's most productive interval, holding over 80% of the country's oil reserves. The majority of the petroleum in Cretaceous reservoirs originated from cyclically bedded Jurassic shales and carbonates (Callovian-Oxfordian-Kemmeridgian ages) (Pitman *et al.*, 2004).

The Gotnia Basin is large and deep basin (Figure 1-5), source rocks are primarily bituminous limestone and shale of the Sargelu Formation (Middle Jurassic). The richest source rocks in the Gotnia Basin are mostly condensed sections deposited during transgression cycles' early stages. Circulation was restricted, allowing huge amounts of organic matter, predominantly algal, to be preserved in the basin centers under anoxic bottom conditions on a regular basis. The oceans got shallower and evaporation rates rose in the late Jurassic (Tithonian age), leading in the precipitation of evaporites that covered the organic-rich source and reservoir facies (Fox & Ahlbrandt, 2002).

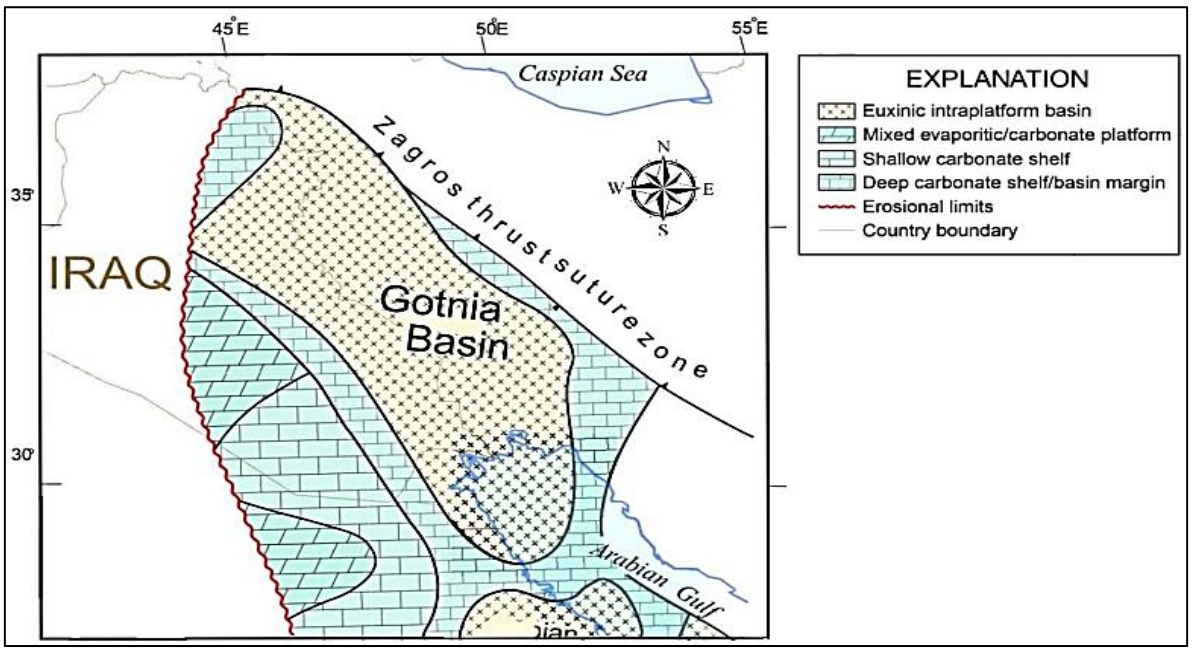

Figure (1-5): Illustrating the extension of the Jurassic Gotnia Basin, modified from (Fox & Ahlbrandt, 2002)

Below is a quick summary of the main formations of the petroleum system of Gharraf oil field from Upper Jurassic Sulaiy Formation to Upper Cretaceous Mishrif Formation (AP8 megasequence) and its sedimentary cycles with the mention of their features. Include the formations that make up the petroleum system of the Gharraf oil field, explained from oldest to youngest as described by (Jassim & Goff, 2006) in the following:

1.3.1. Late Tithonian - Hauterivian sequence (AP8)

1.3.1.1. Sulaiy Formation (inner shelf and deep inner shelf facies)

The Sulaiy Formation as defined in Saudi Arabia comprises chalky, massive bedded limestones, with some interbeds of calcarenite (Powers, 1966) and is of Early Valanginian age. A subsidiary section in Iraq described by Rabanit (Bellen *et al.*, 1959) in well Ratawi-1 in SE Iraq consists of over 331 m (base not reached) of detrital, oolitic limestone and hard recrystallized limestone with rare interbeds of shale. The Sulaiy Formation is conformably overlain by the Ratawi or Yamama Formation except in some parts of the Salman Zone where it is unconformably overlain by the Zubair Formation (Tibor Buday, 1980). The Sulaiy Formation passes to the SW into a sandy unit. A basal sandstone or sandy limestone occurs at the contact with the Gotnia Formation in the W parts of the Salman Zone.

1.3.1.2. Yamama Formation (inner shelf and deep inner shelf facies)

The Yamama Formation was defined by Steinke and Bramkamp in 1952 (Powers, 1966) from outcrops in Saudi Arabia. Bellen *et al.* (1959) described a 257 m interval in Ratawi-1 as the (Yamama-Sulaiy) Formation. The upper 203 m, now assigned to the Yamama Formation (Sadooni, 1993). The formation is up to 400 m thick in the Euphrates area near Najaf and up to 360 m thick in SE

Iraq. In the southern regions of Iraq, Yamama Formation consists of pelloidal, oolitic, pelletal and pseudo-oolitic shoal limestones, plus it includes as well outer shelf argillaceous limestones. Oolitic reservoir units are present in several NW-SE trending depocentres (Sadooni, 1993). The Yamama Formation is Berriasian-Valanginian in age, according to Bellen *et al.* (1959). The Yamama Formation was deposited in alternating deep inner shelf and oolitic shoal environments, according to (Sadooni, 1993), with subtle structural highs within a carbonate ramp controlling the process.

1.3.1.3. Ratawi Formation (inner shelf and deep inner shelf facies)

The Ratawi Formation was defined by Nasr in 1950 (Bellen *et al.*, 1959) from well Ratawi-1 in S Iraq. The formation comprises dark, slightly pyritic, shales; beds of buff, pyritic, pseudoolitic, detrital fossiliferous limestones are present in the lower part of the formation. In some areas E and N of the type well, beds of sandy shale and sandstone occur. Towards the W and N the formation contains a higher proportion of sand. The thickness of the formation in S Iraq ranges from 23 to 629 m. The lower part of the Ratawi Formation was deposited during a highstand in an inner shelf environment; the Upper Ratawi Shale was deposited in a deep inner shelf to middle shelf environment (Douban & Medhadi, 1999). Bellen *et al.* (1959) assigned a Hauterivian age to the upper shale-dominated part of the formation; the lower part of the formation was assumed to be of Valanginian age based on its stratigraphic position. The lower and upper contacts of the formation are conformable (Tibor Buday, 1980).

1.3.2. Barremian-Aptian sequence (AP8)

1.3.2.1. Zubair Formation (clastic-carbonate inner shelf)

The Zubair Formation was introduced by Glynn Jones in 1948 from the Zubair oil field and amended by Nasr and Hudson in 1953 (Bellen *et al.*, 1959). The formation comprises 380-400 m of alternating shale, siltstone and sandstone. The type section was divided into five informal sand and shale units used for reservoir description in the Zubair oil field. To the SW the proportion of shale in the formation rapidly decreases. In the Salman Zone (Awasil Ghalalsan-Safawi areas) the formation consists only of sandstone. The proportion of sandstone in the formation also decreases to the NE; the formation consists almost entirely of shale near Dujalla in Central E Iraq. The Zubair Formation passes laterally into the limestone-marl of the Shu'aiba or Sarmord formations in the Buzurgan area. The formation is thickest in the type area in S Iraq; the depocentre is located at the boundary of the Salman and Mesopotamian zone. Bellen *et al.* (1959) assigned a Hauterivian to Early Aptian age to the formation.

1.3.3. Cenomanian-Early Turonian sequence (AP8)

1.3.3.1. Mishrif Formation (rudist reefs)

The Mishrif Formation was first identified as a heterogeneous formation consisting of organic detrital limestones with beds of rudist, algal, and coral reef limestones, capped by limonitic fresh water limestones by (Bellen *et al.*, 1959). In its type location, the Mishrif Formation is composed of dense, grey-white, algal limestones with shell fragments and gastropods on top, and composed of detrital, brown, porous, partially very shelly and foraminiferal limestones with rudist debris on the bottom. The thickness of the Mishrif Formation in the Rumaila and Zubair oilfields is 270m, and along the Iraq-Iran border the thickness in the Nahr Umr and Majnoon oilfields is 435m, while between Kut

and Amara in the Amud oilfield the thickness is 380m. The Rumaila Formation is usually the underlying unit of the Mishrif Formation in southern regions of Iraq.

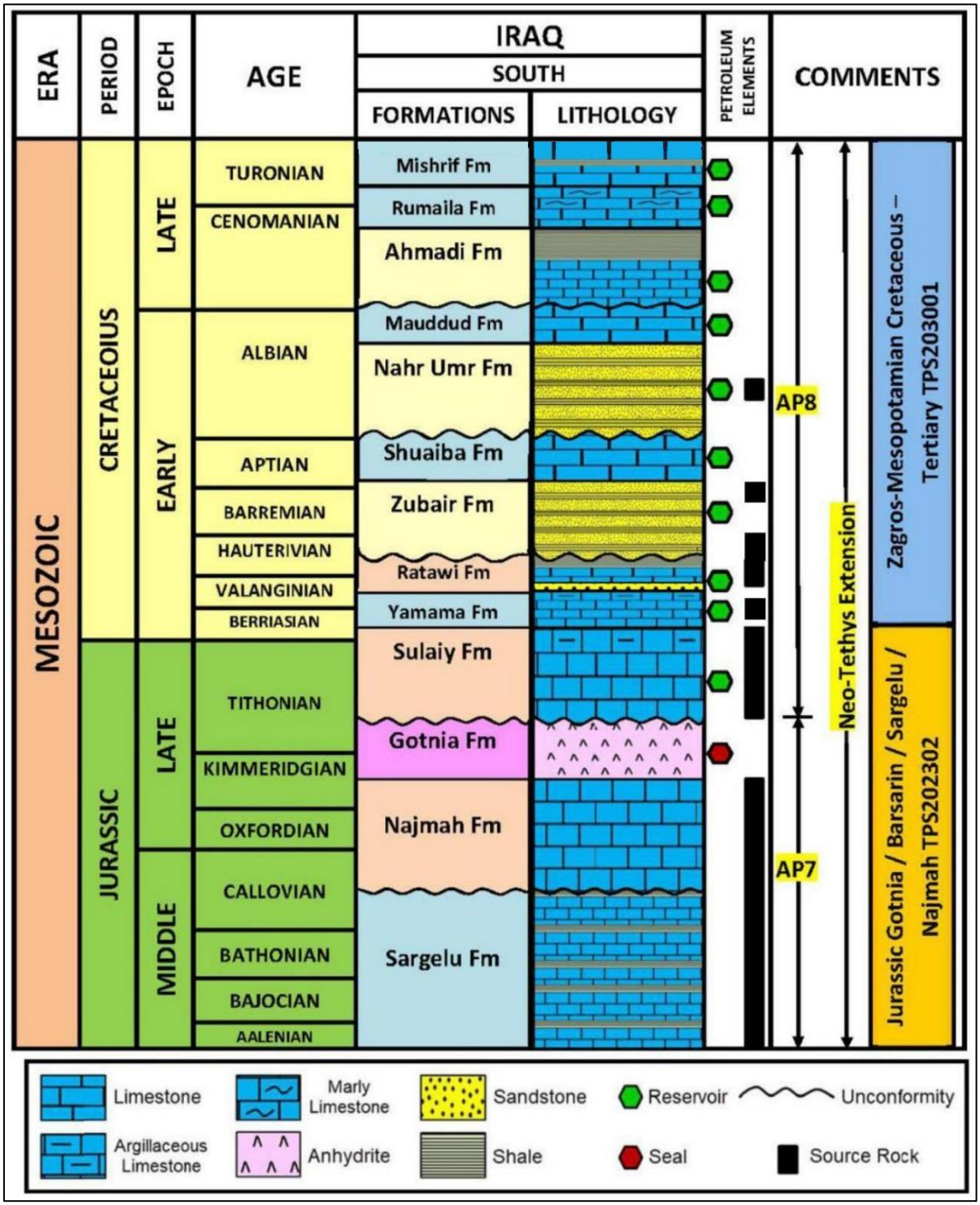

Figure (1-6): General Chronostratigraphic column of the Mesopotamian basin shows the sequence stratigraphy of the formations and petroleum systems and its elements. Modified from (Verma *et al.*, 2004).

Table (1-3): Formations tops and thicknesses of studied wells in Gharraf oil field according to their final well reports (INOC, 1984; SOC, 1987; SOC, 1988; SOC, 2011).

Field Name	Formation Name	Ga-1		Ga-2		Ga-3		Ga-5		Ga-A1P	
		Top (m) RTKB (MD)	Thickness (m)	Top (m) RTKB (MD)	Thickness (m)	Top (m) RTKB (MD)	Thickness (m)	Top (m) RTKB (MD)	Thickness (m)	Top (m) RTKB (MD)	Thickness (m)
Gharraf Oil Field	Mishrif	2236	301	2270	287	2253	296	2276	188	2242	+179
	Rumaila	2537	40	2557	41	2549	39.5	2464	12	---	---
	Ahmadi	2577	12	2598	11	2588.5	12	2476	128	---	---
	Mauddud	2589	202	2609	207	2600.5	209	2604	208	---	---
	Nahr Umr	2791	140	2816	131	2809.5	130.5	2812	128	---	---
	Shuaiba	2931	66	2947	73	2940	70	2940	74	---	---
	Zubair	2997	445	3020	446	3010	438.5	3014	431	---	---
	Ratawi	3442	160	3466	167	3448.5	162.5	3445	175	---	---
	Yamama	3602	269	3633	274	3611	278.5	3620	285	---	---
	Sulaiy	3871	---	3907	---	3889.5	---	3905	---	---	---

Table (1-4): Units tops and bottoms of the lower main unit of Mishrif Formation of studied wells in Gharraf oil field according to their final well reports (SOC, 2011).

Ga-A1P/ RTKB=17.07 m			Ga-3/ RTKB=17.54 m			Ga-5/ RTKB=19.10 m		
Units	RTKB(MD)		Units	RTKB(MD)		Units	RTKB(MD)	
	Top	Bottom		Top	Bottom		Top	Bottom
M1	2305	2306.2	M1	2318.73	2320.45	M1	2340.21	2342.86
M1.2	2306.2	2321	M1.2	2320.45	2333.82	M1.2	2342.86	2389.29
M2	2321	2323	M2	2333.82	2336.71	L2	2389.29	2416.57
L1	2323	2333.71	L1.2	2336.71	2364.93	L2.2	2416.57	2422.53
L1.2	2333.71	2371	L2	2364.93	2375.78	L2.3	2422.53	2446.69
L2	2371	2384	L2.2	2375.78	2394.65	L2.4	2446.69	2464.41
L2.2	2384	2392.56	L2.3	2394.65	2427.15	---	---	---
L2.3	2392.56	2407.44	L2.4	2427.15	2454	---	---	---
L2.4	2407.44	2417.5	---	---	---	---	---	---

Table (1-5): Units tops and bottoms of Yamama Formation of studied wells in Gharraf oil field according to their final well reports (INOC, 1984; SOC, 1987; SOC, 1988).

Ga-1/ RTKB=20 m			Ga-2/ RTKB=18 m			Ga-3/ RTKB=17.54 m		
Units	RTKB(MD)		Units	RTKB(MD)		Units	RTKB(MD)	
	Top	Bottom		Top	Bottom		Top	Bottom
YA	3604	3687	YA	3633	3713	YA	3609.04	3687.54
YB1	3687	3735	YB1	3713	3757	YB1	3687.54	3728.54
YB2	3735	3871	YB2	3757	3907	YB2	3728.54	3889.54

- **M:** Middle units of Mishrif Formation.
- **L:** Lower units of Mishrif Formation.
- **YA:** Yamama Formation upper unit.
- **YB:** Yamama Formation lower unit.

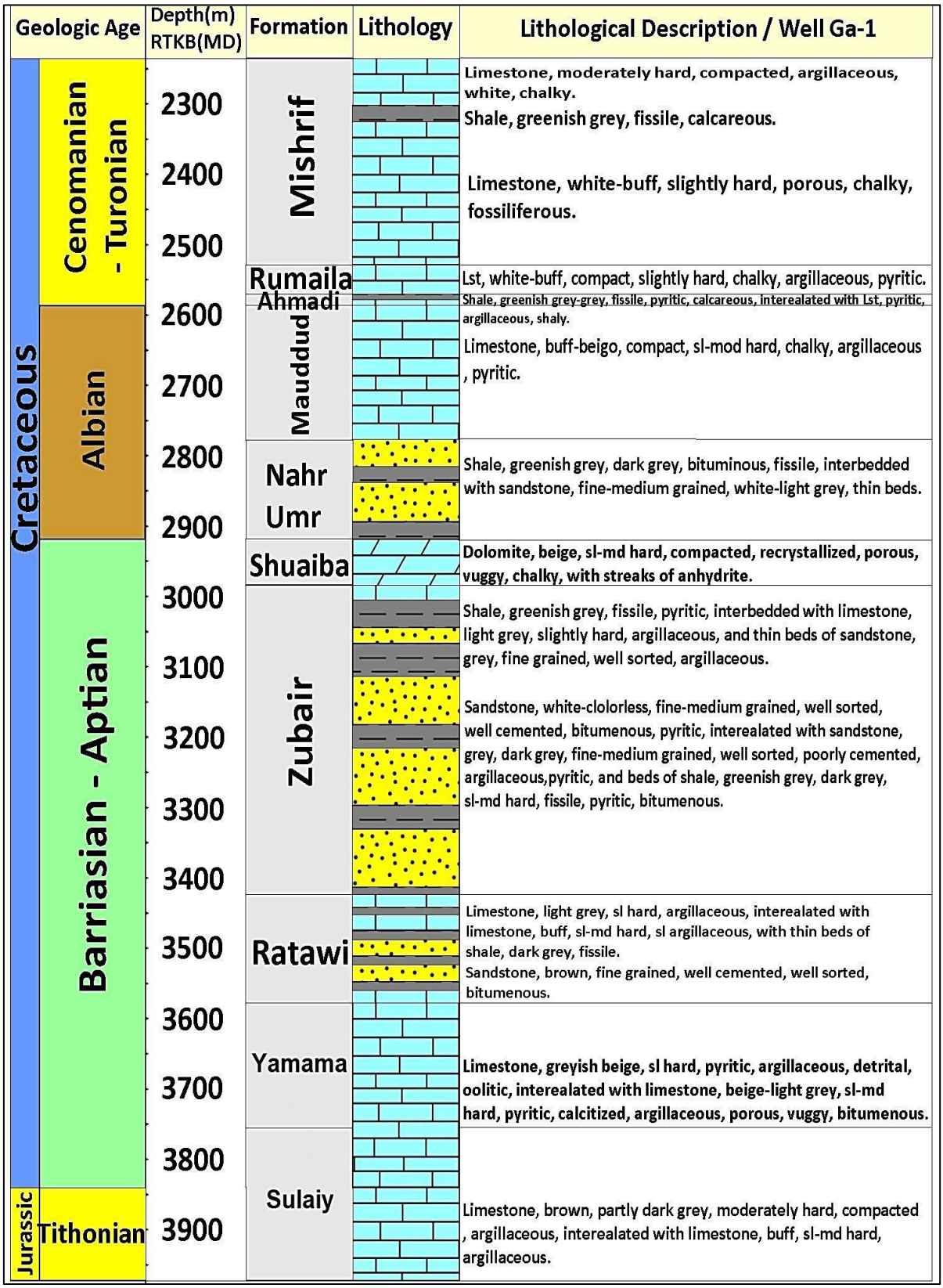

Figure (1-7): Stratigraphic column from U. Jurassic – Cretaceous of Gharraf oil field in well Ga-1 according to the final well report of Oil Exploration Company.

1.4. Previous Studies

1. Al-Ameri & Batten (1997) determined the palynological occurrence and paleoenvironment of Zubair in some oil wells in southern Iraq.
2. A research on the Lower Cretaceous succession of southern Iraq was conducted by Al-Shahwan (2002) and he recommends that the Sulaiy, Yamama, and Ratawi Formations represent source rocks that range from being very good for the Sulaiy Formation to good for the Yamama and Ratawi formations. All of these formations are sited in the oil window's mature region, while the formations of Zubair and Nahr Umr are characterized by good abundance of organic matter and are at early thermal maturation.
3. Pitman *et al.* (2004) are studied the petroleum system in the Mesopotamian Basin and Zagros fold belt of Iraq to determine the generation and migration of petroleum. They indicate that oil and gas fields in the Mesopotamian basin and the folding belt of Zagros are located over the molded petroleum charge plain.
4. In the relationship between Mishrif crude oil and potential source rocks in southern Iraq, Al-Khafaji (2006) used biomarkers and carbon isotopes. He concludes that much of the crude oil accumulated in the Ratawi, North and South Rumaila oil fields in the Mishrif Formation comes from Jurassic source rocks such as the Naokelekan and Sargelu formations, and the rest of the oil comes from the Sulaiy Formation.
5. Al-Yaseri (2007) suggested that the organic facies of southern Iraq are investigated as potential for oils in the Upper most Jurassic (Gotnia Formation) and Lower Cretaceous (Sulaiy, Yamama, Ratawi, Zubair, and Shuaiba formations). He also indicated that Mishrif crude oil is less mature according to bulk parameters and isotopic results as well as molecular parameters, while Nahr Umr and Zubair crude oils are the most mature, these

Cretaceous reservoir oils are generated from a very similar source excluding Nahr Umr oils that have a different source in the South Iraq basin.

6. The Cretaceous Petroleum System of Iraq was studied by Aqrawi *et al.* (2010). They show that in central and southern Iraq, Tithonian (Upper Jurassic) to Lower Cretaceous source rocks have charged Cretaceous reservoirs in anticlinal structures.

7. Jafar, M. S. A. (2010) concluded that three methods confirm that the Upper Jurassic Sulaiy Formation and the Ratawi, Zubair, and Nahr Umr Lower Cretaceous are the candidate source rocks in the stratigraphic portion of an area of interest that might have charged the reservoir of the Lower Cretaceous including the reservoir of Mishrif. The enormous amount of hydrocarbons stored in these reservoirs gives the sense that there are other sources of oils that could be the Middle Jurassic Sargelu Formation that may have charged the Upper Jurassic and Lower Cretaceous reservoirs as well as the Upper Cretaceous reservoir during vertical migration to these reservoirs of produced hydrocarbons.

8. Abeed *et al.* (2011) according to their study, they concluded that the Cretaceous Zubair and Ratawi formations are poor to fair source rocks with a high concentration of Type III kerogen. These formations were typically thermally immature to early mature, with a low thermal maturity. The Yamama Formation, on the other hand, has good source rock potential and includes Type II-S kerogen. It has a low to moderate thermal maturity, and it has yet to reach peak oil output.

9. Najaf, A. A. (2013) in his study of the hydrocarbon generating potential of the Sargelu Formation, North Iraq, Microscopic and chemical analysis performed of 85 rock samples from exploratory wells and outcrops in northern Iraq indicate that limestone, black shale and marl within the Middle Jurassic Sargelu Formation contain abundant oil-prone organic matter. The level of thermal maturity is within the oil window with TAI=3− to 3+, based

on microspore color of light yellowish brown to brown. Accordingly, good hydrocarbon generation potential is predicted for this formation. Two subfamily carbonate oil types, one of Middle Jurassic age (Sargelu) carbonate rock and the other of Upper Jurassic/Cretaceous age.

10. Najaf, A. A. *et al.* (2016) in their study of geochemical correlation of oil and source rocks from selected exploratory wells within Northern Mesopotamian basin, Iraq, two main families recognized (family A) subsidy to subfamily (a) and subfamily (b), generated by different source rock types, and different ages has been established on the basis of biomarker. This family was generated by marine carbonate–intrashelf subbasin source rocks, occurring in Jurassic–Cretaceous–Neogene reservoir rocks in both Zagros Fold Belt and Mesopotamian basin which are geochemically similar to the extracts from the Middle–Upper Jurassic age (Sargelu and Naokelekan Formations), yielding the majority of petroleum oil and gas fields in Iraq. (Family B) of the Upper Triassic Kurra Chine Formation, shallow marine–lagoonal environment, Upper Cretaceous Shiranish formation. Shale beds of the Middle Jurassic Sargelu formations are the major sources of oil in Iraq; these strata were deposited in euxinic marine environment, and most of rock sample are highly mature, with TOC attaining 16.20 wt% and average hydrogen index (HI) of 499 with relatively low values of oxygen index (OI) and maximum temperature (T_{max}) 446.

11. Najaf, A. A. (2018) in his study of basin modeling of the potential sourced Sargelu Formation within Zagros fold belt, North Iraq, one dimension petroleum-system modeling of key wells were developed using Integrated Exploration System (IES). PetroMod software to evaluate burial-thermal history, source-rock maturity, and the timing and extent of petroleum generation; interpreted well logs served as input to the models. The oil generation potential of sulfur-rich Sargelu source rocks was simulated using

closed-system, Type IIs kerogen kinetics. Model results indicate that throughout northern Iraq generation and expulsion of oil from the Sargelu began and ended in the late Miocene. At present, Jurassic source rocks might have generated and between 70 and 100 % of their total oil, or the model indicates that, the majority of Jurassic source rocks in Iraq have reached or exceed peak oil generation and most rocks have completed oil generation and expulsion except Jabal Kand-1, were defiantly unlike the other wells, is still generating today.

12. Al-Khafaji *et al.* (2019) in their study of the source rocks of Zubair Formation and their contribution in generation and expulsion of oil to the Mesopotamian Basin reservoirs they concluded that the kerogen quantity of Zubair source rocks is ranging from poor to excellent. In certain samples, the migration index is greater than 0.1, suggesting the probability of oil expulsion. The genetic potential for producing hydrocarbons ranges from low to excellent, and the gas prone kerogen type III is the most common, followed by oil prone type II and mixed prone type II/III.

13. Al-Khafaji *et al.* (2021) they studied the geochemical properties of crude oils and basin modeling of potential source rocks in the Southern Mesopotamian Basin of Iraq, and they concluded after they collected fifteen samples of crude oil from the clastic reservoirs, and several analyzes were done on it, that marine carbonate-rich source rocks (rich in phytoplankton/benthic algae and bacterial organic matter) deposited under anoxic environmental conditions containing kerogen type II-S is the origin were the analyzed oils derived from, the maturity of source rocks is ranged from early to relatively high stage where both non-biomarker data and biomarker maturity support this result, and the source of oils in the oilfield of this region is from Sargelu, Najmah and Sulaiy formations that belong to the Jurassic-Early Cretaceous and then migrated into the shallow reservoirs through the faults path.

1.5. Objectives of The Study

- Determining the potential source rocks formations of the crude oil accumulated in the Cretaceous reservoirs in the Gharraf oil field.
- Determining the Cretaceous reservoir formations of the crude oil generated from the potential source rocks formations in the Gharraf oil field.
- Determine the seal rocks of the Gharraf oil field petroleum system.
- Determine the overburden rocks of the Gharraf oil field petroleum system.
- Determining the petroleum system processes of the Gharraf oil field represented in the time of trap formation and the time of generation-migration-accumulation processes, as well as the migration pathways of generated hydrocarbons.
- Reservoir rocks formation evaluation for Lower cretaceous Yamama Formation and Upper Cretaceous Mishrif Formation in the Gharraf oil field, in order to determine the petrophysical properties (porosity, permeability, and water saturation) of these reservoirs.
- Oil reserves estimation for Mishrif and Yamama main reservoirs of the Gharraf oil field.
- Potential source rocks formations evaluation for Sulaiy, Yamama, Ratawi, and Zubair formations in the Gharraf oil field, in order to determine the level of thermal maturity of organic matter and the quantity and quality of organic matter (kerogen).
- Analyze a sample of crude oil from Mishrif Formation in the Gharraf oil field in order to determine the potential generated source rocks type, depositional environment, redox conditions, thermal maturity level, and age depending on the crude oil's bulk properties and biomarkers.
- Build 1D petroleum system models of the Gharraf oil field including burial history chart, thermal history chart, and events chart.
- Make oil-source rocks correlation in order to prove the generated source rocks in the Gharraf oil field petroleum system.

1.6. Methodology

1.6.1. Data collecting

Collecting data for any study represents the first essential step for starting this study. The data required in this study were obtained from the concerned authorities in the Ministry of Oil as well as from previous studies of the Gharraf oil field. These data included image of structural contour map of the Gharraf oil field, images of the required well logs represented by (Caliper, GR, SP, Sonic, Neutron, Density, and Resistivity logs) for the studied wells Ga-1, Ga-2, Ga-3, Ga-5, and Ga-A1P, a picture of a seismic section passing through the Gharraf oil field, end-of-well reports for the studied wells including depths of the tops of the studied formations and the lithological description of them to build the stratigraphic column of the field, and the results of the organic geochemical analyzes of the rock core samples of the potential source rocks formations of the petroleum system of Gharraf oil field.

1.6.2. Data processing and interpretation

Data processing and interpretation represents the second basic step after data collection. The necessary software represented by Petrel 2009, IP v3.5, PetroMod v2012.2, and Didger v5 were prepared and installed to digitize, process and interpret these data, and the required results obtained for this study, in the following a brief of each software used in this study:

a. Didger software v5

Didger is a digitizing program that is extremely precise. Didger converts points, lines, and areas from charts, aerial photographs, paper maps, imported vector files, scanned raster images, and GeoTIFF photos to a flexible digital format that can be used with other applications.

There are many functions that this program can perform, including:

- Digitize well logs and contour maps from various pictorial sources.
- Digitize a vector or raster project onscreen.
- Alter the islands and lakes by combining, splitting, and/or reversing them.
- Combine two polygons or make a polygon out of the intersection of two polygons.

b. Interactive petrophysics software v3.5

IP is a powerful and quick software platform for geoscientists who want to make the most of their subsurface findings. This work can be achieved with an interactive interface using IP, which improves Geoscientists' efficiency and productivity. IP is a set of modules for evaluating formations. IP provides an extremely capable and flexible solution for sharing and interpreting well logs and many other important data types, from porosity and pore pressure to reservoir productivity. As standard, IP's Basic package includes advanced data management, calculation, and deterministic workflow features.

The best method for precise subsurface interpretations is Interactive Petrophysics (IP). It is reliable, and its interactive graphical interface reduces user errors. IP provides a powerful, budget solution that allows in-depth analysis for geological and petrophysical decision-making. IP allows for integrated workflows across subsurface disciplines, resulting in increased reservoir quality across the board.

c. Petrel software v2009.1

Schlumberger produced and developed Petrel, a software application used in the petroleum exploration and production industry. It enables users to, perform well correlation, interpret seismic data, build models for studied reservoirs, build maps, design development strategies to increase reservoir

production, and view the results of reservoir simulations, estimate volumes. Throughout the reservoir's lifetime, risk and uncertainty may be measured.

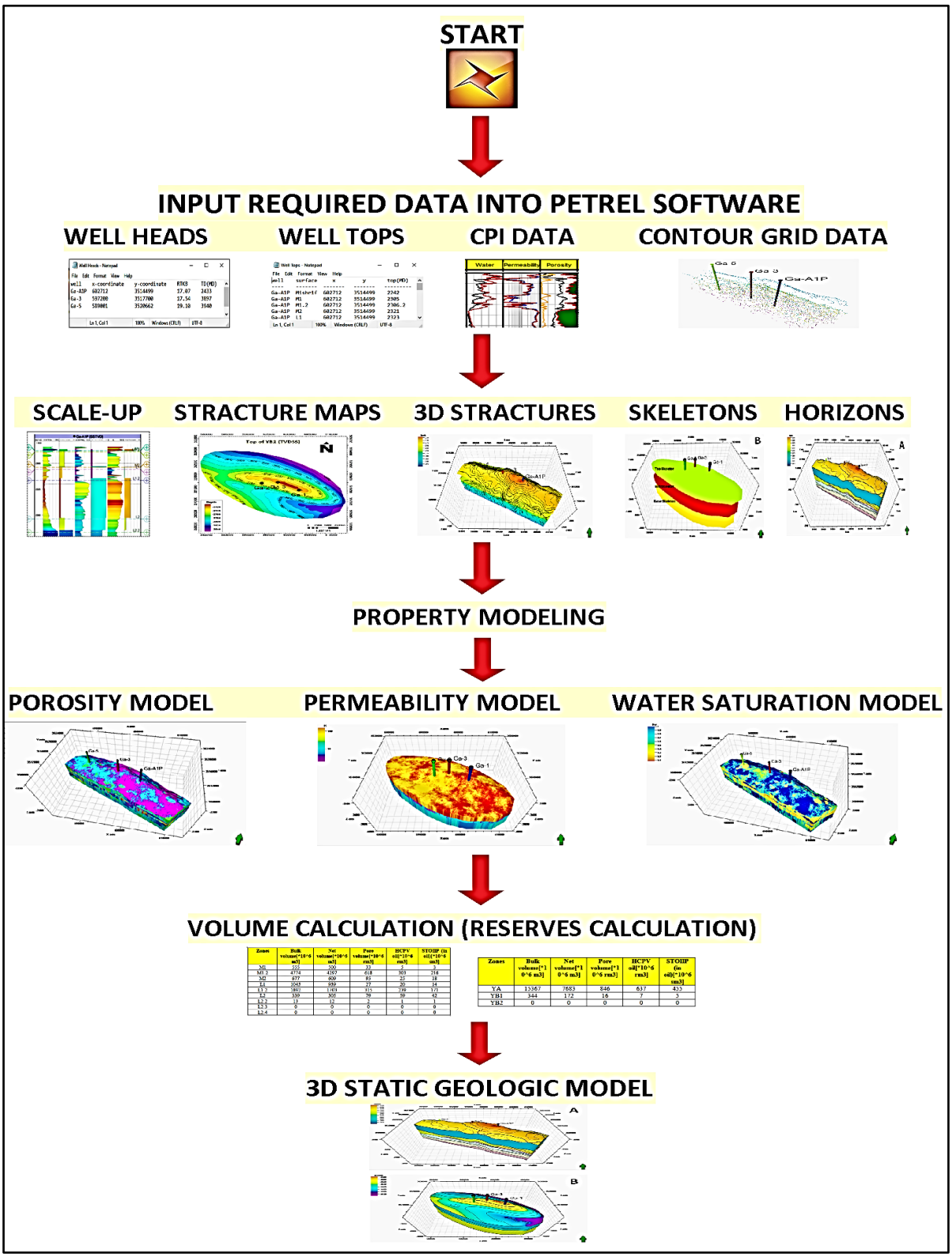

Figure (1-8): Work-flow of petrel software to build a 3D static geologic model.

d. PetroMod software v11

PetroMod software package is used in this work to model the hydrocarbon generation, migration and accumulation. PetroMod incorporates multi-dimensional models of compaction, thermal, petroleum migration histories, and fluid flow in sedimentary basins with stratigraphic, seismic, and geological interpretations.

PetroMod has proved to be a useful tool in science, but it is still used in exploration. PetroMod's primary goal is to determine the most precise timing and location of petroleum generation, expulsion, and migration processes. PetroMod has proven to be a valuable tool in research applications, but it mostly used in exploration work.

The fundamental task of PetroMod is to obtain the most accurate prediction of timing and location of petroleum generation, expulsion and migration processes (IES, 2009).

PetroMod consists of a number of modules for 1D, 2D, 3D basin modeling with unique user interface and workflow. N-component, 3-phase flash calculation is readily integrated for 2D and 3D packages (Jia, 2010). In this program, basic data is entered and then the required models are made, which give clear and different explanations.

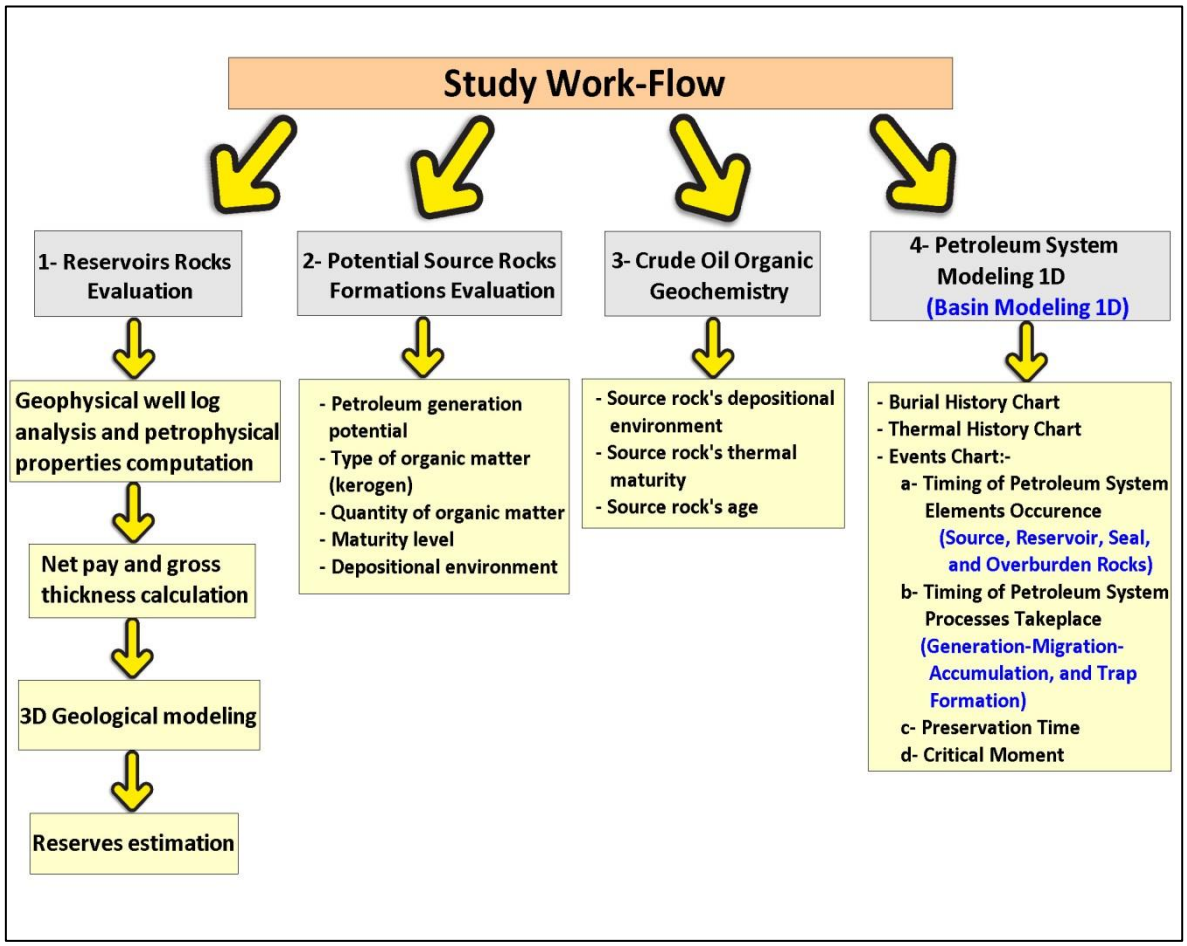

Figure (1-9): Showing workflow of this study.

Chapter Two

Source, Seals, and Overburden Rocks

2.1. Preface

To define the petroleum system, we must first define the two concepts separately, and then integrate them to form a full description of the petroleum system. When we talking about petroleum, we should know the source of the term "petroleum". Where the term of petroleum derived from the Latin word, where the first part of the term "petra" means "rock", and the second part of the term "oleum" means "oil". Petroleum is a term used to describe a combination of solid, liquid, and gaseous hydrocarbons. These hydrocarbons occur naturally under the earth's surface. It is also referred to as crude oil. Petroleum is used as raw resources for a variety of products, including: gasoline, naphtha, diesel, kerosene, natural gas, paraffin wax, lubricating oils, and asphalt. Now let's describe system to get the petroleum description. A collection of elements that all work together to accomplish the same goal, referred to as a "system". As a result, the petroleum system can be described as a collection of geological components and processes that contribute to hydrocarbon generation and accumulation (Magoon & Schmoker, 2000).

Source-rock, reservoir-rock, seal-rock, as well as overburden rock, all represent the fundamental elements of a TPS. The main processes of a petroleum system including; generation, migration, accumulation, and trap formation. Both of genetically related petroleum that happening in shows, seeps, and accumulations of discovered and undiscovered, which its root is a pod or closely related pods of active source rock. The Total Petroleum System represents a hydrocarbon fluid system, this system can be identified in particular part of the lithosphere, where formed naturally and includes the fundamental elements and processes necessary for the accumulation of oil and gas. The TPS definition assumes that migration paths must occur; either now or in the past, linking the provenance with the accumulations using petroleum geology and geochemistry principles, in order to better understand how it developed over time. Plotting this natural fluid system, or TPS, in three-dimensional space over

time, represents the main objective, in order to find, describe, and evaluate particular areas for undiscovered hydrocarbons (Magoon & Schmoker, 2000).

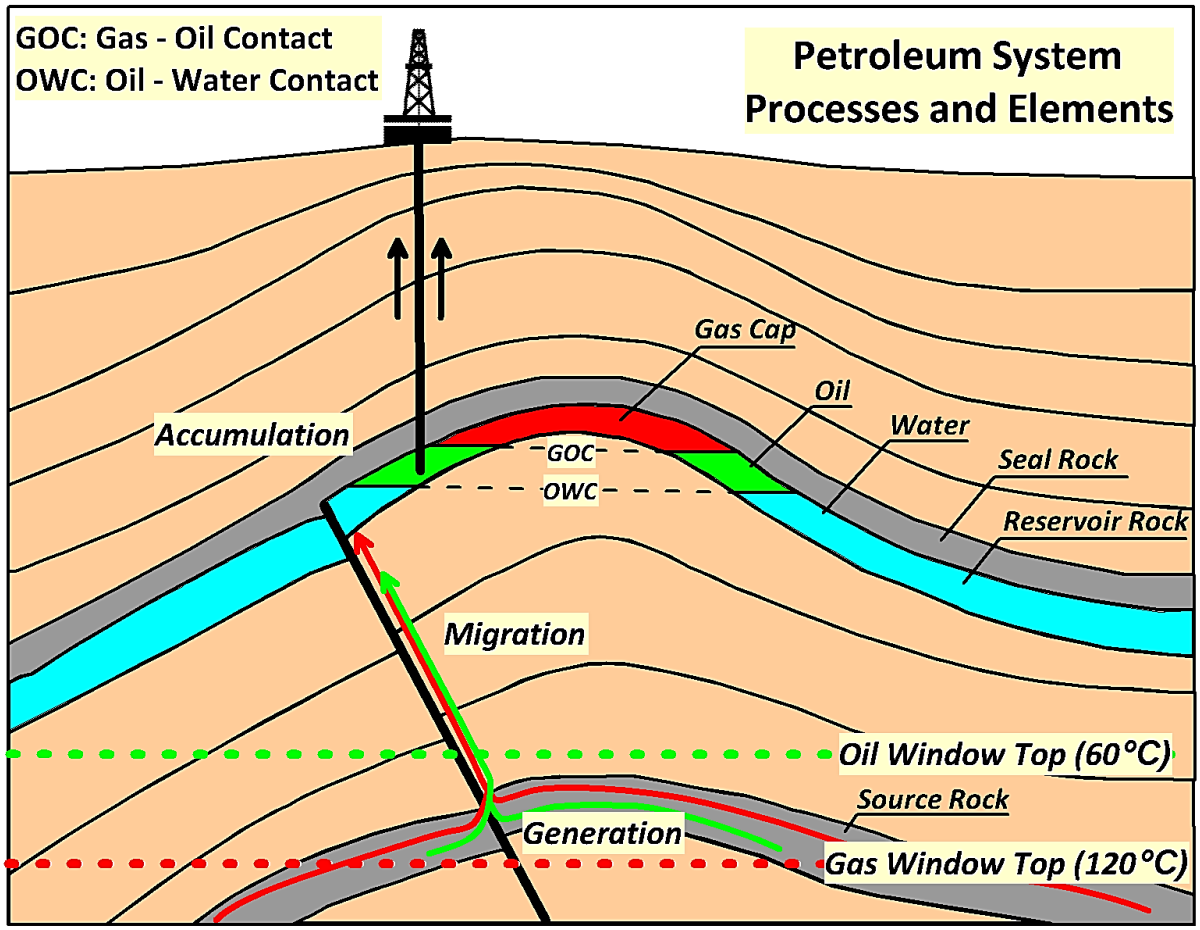

Figure (2-1): Scheme illustrating a typical petroleum system. Modified from (Magoon & Dow, 1991)

2.2. Petroleum System Elements

2.2.1. Overview

For every oil or gas play, there must be a source rock that generated it .The efficiency of each paly, whether conventional or unconventional, oil or gas, is determined by the source rock. Without source rock element for petroleum generating, it become unnecessary to present all other elements and processes required to develop a play. Any fine-grained, organic-rich rock capable of generating petroleum is referred to as a source rock. Its petroleum-generating

potential is proportional to its volume, organic richness, and thermal maturity. The volume and type of organic matter present within the rock is referred to as organic richness. Thermal maturity refers to how long a source rock has been exposed to heat. When the burial of the source rock increases to a certain depth beneath lithologic column, the heat produced increases, then petroleum is generating by the thermal transformation of organic matter in a source rock (McCarthy *et al.*, 2011). Kerogen refers to the insoluble component of organic matter in sedimentary rocks, whereas bitumen refers to the soluble part (Tissot & Welte, 1984).

Table (2-1): Kerogen types and its source material after (McCarthy *et al.*, 2011).

Kerogen type	Source material	General environment of deposition
I	Mainly algae	Lacustrine setting
II	Mainly plankton, some contribution from algae	Marine setting
III	Mainly higher plants	Terrestrial setting
IV	Reworked, oxidized material	Varied settings

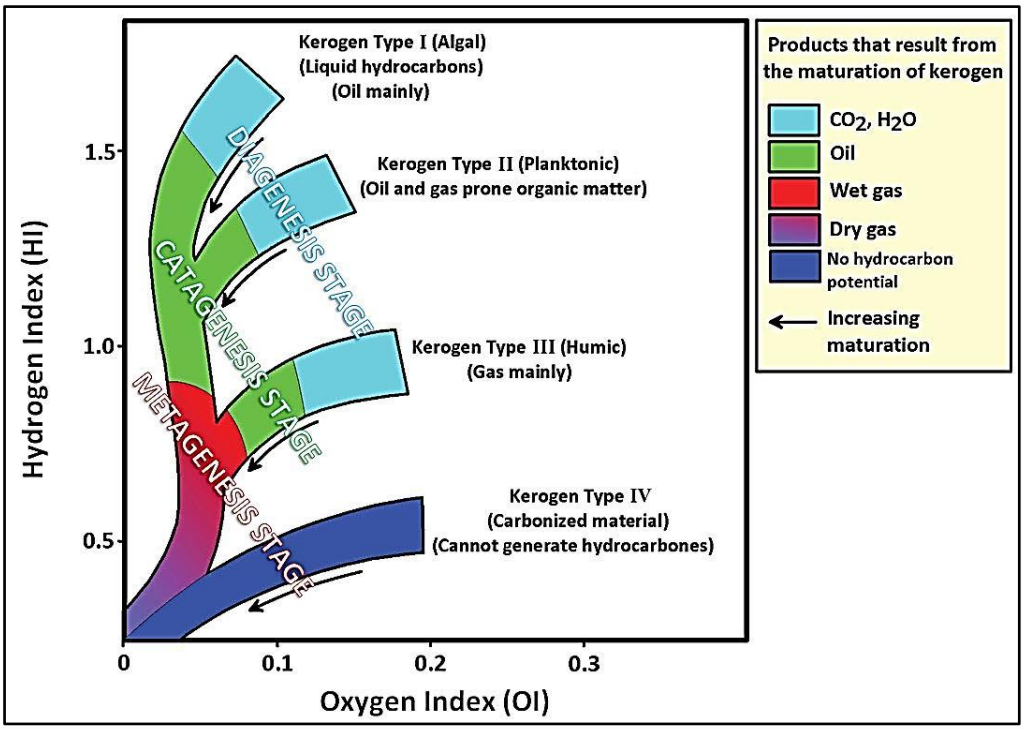

Figure (2-2): Van Krevelen diagram shows changes in kerogen types caused by increased heat during burial. Modified from (Tissot *et al.*, 1974).

The generative potential of the source rock depending on the quality and quantity of organic material that have been preserved during diagenesis of sediment, whether it will be prone to expel oil or gas. Quantity is determined by a mount of organic input, the degree to which it is preserved (either as primary or secondary biogenic) (Hsu & Robinson, 2007). The quality of kerogen is mostly determined by hydrogen content; kerogen with a high H/C ratio (>1.2) is oil-prone, while kerogen with a lower H/C ratio (0.5-0.8) generates mostly gas (Tissot & Welte, 1984). Rock-Eval pyrolysis tool represents almost the best tool in determining the type of kerogen (Espitalie *et al.*, 1977).

2.2.1.1. Basic source rock analysis and analysis techniques

Geochemists can determine the amount of generated petroleum in comparison to a rock's total potential by monitoring the compounds generated during a steady increase in temperature. Furthermore, the temperature at which the maximum gas evolution occurs indicates the maturity of the source rock. To determine the capacity of source rocks to generating hydrocarbons (oil and gas), geoscientists employ a number of analysis techniques. Formation cuttings, sidewall cores, outcrop samples as well as conventional cores can all be geochemically tested using a variety of techniques to specify the amount, type, and thermal maturity of organic matter in the source rock (McCarthy *et al.*, 2011). The analysis techniques are:

a. TOC measurement

b. Rock-Eval pyrolysis

c. Vitrinite reflectance (Ro)

d. Thermal Alteration Index (TAI)

e. Conodont Alteration Index (CAI)

f. Gas chromatography (GC)

Carbon represents an essential component of any organic matter, and measuring the carbon content of a rock is one way to determine its organic richness (TOC) (Jarvie, 1991). The TOC measurement considered as a priority in source rock evaluation because a formation's oil or gas generating potential is proportional to its carbon content. After the assessment of this initial carbon, other screening techniques like pyrolysis and vitrinite reflectance are used. Pyrolysis and vitrinite reflectance tests can be used to evaluate a wide number of rock samples quickly, and they can be supported by more extensive test methods (McCarthy *et al.*, 2011). The source rock samples that were taken from the studied source rock formations were subjected first to the process of calculating the total organic carbon (TOC) and then to the process of Rock-Eval pyrolysis to obtain the important parameters in evaluating the source rocks of the studied formations, and below is a summary of each of these two assessment techniques:

a. TOC content

The total organic carbon (TOC) measurement represents the first screening for determining organic richness in source rock. Only a semi-quantitative scale of petroleum generating potential is provided by TOC values. The TOC values indicate the quantity of organic matter, but not its quality (McCarthy *et al.*, 2011). The values of TOC can be calculated by using a direct-combustion technique which requires 1gm only of rock samples (Peters & Cassa, 1994). In order to calculate the values of TOC in rock samples, samples should be pulverized and treated to remove any carbon or other contaminants found in carbonate samples. After that, a high-frequency induction furnace used to burn the rock samples at 1200 ˚C. Carbon involving in kerogen transformed into CO and CO2, where the transformed carbon ratio are calculated in an infrared cell, then, calculated value converted to TOC and recorded as mass weight percent of rock.TOC indicates the quantity, but not the quality, of the organic matter. If the

initial screening test reveals adequate content of organic material, the source rock should be subjected to additional tests to determine the quality and maturity of the organic matter (McCarthy *et al.*, 2011).

b. Rock-Eval pyrolysis

The Francais du Petrole Institute was the first to develop this screening technique, which called the Rock-Eval pyrolysis. This analyzer has become an industry standard in source rock evaluation (Espitalie *et al.*, 1977). This programmed pyrolysis technique, a significant development in petroleum geochemistry, exposes rock samples to high temperatures, allowing researchers to obtain results that would have taken millions of years in a sedimentary basin. Only 100 mg from pulverized rock required for this analyzing technique, and the analysis of a sample can take a matter of minutes. The most recent iteration of the Rock-Eval device heats samples in a programmed sequence of stages varying from 100 to 850 ˚C using both pyrolysis and oxidation ovens (Lafargue *et al.*, 1998). Sample analyses are automated, and results are computed before they are tabulated and output to a log (McCarthy *et al.*, 2011). Samples are heated in an inert atmosphere of helium or nitrogen during Rock-Eval pyrolysis. A flame ionization detector (FID) senses organic compounds emitted during each stage of heating. Sensitive infrared (IR) detectors measure CO and CO2 during pyrolysis and oxidation. A thermocouple monitors temperatures. These measurements are recorded on a chart known as a pyrogram. The results of the Rock-Eval pyrolysis help geochemists in identifying the type of organic material exist in a source rock, as well as determining a sample's thermal evolution and hydrocarbon-generation potential of residual (Espitalié & Bordenave, 1993). Rock-Eval pyrolysis involves two main stages in order to heat rock samples. In first stage heating held at a steady 300 ˚C for several minutes, then in second stage programmed heating of 25 ˚C per minute to a peak temperature of about 850 ˚C. Any free oil and gas previously generated by

the bitumen are extracted and released from the source rock through the first stage. The insoluble kerogen is thermally cracked to produce hydrocarbon compounds in the next stage. As temperatures rise, the kerogen releases CO2 in addition to hydrocarbons (Peters, 1986). This controlled heating program is illustrated by a series of peaks on the pyrogram, see Figure (2-5) (Espitalie *et al.*, 1977).

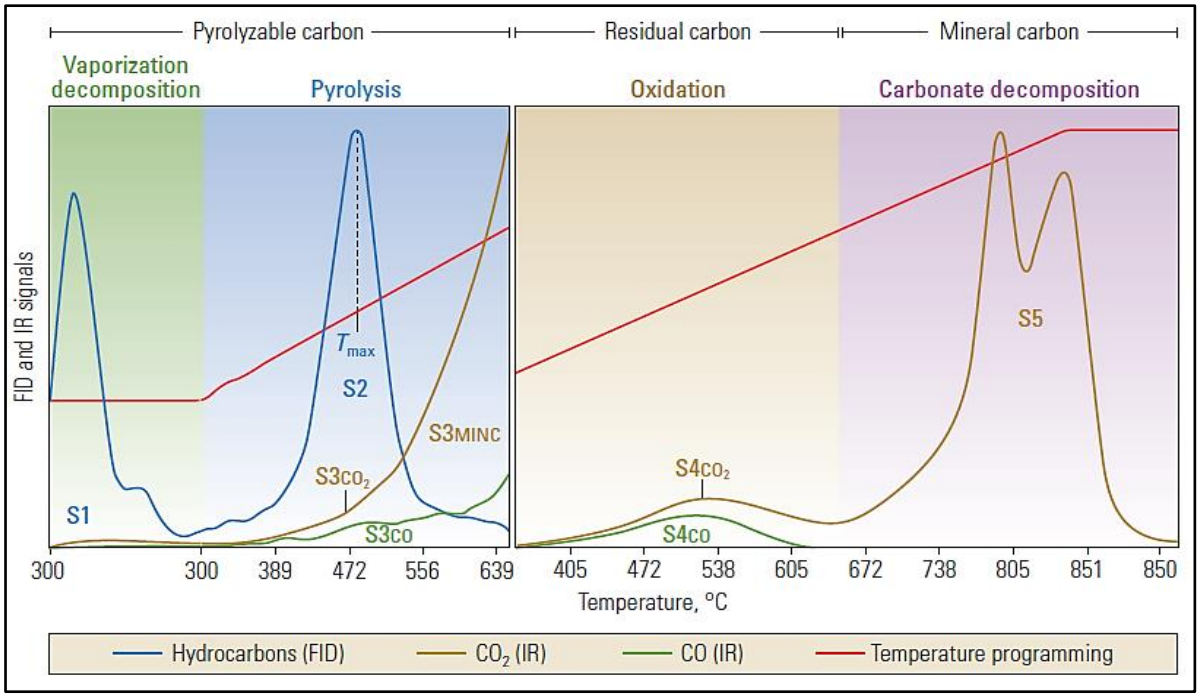

Figure (2-3): Illustrates the typical curves generated from Rock-Eval pyrolysis technique after (Lafargue *et al.*, 1998) and (McCarthy *et al.*, 2011).

- During the first stage of heating at 300 ˚C, the first peak, S1, corresponds to free oil and gas that emerge from the rock samples without cracking the kerogen. These hydrocarbons (oil and gas) were generated in the subsurface, but only pyrolysis analyzing technique enabled them to be expelled from the source rock. S1 peak in the pyrogram of the Rock-Eval pyrolysis represents the number of milligrams of free hydrocarbons that can be thermally distilled from a gram of sample (Espitalie *et al.*, 1977).

- The hydrocarbons (oil and gas) that extract from the sample during the second programmed heating stage of pyrolysis are represented by the second peak in the pyrogram, S2. The cracking of heavy hydrocarbons and the thermal degradation of kerogen produce these hydrocarbons. S2 in the pyrogram of the Rock-Eval pyrolysis indicates the quantity in milligrams of residual hydrocarbons in one gram of rock, indicating the amount of hydrocarbons the source rock could still produce if thermal maturation continues. This reading can have important implications for the evaluation of oil shales. The Rock-Eval technique yields a variety of CO2 measurements (McCarthy *et al.*, 2011).
- The S3 peak in the pyrogram of the Rock-Eval pyrolysis corresponds to CO2 produced by thermal cracking of the kerogen which expressed in milligrams per gram of rock. The S4 peak in the pyrogram is produced by oxidizing residual organic carbon, this process is following pyrolysis in a separate oven (McCarthy *et al.*, 2011).
- The S4CO2 and S4CO peaks are formed in the pyrogram of the Rock-Eval pyrolysis as the S4 measurement is broken down into carbon dioxide and carbon monoxide components (McCarthy *et al.*, 2011).
- A separate CO2 peak, in the pyrogram of the Rock-Eval pyrolysis, marked S5, represents CO2 that produced from decomposition of the sample's carbonate minerals (McCarthy *et al.*, 2011).

Pyrolysis temperatures are also recorded, resulting in a Tmax peak, which corresponds to the pyrolysis oven temperature at maximum hydrocarbon generation. Tmax of pyrolysis is reached during the second stage of pyrolysis, when the S2 peak is produced by cracking of the kerogen and heavy hydrocarbons in rock sample (Peters & Cassa, 1994). Geochemists can use the amount of heat required to generate different chemical compounds in the rock, this gives better understand the rock's history and also the stage of thermal maturation that the rock has already undergone. There is a difference between

Tmax and geologic temperature, although it does help characterize thermal evolution of the organic matter (McCarthy *et al.*, 2011). Tmax is the primary Rock-Eval parameter for assessing thermal maturity for different types of organic matter. It was recognized early that Tmax would increase with increasing depth (Espitalie *et al.*, 1977) and was eventually related to other maturity indicators such as vitrinite reflectance. Typical Tmax values for the top and bottom of the oil window are shown in Table (2-2).

Table (2-2): Thermal maturity interpretations for Rock-Eval Tmax, after (Espitalié, 1986).

Maturation	T_{max} (˚C)
Top of Oil Window	~435 - 445
Bottom of Oil Window	~470

The range of temperature for the upper portion of the oil window, reflects that the absolute changes in Tmax vary according to kerogen type as well as maturity (Espitalie *et al.*, 1985; Espitalié, 1986; Peters, 1986). While Tmax values for Type II kerogen will be approximately 435°C at the top of the oil window, Type I kerogen will have Tmax values of about 445°C. Significant hydrocarbon generation in Type III will be indicated by Tmax values of about 440°C. As maturity progresses, the kerogen type influence diminishes, and all three kerogen types have Tmax values of approximately 470°C at the bottom of the oil window. The observed relationship between Tmax and vitrinite reflectance, displays a range of variation in Tmax at any given maturity level (Dembicki, 2016). There are many important indices mentioned below, taken together, these pyrolysis measurements provide insight into the chemical makeup and maturity of the organic matter contained within the source rock. The relationship between these components forms the basis for various indices used in the interpretation of rock characteristics (Espitalie *et al.*, 1977).

- The hydrogen index, HI, is determined using the hydrogen to TOC ratio, and is defined as 100 * S2/TOC. The HI is equal to the amount of hydrogen in the kerogen, and a high HI indicates a higher potential for oil generation. Kerogen type can be inferred from this index as well (McCarthy *et al.*, 2011).
- The oxygen index, OI, is determined using the CO2 to TOC ratio, and is defined as 100 * S3/TOC. The OI is a measurement of the amount of oxygen in kerogen which can be used to monitor kerogen maturation or type (McCarthy *et al.*, 2011).
- The production index (PI): this index is determined from the relationship between hydrocarbons generated in the first (S1) and second (S2) stages of pyrolysis. PI is identified as S1/(S1 + S2).

  Because PI tends to increase with depth for fine-grained rock, this relationship is used to identify the evolution of organic matter. This index tends also to increase with maturity increment of source rock before expulsion of hydrocarbon, while thermally degradable components within kerogen are transformed to free hydrocarbons. S1 and PI values that are abnormally high can be used to identify petroleum accumulations or stained carrier beds (McCarthy *et al.*, 2011).
- The petroleum potential represents the maximum quantity of hydrocarbons that a sufficient matured source rock might generate; it is defined as the sum of S1 + S2. As a result, it accounts for the hydrocarbons amount, that already generated by the source rock, represented by (S1), as well as those that the source rock will emit in the future if maturation proceeds, represented by (S2). The petroleum potential is measured in kilograms of hydrocarbons per metric ton of source rock (McCarthy *et al.*, 2011).

Table (2-3): Illustrate source rock evaluation criteria (McCarthy *et al.*, 2011).

Source rock quality	TOC (%)	Pyrolysis S2 (Mg hydrocarbons/g rock)	EOM weight (%)	Hydrocarbons (ppm)
None	< 0.5	< 2	< 0.05	< 200
Poor	0.5 – 1	2 – 3	0.05 – 0.1	200 – 500
Fair	1 – 2	3 – 5	0.1 – 0.2	500 – 800
Good	2 – 5	5 – 10	> 0.2	> 1200
Very good	> 5	> 10		

Stage	Tmax
Onset of oil	
Type I kerogen	~445 ˚C
Type II kerogen	~435 ˚C
Type III kerogen	~440 ˚C
Onset of gas	~460 ˚C

Product type	Hydrogen index
Gas	50 – 200
Gas and oil	200 – 300
Oil	> 300

c. Gas chromatography (GC)

Gas chromatography represents another screening method, this method measures the composition and concentration of light hydrocarbons (oil and gas) released from formation cuttings while drilling (Noble, 1991). Fine-grained formation cuttings, such as those produced by source rocks, can retain hydrocarbons even after reaching the surface, making them suitable samples for this type of analysis. The gas chromatography technique can be performed at the well site or in a laboratory under strictly controlled conditions (McCarthy *et al.*, 2011).

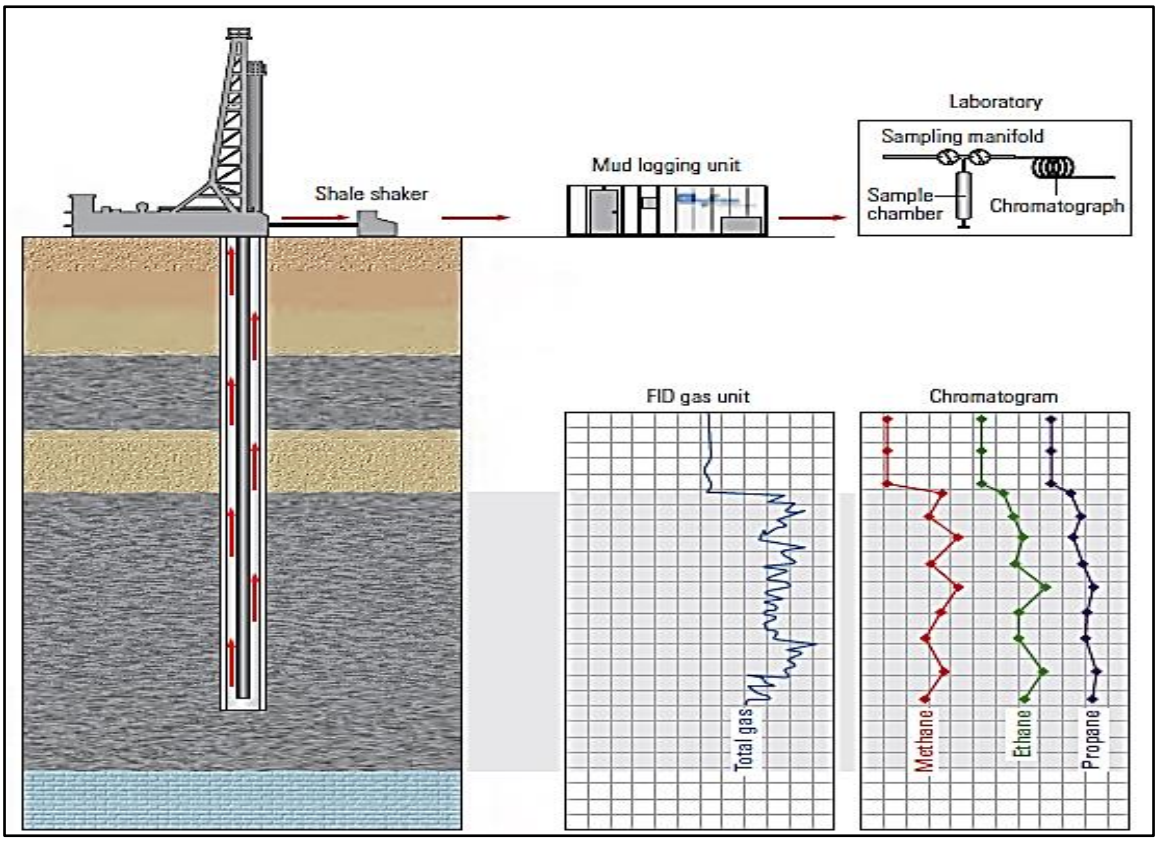

Figure (2-4): Illustrating formation cuttings analysis using gas chromatography technique. After (McCarthy *et al.*, 2011).

A gas chromatograph evaluates gas liberated during the drilling process and records individual peaks for methane (C1), ethane (C2), propane (C3), isobutene (iC4) and normal butane (nC4); a single peak is typically recorded for pentanes (iC5 and nC5) and heavier hydrocarbons (C5+). Geoscientists can evaluate the types of hydrocarbons that may be produced within a prospective reservoir by determining the composition and concentration of these gases (McCarthy *et al.*, 2011).

Gas chromatography (GC), when supplemented by mass spectrometry (MS), can provide a detailed analysis of organic compounds found in trace amounts. This technique, known as GCMS, is commonly used by geochemists to determine the masses and relative concentrations of organic compounds called biological markers or biomarkers. Biomarkers constitute molecular fossils and are synthesized only through biogenic processes (Noble, 1991).

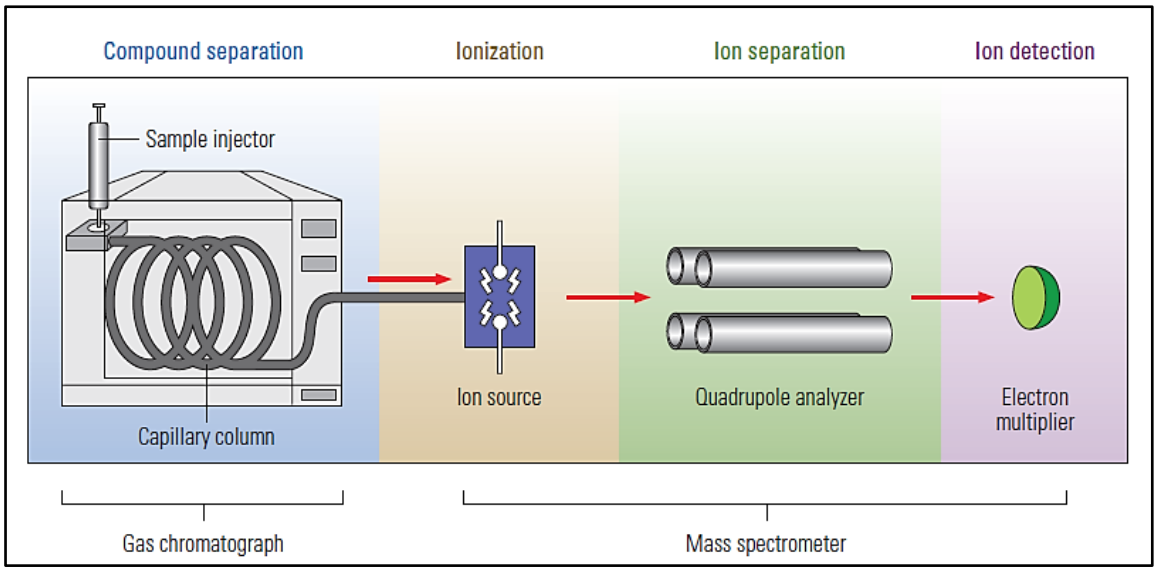

Figure (2-5): Biomarker analysis using GCMS technique. After (McCarthy *et al.*, 2011)

Their organic structures can be classified into basic groups, which, in turn, contain members having variations of the same basic structure. These groups can be related to specific organisms, and they can help geochemists in determining the environment in which an assemblage was deposited. The types of organic matter incorporated into the sediment, as well as chemical changes that occurred after deposition, are reflected in biomarker compositions. The combination of precursor molecules and their chemical reactions differs from one basin or field to another, producing a biomarker distribution that is often unique to a particular location. By comparing oil to samples of potential source rock, this chemical fingerprint can help link oil to its source. Because biomarker patterns tend to change systematically with respect to time and temperature, they can help geochemists infer maturation trends (McCarthy *et al.*, 2011). When a basin have not been encountered potential source rocks in it, this lead to indirect correlations between source rock and oil may be obtained through source-related biomarker ratios (Peters & Fowler, 2002). Geochemists use these biomarker ratios to determine the thermal maturity, depositional environment,

lithology, organic matter input, and age of source rocks. Vitrinite reflectance and spore coloration used as maturity indicators, biomarkers can also supplement these maturity indicators (Noble, 1991).

2.2.2. Source rocks evaluation

Source rock formations in the middle and south Mesopotamian Basin of Iraq are mostly Bathonian-Kimmeridgian and Tithonian – Lower Cretaceous shales and carbonate. (Pitman *et al.*, 2004; Al-Amer *et al.*, 2009; Abeed *et al.*, 2011; Al-Ameri *et al.*, 2014; Al-Khafaji, *et al.*, 2019; Al-Khafaji *et al.*, 2021). The obtained analytical data was used to assess the potential source rocks which are quantity, quality, and maturity of organic matter as well as source rock depositional environment. The analysis samples data is from the Upper Jurassic - Lower Cretaceous succession at the Gharraf oil field and adjacent Nasiriya oil field due to the great similarity in the geological situation between the two fields, where both marginal fields and their source rocks formations located at shallower depth (less maturity), compared with analysis samples data from Sulaiy Formation at the North Rumaila oil field in Basra which is basinal field at deeper depth (more maturity).

Table (2-4): Showing Rock-Eval/TOC data for the analyzed samples of the Upper Jurassic - Cretaceous source rocks formations in the Gharraf oil field Well Ga-1, Nasiriyah oil field Well NS-1, and North Rumaila oil field Well R-167 (Al-Ameri *et al.*, 2009; Abeed *et al.*, 2011; Al-Khafaji, 2015).

Well Name	Fn. Name	Depth (m)	Sample type	TOC (%)	S1 (mg HC/g)	S2 (mg HC/g)	S3 (mg CO2/g)	Tmax (°C)	Ro (%)	HI	OI	S2/S3	S1/TOC	PI
NS-1	Nahr Umr	2424	Core	1.71	0.59	4.30	0.72	426	0.51	251	42	6	35	0.12
NS-1	Nahr Umr	2436	Core	1.04	1.05	2.86	0.51	428	0.54	275	49	6	101	0.27
Ga-1	Zubair	3430	Core	1.68	0.23	1.27	0.46	428	0.54	76	27	3	14	0.15
Ga-1	Zubair	3198	Core	1.81	0.22	2.01	0.60	425	0.49	111	33	3	12	0.10
Ga-1	Zubair	3130	Core	0.65	0.25	0.75	0.29	433	0.63	115	45	3	38	0.25
NS-1	Ratawi	3093	Core	0.39	0.48	0.71	0.26	431	0.60	182	67	3	123	0.40
NS-1	Ratawi	3117	Core	0.81	2.72	1.58	1.04	432	-	195	128	2	336	0.63
NS-1	Yamama	3187	Core	0.34	0.53	0.61	0.70	433	0.63	179	206	1	156	0.46
NS-1	Yamama	3240	Core	0.18	0.15	0.46	0.10	432	0.62	256	56	5	83	0.25
NS-1	Yamama	3267	Core	1.55	3.72	8.73	0.26	427	0.53	563	17	34	240	0.30
NS-1	Yamama	3351	Core	0.16	0.26	0.39	0.28	428	0.54	244	175	1	163	0.40
NS-1	Sulaiy	3630	Core	0.71	1.22	1.33	0.64	430	0.58	187	90	2	172	0.48
NS-1	Sulaiy	3613	Core	0.66	1.66	1.86	0.48	426	0.51	282	73	4	252	0.47
NS-1	Sulaiy	3568	Core	0.29	0.59	0.68	0.46	432	0.62	234	159	1	203	0.46
NS-1	Sulaiy	3526	Core	0.39	0.72	1.48	0.29	432	0.62	379	74	5	185	0.33
NS-1	Sulaiy	3503	Core	0.21	0.48	0.55	0.33	430	0.58	262	157	2	229	0.47
R-167	Sulaiy	4487	Core	2.05	0.84	1	0.42	464	1.19	49	20	2.38	17	0.27
R-167	Sulaiy	4482	Core	5.90	1.82	4.15	0	470	1.30	70	0	-	31	0.30

2.2.2.1. Sulaiy Formation

The average of the TOC contents present in the Sulaiy Formation in the Gharraf oil field Well Ga-1 is 2.4%, (Table 4-2), and in the Nasiriyah oil field Well NS-1 is 0.71%, and is 7.33% in the North Rumaila oil field Well R-167. So, it is considered to have the potential to act as efficient petroleum source rocks.

The value of Tmax was only assessed for the samples with S2 values > 0.2 mg HC/g (Table 2-4) and vary for the Sulaiy Formation between 426°C and 432 °C in Gharraf oil field Well Ga-1 and Nasiriyah oil field Well NS-1, indicating that the formation in these fields is ranged between immature to early mature, while Tmax of Sulaiy Formation is between 464-470°C in North Rumaila oil field Well R-167 indicating late stage of maturity, Figure (2-6).

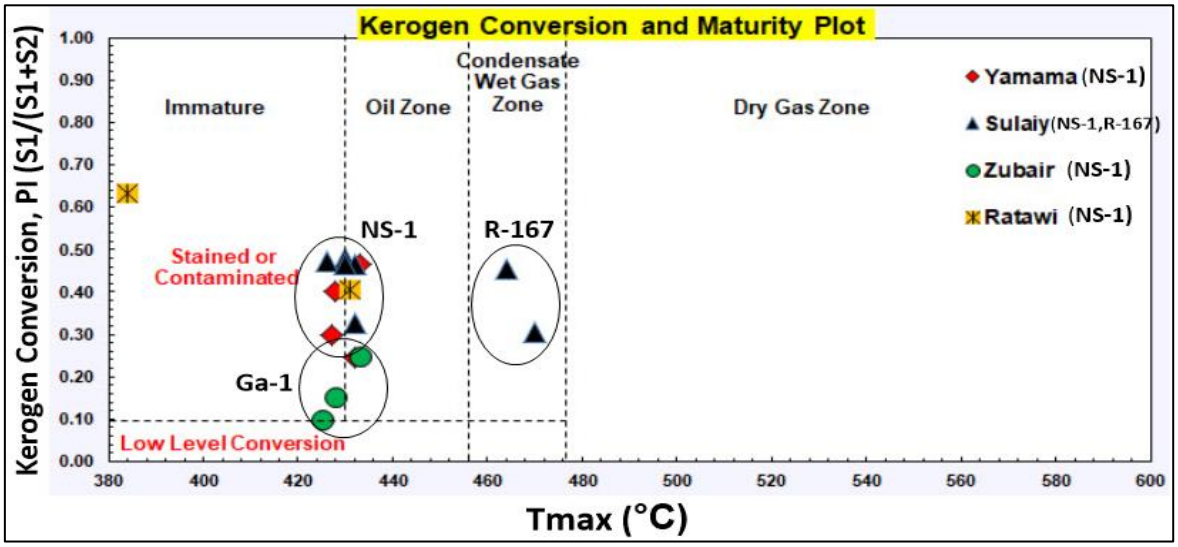

Figure (2-6): Showing the conversion and maturity of kerogen contained within the source rocks core samples from Gharraf oil field Well Ga-1, Nasiriyah oil field Well NS-1, and North Rumaila oil field Well R-167.

The PI values vary between 0.33 and 0.48 for Sulaiy Formation in the Gharraf oil field Well Ga-1 and Nasiriyah oil field Well NS-1, while PI of Sulaiy Formation is between 0.27 and 0.30 in North Rumaila oil field Well R-167. The high PI values of the formation refer to petroleum generation, (Figure 2-6).

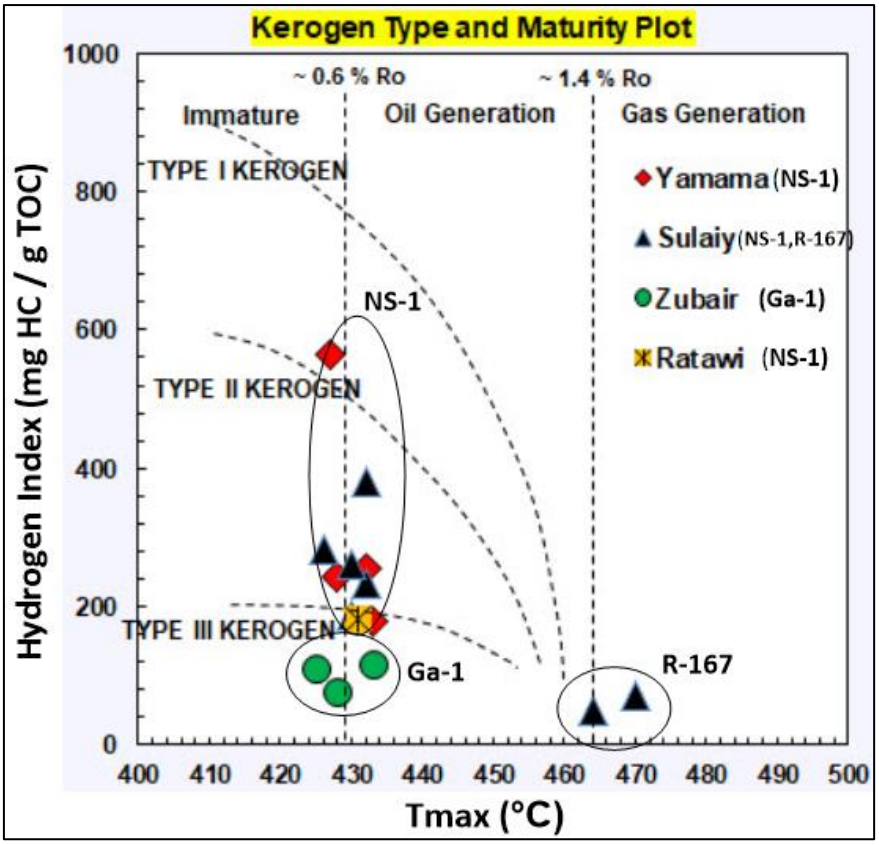

Figure (2-7): Showing the type and maturity of kerogen contained within the source rocks core samples from Gharraf oil field Well Ga-1, Nasiriyah oil field Well NS-1, and North Rumaila oil field Well R-167.

The HI values for Sulaiy Formation are moderate in the Gharraf oil field Well Ga-1 is 367.1 mg HC/g TOC, Table (4-2), and moderate - high in the Nasiriyah oil field Well NS-1 is between 187 – 379 mg HC/g TOC, Table (2-4), indicated immature to early peak oil, while in the North Rumaila oil field Well R-167, HI values of Sulaiy Formation is between 49 and 70 mg HC/g TOC (Table 2-4), indicating over-mature stage (gas generation) (Figure 2-7). The kerogen type of Sulaiy Formation in both Gharraf and Nasiriyah oil fields can be classified as Type II-III, and Type II-S kerogen (Figure 2-8; Table 2.4) indicated a high petroleum generation potential.

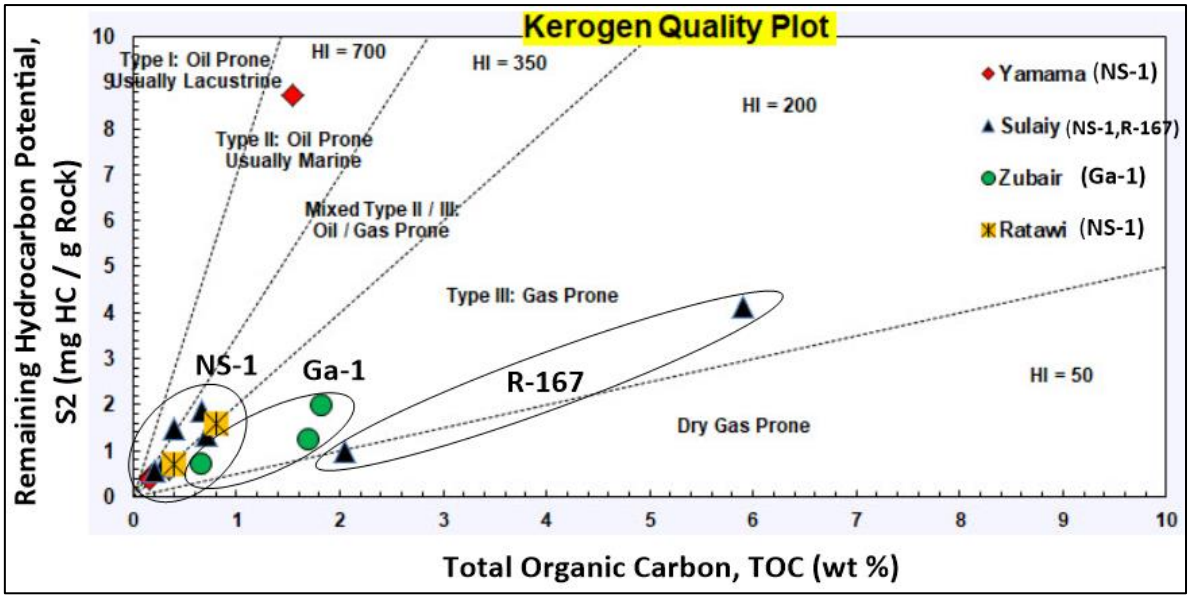

Figure (2-8): Showing the quality of kerogen contained within the source rocks core samples from Gharraf oil field Well Ga-1, Nasiriyah oil field Well NS-1, and North Rumaila oil field Well R-167.

2.2.2.2. Yamama Formation

The TOC content value for the Yamama Formation is 1.1 % in the Gharraf oil field Well Ga-1 (Table 4-2), between 0.16-1.55 % in Nasiriyah oil field Well NS-1 (Table 2-4), and between 2.05-5.90% in North Rumaila oil field Well R-167, it is considered to have the potential to act as good petroleum source rocks. Tmax values of the Yamama Formation in Gharraf oil field Well Ga-1and Nasiriyah oil field Well NS-1 are between 427°C and 433°C (Table 2-4), which indicate immature to early peak oil generation. The PI values are range from 0.25 to 0.46 in the Gharraf oil field Well Ga-1 and Nasiriyah oil field Well NS-1 oil fields, (Figure 2-6). The values over 0.4 may indicate re-migrated hydrocarbons. The S2 values of the Yamama Formation in both Gharraf oil field Well Ga-1 and Nasiriyah oil field Well NS-1 are between 0.39 – 8.73 mg HC/g. HI is 434.5 mg HC/g TOC in the Gharraf oil field Well Ga-1 (Table 4-2), and between 179-563 mg HC/g TOC in the Nasiriyah oil field Well NS-1(Table 2-4) (Figure 2-7). The kerogen type therefore is Type II of Yamama source

rocks in both Gharraf Well Ga-1 and Nasiriyah Well NS-1 oil fields, which is considered to be high hydrocarbon generating potential (oil-prone mainly), (Figure 2-8), while in North Rumaila oil field Well R-167 the Yamama source rocks contain kerogen Type III which is mainly gas-prone organic matter, (Figure 2-8).

2.2.2.3. Ratawi Formation

The TOC value of the Ratawi Formation samples in Gharraf oil field Well Ga-1 is 0.6%, (Table 4-2), and between 0.39-0.81% in Nasiriyah oil field Well NS-1, (Table 2-4). The T*max* values were between 431°C and 432°C of the formation in both oil fields, indicated immature to early peak oil generation. PI values range from 0.40-0.63, indicating migrated oil. Kerogen type is Type III which is mainly gas-prone organic matter.

2.2.2.4. Zubair Formation

The TOC values of the Zubair Formation samples in Gharraf oil field Well Ga-1 are between 0.65-1.81%, (Table 2-4). T*max* values were between 425°C and 433°C, indicated immature to early peak oil generation. PI values range from 0.10 to 0.25 in Gharraf oil field Well Ga-1, indicating non-migrated oil. The kerogen type in the formation source rocks is Type III which is mainly gas-prone organic matter, (Table 2-4; Figures 2-6, 2-7 and 2-8).

2.2.2.5. Discussion

The two Cretaceous Zubair and Ratawi source rocks in both Gharraf oil field Well Ga-1 and Nasiriyah oil field Well NS-1 are considered as poor to fair hydrocarbon generating potential source rocks. They were immature to early mature Type/III kerogen and may be contributing to petroleum generation. The Sulaiy and Yamama formations source rocks, in both Gharraf oil field Well Ga-1 and Nasiriyah oil field Well NS-1, have fair to good hydrocarbon generating potential, immature to early peak oil generation, and have Type II kerogen

which is mainly oil-prone organic matter, while the Sulaiy Formation source rocks in North Rumaila oil field Well R-167 have excellent hydrocarbon generating potential, they were at over-mature stage mainly gas generation stage due to its high TOC and Tmax values in this oil field, (Figures 2-7 and 2-8). The Sulaiy Formation due to moderate to high TOC contents value and moderate to high HI indicated that the formation was released some to most of its petroleum generation potential in the Gharraf Well Ga-1, Nasiriyah Well NS-1, and North Rumaila Well R-167 oil fields.

2.2.3. Seal rocks

The seal rocks in the petroleum system of Gharraf oil field are considered as intraformational seals, where argillaceous limestones of the Upper Member of the Ratawi Formation seal underlying Yamama Formation reservoir and seal lower reservoir part of Ratawi Formation as well. Shale units within the Zubair Formation are considered as internal seals for the Zubair reservoir. There are tight and/or muddy layers within the Mishrif Formation may locally act as intraformational seals, also the shales overlying the lower main unit of Mishrif Formation may act as seals for Mishrif reservoir.

2.2.4.Overburden rock

The overburden rock is a sequence of sedimentary rocks that covers source rock, reservoir rock, and seal rock, where it is considered as an important part of the petroleum system. The hydrocarbons produced by the thermal degradation of organic matter in source rocks depend on the thickness of the overburden and the physical properties and processes that determine the temperature of the sedimentary basin (Magoon & Dow, 1991). Overburden Rocks of the Gharraf oil field represented by the stratigraphic sequence from upper Cretaceous formations to the end of Cenozoic.

Chapter Three

Reservoirs

3.1. Preface

One of the seven essentials elements for a commercial accumulation of hydrocarbons is the existence of a reservoir. Any rock, theoretically, could act as an oil or gas reservoir. In practice, the major known reserves are found in sandstones and carbonates, although fields can also be found in shales and a variety of igneous and metamorphic rocks. In order to a rock working as a reservoir, it must have these two essential characteristics: It must have pores (porosity) to contain the hydrocarbons (oil or gas) within it. And, the pores must be connected to allow the movement of fluids; in other words, the rock must have permeability (Selley, 1998).

Cretaceous reservoir rocks are abundant, especially in S Iraq. However, four reservoir units contain most of the oil of the region; the Yamama, Zubair, Nahr Umr and Mishrif. Other formations are locally important and include the: Sulaiy, Ratawi, Shu'aiba, Mauddud, Rumaila, Khasib-Tanuma-Sa'di, Hartha and Tayarat (Jassim & Goff, 2006).

In the Gharraf oil field, the major field reservoirs which involve the largest quantity of oil accumulations are the Mishrif and Yamama formations, while the minor reservoirs of the oil field which involve less quantity of oil accumulations are Ratawi and Zubair formations.

This work focused on studying the two main reservoirs, Mishrif and Yamama, due to the availability of data needed to study them, where we have studied below the petrophysical properties of these two reservoirs, depending on the well logs data available to them, and to study this, we must address the basic principles of a topic of well logs and of the petrophysical properties of reservoirs and how computing it. This is followed by the building of the three-dimensional models using Petrel software for the petrophysical properties inferred from the well logs of the studied reservoirs using the IP software to clarify and understand the nature of these reservoirs.

There are many 3D models, well logs plots, petrophysical properties plots, cross plots, and CPI plots related to the reservoir evaluation of both Yamama Formation and Mishrif Formation for the rest of the wells studied it has been removed from this chapter and compiled in Appendix (A) in the end of this thesis, it is necessary to review it in order to reach a full understanding of the subject.

3.2. Basic Principles of Well Logs

Below is a brief explanation of the basic principle of used well logs.

3.2.1. Borehole environment

When a hole is drilled into a formation, the rock and fluids (rock-fluid system) in the area around the borehole are changed. The drilling mud contaminates the borehole of the well and the adjacent rock, affecting logging measurement (Gibson, 1982). Adjacent to the borehole, most of the original formation water and hydrocarbons, if present, may be flushed away by filtration, this zone is known as flushed zone (of resistivity R_{xo}). Farther from the borehole, the displacement of the formation fluids is gradually less complete resulting in a transition zone between mud filtrate and original formation fluid saturation, this zone is known as transition or invaded zone (of resistivity R_{xo}). Then comes the part of the formation where the pores are uncontaminated by mud filtrate; instead, they are saturated with formation fluids (water, oil and/or gas). This zone is known as uninvaded zone (of resistivity R_t) see Figure (3-1). The extent of flushed zone is referred to as diameter of invasion (D_i) (Halliburton, 2001). The diameter of invasion, which is measured in inches depends on many factors (Gibson, 1982):

1- The nature of drilling mud.
2- The formation porosity and permeability.
3- The pressure differential between mud column and the formation.
4- The time since the formation was first drilled.

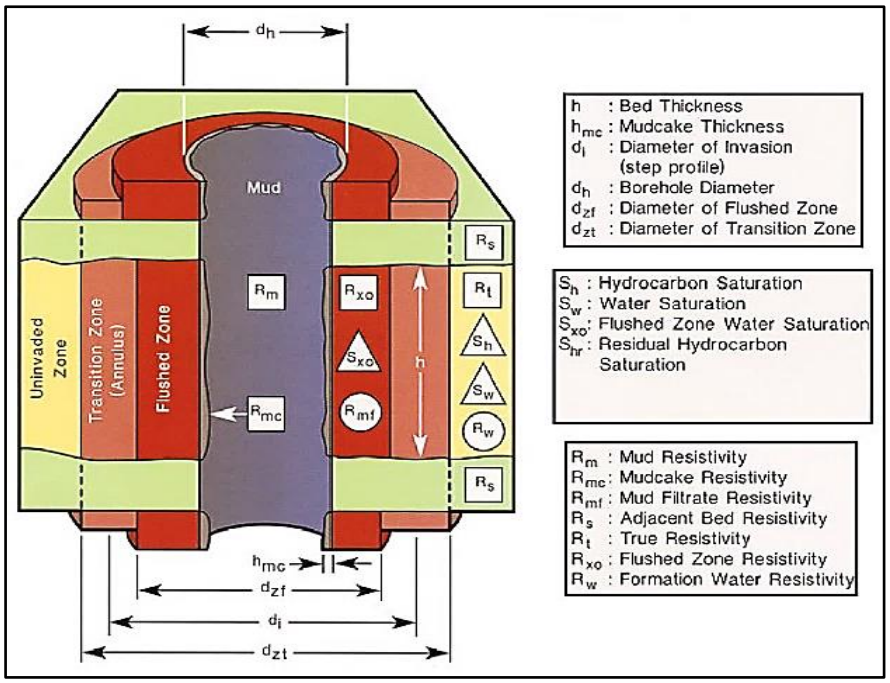

Figure (3-1): Showing the borehole environment (Halliburton, 2001).

3.2.2. Resistivity logs

Resistivity logs are electric logs which are used to determine:

a. Determine hydrocarbon-bearing versus water-bearing zones.

b. Indicate permeable zones.

c. Determine porosity.

The determination of hydrocarbon- and water-bearing zones is usually one of the most relevant uses of resistivity logs. Since the material or grains of the rock are nonconductive, as are any hydrocarbons in the pores, the rock's ability to transfer a current is almost completely dependent on water in the pores. The resistivity of a formation increases while the hydrocarbon saturation of the pores increases (and the water concentration decreases at the same time). The resistivity of the rock increases while the salinity of the water in the pores decreases (and Rw increases at the same time) (Asquith & Krygowski, 2004).

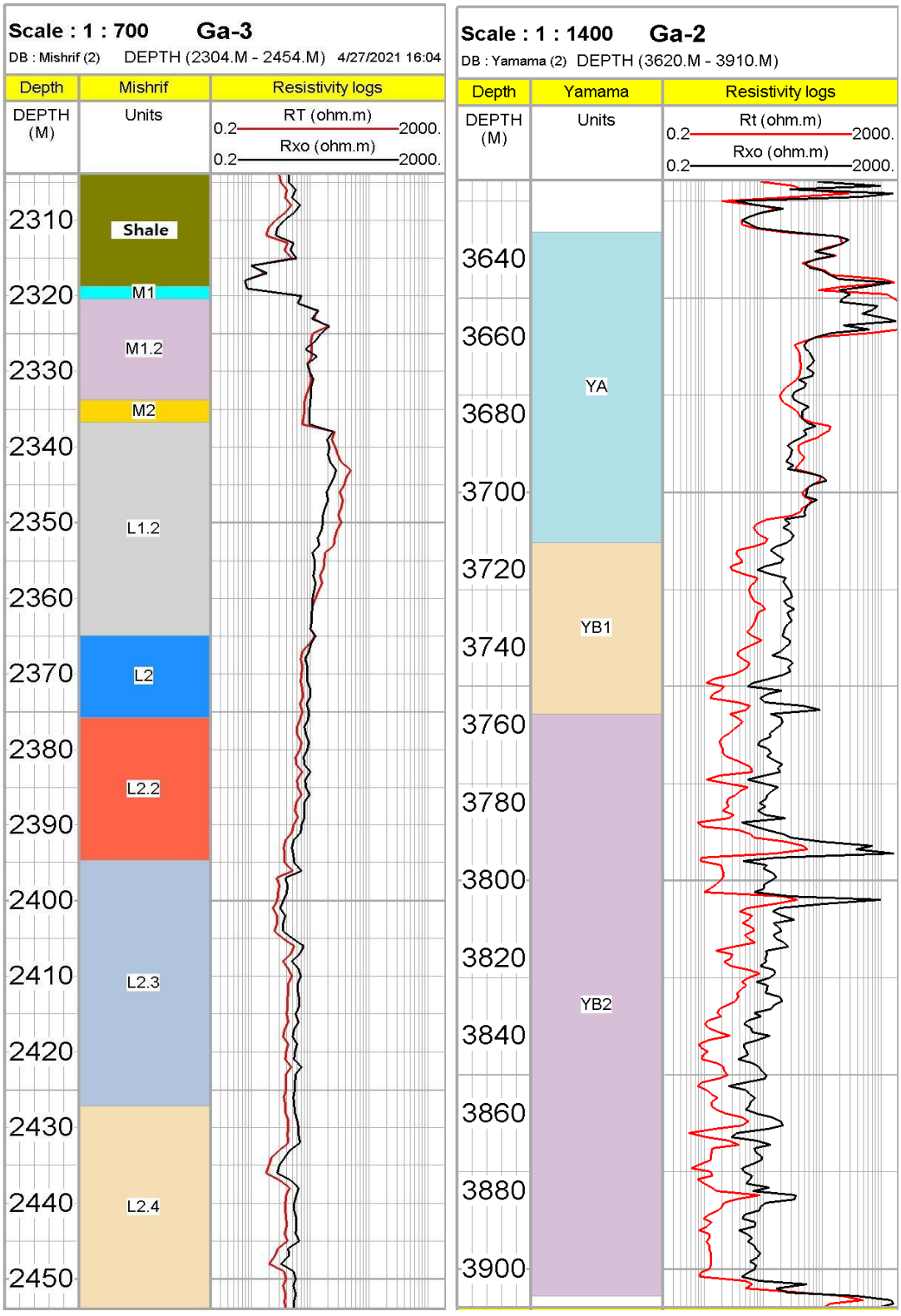

Figure (3-2): Resistivity log plots of Well Ga-2 of Yamama Formation and Well Ga-3 of the lower main unit of Mishrif Formation in Gharraf oil field.

3.2.3. Gamma ray and caliper logs

Gamma ray logs, abbreviated as GR, are used to quantify natural radioactivity in drilled formations as well as to distinguish lithology of studied formations and correlation zones. Clean lithology of sandstones and carbonates, referred to as Shale-free, give low gamma ray responses due to low concentrations of radioactive material. When shale content increase in a formation, the response of gamma ray log increases because of the increase in the concentration of radioactive materials in shale (Asquith & Krygowski, 2004). Since the gamma ray log is influenced by the diameter of the borehole, it is usually run in conjunction with a caliper log, a mechanical instrument that tracks the diameter of the borehole. The caliper log indicates where the hole could have been locally widened by washing out or caving, causing the gamma ray and other log responses to deviate from the intended. The hole can also be narrower than the gauge of the bit where bridging happens. Bridging is caused by either sloughing of the hole's slide and the initiation of collapse, or by an accumulation of mud cake opposite permeable zones (Selley, 1998). In this study, the gamma-ray logs were used in determining the lithology of the studied rock formations represented in the Mishrif and Yamama formations, in calculating the volume of shale in these formations, as well as used in the correlation between the wells studied.

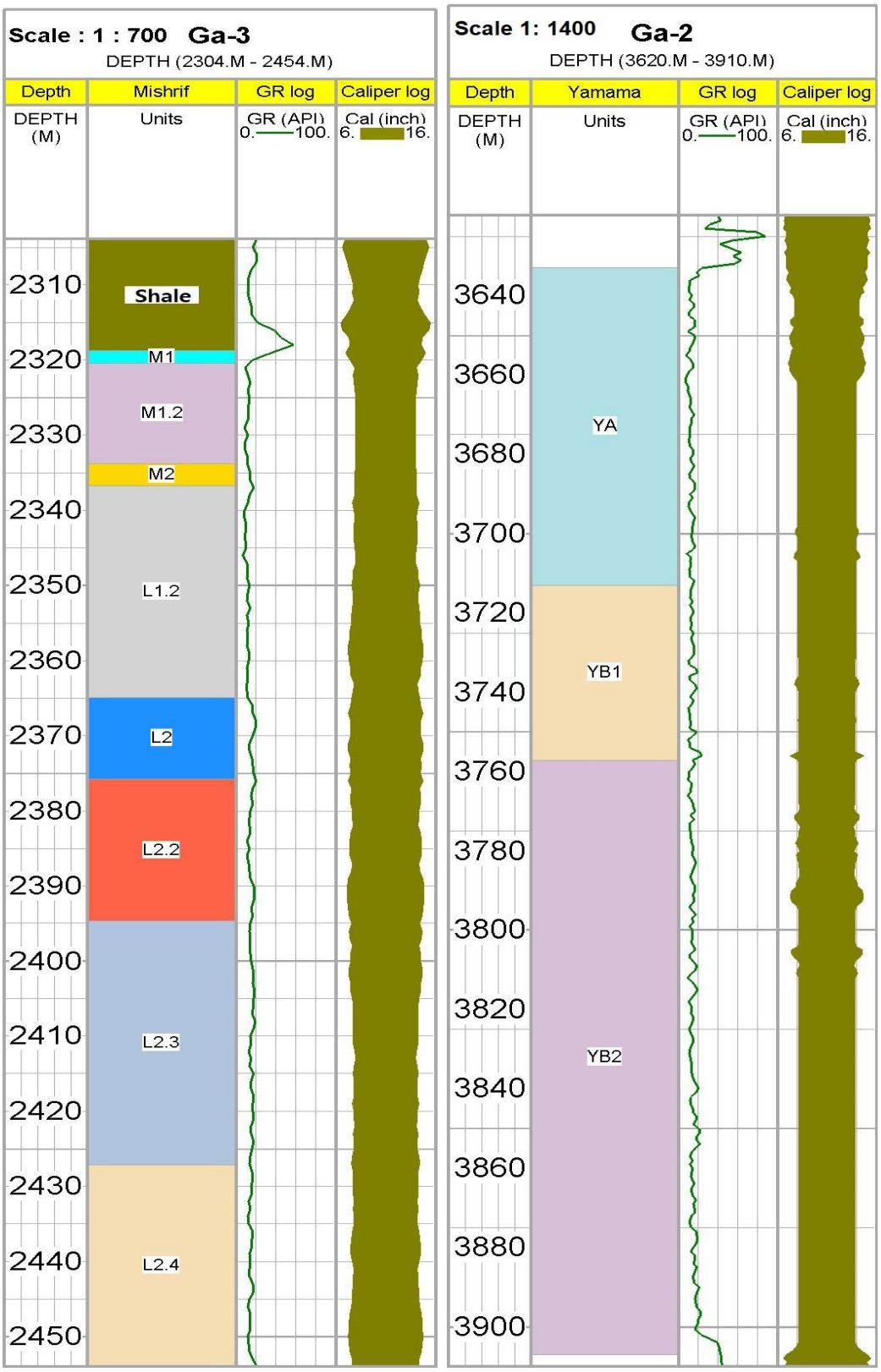

Figure (3-3): Caliper and GammaRay log plots of Well Ga-2 of Yamama Formation and Well Ga-3 of the lower main unit of Mishrif Formation in Gharraf oil field.

3.2.4. Spontaneous potential log (SP)

The Spontaneous Potential (SP) log was one of the first electric logs used in the petroleum industry and has played an important role in well log analysis since then. This kind of log is used in the log suit of the vast majority of wells today. The Spontaneous Potential log is primarily used to distinguish impermeable zones such as shale and permeable zones such as sand. It is expressed in millivolts (Gibson, 1982). The SP log is a record of direct current (DC) voltage (or potential) that develops naturally (or spontaneously) between a moveable electrode in the well bore and a fixed electrode located at the surface (Asquith & Krygowski, 2004). The SP log behavior depends primarily on difference in salinity between drilling mud and the formation water (Selley, 1998).

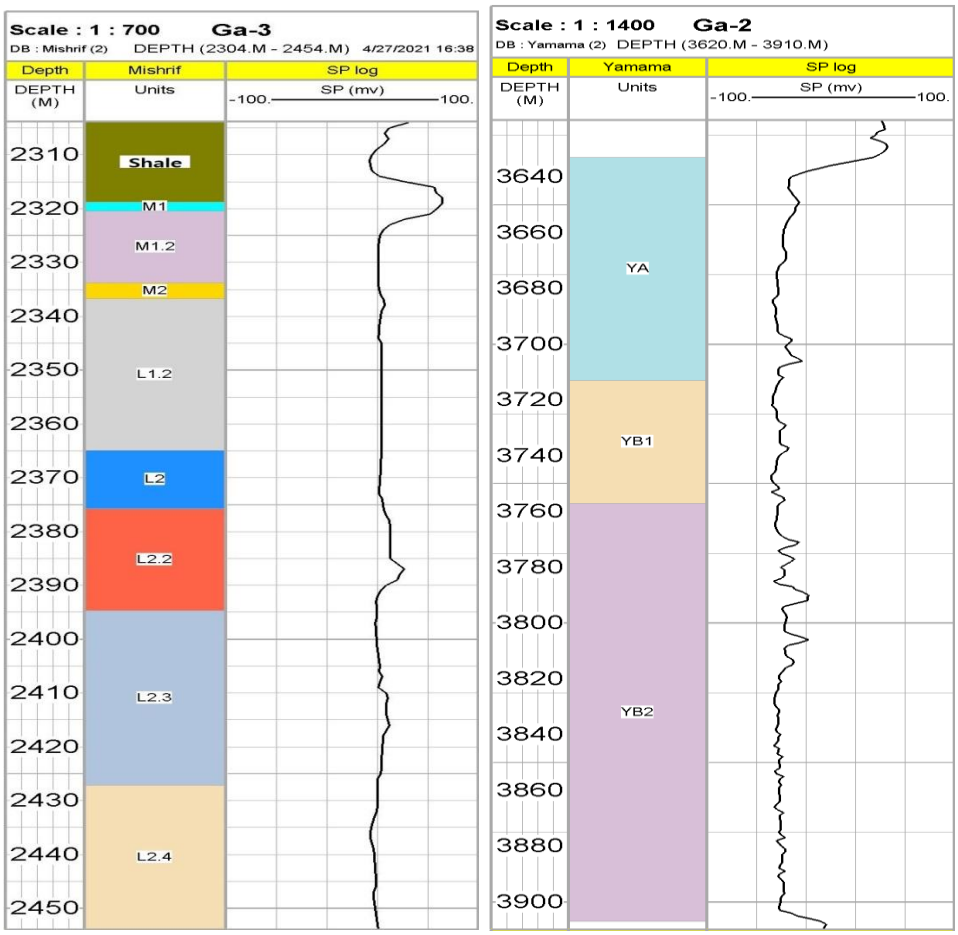

Figure (3-4): SP log plots of Well Ga-2 of Yamama Formation and Well Ga-3 of the lower main unit of Mishrif Formation in Gharraf oil field.

3.2.5. Porosity logs

Porosity may be measured in three ways; directly from cores, indirectly from geophysical well logs or from seismic data (Selley, 1998). Porosity was measured in this study from three types of logs, these logs are Density, Neutron and Sonic logs.

a. Density log

The density log measures formation density by emitting gamma radiation from the tool and recording the amount of gamma radiation returning from the formation. For this reason the device is often called the gamma-gamma tool (Selley, 1998). The Greek letter (ρ) represents density, which is expressed in grams per cubic centimeter, or g/cm3. The density log includes two separate density values: RHOB (bulk density) and matrix density formation (solid and fluid parts) as determined by the logging device. The matrix density refers to the density of the rock's solid framework (Asquith & Krygowski, 2004). The gamma radiation reading can be related to the electron density of the formation. Bulk density of a rock is a function of lithology and porosity. Mud filtrate is usually the fluid contained in the pores around the borehole of well. This value for porosity is read because the tool only has a limited depth of investigation and essentially only investigates the region of the formation invaded by filtrate from the drilling mud. Thus the density of the fluid may vary from 1.0 g/cm³ for fresh water mud to 1.1 g/cm³ for salty mud. Shale also affects the accuracy of the density- derived porosity of reservoir .Also several minerals have anomalous densities. The presence of oil has little effect on porosity values, but gas lowers the density of a rock and thus causes the log to give too high a porosity (Selley, 1998). The formation density log is useful as a porosity-logging tool. Other uses of density measurements include identification of minerals in evaporate deposits, detection of gas determination of hydrocarbon density, evaluation of shaly sands and complex lithologies and determination of

oil shale yield (Schlumberger, 1972). Porosity is derived from the bulk density of clean liquid-filled formations when the matrix density (*ρma*) and the density of the saturating fluids (*ρf*) are known (Asquith & Krygowski, 2004):

$$\emptyset_D = \frac{\rho ma - \rho b}{\rho ma - \rho f} \quad \text{..... (3-1)}$$

Where:

- $\emptyset_D$: Porosity by density log.
- ρma : Density of the dry rock (gm/cm^3), see Table (3-1).
- ρf : Density of fluid (gm/cm^3) = 1 gm/cm^3 for fresh water or 1.1 gm/cm^3 for salt mud.

Table (3-1): Matrix densities values of common lithologies. Modified after (Asquith & Krygowski, 2004)

Lithology / Fluid	ρma or ρf gm/cm3 (kg/m3)
Sandstone	2.644 (2644)
Limestone	2.710 (2710)
Dolomite	2.877 (2877)
Anhydrite	2.960 (2960)
Salt	2.040 (2040)
Fresh water	1.0 (1000)
Salt water	1.15 (1150)

b. Neutron log

The hydrogen amount in a formation is estimated using neutron logs, which are porosity logs. The neutron log, (NPHI), computes liquid fluid porosity in clean formations (no shale) where the porosity is filled with oil or water (Asquith & Krygowski, 2004). Neutron logs are used principally for delineation of porous formation and determination of their porosity. They respond primarily to the amount of hydrogen present in the formation (Schlumberger, 1972). The neutron log was recorded in API units. Because shale always contains some bonded water, the neutron log will always give a higher apparent porosity reading in dirty reservoirs than actually exists. The

hydrogen content of oil and water is about equal, but is lower than that of hydrocarbon gas. Thus the neutron log may give a porosity reading in gas reservoirs (Selley, 1998). Figure (3-5) shows the correlation among porosity logs (Sonic, Density and Neutron logs) of the studied wells of Mishrif and Yamama formations in Gharraf oil field.

c. Sonic log

The sonic log is a porosity log that calculates the interval of transit time (Δt) of a compressional acoustic waves as it travels across the formation along the borehole's axis. The unit of sonic log contains one or more transmitters of ultrasonic waves and two or more receivers (Gibson, 1982). The percentage of vuggy or fracture secondary porosity can be calculated by subtracting sonic porosity from total porosity. Total porosity values are obtained from one of the nuclear logs (density, neutron, or preferably the combination of density and neutron) (Asquith & Krygowski, 2004). In this study, the sonic logs used to make correlation between studied wells and in the determination of lithology, as well as in calculating the amount of porosity of the studied formations (Mishrif and Yamama). The response of sonic log of Mishrif and Yamama formations in the studied wells is shown in Figure (3-5). Sonic log (Δt) based on Wyllie time-average equation was used to determine primary porosity (Wyllie *et al.*, 1958):

$$\emptyset S = \frac{\Delta tlog - \Delta tma}{\Delta tfl - \Delta tma} \quad \text{..... (3-2)}$$

Where:

- $\emptyset S$: Sonic derived porosity.
- $\Delta tlog$: Interval transit time in the formation.
- Δtma : Interval transit time in the matrix.
- Δtfl : Interval transit time in the fluid in the formation.

Table (3-2): Interval transit times and sonic velocities for various matrixes (Asquith & Krygowski, 2004)

Lithology/Fluid	Matrix Velocity ft/sec	ΔtMatrix or ΔtFluid(Wyllie) μsec/ft (μsec/m)	ΔtMatrix (RHG) μsec/ft (μsec/m)
Sandstone	18000 - 19500	55.5-51 (182-186)	56 (184)
Limestone	21000 - 23000	47.6 (156)	49 (161)
Dolomite	23000 - 26000	43.5 (143)	44 (144)
Anhydrite	20000	50 (164)	
Salt	15000	66.7 (219)	
Casing (iron)	17500	57 (187)	
Freshwater mud filtrate	5280	189 (620)	
Saltwater mud filtrate	5980	185 (607)	

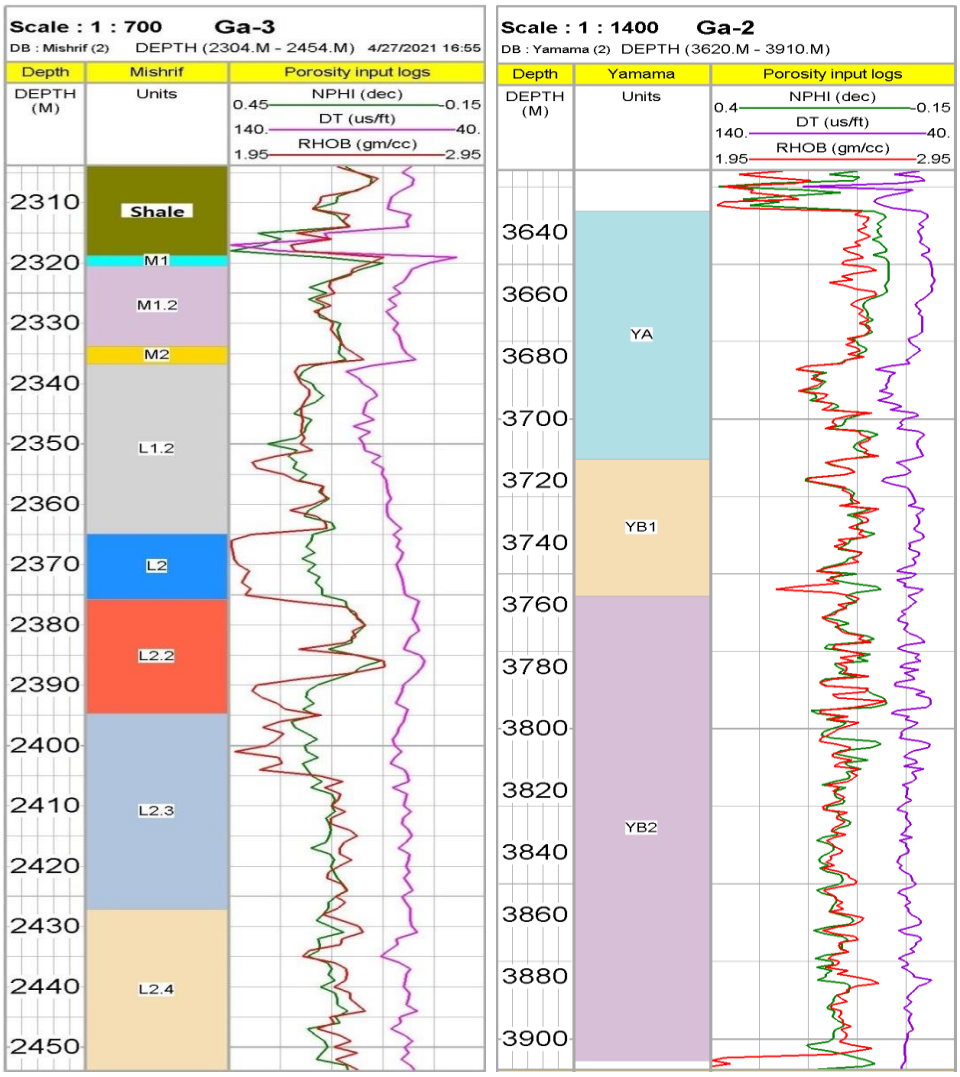

Figure (3-5): Porosity input logs plots of Well Ga-2 of Yamama Formation and Well Ga-3 of the lower main unit of Mishrif Formation in Gharraf oil field.

3.3. Petrophysical Properties Computation

Petrophysics is the study of the chemical and physical characteristics that define the behavior and presence of rocks and liquids. Logging aid describes physical characteristics of rocks for example, porosity, lithology, permeability and pore geometry. Logging data are utilized to detect pay zone to fix thickness and depth of intervals, to distinct amongst gas, oil or water in reservoir and to estimate oil reserve (Asquith & Krygowski, 2004). Petrophysical properties that are discussed in this study include:

- Lithology determination
- Shale volume computation
- Porosity
- Water saturation
- Hydrocarbon saturation
- Permeability

3.3.1. Lithology determination

The lithology and mineral composition of the Mishrif and Yamama formations were determined using four types of cross plots as mentioned in the following:

a. Neutron-density lithology cross plot:

These logs combination are used to identify lithology and porosity. The horizontal axis represents the neutron log; while the vertical axis represents density log (Jia, 2010), Figure (3-6).

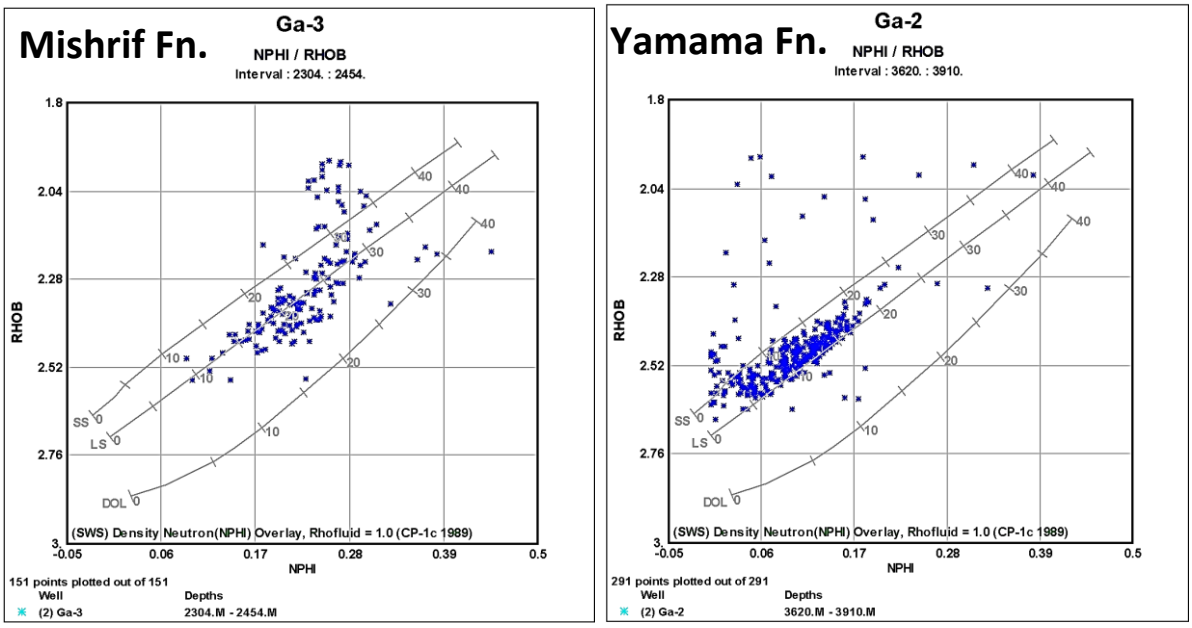

Figure (3-6): Neutron – Density cross plots of the lower main unit of Mishrif Formation in Well Ga-3 and of Yamama Formation in Well Ga-2 in Gharraf oil field.

b. Neutron - Sonic lithology cross plot:

These logs are also used for identifying lithology and porosity. The horizontal axis represents the neutron log, while the vertical axis represents the sonic log. These logs show that the main lithology of Mishrif and Yamama formations is limestone and dolomitic limestone as shown in Figure (3-7). A comparison of the two cross plots show that the neutron - sonic plot indicates a much more dolomitic lithology compared to neutron - density plot. This differ is due to the presence of vuggy porosity (Jia, 2010). The sonic log measures only matrix porosity (intergranular and intercrystalline) and the nuclear logs (neutron and density) measure total porosity (Asquith & Krygowski, 2004).

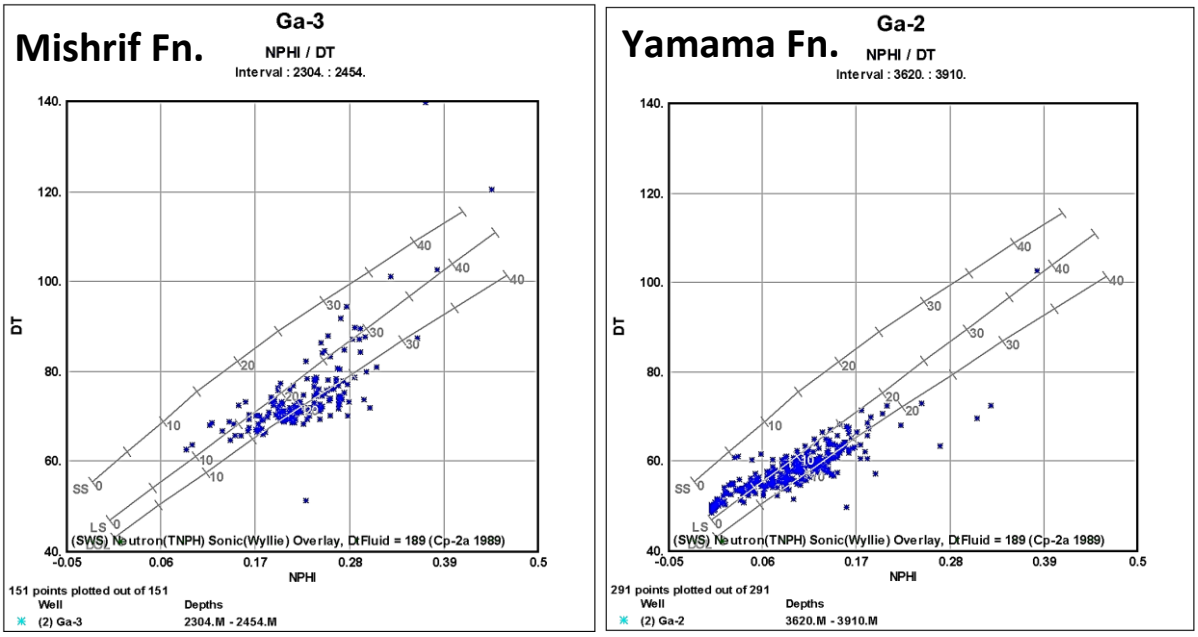

Figure (3-7): Neutron – Sonic cross plots of Well Ga-2 of Yamama Formation and Well Ga-3 of the lower main unit of Mishrif Formation in Gharraf oil field.

c. M-N Lithology cross plot:

The main goal of this cross plot is to analyze the data from all three porosity logs in order to determine the lithology-dependent quantities of M and N. The M and N variables are essentially represents the slopes of the specific lithology lines on the Sonic-Neutron and the Sonic-Density cross plot charts, therefore, these variables (M and N) are essentially independent of porosity, and then mineralogy can be identified from a cross plot of these two variables. (Gibson, 1982). M and N are defined as (Schlumberger, 2005), Figure (3-8):

$$M = \frac{\Delta tf - \Delta tlog}{\rho b - \rho f} * 0.01 \quad \text{..... (3-3)}$$

$$N = \frac{\emptyset NF - \emptyset N}{\rho b - \rho f} \quad \text{..... (3-4)}$$

Where:

- ***Δtf*** **:** interval transit time in fluid (189 m/s for fresh water and 185 m/s for salt mud).
- ***Δt*** **:** interval transit time (the log reading).
- ***ρb*** **:** formation bulk density (the log reading).
- ***ρf*** **:** fluid density (1 gm/cm^3 for fresh water or 1.1 gm/cm^3 for salt mud).
- ***ØNF*** **:** neutron porosity for fluid = 1.
- ***ØN*** **:** neutron porosity.

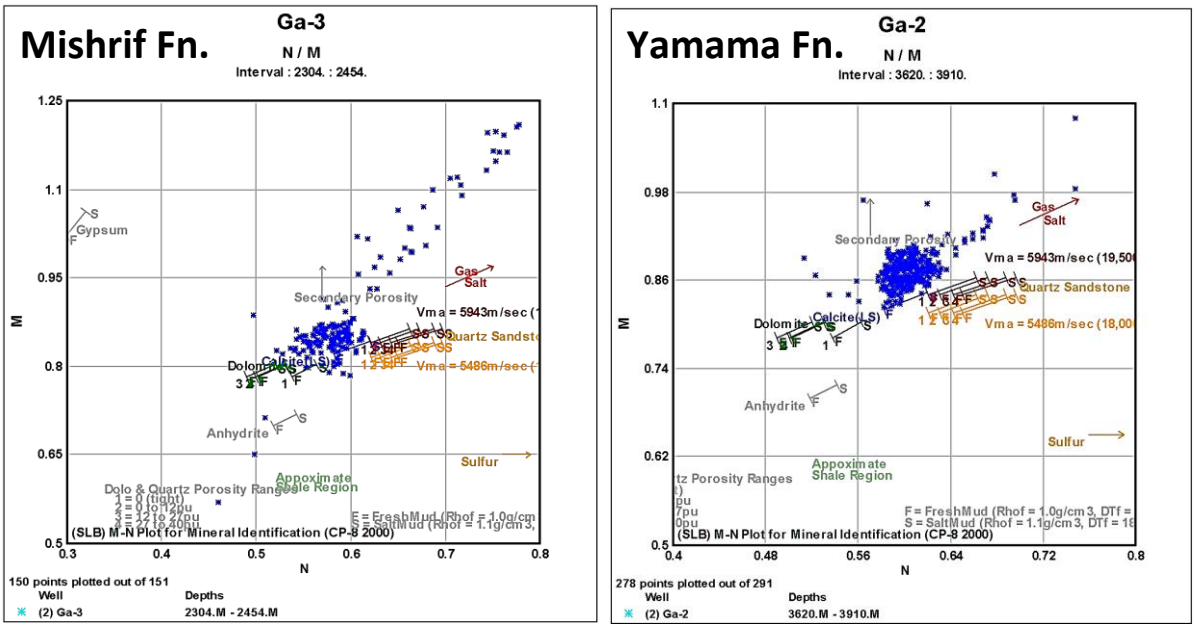

Figure (3-8): M – N cross plots of the lower main unit of Mishrif Formation in Well Ga-3 and of Yamama Formation in Well Ga-2 in Gharraf oil field.

d. Matrix identification (MID) cross plot:

Identification of lithology, gas and secondary porosity can also be obtained using the matrix identification (MID) cross plot (Schlumberger, 1991). Determination of lithology is readily accomplished by comparison of the apparent transit time in rock matrix (Δtma). To use the MID cross plot, three logs are required the sonic, neutron, and density logs. These logs are sensitive to lithology (Asquith & Krygowski, 2004). The apparent total porosity (Øta) must be determined using the derived neutron-density. The values of the apparent

density of matrix (ρmaa) and the apparent transit time (Δtmaa) are determined from the following equations according to Schlumberger (2005), Figure (3-9):

$$RHOmaa = \frac{\rho b - \emptyset ta.\rho f}{1 - \emptyset ta} \quad \text{..... (3-5)}$$

$$\Delta tmaa = \frac{\Delta tlog - \emptyset ta.\Delta tf}{1 - \emptyset ta} \quad \text{..... (3-6)}$$

Where:

- ***RHOmaa*:** apparent density of matrix (gm/cc).
- ***Δtmaa*:** apparent transit time in rock matrix (µsec/ft).
- ***Øta*:** is the apparent total porosity.

Figure (3-9) of MID cross plot shows type of matrix in Mishrif and Yamama formations in Gharraf oil field, which is represented by mainly calcite with few points falling in dolomite zone and some of them in quartz zone.

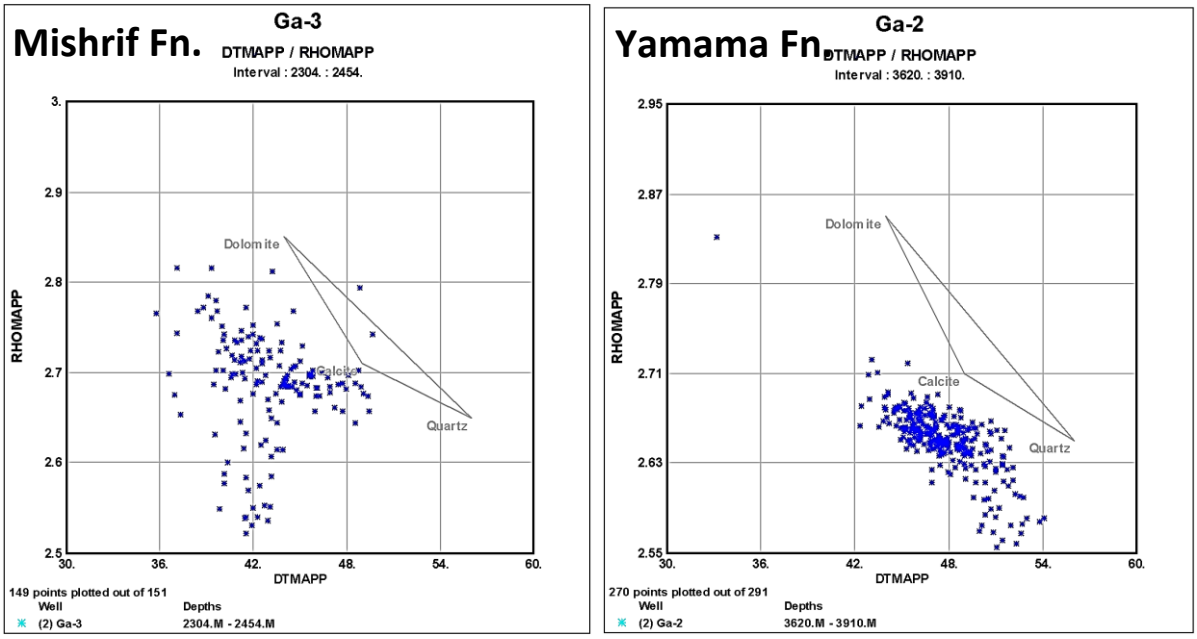

Figure (3-9): MID cross plots of lower main unit of Mishrif Formation in Well Ga-3 and of Yamama Formation in Well Ga-2 in Gharraf oil field.

3.3.2. Shale volume computation

Because clay is typically further radioactive than carbonate, GR tool will be suitable candidate to calculate the amount of clay in permeable reservoir. The shale volume is expressed as a decimal fraction or percentage is named V*shal*e. The measurement of the Gr index is the principal stage required for define the shale volume by GR log (Asquith & Krygowski, 2004):

$$I_{GR} = \frac{GRlog - GRmin}{GRmax - GRmin} \quad \text{..... (3-7)}$$

$$V_{sh} = 0.33\,(2^{(2\times I_{GR})} - 1) \quad \text{..... (3-8)}$$

Where:

- I_{GR}: is the gamma ray index.
- GR_{log}: is the gamma ray log reading in zone of interest, API units.
- GR_{min}: is the minimum gamma ray reading in clean zone, API units.
- GR_{max}: is the maximum gamma ray reading in shale zone, API units.

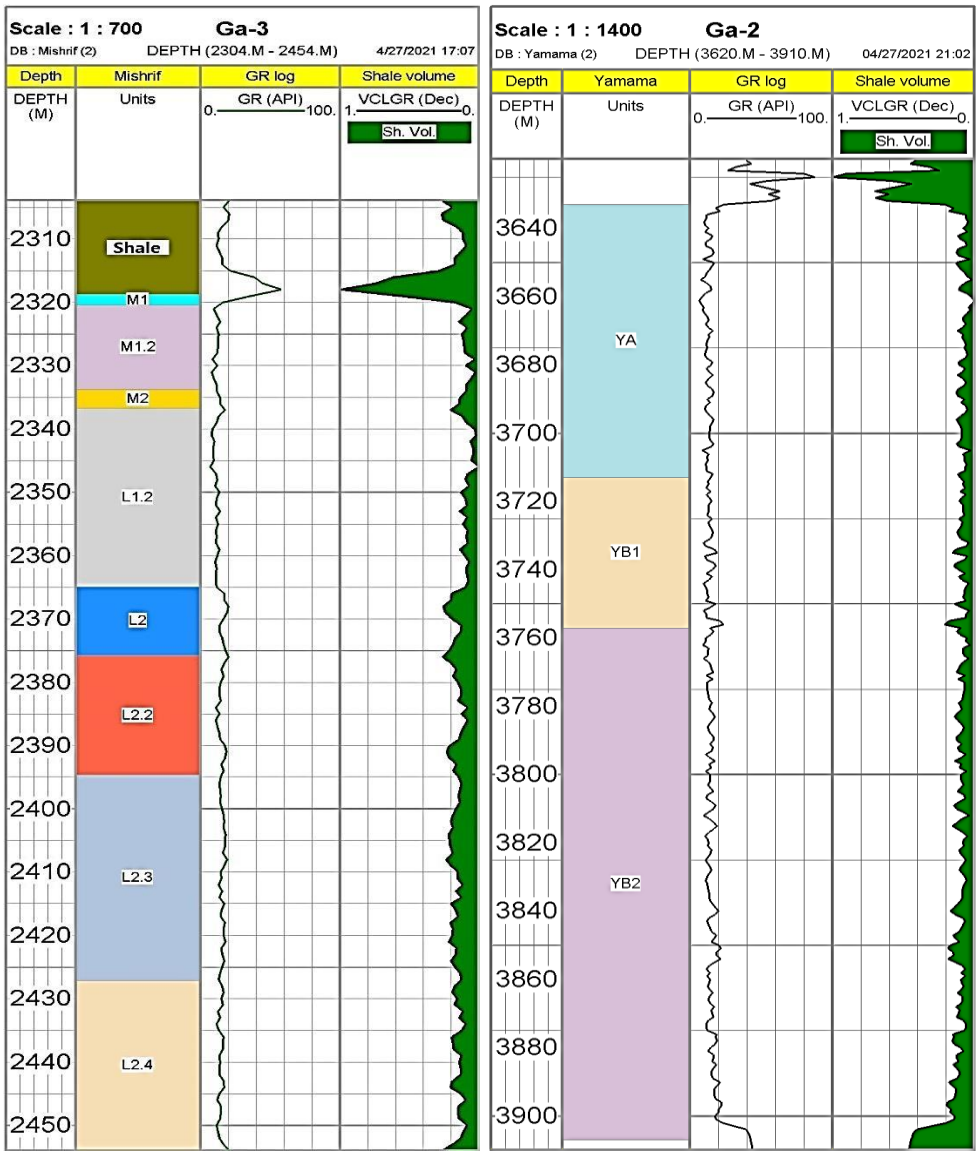

Figure (3-10): Shale volume of Well Ga-2 of Yamama Formation and Well Ga-3 of the lower main unit of Mishrif Formation in Gharraf oil field.

3.3.3. Porosity and porosity calculation

Porosity is the first of the several essential attributes of a reservoir. The pore spaces, or voids, within a rock are generally filled with connate water, but contain oil or gas within a field. Porosity is either expressed as the void ratio, which is the ratio of voids to solid rock, or, more frequently, as a percentage **(Selley, 1998)**:

$$\boldsymbol{Porosity}(\%) = \frac{\boldsymbol{volume\ of\ voids}}{\boldsymbol{total\ volume\ of\ rock}} * \mathbf{100} \quad \text{..... (3-9)}$$

Porosity is the ratio of spaces to the total volume of rock. Porosity is signified as a percentage by the Greek letter phi, Ø (Asquith & Krygowski, 2004). Porosity logs Neutron, Density, and Sonic are mainly related to porosity, and they also influenced by lithology, formation matrix, kind of porosity and degree of shaliness and kind of liquid existing in the pores (Schlumberger, 1974). The neutron –density logs provide the best combination to identify gas zones and determining their porosity. The combination also provides porosity in complex lithology and volume of shale for shaly formation evaluation. Porosity logs include sonic logs, density logs, and neutron logs. The sonic log records matrix porosity, whereas the nuclear logs (density or neutron) determine the total porosity (Asquith & Krygowski, 2004). Porosity can be determined (Al-musawi & Nasser, 2019):

a. Directly from cores, plugs, or samples in the core-laboratory.

b. Indirectly from logs nuclear and acoustic measurements, and by NMR measurements.

Porosity should be calculated from the density and sonic logs using the following equations **(Darling, 2005)**:

$$Ø_D = \frac{\rho ma - \rho b}{\rho ma - \rho f} \quad \text{..... (3-10)}$$

Where:

- ϕ_D: is the density-derived porosity, fraction.
- ρ_{ma}: is the matrix density, (whose value is 2.71 gm/cc for limestone and 2.87 gm/cc for dolomite).
- ρ_b: is the formation bulk density, gm/cc.
- ρ_f: is the fluid density (for fresh water mud = 1 gm/cc, for salt water Mud =1.1gm/cc).

$$Ø_s = \frac{\Delta tlog - \Delta tma}{\Delta tf - \Delta tma} \quad \text{..... (3-11)}$$

Where:

- ϕ_s: is sonic-derived porosity, fraction,

- Δt_{ma}: is the interval transit time in the matrix (whose value is 47.6 μsec/ft for limestone and 43.5 μsec/ft for dolomite)
- Δt_{log}: is the interval transit time in the formation, μsec/ft; and
- Δt_f : is the interval transit time in the fluid within the formation (For fresh water mud = 189 μsec/ft; for salt-water mud = 185μsec/ft)

It is necessary to distinguish between the types of porosity (Al-musawi & Nasser, 2019).

a- Total porosity (*Øt*)

Total porosity (PHIT) is described as the ratio of all pores' volume to the bulk volume of a substance, whether all pores are related or not (Bowen, 2003).

$$Øt = \frac{Ø_N + Ø_D}{2} \quad \text{..... (3-12)}$$

b- Effective porosity (*Øeff*)

Effective porosity is another essential type of porosity, it represents the ratio of the volume of only interconnected pore in a material to the total volume of reservoir rock (Bowen, 2003).

$$Øeff = Øt * (1 - Vsh) \quad \text{..... (3-13)}$$

c- Secondary porosity

Secondary porosity is another minor type of porosity, this type formed within a reservoir after deposition. Vuggy or fracture secondary porosity can be calculated by secondary porosity index (SPI) (Bowen, 2003).

$$SPI = Øt - Øsonic \quad \text{..... (3-14)}$$

Secondary porosity arises as a result of secondary geological processes represented by the diagenesis process that occurs after sediments deposition (Tiab & Donaldson, 2004). The secondary porosity involves vugular spaces found in carbonate rocks that was formed due to the leaching, or fracture openings that was formed in fractured reservoirs (Ezekwe, 2010). The intervals of higher secondary porosity mean existence the effect of digenesis processes on

the porosity of Mishrif Formation such as dolomatization and dissolution (Al-musawi & Nasser, 2019).

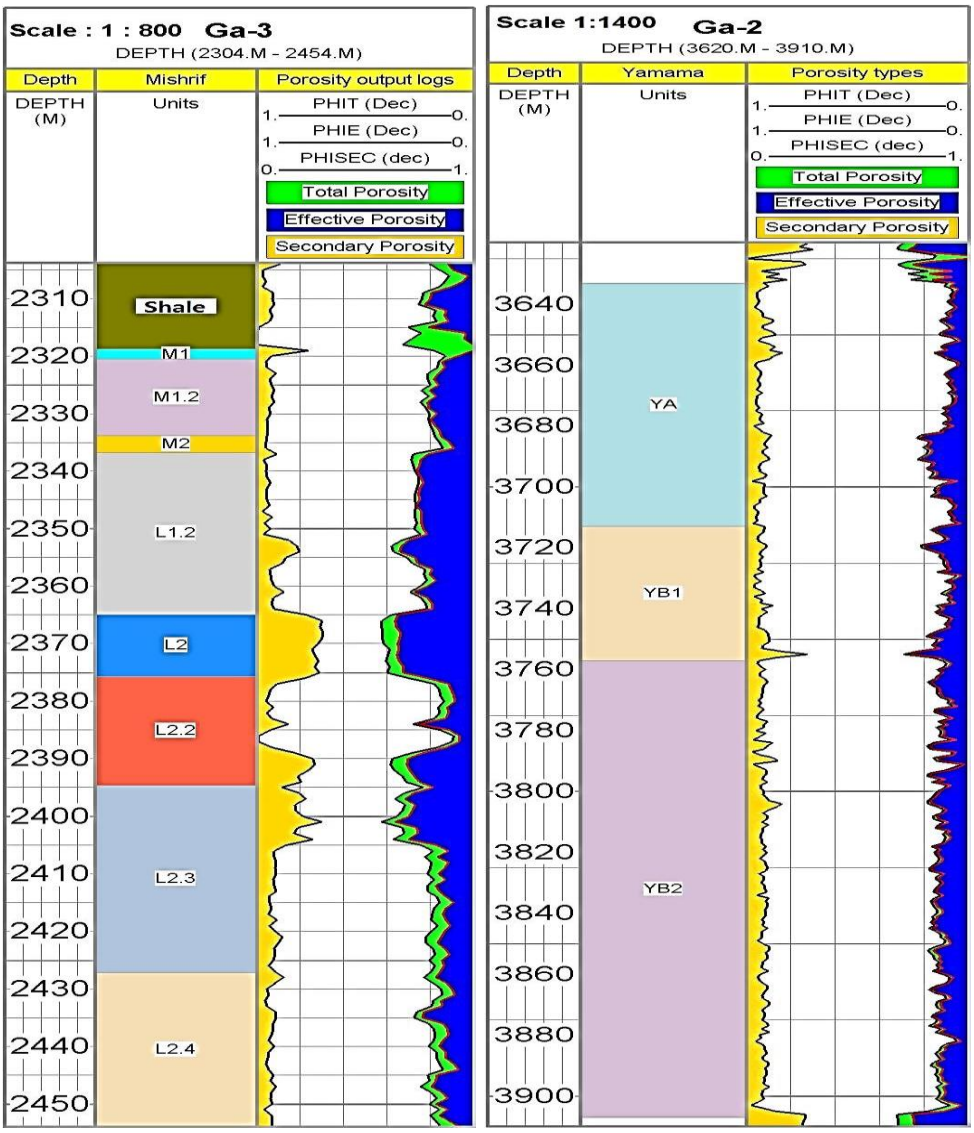

Figure (3-11): Porosity types log plots of Well Ga-2 of Yamama Formation and Well Ga-3 of the lower main unit of Mishrif Formation in Gharraf oil field.

3.3.4. Water saturation calculation

It's the measure of pore volume in a rock that is engaged by formation water, it is signified as decimal portion or as percentage and has the symbol (Sw) (Asquith & Krygowski, 2004). Water saturation is very important petrophysical parameters in exploration and production of petroleum. The evaluation of water saturation (Sw) is still difficult regarding well logging

interpretation, especially for organic-rich shale reservoirs featuring low porosity and permeability. (Archie, 1942) was the first to propose a water saturation model for clean sand formation that considering porosity and resistivity. The Simandoux model which was created by (Simandoux, 1963), modified Simandoux model which was created by (Fertl and Hammack, 1971), total shale model which was created by (Schlumberger, 1972), Indonesian model which was created by (Poupon and Leveaux, 1971), and model of dual water that created by (Bassiouni, 1994). These different types of models represent the most important models of water saturation for non-clean or shale-bearing sandstone reservoirs according to traditional logging data. For non-clean or shale-bearing as well as heterogeneous formations, the formula of Archie does not work well. In the measurement of water saturation, Simandoux took into consideration another conductivity source emerging from clay, as seen in Equation (3-15) (Zhang & Xu, 2016):

$$C_t = Sw^n * \frac{Cw}{F+X} \quad \text{..... (3-15)}$$

Where:

- $\mathbf{C_t}$: total conductivity
- **F** : formation factor
- $\mathbf{C_w}$: conductivity of the formation water
- $\mathbf{S_w}$: water saturation
- **X** : additional conductivity of clay

The Indonesian equation was developed by Poupon and Leveaux (1971) to account for the high amount of shale and fresh water formations contained in Indonesia reservoirs. The equation was developed by using computer-made cross-plots to determine the relationship between the value of water saturation and the value of the true resistivity of the formation (Marcus *et al.*, 2018).

$$\frac{1}{\sqrt{R_t}} = \left[\frac{(Vclay)^d}{\sqrt{Rclay}} + \frac{(\emptyset)^{m'2}}{\sqrt{aRw}}\right] * Sw^{n'2} \quad \text{..... (3-16)}$$

Where:

- ***Vcaly***: is volume of shale
- ***Rt*****:** formation true resistivity
- ***Rw*****:** formation water resistivity
- ***a*****:** tortuosity
- ***Ø*****:** porosity
- ***Sw*****:** water saturation
- $d = 1 - \frac{Vsh}{2}$

Mishirif and Yamama formations in Gharraf oil field are non-clean carbonate formations with variable quantities of shale within the different units of the studied formations. Therefore, Archie's model does not work fine in interpretation of water saturation. Simandoux and Indonesian models used in this study in calculation of water saturation to the studied formations.

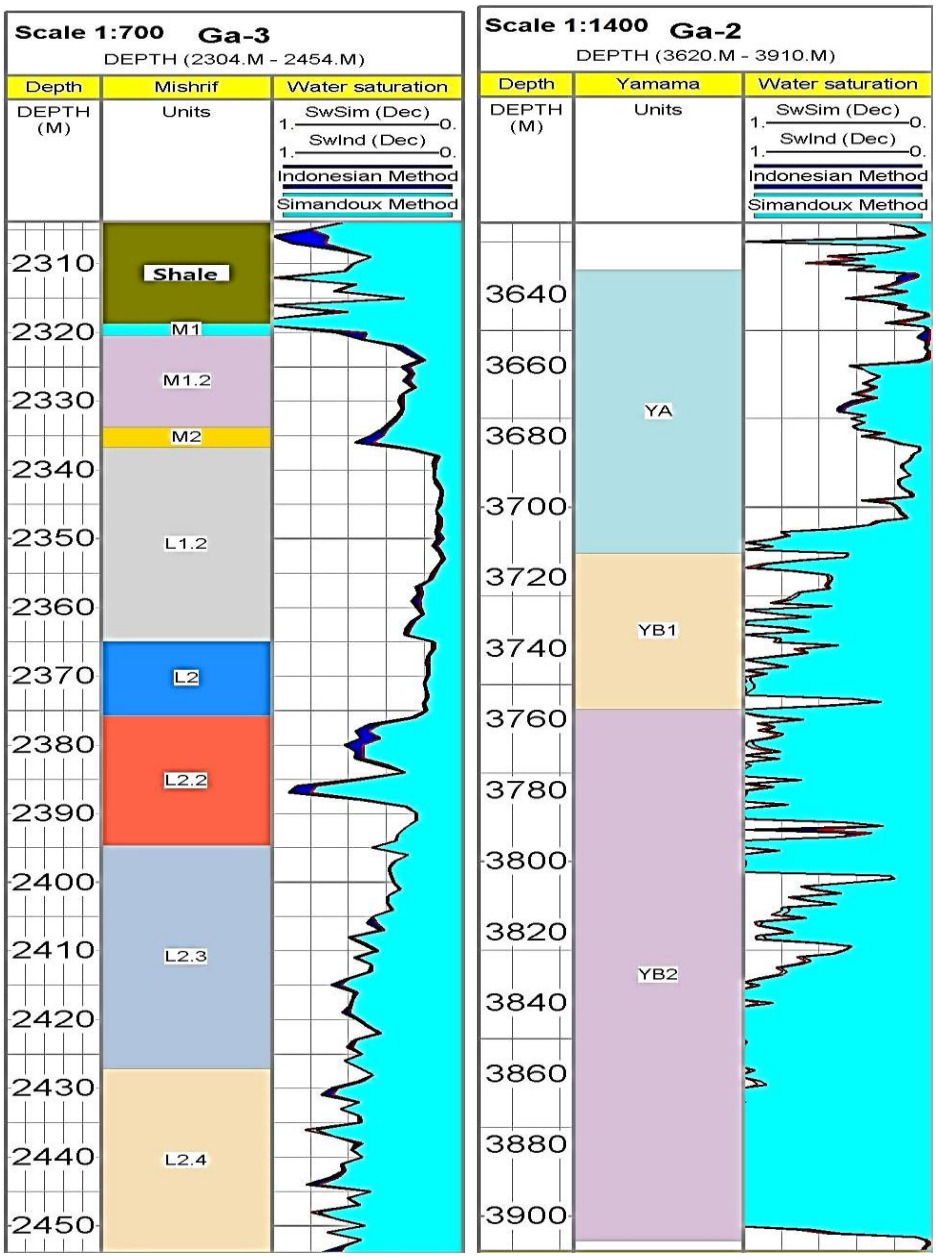

Figure (3-12): Water saturation log plots of Well Ga-2 of Yamama Formation and Well Ga-3 of the lower main unit of Mishrif Formation in Gharraf oil field.

3.3.5. Hydrocarbon saturation calculation

The hydrocarbon saturation is the quantity of pore volume in a stone which occupied by oil, typically detected by the difference amongst unity and water saturation, though the residual hydrocarbon saturation is the difference amongst unity and water saturation in flushed interval (Rider, 1986):

$$Sh = 1 - Sw \quad \text{..... (3-17)}$$

$$Sor = 1 - Sxo \text{..... (3-18)}$$

Where:

- S_h: hydrocarbon saturation
- S_{or}: residual hydrocarbon saturation

Both S_w as well as S_{xo} can be used to calculate the amount of moveable hydrocarbon, as seen in Equation (3-19) (Serra, 1989):

$$Movable\ Hydrocarbon\ Saturation\ (Smo) = Sxo - Sw \text{ ... (3-19)}$$

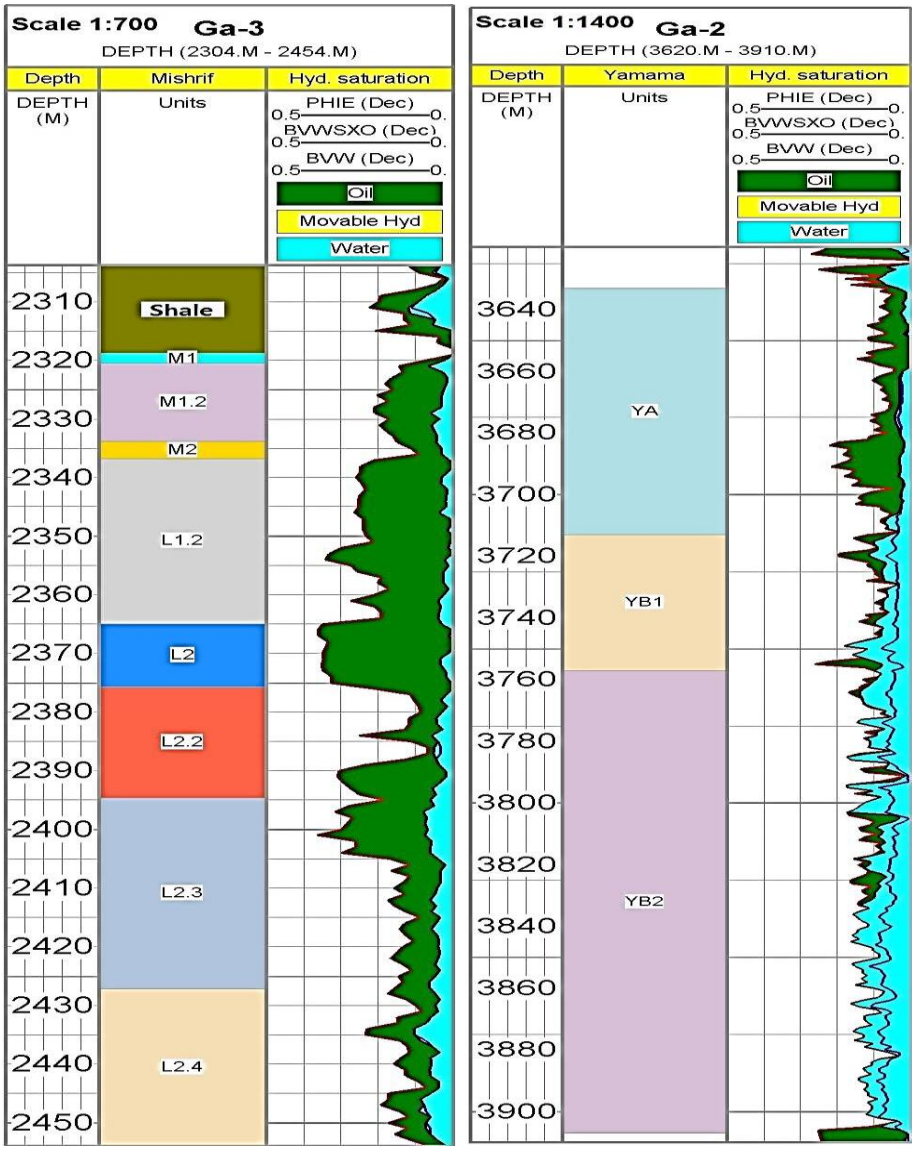

Figure (3-13): Hydrocarbon saturation log plots of Well Ga-2 of Yamama Formation and Well Ga-3 of the lower main unit of Mishrif Formation in Gharraf oil field.

3.3.6. Permeability computation

The capacity of a rock to transmit fluid is defined by its permeability. It links the fluid flow rate to the applied pressure gradient as well as the viscosity of the fluid. The related passages of the pore space (pore throats) regulate permeability. The permeability value is expressed in the Darcy unit (d) or milli-darcy unit (md). Indirect method using wireline logs and complex interpretation is used to evaluate permeability. A distinction must be made depending on the fluid composition (Al-musawi & Nasser, 2019):

a. Absolute permeability for a single non-reactive fluid in laminar flow.

b. Effective permeability in the presence of another fluid for the movement of one fluid.

c. The ratio of efficient to absolute permeability is known as relative permeability.

There are many methods of estimating permeability from wireline tool, but the Timur and Morris equations are used to calculate the permeability of Mishrif and Yamama formations in studied wells because it's the more reliable for Iraq's carbonate reservoirs:

$$K = a * (\frac{Ø^b}{\boldsymbol{Swirr}^c}) \quad \text{..... (3-20)}$$

Where:

- ***K***: permeability
- *Ø*: porosity
- $\boldsymbol{S_{wirr}}$: irreducible water saturation (has been used the minimum values of Sw)
- **a, b and c**: constants depending on the used method.

The constants for calculation permeability in Interactive Petrophysics (IP V 3.5) are: Timur : a = 8581 b = 4.4, and c = 2 and Morris Biggs Oil: a = 62500 b = 6, and c = 2. These equations apply only to zones of irreducible water saturation, such as the hydrocarbon zones above the transition zone.

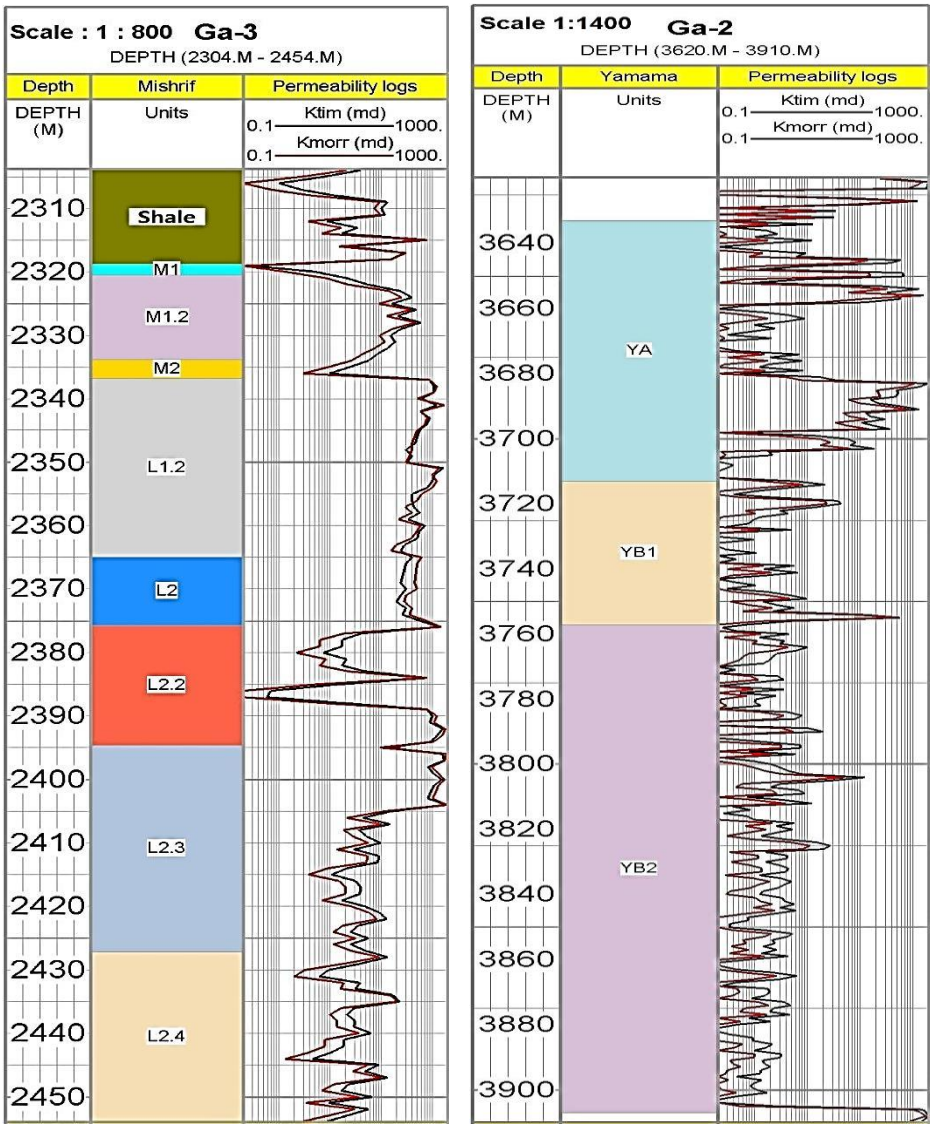

Figure (3-14): Permeability log plots of Well Ga-2 of Yamama Formation and Well Ga-3 of the lower main unit of Mishrif Formation in Gharraf oil field.

3.3.7. Computer processes interpretation (CPI)

The main purpose of well logs in the formation evaluation is to show a detailed plot of the physical and chemical properties of the formation as a function of depth in a borehole. The process of detecting physical properties of in-situ rocks such as density, gamma ray, resistivity, interval transits time, and borehole size is known as geophysical logging. The measured parameters are used to obtain other petro-physical parameters such as lithology, porosity, water saturation, porous and non-porous rocks, pay zones in the subsurface,

hydrocarbon saturation and possibly permeability. The formation fluid, bore hole surface irregularities, shale, and adjacent beds all affect the measured petrophysical parameters (Nwosu & Emujakporue, 2017).

Geophysical well logs data processing and interpretation are complex processes and they involve mathematical, statistical and numerical techniques. Well log data evaluation and analysis can be carried out by manual and/or by employing a computer (Aboelhassan *et al.*, 2017). The first and most common technique is the manual evaluation, which makes use of charts and cross-plot. Recently, computer methods based processed interpretations are increasingly been used. Computer processed interpretation has been used by many researchers (Mayer, 1980). In this study, computer processed interpretation (CPI) of geophysical well logs data was carried out with the aid of Interactive Petrophysics (IP) software V3.5 (Selley, 1998). It gives a continuous reading of lithology, porosity, fluid saturation and other petrophysical properties. The quality of the logs was assessed before the application of the computer processed interpretation to avoid errors in the derived parameters. Well log analysis is the most crucial stage in petro-physical data evaluation. The software package used for this study has a predefined work flow that follows the basic steps of formation evaluation and analysis. Interactive Petrophysics (IP) software was used to conduct this study. The standard procedure for formation evaluation used by oil and gas companies was followed. The techniques involve lithology and reservoir identifications, shale volume estimation, porosity and fluid saturation determination. The default computer processed interpretation format of the Interactive Petrophysics (IP) software was used for generating the results (Nwosu & Emujakporue, 2017). In order to prepare the Computer Processes Interpretation (CPI) plots for Mishrif and Yamama formations, the data of necessary logs were uploaded to IP software. After uploading and processing all reservoirs parameters, the CPI plots for the studied wells for both formations were achieved as shown in the Figures (3-15) and (3-16).

3.3.7.1. CPI interpretation of Mishrif and Yamama reservoirs

Computer Processes Interpretation (CPI) of the lower main unit of Mishrif Formation in Well Ga-3 of Gharraf oil field. Units L1.2 and L2 have good petrophysical properties Øeff = 18-22%, Sw = 16-38%, K = 80-343md. They are considered as the best reservoir units for oil. They contain economical quantity of oil reserves 584 million cubic meters. Units M1, M1.2, and M2 have less petrophysical properties and less quantity of oil reserves 229 million cubic meters, while lower units L2.2, L2.3, and L2.4 are almost fully saturated with reservoir water Sw=68-87% with small quantity of oil reserve 125 million cubic meters (Figure 3-15).

Computer Processes Interpretation (CPI) of Yamama Formation in Well Ga-2 of Gharraf oil field. Unit YA has good petrophysical properties Øeff = 11%, Sw = 26%, K = 119md, and it is considered as the best reservoir unit for oil reserve of Yamama Formation. It contains economical quantity of oil reserve 469 million cubic meters. Units YB1 and YB2 have low petrophysical properties, they contain a large percentage of reservoir water Sw=61-70% (Figure 3-16).

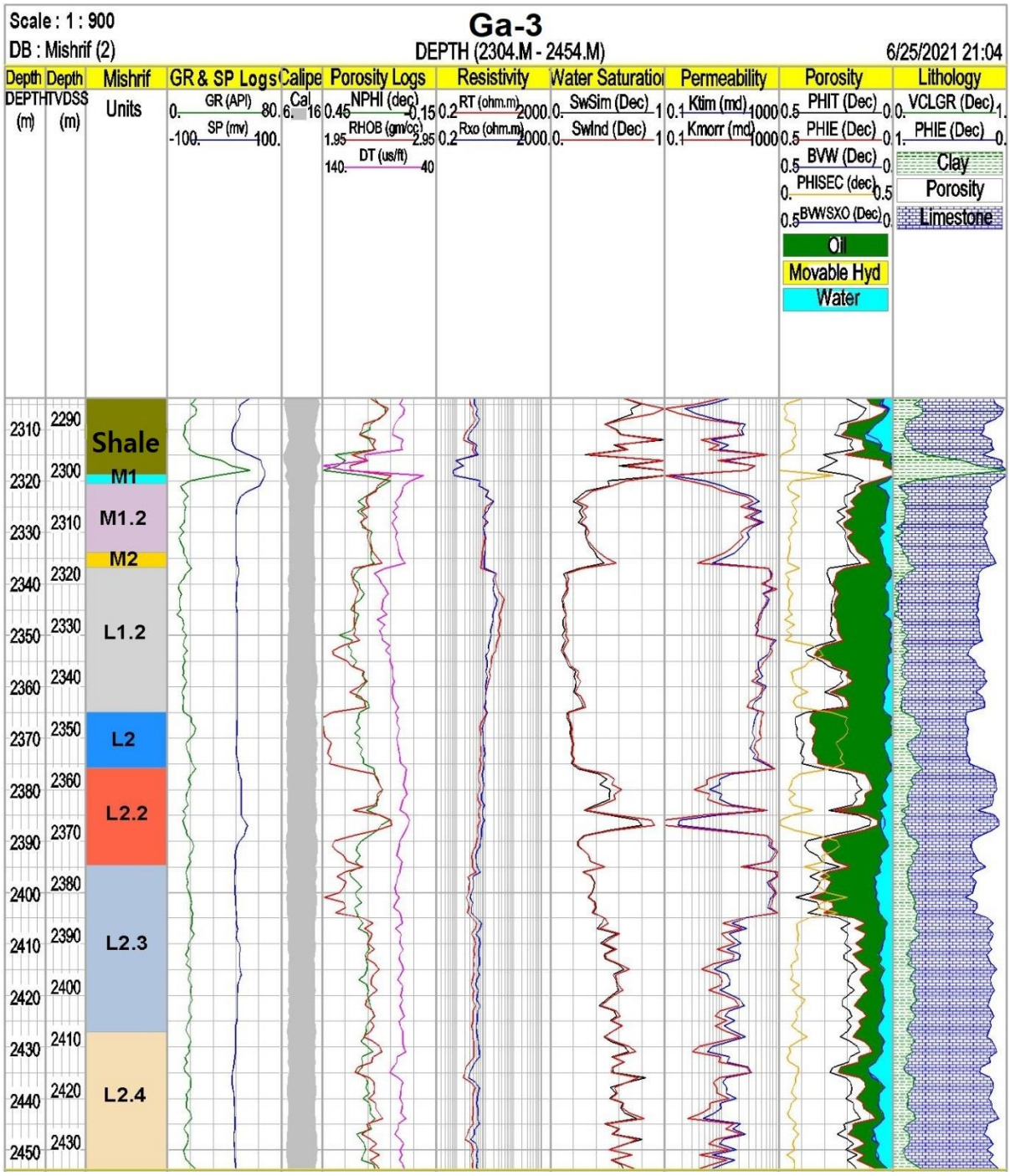

Figure (3-15): Computer Processes Interpretation (CPI) of the lower main unit of Mishrif Formation in Well Ga-3 of Gharraf oil field.

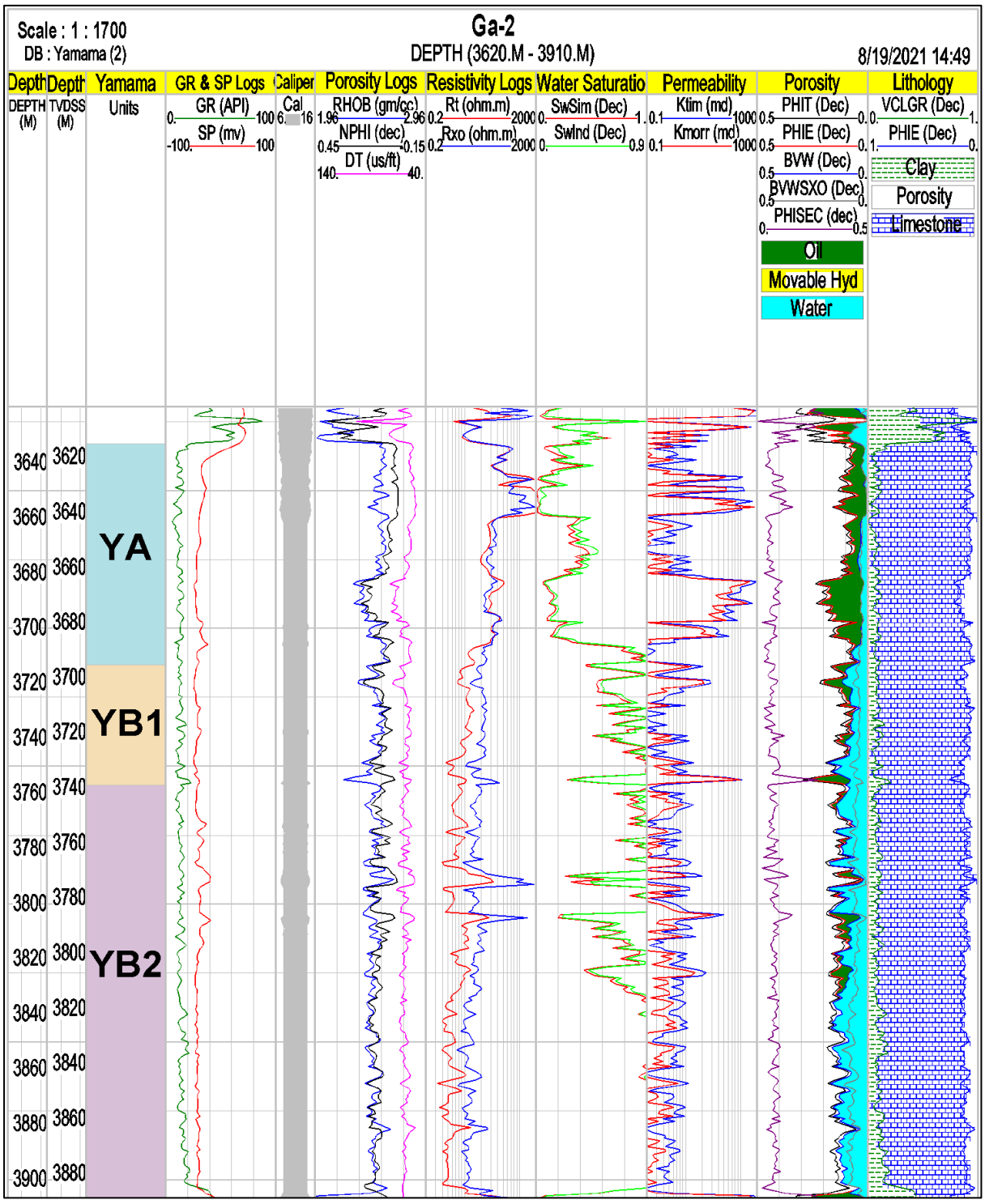

Figure (3-16): Computer Processes Interpretation (CPI) of Yamama Formation in Well Ga-2 of Gharraf oil field.

3.3.8. Net pay and gross thickness measurements

In order to evaluate studied reservoirs, net pay and gross thickness must be calculated; where net pay represents the thickness of the porous and permeable zone of an evaluated formation that containing commercial amounts of hydrocarbon. The net to gross ratio (N/G %) can be defined as the ratio between the thickness of net pay and the thickness of total pay zone. This is an important factor in hydrocarbon volumetric calculation of reservoir (Katz & Thompson, 1986).

The zone of a reservoir which effectively contributes in petroleum production represents the net pay of that reservoir. This value is calculated used appropriate cut-off values applied to petrophysical parameters. Shale volume, water saturation, and porosity cut-off values represent important petrophysical parameters in order to calculate net pay of the studied reservoirs, where using these petrophysical parameters is important to identify between reservoir zone from non-reservoir zone of studied formations, We can also distinguish between wet or dry zone and oil-filled zone depending on the cut-off value of water saturation (Sw).

The main purpose of the calculation of net-pay for studied reservoirs is to exclude non-productive reservoir zones, and to give a solid basis for the processes of a quality 3D reservoir analysis and measurable hydrocarbons in place and flow calculations (Ahmed, 2009). In the net pay thickness measurement, 50%, 50%, and 8% as the default values of water saturation, shale volume, and porosity respectively for the lower main unit of Mishrif Formation, and 50%, 50%, and 6% as the default values of water saturation, shale volume, and porosity respectively for Yamama Formation in Gharraf oil field have been applied, Figures (3-17) and (3-18). Tables (3-3) and (3-4) show the calculations of net-pay and other reservoir parameters of reservoir units of Mishrif (Ga-3) and Yamama (Ga-2) formations in Gharraf oil field.

Table (3-3): Net pay and average of the main petrophysical properties of the lower main unit of Mishrif Formation in Well Ga-3

Gharraf oil field / Mishrif Reservoir / Well Ga-3 RTKB = 17.54 m											
Units	Top		Bottom		Gross Thick.	Net Thick.	N/G	Av. PHIE%	Av. Sw%	Av. Vcl%	Av. Sh%
	MD	TVDSS	MD	TVDSS							
M1	2318.73	2301.19	2320.45	2302.91	1.72	0.00	0.00	---	---	---	---
M1.2	2320.45	2302.91	2333.82	2316.28	13.37	12.32	0.92	17.90	28.70	08.80	71.30
M2	2333.82	2316.28	2336.71	2319.17	2.89	2.89	1.00	12.30	40.40	13.30	59.60
L1.2	2336.71	2319.17	2364.93	2347.39	28.22	28.22	1.00	24.50	15.50	08.40	84.50
L2	2364.93	2347.39	2375.78	2358.24	10.85	10.85	1.00	34.20	18.00	18.80	82
L2.2	2375.78	2358.24	2394.65	2377.11	18.87	11.87	0.63	21.50	31.60	18.00	68.40
L2.3	2394.65	2377.11	2427.15	2409.61	32.50	17.85	0.55	22.80	39.80	17.00	60.20
L2.4	2427.15	2409.61	2454	2436.46	26.85	02.00	0.07	17.30	47.40	15.10	52.60

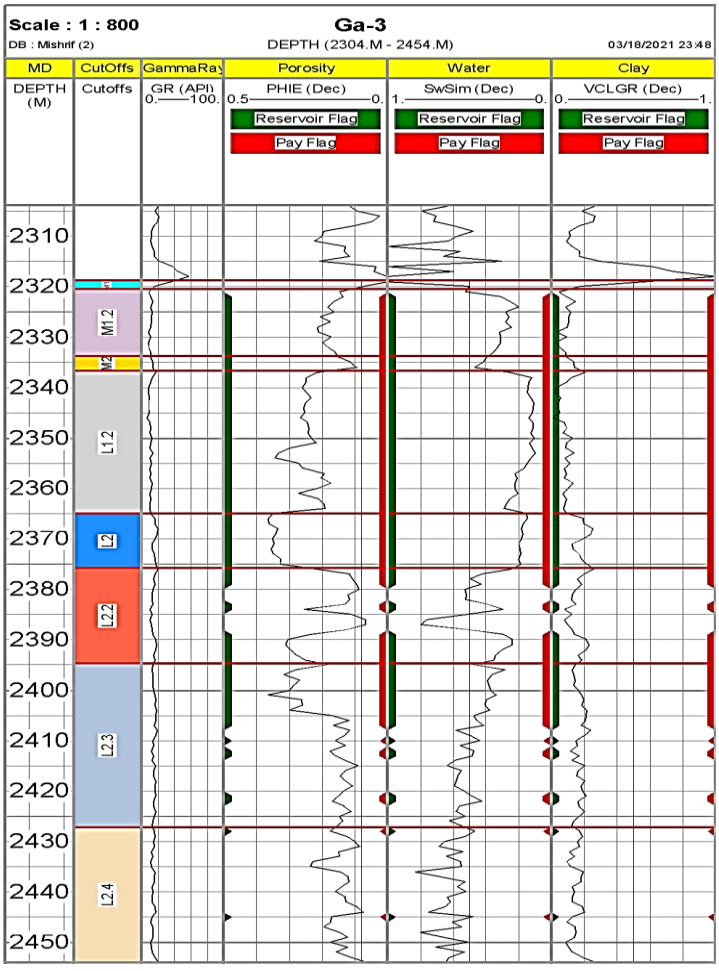

Figure (3-17): Net-pay and reservoir parameters of the lower main unit of Mishrif Formation in Well Ga-3 of Gharraf oil field. According to these measurements it was concluded that the zones that have petrophysical properties most suitable for storing oil in the Mishrif reservoir are mainly represented by units L1.2 and L2, as both contain the largest reserves of oil (584 million cubic meters).

Table (3-4): Net pay and average of the main petrophysical properties of Yamama Formation in Well Ga-2.

Gharraf oil field / Yamama Reservoir / Well Ga-2 RTKB = 18 m											
Units	Top		Bottom		Gross Thick.	Net Thick.	N/G	Av. PHIE%	Av. Sw%	Av. Vcl%	Av. Sh%
	MD	TVDSS	MD	TVDSS							
YA	3633	3615	3713	3695	80.00	67.00	0.84	11.10	20.20	07.90	79.80
YB1	3713	3695	3757	3739	44.00	41.00	0.93	12.20	72.90	08.90	27.10
YB2	3757	3739	3907	3889	150.00	138.50	0.92	12.30	89.70	10.50	10.30

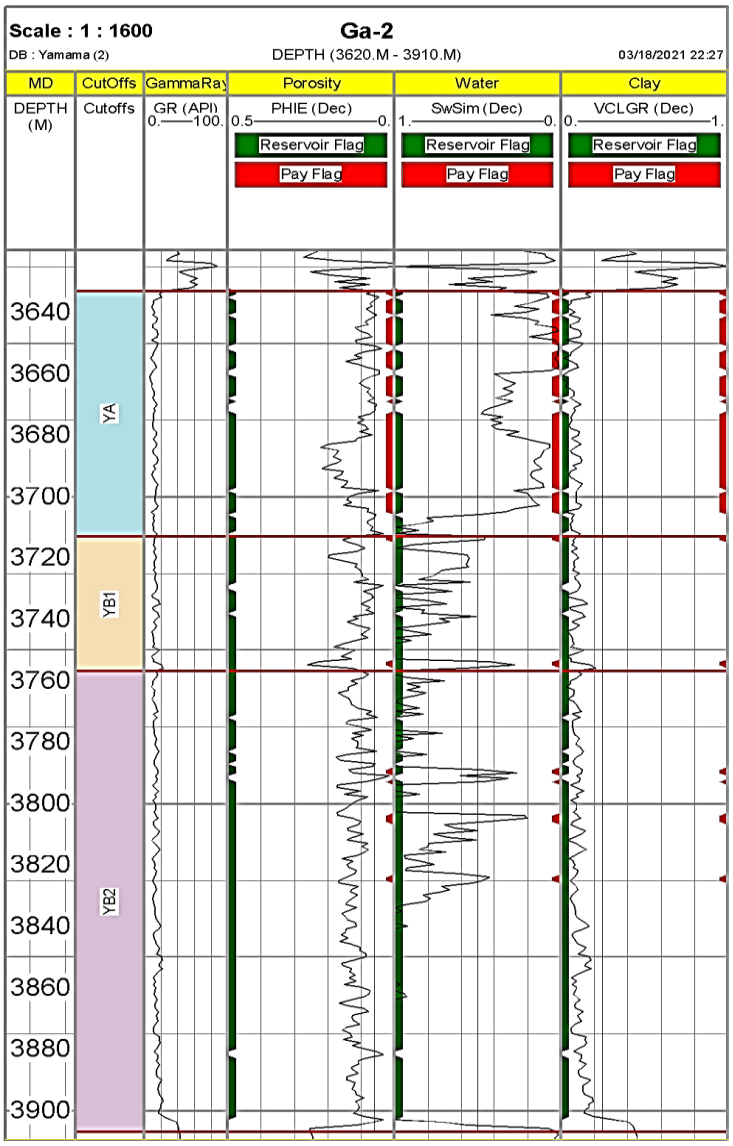

Figure (3-18): Net-pay and reservoir parameters of Yamama Formation in Well Ga-2 of Gharraf oil field. According to these measurements it was concluded that the zone that has petrophysical properties most suitable for storing oil in the Yamama reservoir is mainly represented by unit YA, as it contains the largest reserve of oil (469 million cubic meters).

3.3.9. 3D Geological modeling and formation evaluation

Geological modeling can be defined as the process of using computer to create computerized representations of parts of the Earth's crust, including oil and gas fields. The process of realistic geologic models in the oil and gas industry are required as input to reservoir simulator programs, these programs can predict the rock's behavior under different scenarios of hydrocarbon recovery. Using reservoir simulation allows reservoir engineers to identify which recovery options offer the safest and most economic, efficient, and effective development plan for a particular reservoir (Kessler *et al.*, 2008). In geological studies, the process of building a three-dimensional geological model from subsurface data is considered as a typical task involving natural resource evaluation and hazard assessment (Schlumberger, 2013).

3D geological models were built for Mishrif and Yamama formations in Gharraf oil field using Petrel software. These models include structural models and reservoir properties models (porosity, water saturation, and permeability) in three dimensions. In order to build 3D geological models, the following steps were followed:

1) Geo referencing

Geo referencing is the first step before starting a geo modeling, whereby all available information are combined and organized in common coordinate system. Coordinate system selection is a critical step in defining the project parameters and care must be taken in picking the right value. For this study, according to the study area, the coordinate system which has been introduced is WGS 1984 UTM, Zone 38˚ North, Figure (3-19).

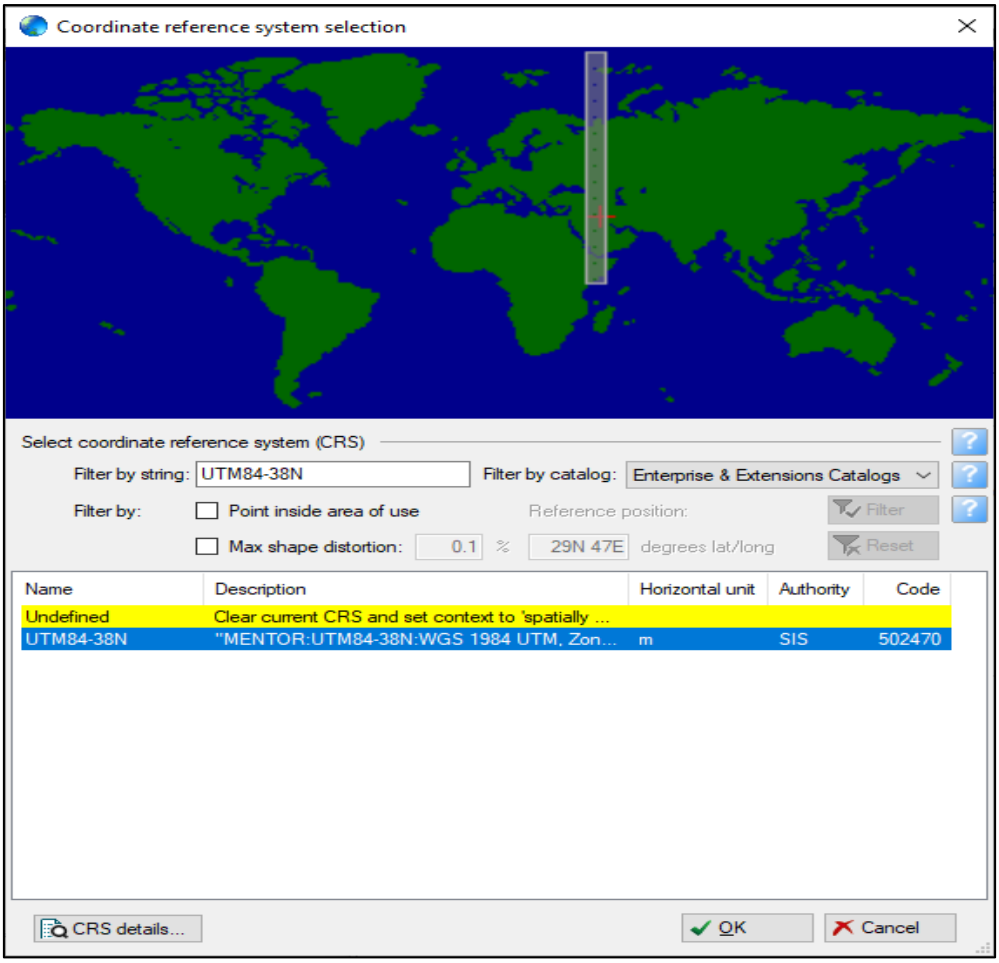

Figure (3-19): Illustrating coordination system selected in Petrel software of Gharraf oil field.

2) Data import

To build 3D models of the studied formations, there are many types of data that should be supplied to the Petrel software, they are included:

a. Well heads and well tops

Well heads of 3 boreholes (Ga-A1P, Ga-3 and Ga-5) of Mishrif Formation and 3 boreholes (Ga-1, Ga-2 and Ga-3) of Yamama Formation have been imported as ASCII file containing well header information organized in columns to the Petrel software, they included eastern (x), northern (y), Rotary Table Kelly Bushing (RTKB) and vertical measured depth (MD).

Well tops are used to make boundary between geological units as seen in the boreholes (Schlumberger, 2008). Well tops of the studied reservoirs units of the

lower main unit of Mishrif Formation and Yamama Formations have been imported as ASCII file containing well header information organized in columns to Petrel also, they included surface name, eastern (x), northern (y) and surface top (MD) for each of the studied wells.

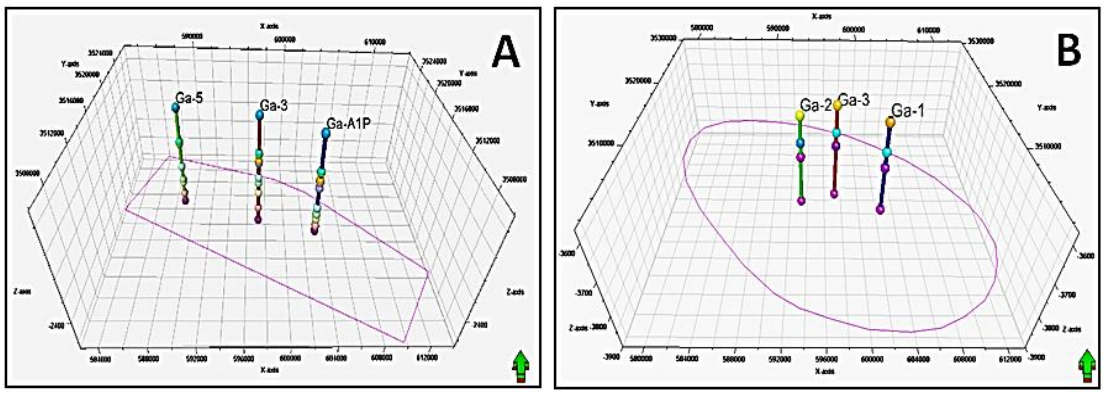

Figure (3-20): Well heads and well tops for the studied wells of (A) The lower main unit of Mishrif Formation, and (B) Yamama Formation.

b. Well logs

This type of data included importing well logs data to the Petrel software (gamma ray, SP, neutron, sonic, density and resistivity logs) and CPI (porosity, permeability and water saturation) that exported from Interactive Petrophysics software (IP) as a LAS files for the studied wells (Ga-1, Ga-A1P, Ga-2, Ga-3, Ga-5) of the Gharraf oil field**.**

3) 3D grid construction

A 3D grid, in simple terms, divides a model into boxes, each one is referred to as a grid cell, each grid cell have one type of rock properties, one value of porosity, one value of permeability, one value of water saturation, etc. (Schlumberger, 2009). A 3D grid construction is the first step to set up 3D model in simple terms (Schlumberger, 2007). The process of generating the grid, which acts as a foundation for all modeling, is known as pillar gridding. The skeleton grid is made up of top, middle, and bottom skeleton grids (Figure 3-21).

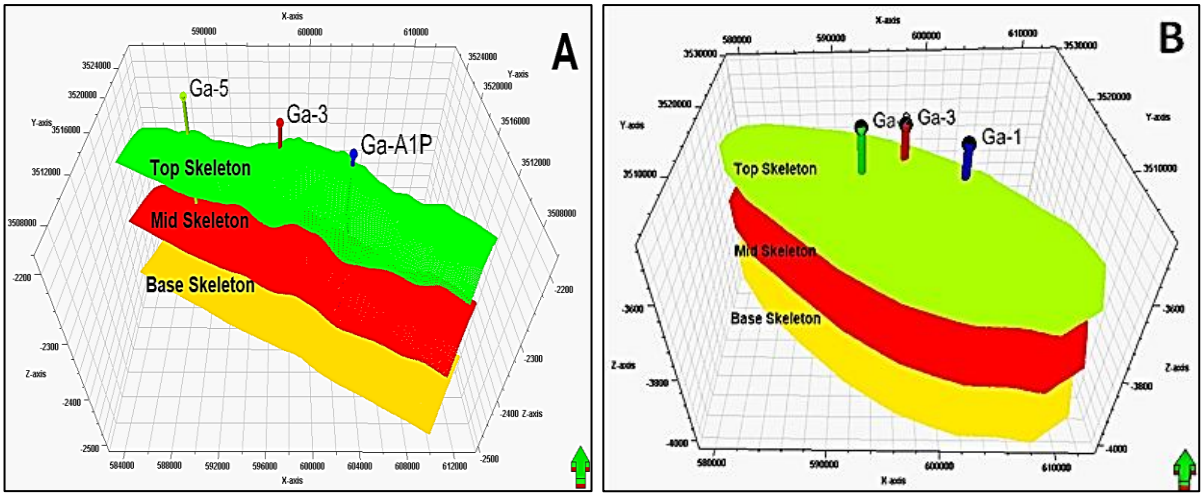

Figure (3-21): The Skeletons of (A) the lower main unit of Mishrif Formation, and (B) Yamama Formation in Gharraf oil field.

4) 3D Structural modeling and structural contour map

Structural modeling represents building a 3D structural model and setting up structural contour map for each unit's top of the studied formations, as it was done for Mishrif and Yamama formations using Petrel software, as illustrated in Figure (3-22) and Figure (3-23). Structural modeling is involving three processes represented as follows:

a. Fault modeling

b. Pillar gridding

c. Vertical layering

The all three processes of structural modeling are performed respectively in order to create a single data model (Schlumberger, 2010.a). Contour maps can be made by computer from the surface information and correlated boreholes (Hamdan, 2011). Figure (3-24) and Figure (3-25) represent the structural contour maps for all units and barrier beds of Mishrif and Yamama formations are deduced using Petrel software.

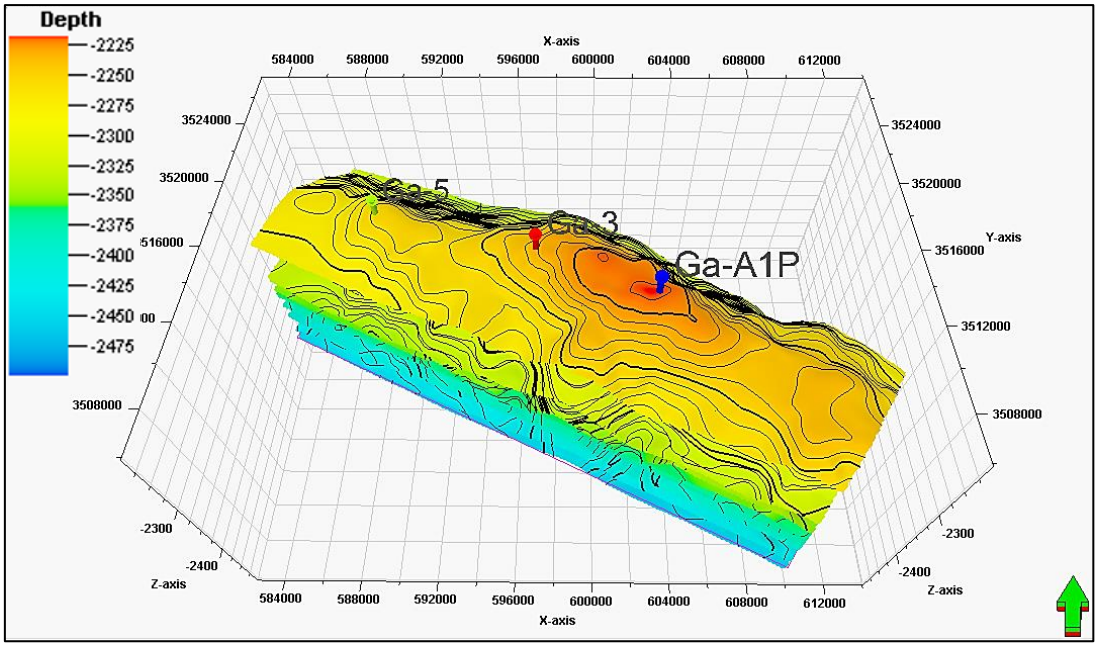

Figure (3-22): 3D structural model of the lower main unit of Mishrif Formation in Gharraf oil field.

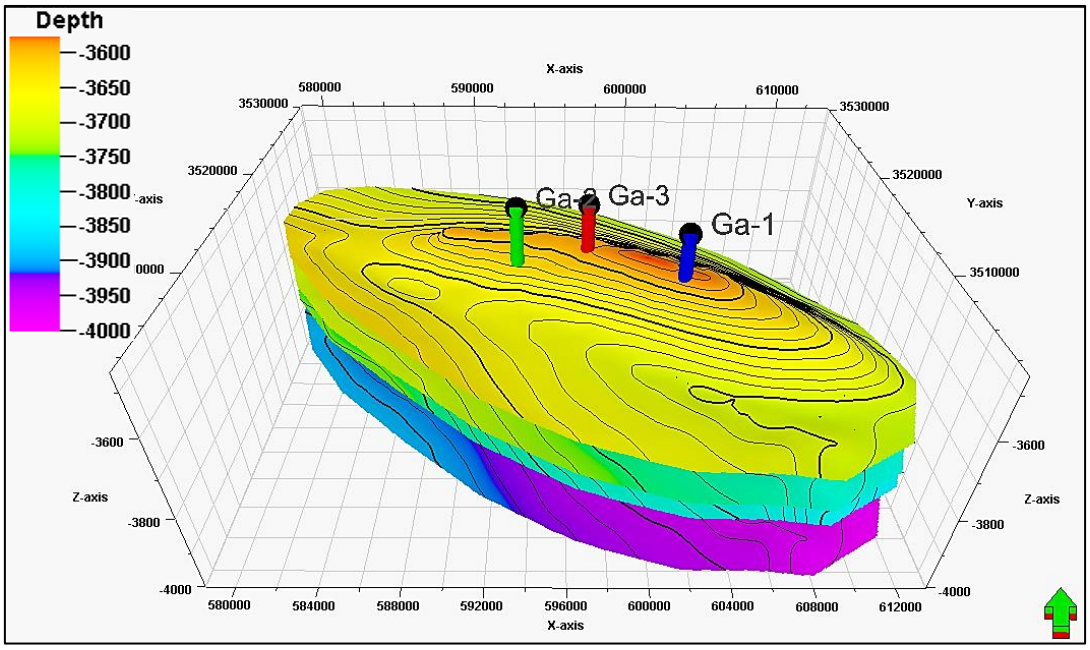

Figure (3-23): 3D structural model of Yamama Formation in Gharraf oil field.

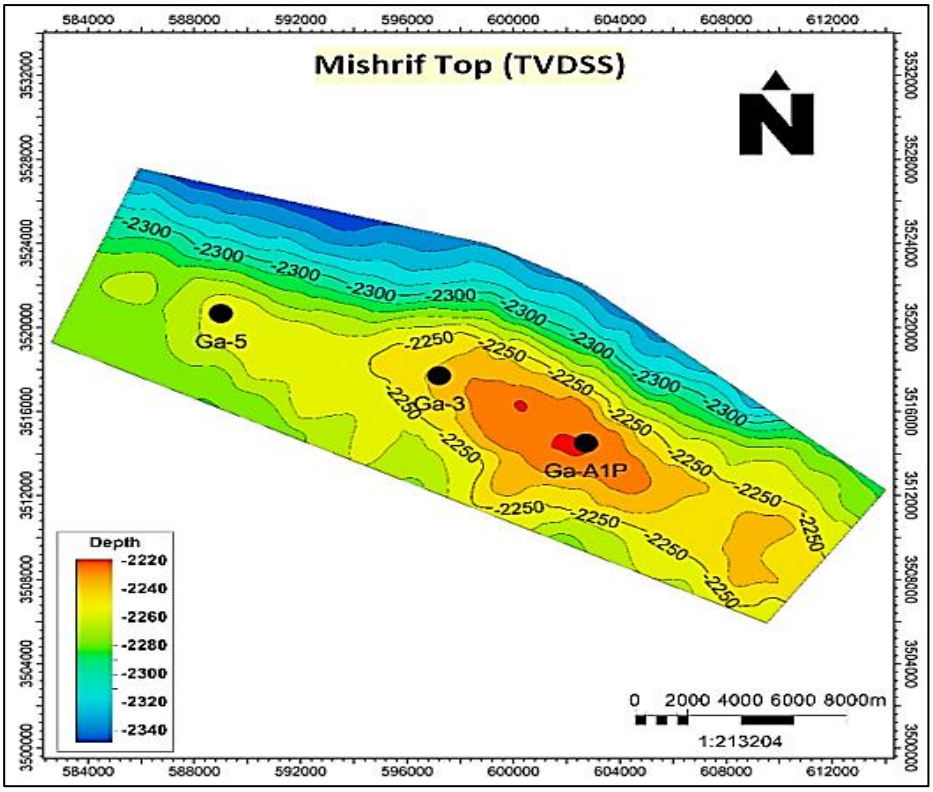

Figure (3-24): Structure contour map of Mishrif Formation top in Gharraf oil field.

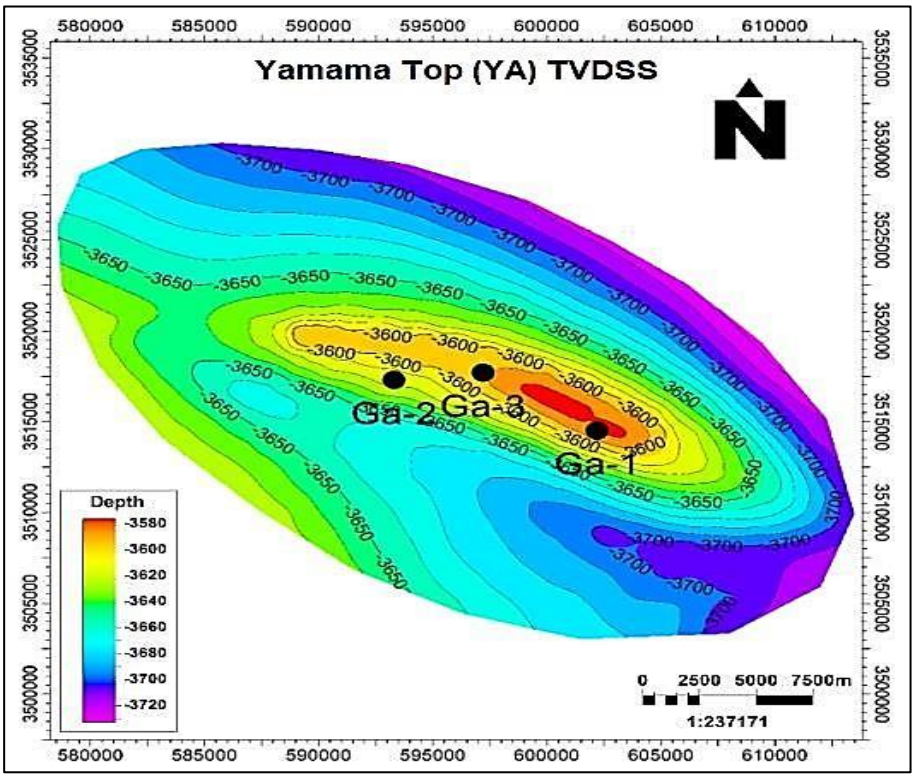

Figure (3-25): Structure contour map of Yamama Formation top in Gharraf oil field.

5) Well correlation

The well correlation concept may provide an idea about the quality and the distribution of petrophysical properties, as well as the extents and thickness of various lithological units in reservoirs (Schlumberger, 2008). Two correlation sections of the studied wells in Gharraf oil field were made by using Grapher software, see Figure (3-26). First correlation section, see Figure (3-27), is between Mishrif Formation studied wells (Ga-A1P, Ga-3 and Ga-5) from NW to SE, and the second correlation section, see Figure (3-28), is between Yamama Formation studied wells (Ga-1, Ga-2 and Ga-3) from NW to SE. These sections illustrate the variation in thickness of units of the Mishrif and Yamama reservoirs in the studied wells.

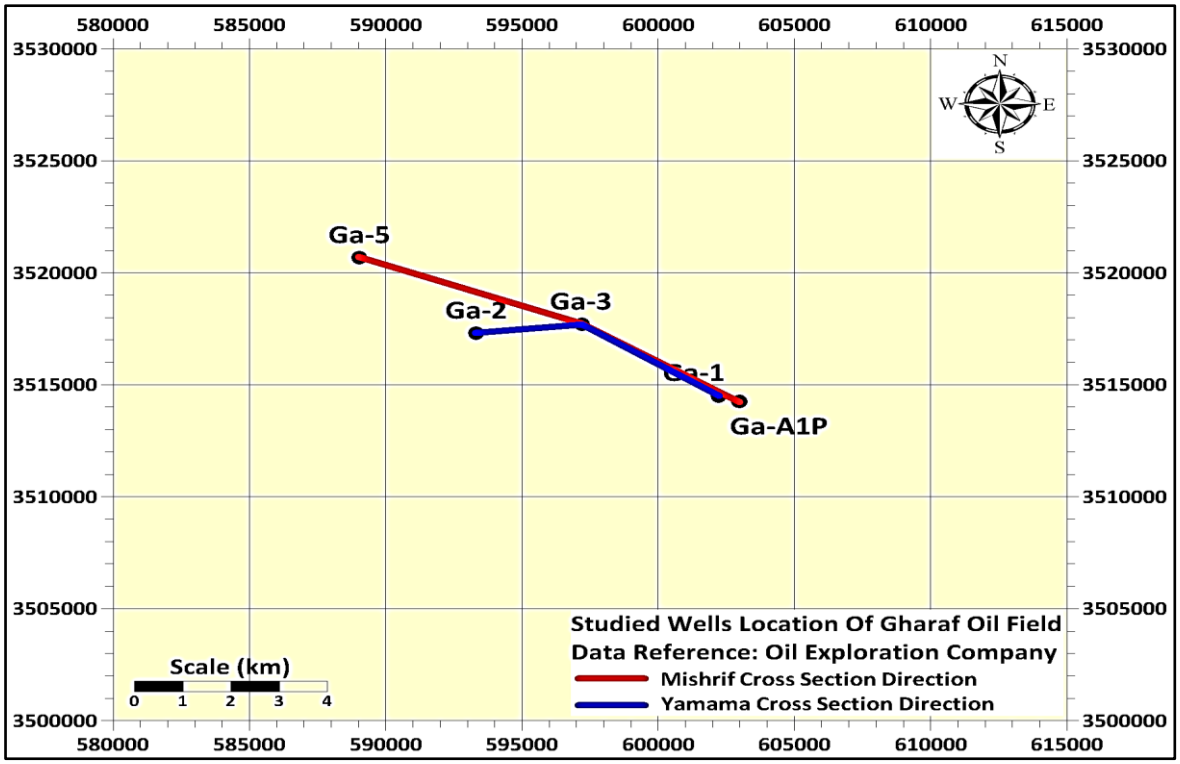

Figure (3-26): Location of the studied wells and the cross sections directions in Gharraf oil field.

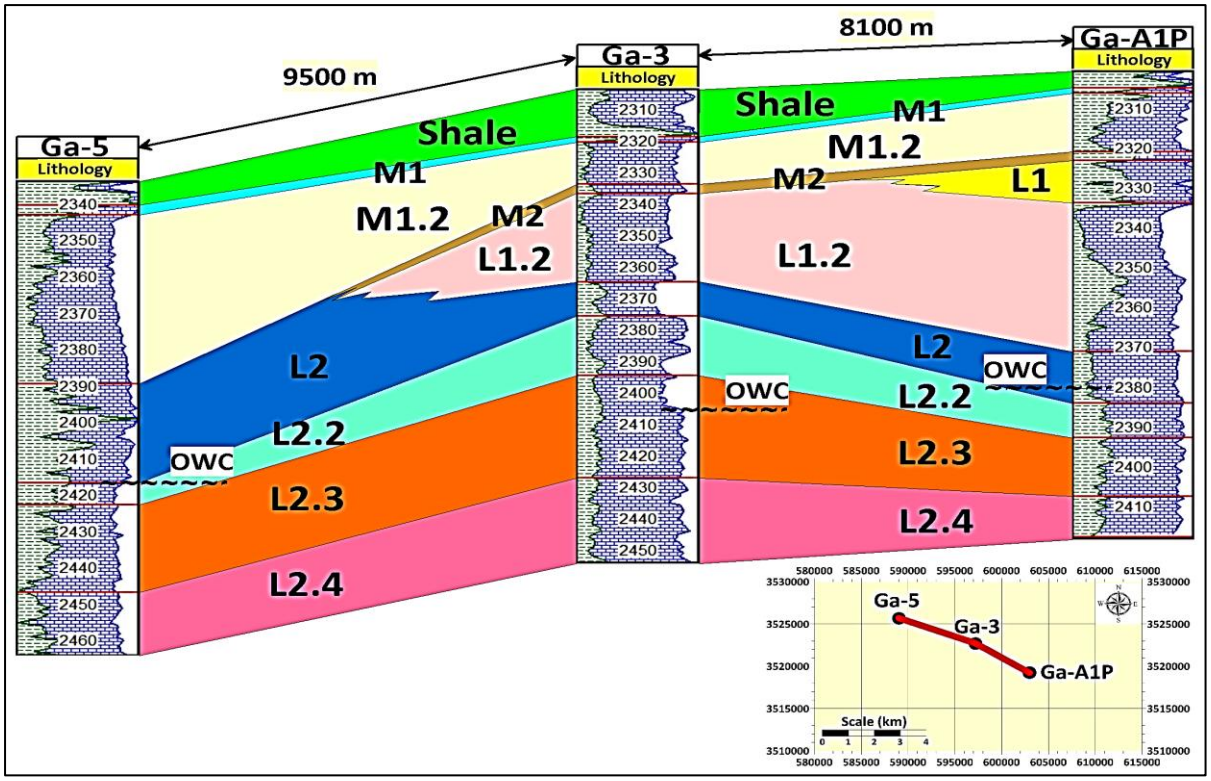

Figure (3-27): Correlation section between studied wells of the lower main unit of Mishrif Formation in Gharraf oil field (RTKB MD).

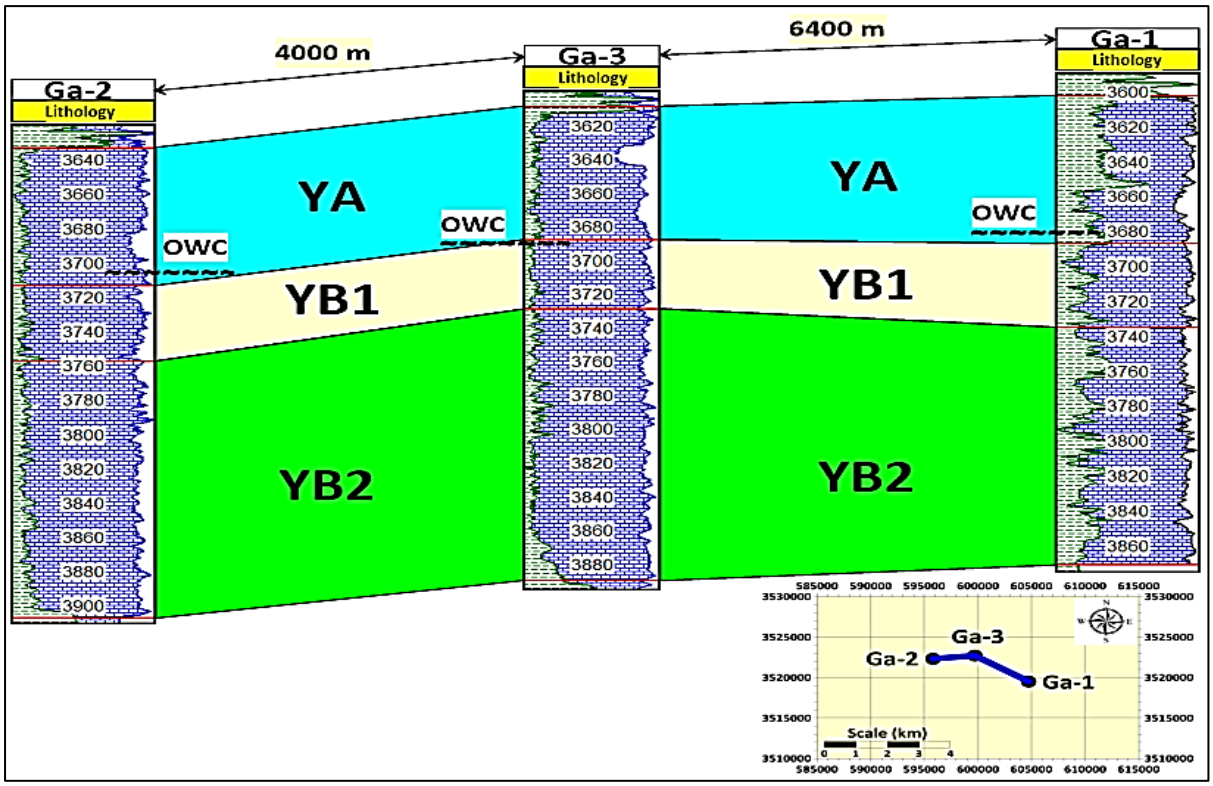

Figure (3-28): Correlation section between studied wells of Yamama Formation in Gharraf oil field (RTKB MD).

6) Horizons

The process of inserting the structural horizons into the pillar grid represents the next step in the building of structural modeling, where this step is for creating the vertical layering of the 3D grid model by using Petrel software. The contraction of horizons generates independent geological horizons from X, Y, and Z input data and it is used to generate additional horizons using relative distance to existing horizons (Schlumberger, 2009), Figure (3.29).

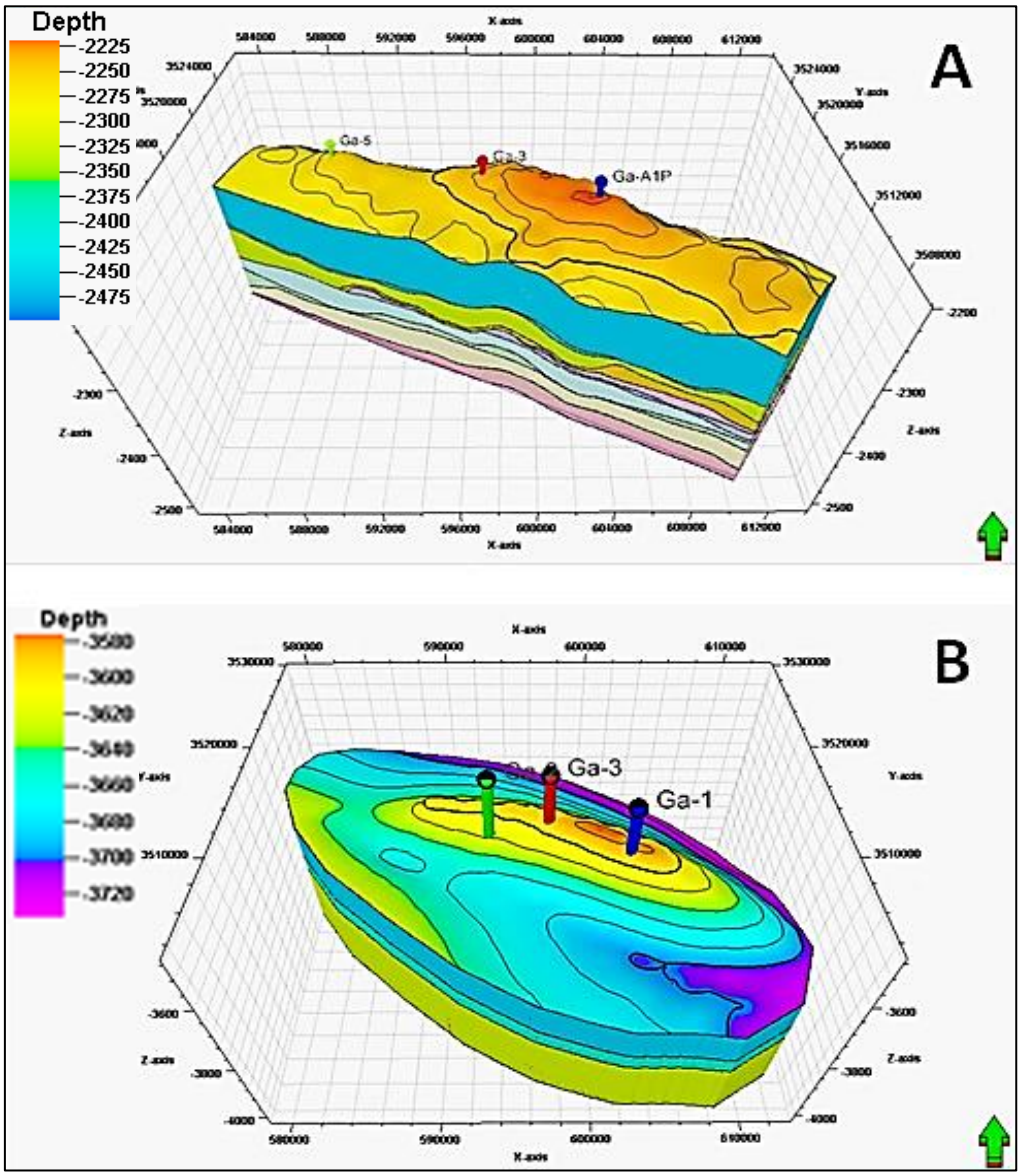

Figure (3-29): 3D model shows main horizons of (A) The lower main unit of Mishrif Formation, and (B) Yamama Formation in Gharraf oil field.

7) Scale up of well logs

When building a model of petrophysical properties of a reservoir, the represented zone in modeling is divided up by generating a 3D grid, where each single grid cell has a single value for each property. As the grid cells are often much larger than the sample density for well logs, well log data must be scaled up before they can be entered into the grid. This process is also called blocking of well logs (Schlumberger, 2008). Petrophysical properties can be scaled up by using many statistical methods existed in Petrel software such as (arithmetic, harmonic, and geometric methods), where values of petrophysical properties represented by the porosity, permeability and water saturation in the current model have been scaled up by using most of the previously mentioned methods.

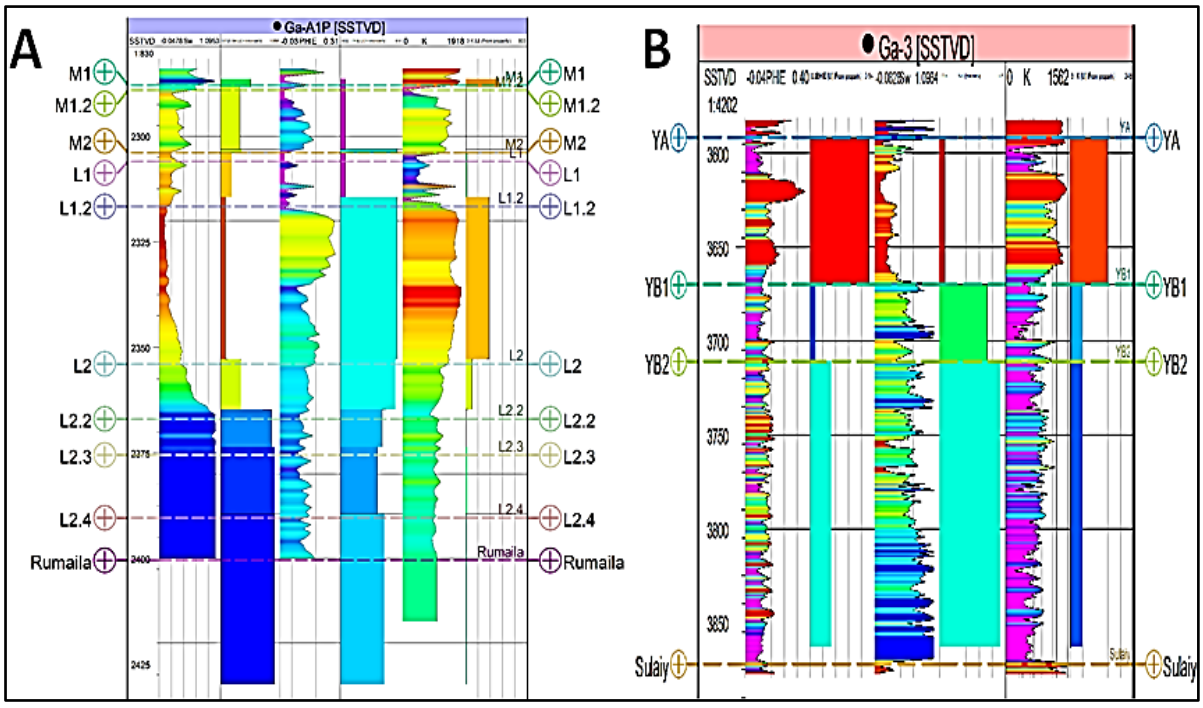

Figure (3-30): Shows the Scale up of Sw, PHIE and K logs of (A) Studied well Ga-A1P of the lower main unit of Mishrif Formation, and (B) Ga-3 of Yamama Formation in Gharraf oil field.

8) Property modeling

The modeling process of petrophysical properties for a reservoir is assigning values of porosity, permeability and water saturation, for each single cell of a 3D grid. The process of filling the grid cells with petrophysics properties (porosity, permeability, and water saturation) to match well data and realistically preserve reservoir heterogeneity is defined as property modeling. The objective of property modeling is to distribute properties between the available wells (Schlumberger, 2010a). Well logs data represent the base in the 3D property modeling, where this process comprises computation for solving complicated mathematical equations including one or several 3D property models, in other words, Sw transforms based on porosity 3D model (Schlumberger, 2007). Petrophysical model can be defined as the process of simulation for petrophysical properties porosity, permeability and water saturation of a reservoir, where this process can be achieved by using Petrel software which offers several algorithms for modeling the distribution of petrophysical properties in a reservoir model (Schlumberger, 2009).

a. Porosity model

The porosity model has been built using the outputs of porosity logs (neutron, density and sonic), which have been corrected and interpreted using IP software. The Sequential Gaussian Simulation Algorithm has been used as a statistical method that fits with the amount of data available (Schlumberger, 2010, b). The Figures below show the 3D porosity models of the lower main unit of Mishrif Formation and Yamama Formation.

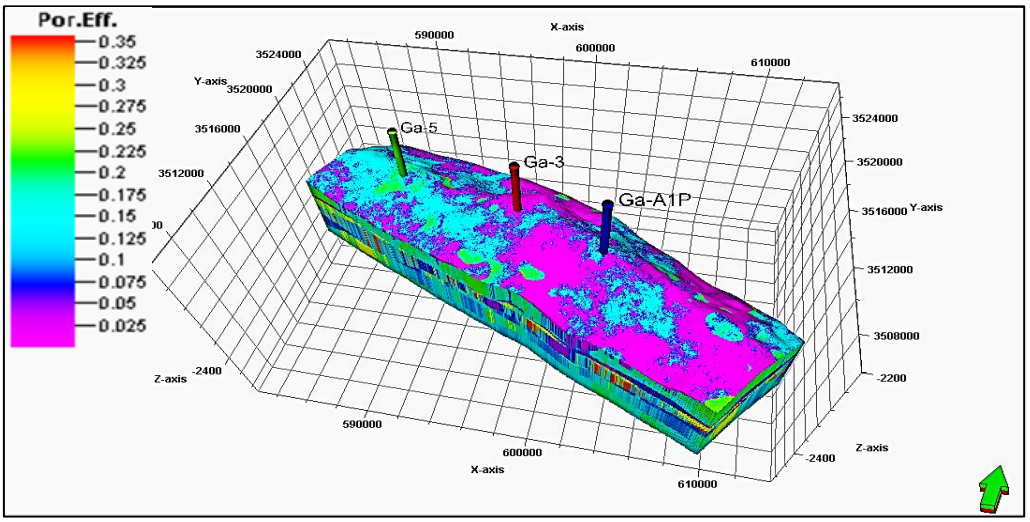

Figure (3-31): Effective porosity model of the lower main unit of Mishrif Formation in Gharraf oil field (values in decimal).

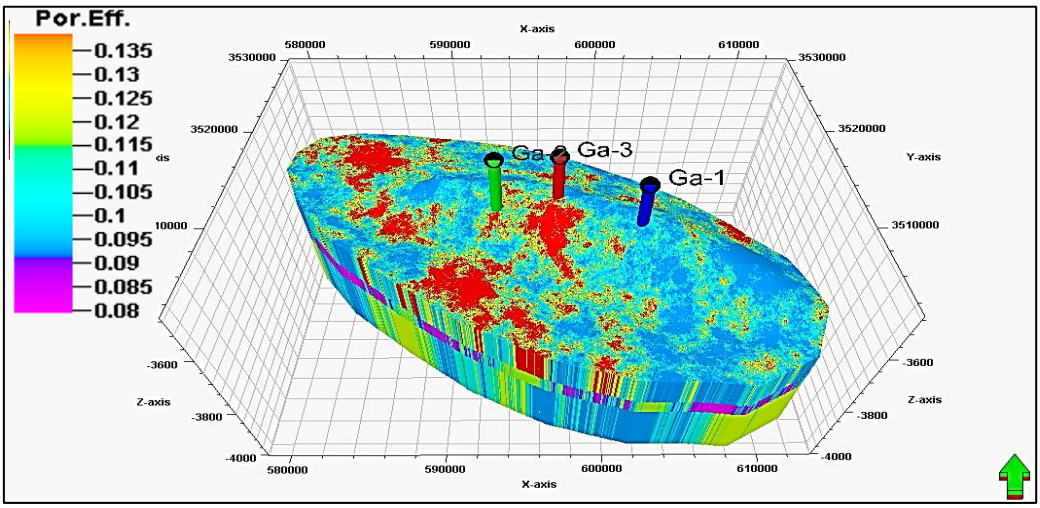

Figure (3-32): Effective porosity model of Yamama Formation in Gharraf oil field (values in decimal).

b. Water saturation model

Water saturation model was built after the scale up of water saturation that exported from IP software for each reservoir unit of the Mishrif and Yamama formations. The same geostatistical method was used in the porosity models (Statistical Gaussian Simulation Algorithm) according to the available data. The Figures below show the 3D water saturation models of the lower main unit of Mishrif Formation and Yamama Formation.

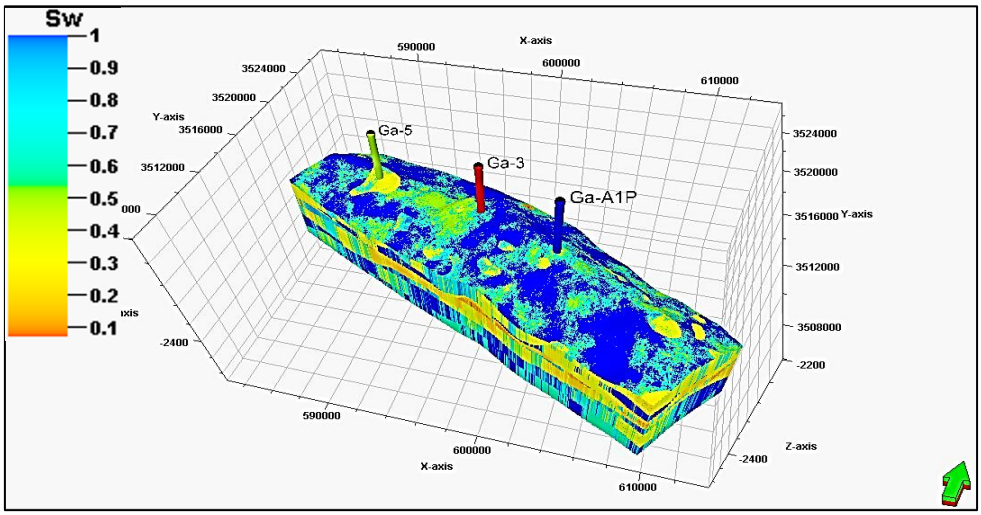

Figure (3-33): Water saturation model of the lower main unit of Mishrif Formation in Gharraf oil field (values in decimal).

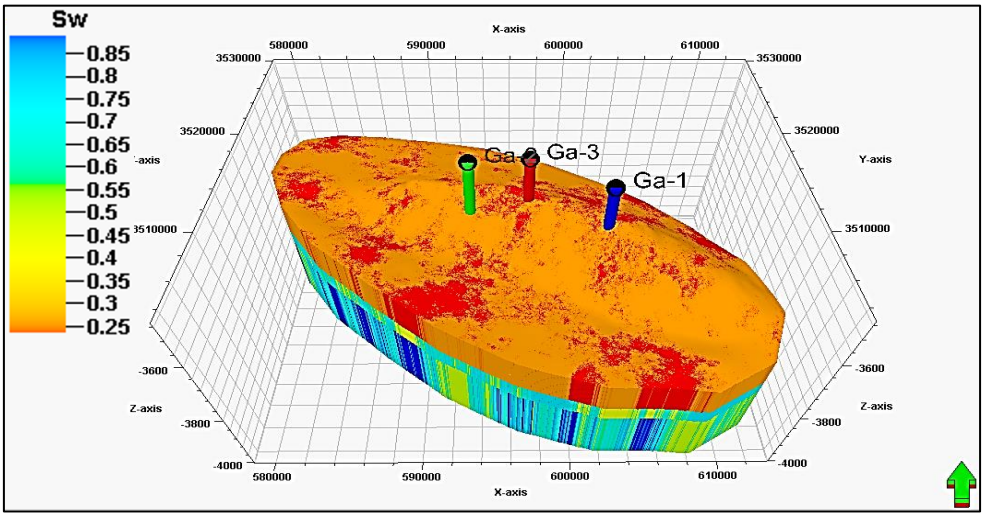

Figure (3-34): Water saturation model of Yamama Formation in Gharraf oil field (values in decimal).

c. Permeability model

Permeability model was built after the scale up of permeability that exported from IP software for each reservoir unit of the Mishrif and Yamama formations. The same geostatistical method, which is (Statistical Gaussian Simulation Algorithm), has been used in the porosity and water saturation models according to the available data. The Figures below illustrate the 3D permeability models of lower main unit of Mishrif Formation and Yamama Formation.

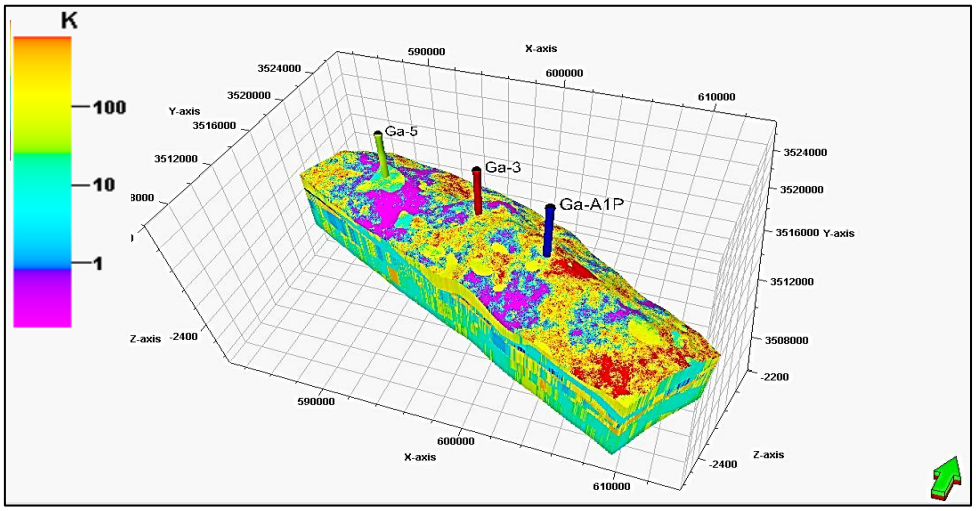

Figure (3-35): Permeability model of the lower main unit of Mishrif Formation in Gharraf oil field (values in milli-Darcy).

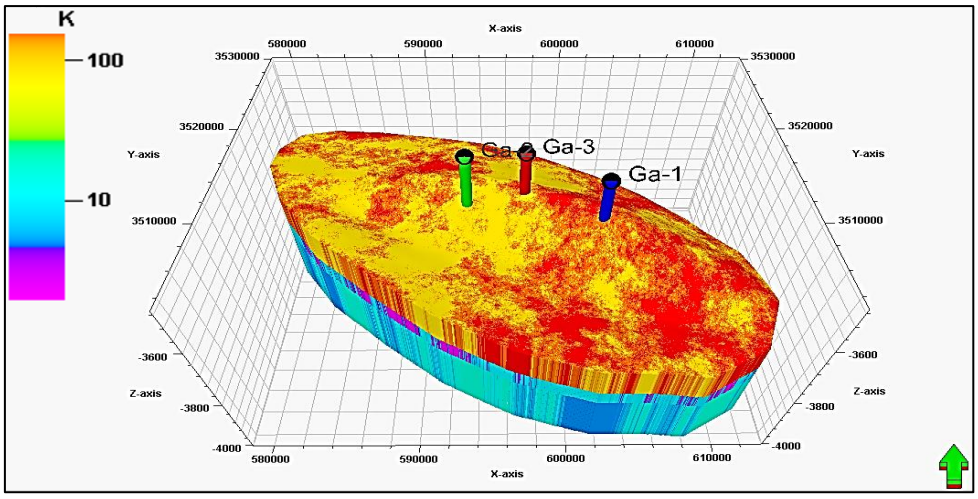

Figure (3-36): Permeability model of Yamama Formation in Gharraf oil field (values in milli-Darcy).

3.3.10. Petrophysical evaluation of Mishrif reservoir units

a. M1 unit

This unit represents the first reservoir unit of the lower main unit of Mishrif Formation. The thickness of this unit is tight in the studied wells (1.2 - 2.65m), where the thickness increases towards the wells Ga-A1P in the SE and Ga-5 in the NW of the oilfield. The average value of effective porosity (PHIE), water saturation (Sw_{sim}) and permeability (K_{tim}) for this unit are: 4%, 58% and 68md respectively, and the very low porosity of this unit make it ineligible to be an oil reservoir.

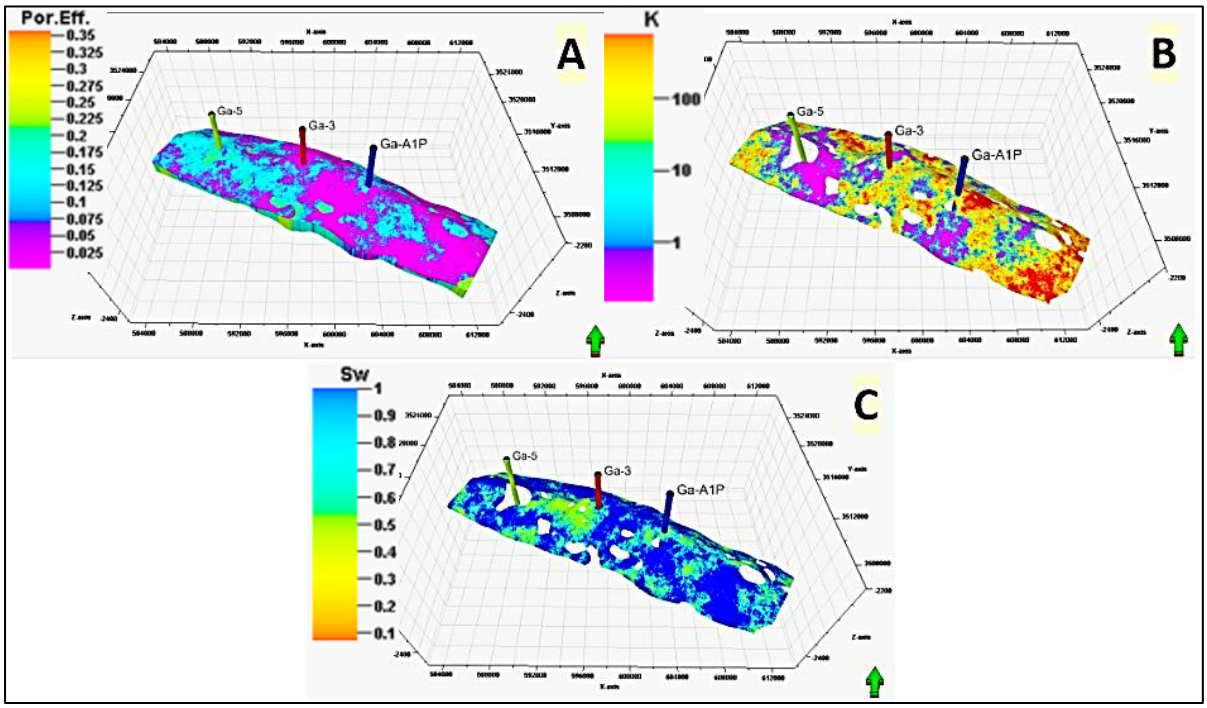

Figure (3-37): (A) Effective porosity (dec) (B) Permeability (mD) (C) Water saturation (dec) of M1 unit of the lower main unit of Mishrif Formation in Gharraf oil field.

b. M1.2 reservoir unit

M1.2 unit represents the second unit of the lower main unit of Mishrif Formation. The thickness of this unit is relatively uniform in the studied wells (13.37 - 46.43m). The average value of effective porosity (PHIE), water saturation (Sw_{sim}) and permeability (K_{tim}) for this unit are: 11%, 50% and 64md respectively. This unit characterized by good petrophysical properties, as it is saturated with reservoir water in the well Ga-5 and contains oil in a large proportion in the wells Ga-A1P and Ga-3. The oil reserve of this unit is 189 million cubic meters.

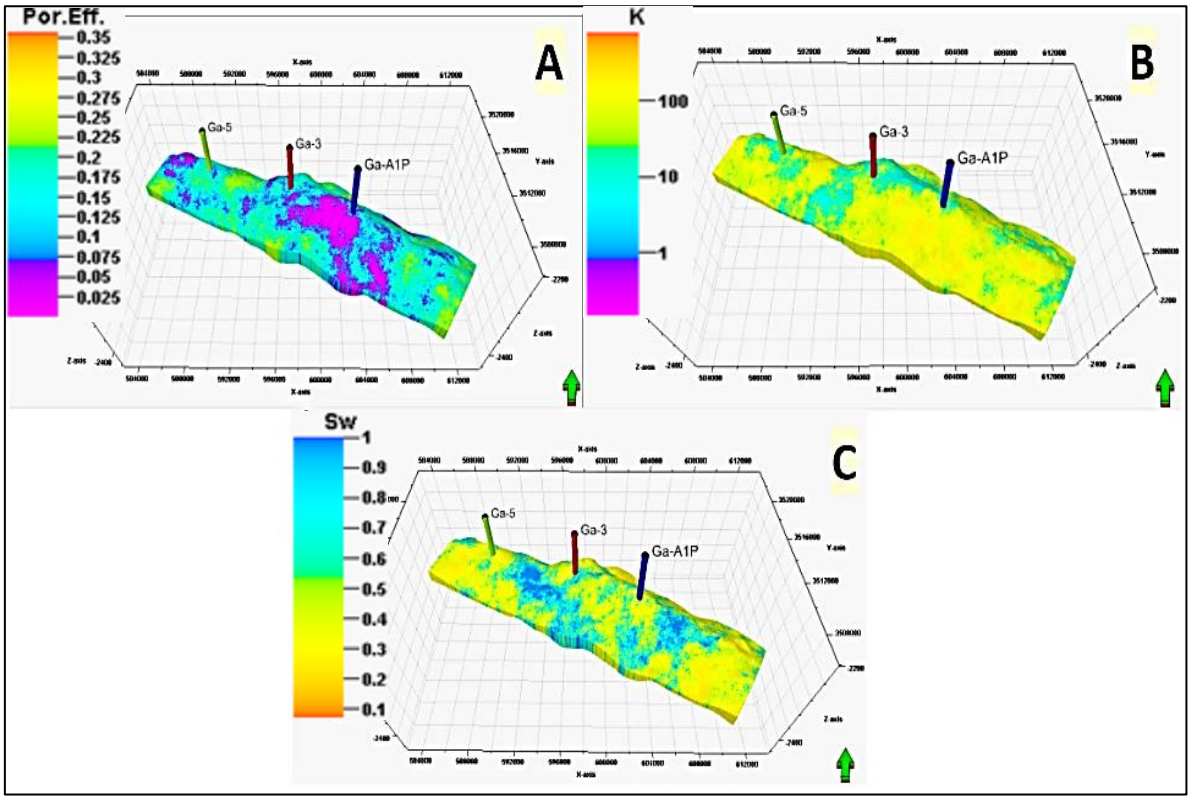

Figure (3-38): (A) Effective porosity (dec) (B) Permeability (mD) (C) Water saturation (dec) of M1.2 unit of the lower main unit of Mishrif Formation in Gharraf oil field.

c. M2 reservoir unit

M2 unit represents the third unit of the lower main unit of Mishrif Formation. The thickness of this unit is tight and ranges between 2-2.89m in the studied wells. The extension and thickness of this reservoir unit disappears towards the northwest of the Gharraf oil field, and it does not appear in well Ga-5. The average value of effective porosity (PHIE), water saturation (Sw_{sim}) and permeability (K_{tim}) for this unit are: 14%, 30% and 71md respectively. This unit has good petrophysical properties and does not contain oil in the well Ga-A1P while in the well Ga-3 it contains small quantity of oil reserve. The oil reserve of this unit is 19 million cubic meters.

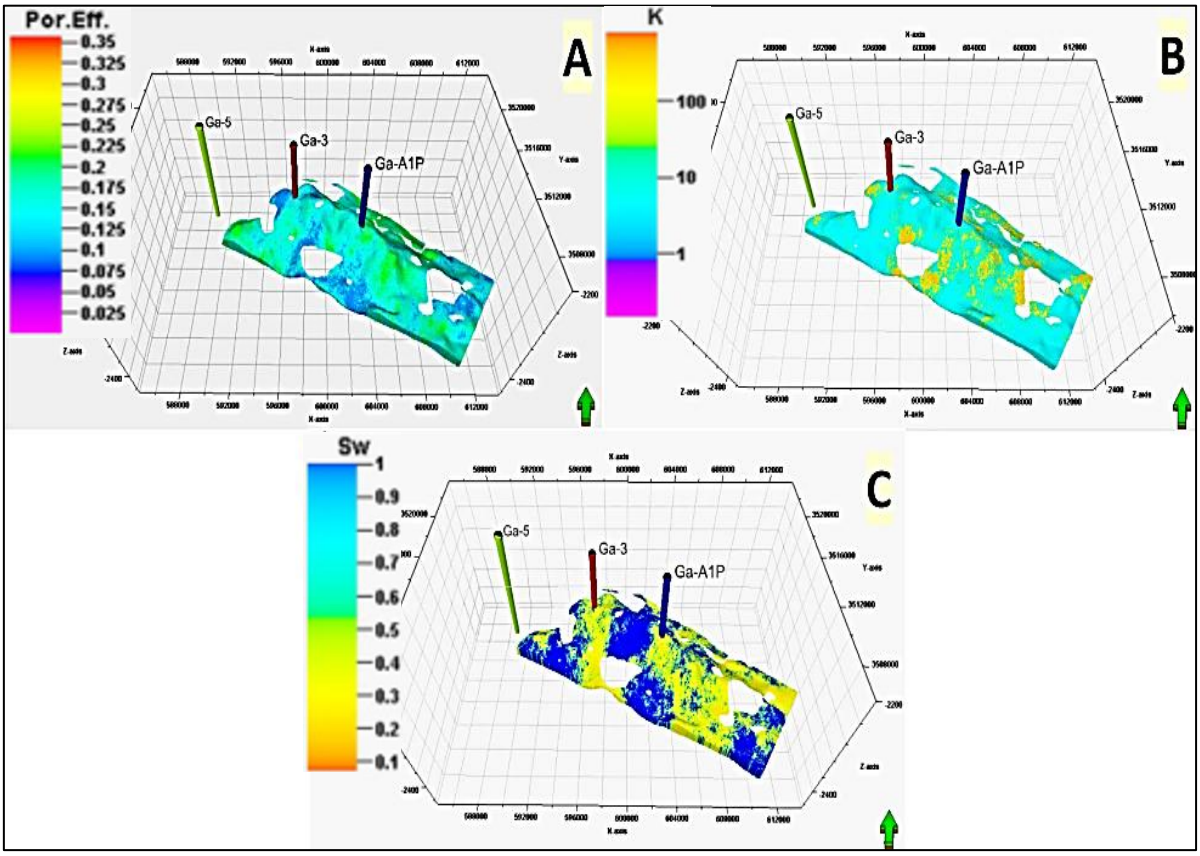

Figure (3-39): (A) Effective porosity (dec) (B) Permeability (mD) (C) Water saturation (dec) of M2 unit of the lower main unit of Mishrif Formation in Gharraf oil field.

d. L1 reservoir unit

L1 unit represents the fourth unit of the lower main unit of Mishrif Formation. The thickness of this unit is 10.71m in well Ga-A1P. The extension of this reservoir unit disappears towards the northwest of the Gharraf oil field, and it does not appear in wells Ga-3 and Ga-5. The average value of effective porosity (PHIE), water saturation (Sw_{sim}) and permeability (K_{tim}) for this unit are: 6%, 23% and 41md respectively. This unit has low petrophysical properties and it contains small quantity of oil reserve in the well Ga-A1P. The oil reserve of this unit is 17 million cubic meters.

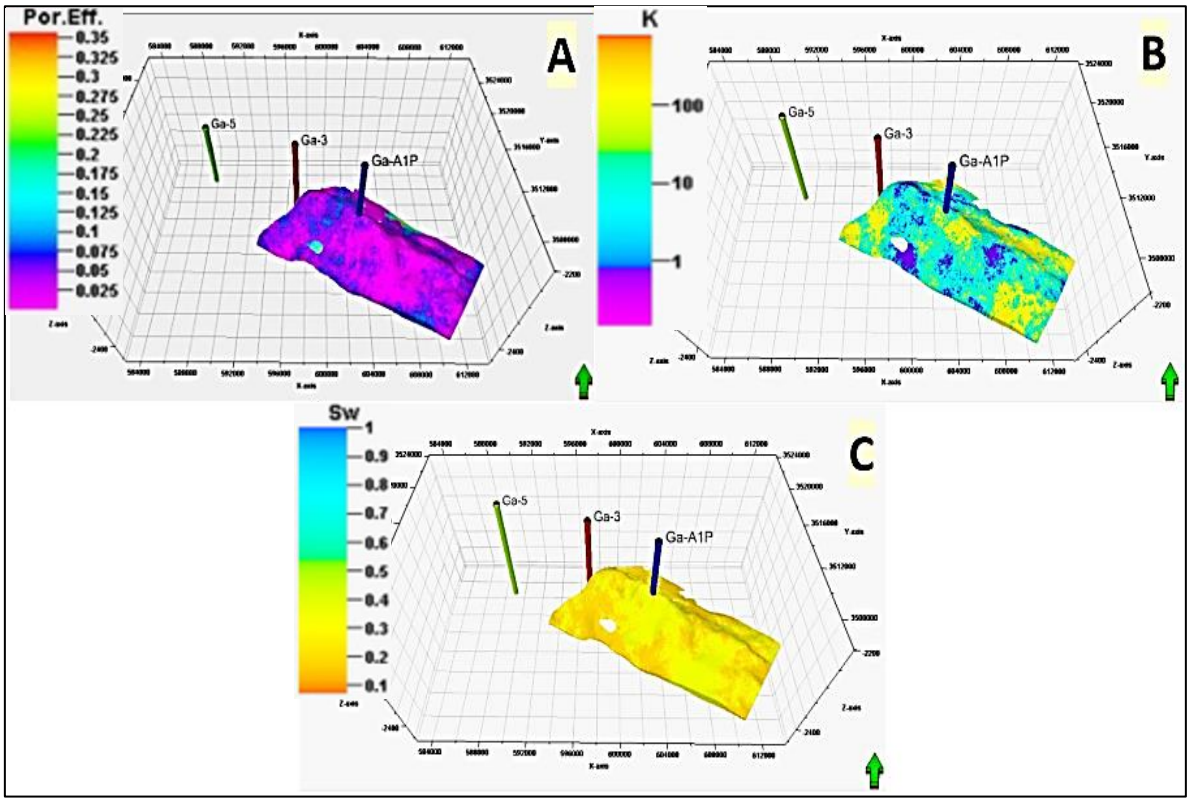

Figure (3-40): (A) Effective porosity (dec) (B) Permeability (mD) (C) Water saturation (dec) of L1 unit of the lower main unit of Mishrif Formation in Gharraf oil field.

e. L1.2 reservoir unit

L1.2 unit represents the fifth unit of the lower main unit of Mishrif Formation. The thickness of this unit ranges between 28.22-37.29m in the studied wells. The extension and thickness of this reservoir unit disappears towards the northwest of the Gharraf oil field, and it does not appear in Well Ga-5. The average value of effective porosity (PHIE), water saturation (Sw_{sim}) and permeability (K_{tim}) for this unit are: 22%, 16% and 343md respectively. This unit has good petrophysical properties, and it is considered as one of the best reservoir unit for oil. It is the largest reservoir unit for the Mishrif Formation, where it contains a large quantity of oil reserve in the two wells Ga-A1P and Ga-3. The oil reserve of this unit is 220 million cubic meters. Both units L1.2 and L2 are considered as the best reservoir units of Mishrif Formation, where they contain economical quantity of oil reserves in the reservoir (584 million cubic meters).

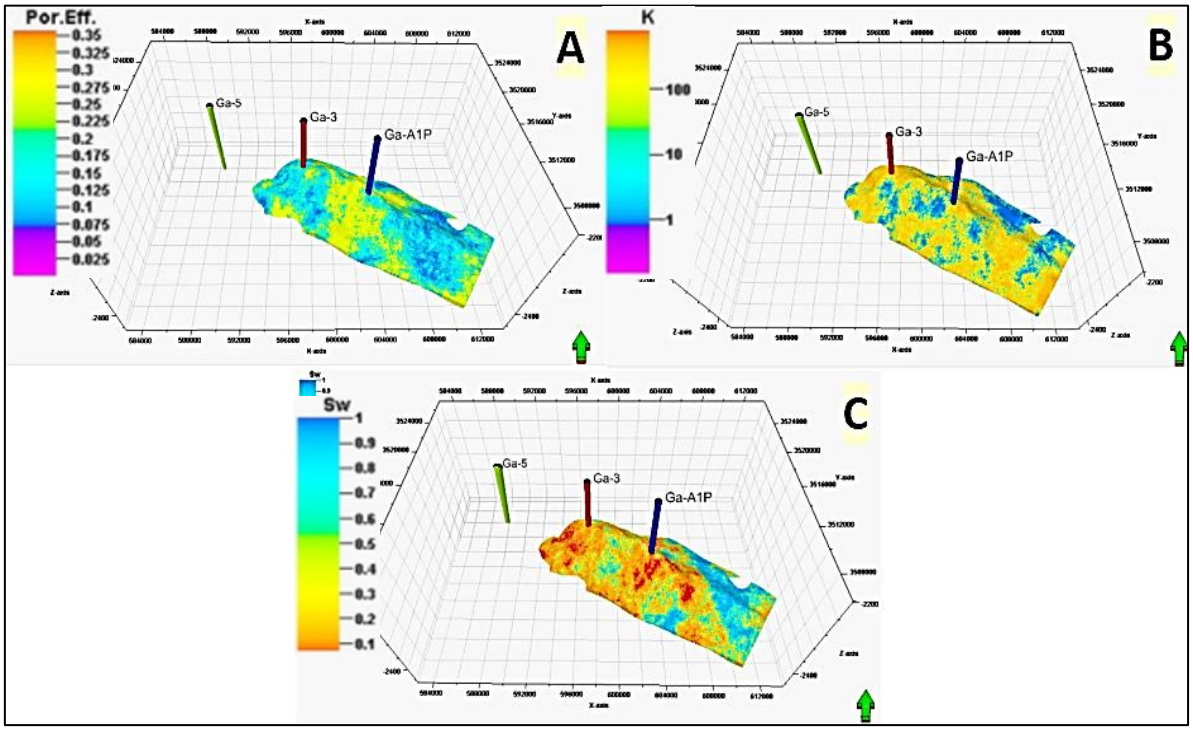

Figure (3-41): (A) Effective porosity (dec) (B) Permeability (mD) (C) Water saturation (dec) of L1.2 unit of the lower main unit of Mishrif Formation in Gharraf oil field.

f. L2 reservoir unit

L2 unit represents the sixth unit of the lower main unit of Mishrif Formation. The thickness of this unit ranges between 10.85-27.28m in the studied wells. This unit extends over the entire oil field and appears in all wells and thickens towards well Ga-5. The average value of effective porosity (PHIE), water saturation (Sw_{sim}) and permeability (K_{tim}) for this unit are: 18%, 38% and 80md respectively. This unit has good petrophysical properties but contains less quantity of oil in the two wells Ga-A1P and Ga-5 and a large quantity of oil in the well Ga-3. It is considered as one of the best reservoir unit for oil. The oil reserve of this unit is 364 million cubic meters. Both units L2 and L1.2 are considered as the best reservoir units of Mishrif Formation, where they contain economical quantity of oil reserves in the reservoir (584 million cubic meters).

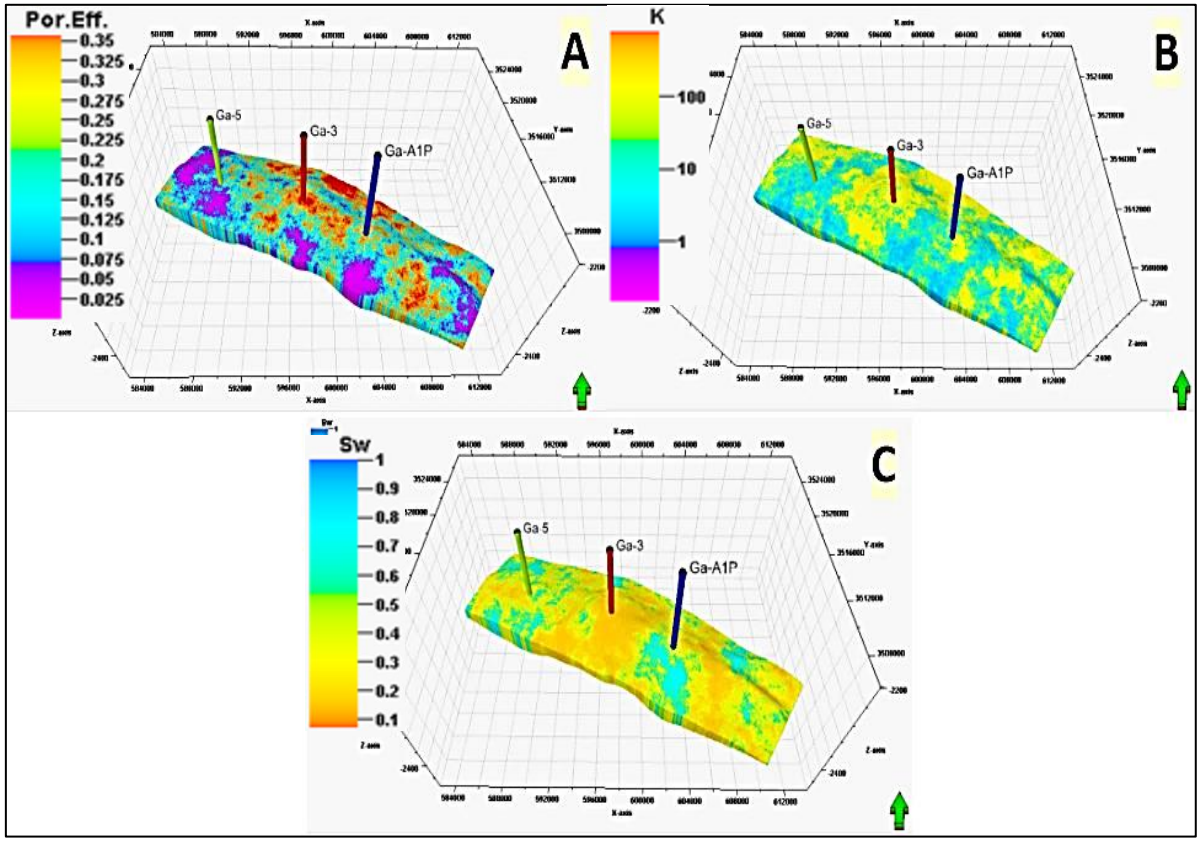

Figure (3-42): (A) Effective porosity (dec) (B) Permeability (mD) (C) Water saturation (dec) of L2 unit of the lower main unit of Mishrif Formation in Gharraf oil field.

g. L2.2 reservoir unit

L2.2 unit represents the seventh unit of the lower main unit of Mishrif Formation. The thickness of this unit ranges between 5.96-18.87m in the studied wells. This unit extends over the entire oil field and appears in all wells and the highest thickness of this unit appears at well Ga-3. The average value of effective porosity (PHIE), water saturation (Sw_{sim}) and permeability (K_{tim}) for this unit are: 15%, 68% and 94md respectively. This unit has medium to low petrophysical properties as it is almost completely saturated with reservoir water in the well Ga-A1P and contains a medium quantity of oil in the well Ga-3 and a small quantity in the well Ga-5. The oil reserve of this unit is 40 million cubic meters.

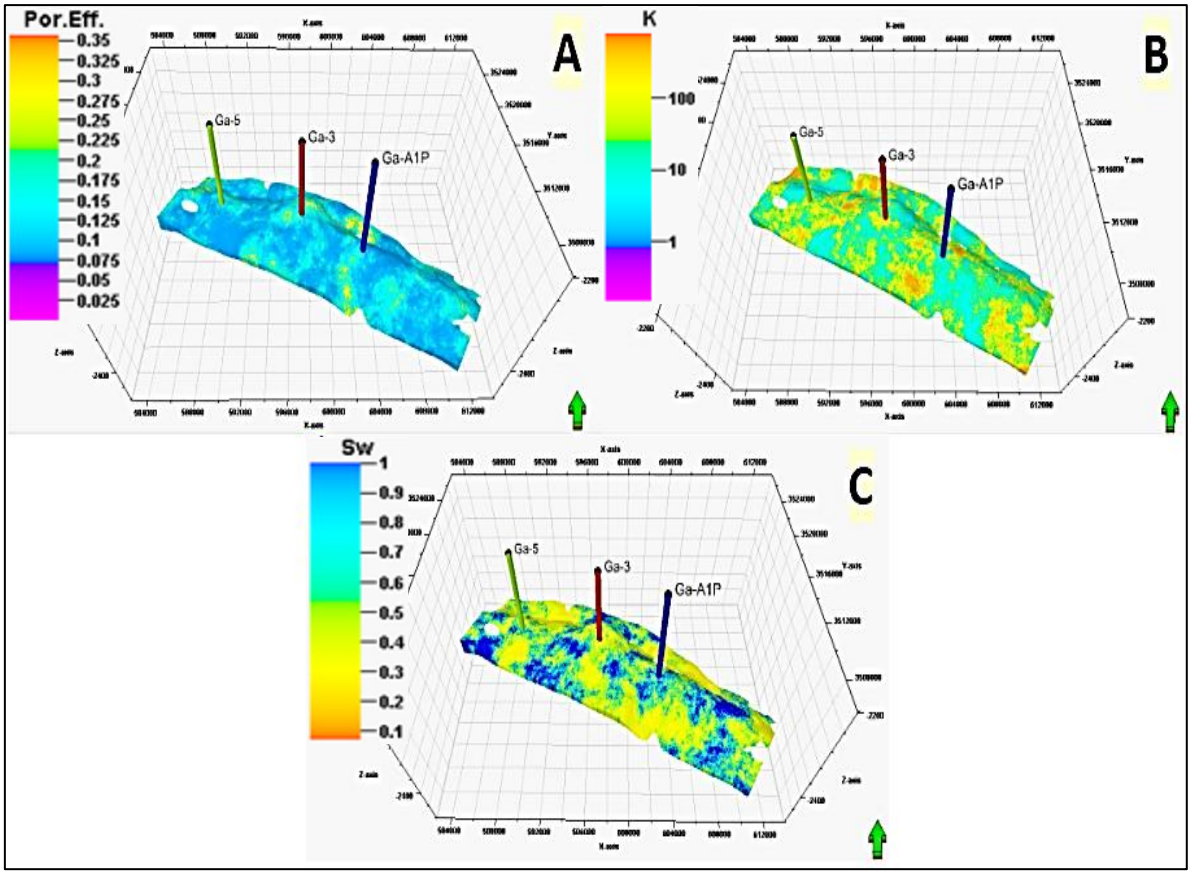

Figure (3-43): (A) Effective porosity (dec) (B) Permeability (mD) (C) Water saturation (dec) of L2.2 unit of the lower main unit of Mishrif Formation in Gharraf oil field.

h. L2.3 reservoir unit

L2.3 unit represents the eighth reservoir unit of the lower main unit of Mishrif Formation. The thickness ranges between 14.88-32.50m in the studied wells. This unit extends over the entire oil field and appears in all wells and the highest thickness of this unit appears at well Ga-3. The average value of effective porosity (PHIE), water saturation (Sw_{sim}) and permeability (K_{tim}) for this unit are: 16%, 78% and 77md respectively. This unit has medium to low petrophysical properties as it is completely saturated with reservoir water in the well Ga-A1P and a large proportion of it in the well Ga-5 and contains a medium quantity of oil in the well Ga-3. The oil reserve of this unit is 81 million cubic meters.

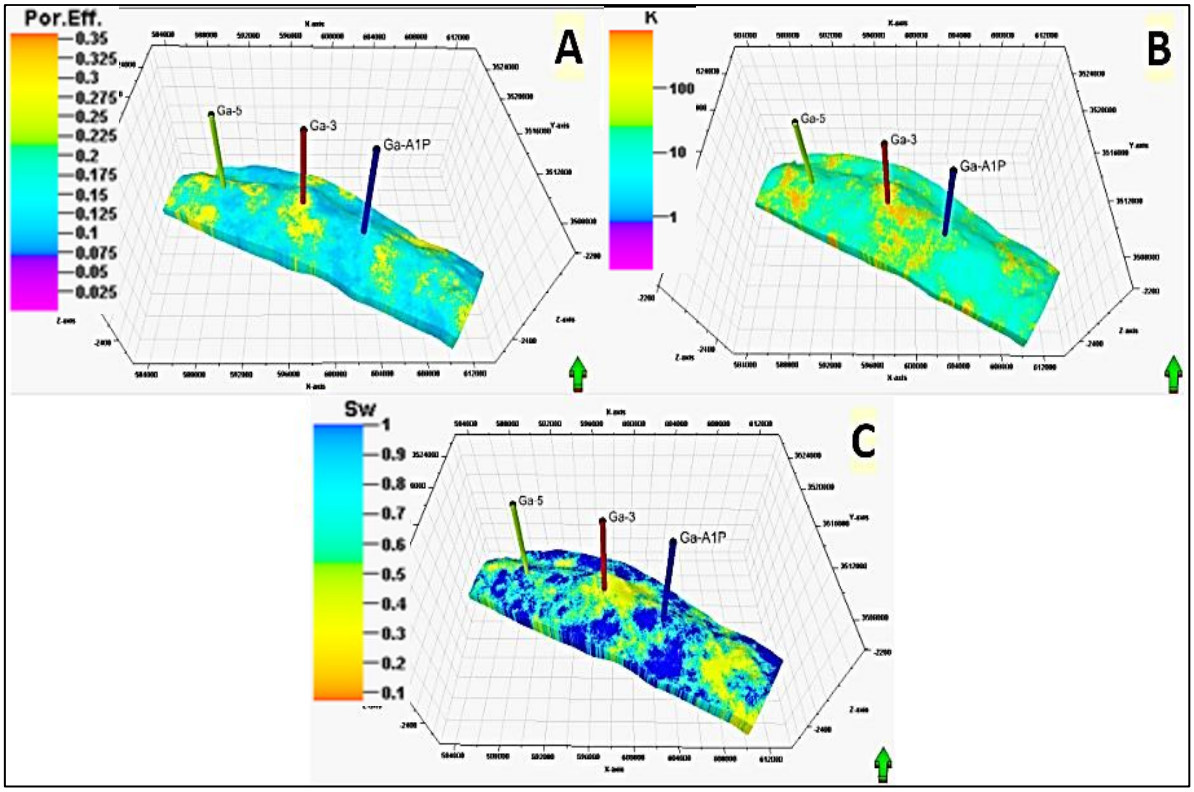

Figure (3-44): (A) Effective porosity (dec) (B) Permeability (mD) (C) Water saturation (dec) of L2.3 unit of the lower main unit of Mishrif Formation in Gharraf oil field.

i. L2.4 reservoir unit

L2.4 unit represents the ninth reservoir unit of the lower main unit of Mishrif Formation. The thickness of this unit ranges between 10.06-26.85m in the studied wells. This unit extends over the entire area of the oil field and appears in all studied wells and the highest thickness of this unit appears at well Ga-3. The average value of effective porosity (PHIE), water saturation (Sw_{sim}) and permeability (K_{tim}) for this unit are: 14%, 87% and 15md respectively. This unit has low petrophysical properties as it is completely saturated with reservoir water in the wells Ga-A1P and Ga-5, and a large quantity of it in the well Ga-3. The oil reserve of this unit is 4 million cubic meters.

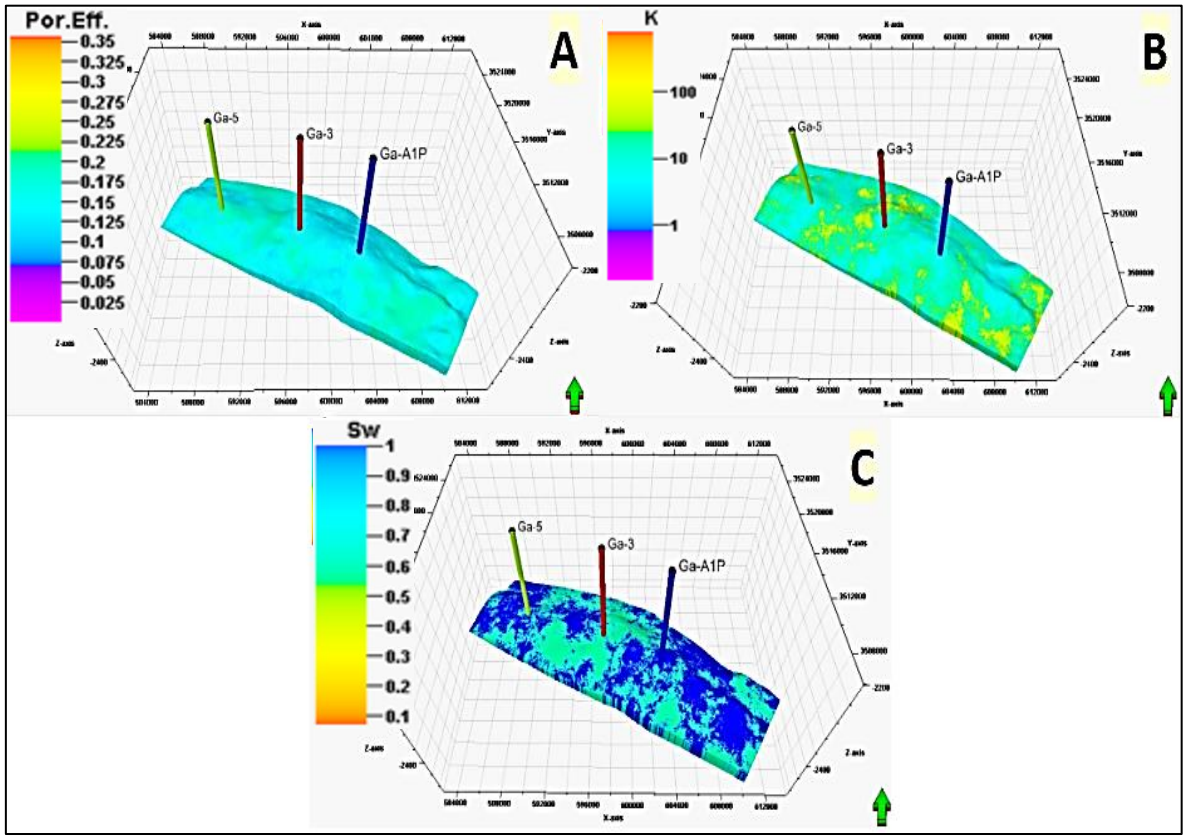

Figure (3-45): (A) Effective porosity (dec) (B) Permeability (mD) (C) Water saturation (dec) of L2.4 unit of the lower main unit of Mishrif Formation in Gharraf oil field.

3.3.11. Petrophysical evaluation of Yamama reservoir units

a. YA unit

YA unit represents the upper reservoir unit of Yamama Formation. The thickness of this unit ranges between 78.54-85m in the studied wells. The average value of effective porosity (PHIE), water saturation (Sw_{sim}) and permeability (K_{tim}) for this unit are: 11%, 26% and 119md respectively. This unit has good petrophysical properties, and it is considered the best reservoir unit for oil of Yamama Formation. It contains a large quantity of oil in the studied wells Ga-1, Ga-2 and Ga-3. The oil reserve of this unit is 469 million cubic meters.

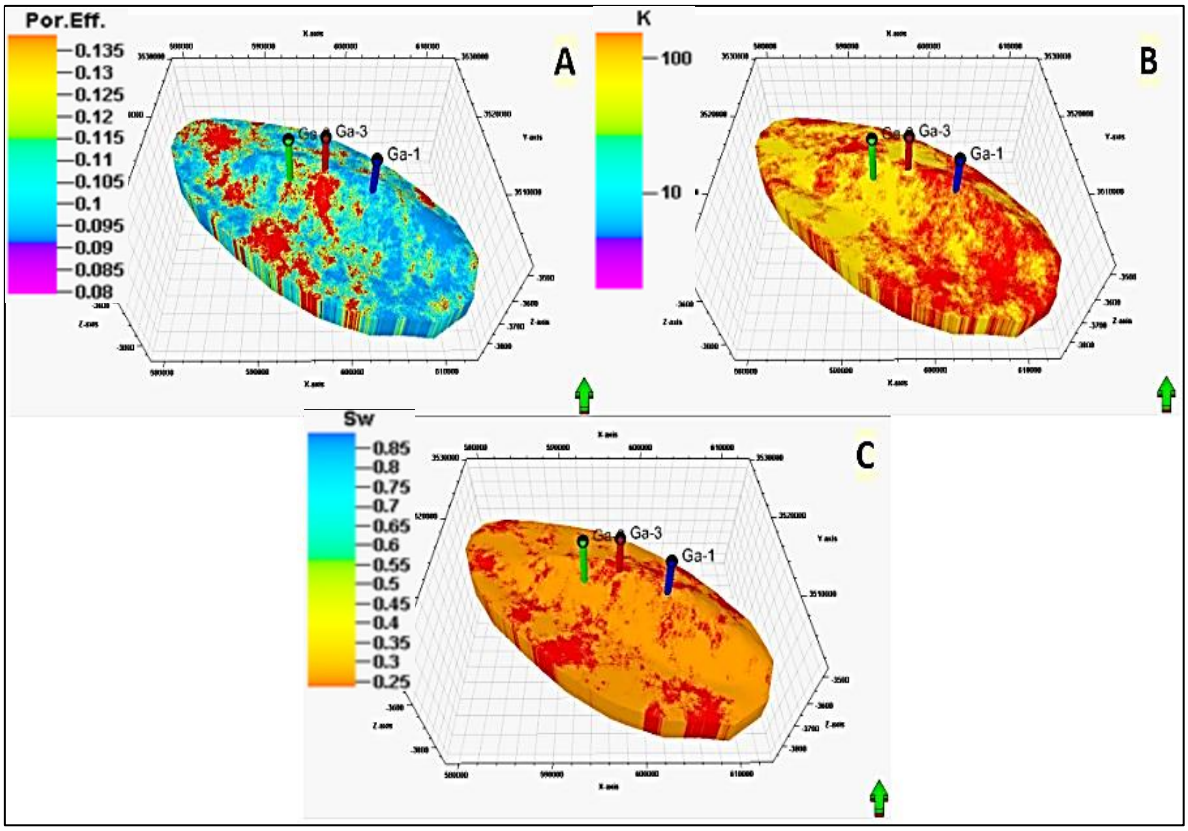

Figure (3-46): (A) Effective porosity (dec) (B) Permeability (mD) (C) Water saturation (dec) of YA unit of Yamama Formation in Gharraf oil field.

b. YB1 unit

YB1 unit represents the middle reservoir unit of Yamama Formation. The thickness of this unit ranges between 41-48m in the studied wells. The average value of effective porosity (PHIE), water saturation (Sw_{sim}) and permeability (K_{tim}) for this unit are: 10%, 61% and 7md respectively. This unit has medium to low petrophysical properties as it contains a large quantity of reservoir water in the studied wells with a small proportion of oil. The oil reserve of this unit is 8 million cubic meters.

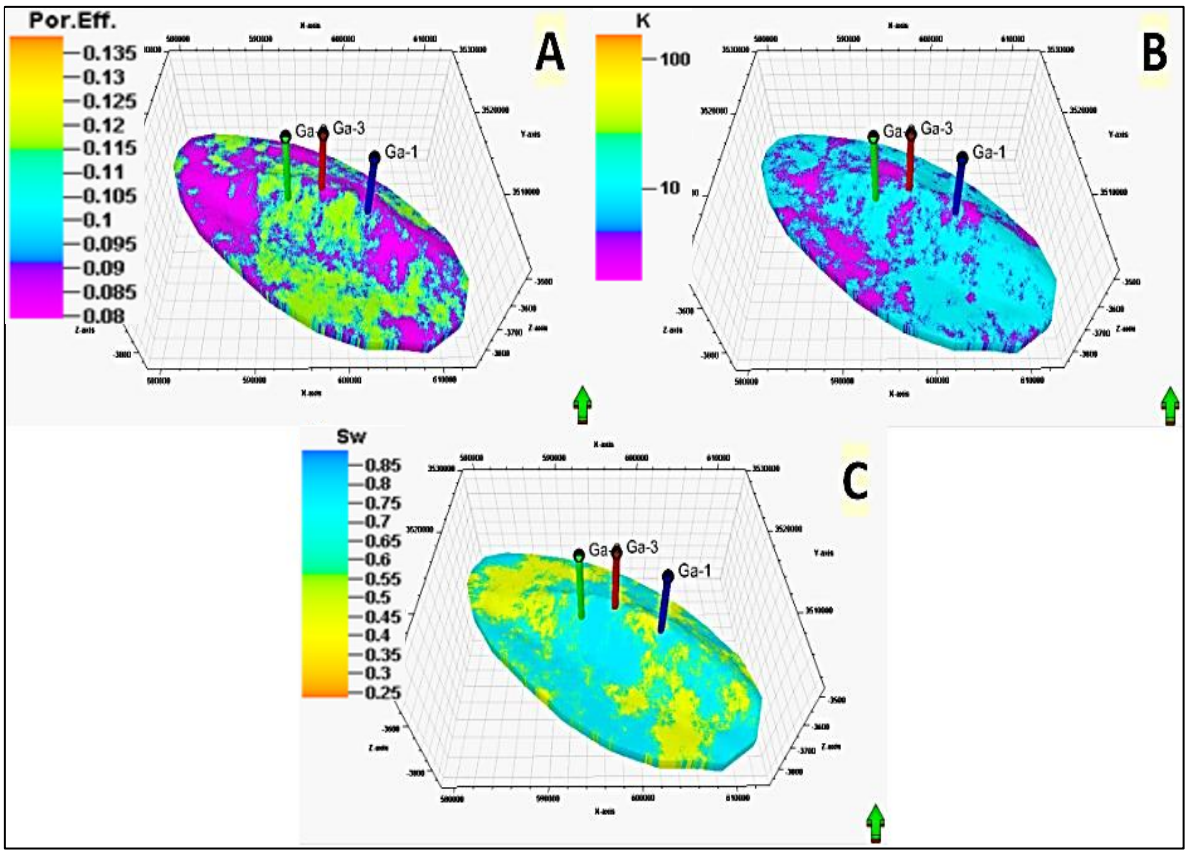

Figure (3-47): (A) Effective porosity (dec) (B) Permeability (mD) (C) Water saturation (dec) of YB1 unit of Yamama Formation in Gharraf oil field.

c. YB2 unit

YB2 unit represents the lower reservoir unit of Yamama Formation. The thickness of this unit ranges between 136-161m in the studied wells. The average value of effective porosity (PHIE), water saturation (Sw_{sim}) and permeability (K_{tim}) for this unit are: 11%, 70% and 14md respectively. This unit has low petrophysical properties as it contains a large quantity of reservoir water in the studied wells. There is no oil reserve in this unit.

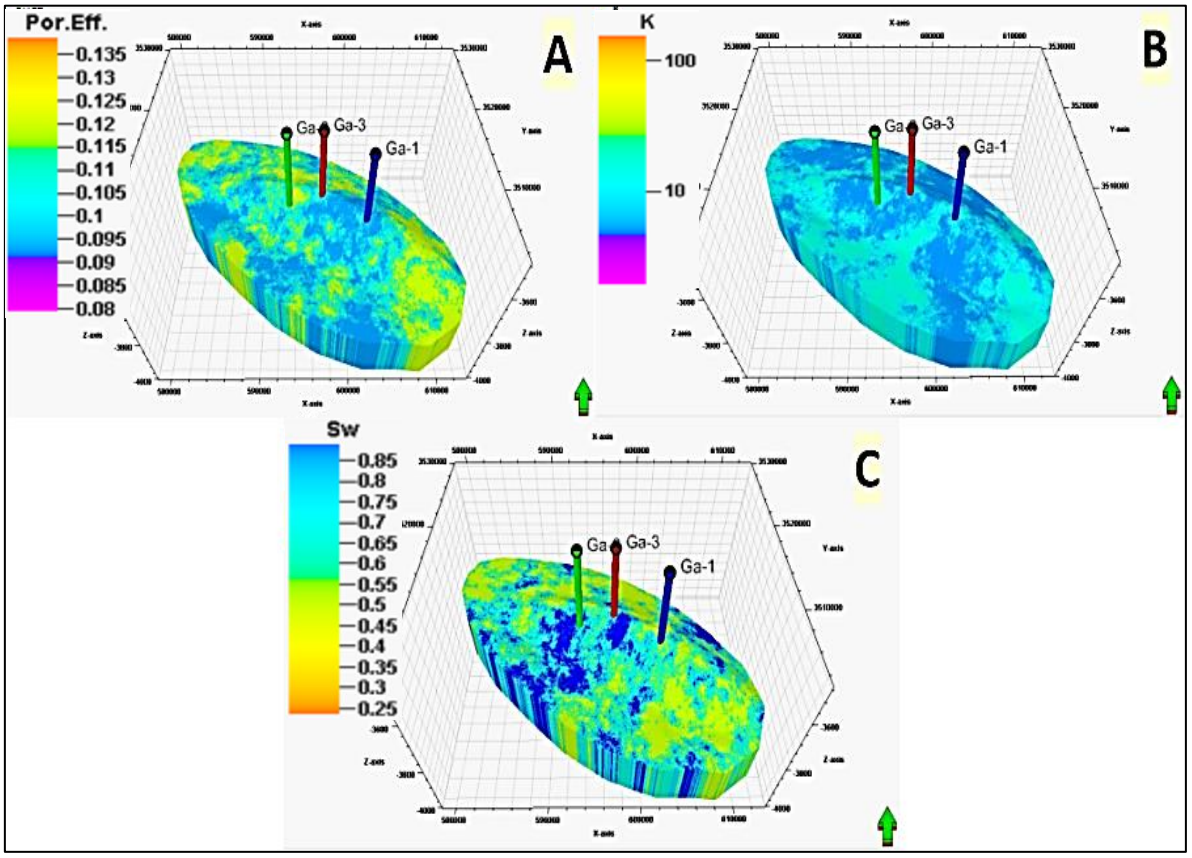

Figure (3-48): (A) Effective porosity (dec) (B) Permeability (mD) (C) Water saturation (dec) of YB2 unit of Yamama Formation in Gharraf oil field.

3.3.12. Fluid contacts

The oil water contacts for the Mishrif and Yamama reservoirs were used by Petrel software in order to calculate the oil reserves in the studied reservoirs. As it is known, no clear limit can be determined for oil-water contact, so these contacts have been predicted of some of studied wells depending on the net pay and gross thickness measurements and also from the comparison between resistivity logs (Rt and Rxo) depending on their crossing which occurs due to the direct decrease in the value of the true resistivity (Rt) of the formation relative to the resistivity of the invaded zone (Rxo) because of the increase in water saturation relative to hydrocarbon saturation, and the other contacts of the studied wells were taken from the final reports of these wells (Figure 3.27 and Figure 3.28) (Table 3-5).

Table (3-5): The oil-water contacts in the studied wells of Gharraf oil field**.**

Formations	Wells	OWC depth(m) (RTKB)
Mishrif	Ga-A1P	2383
	Ga-3	2407
	Ga-5	2417
Yamama	Ga-1	3678
	Ga-2	3703
	Ga-3	3688

3.3.13. Hydrocarbon reserves estimation

Reserves are the part of the stock tank oil initially in place (STOIIP) that may be in fact produced for a given development date, or those quantities of petroleum which are expected to be commercially regained from known accumulations from a certain date onward, all reserve estimates include some degree of uncertainly**.** The most important methods used to calculate the volume of hydrocarbons stored within oil or gas reservoirs are:

1. Volumetric method.

2. Material balance method.

3. Production decline method.

The first method is used after the exploration and development of the field, the other methods are used after a period of time on production and provide data on reservoir pressure change with a time and provide sufficient data on the properties of reservoir fluids and production data (Darling, 2005).

After the static geological model of the studied formations has been completed and the fluid contacts (OWC) as well as the distribution of reservoir petrophysical properties has been determined, initial oil in place (STOIIP) of the studied reservoirs has been calculated using Petrel software. This study shows that the volume of initial oil in place (STOIIP) in the reservoir part of Mishrif Formation of Gharraf oil field is 938 million cubic meters, which is equal to 5900.02 million barrels, see Table (3-6), and in the Yamama Formation of Gharraf oil field is 477 million cubic meters, equal to 3000.33 million barrels, see Table (3-7). The calculations of this study were achieved by using Petrel software after fluid contacts was determined and entered, as well as the dependence of the estimation on the petrophysical properties (porosity, permeability and water saturation) of the studied reservoirs.

Table (3-6): Illustrating Hydrocarbon reserve estimation results of the lower unit of Mishrif Formation in Gharraf oil field.

Mishrif zones	Bulk volume [*10^6 m3]	Net volume [*10^6 m3]	Pore volume [*10^6 rm3]	HCPV oil [*10^6 rm3]	STOIIP (in oil) [*10^6 sm3]
M1	964	675	43	6	4
M1.2	5192	3635	528	264	189
M2	869	608	96	26	19
L1	1533	1073	33	24	17
L1.2	3903	2732	485	308	220
L2	6091	4264	777	509	364
L2.2	1825	1278	150	56	40
L2.3	3083	2158	367	114	81
L2.4	393	275	38	5	4
Total	**23853**	**16698**	**2517**	**1312**	**938**

Table (3-7): Illustrating hydrocarbon reserve estimation results of Yamama Formation in Gharraf oil field.

Yamama zones	Bulk volume [*10^6 m3]	Net volume [*10^6 m3]	Pore volume [*10^6 rm3]	HCPV oil [*10^6 rm3]	STOIIP (in oil) [*10^6 sm3]
YA	19666	7866	872	657	469
YB1	782	313	30	11	8
YB2	0	0	0	0	0
Total	**20488**	**8179**	**902**	**668**	**477**

- ✓ **rm^3:** reservoir cubic meter.
- ✓ **sm^3:** standard cubic meter.
- ✓ **HCPV:** hydrocarbon pore volume.
- ✓ **STOIIP:** stock-tank oil initially in place.

Chapter Four

Oil Generation

and

Basin Modeling

4.1. Preface

This chapter includes interpretation of the organic geochemistry analysis results for the Mishrif crude oil sample took from Gharraf oil field Well Ga-1, bulk properties and biomarkers ratios, in order to determine the type of generated source rocks, type of depositional environment, redox conditions, type of organic matter (kerogen), and age of generated source rocks of the Gharraf oil field petroleum system. Also includes building 1D petroleum system models (burial history chart, thermal history chart, and events chart) for Well Ga-1 of Gharraf oil field and determine the temporal relationship between essential elements, the rock units, preservation time, processes, and critical moment for the Gharraf oil field total petroleum system. Finally, oil-probable source rocks correlation using the bulk geochemical, molecular and carbon isotopic characteristics of the crude oil sample from Mishrif reservoir Well Ga-1 were established in order to confirm the relationship between the Mishrif formation crude oil and the source rocks generating this oil.

Many basin models of the Gharraf oil field of the southern Mesopotamian Basin, were built in this study so as to quantify key aspects of this petroleum system. The model's required inputs are seismic interpretation, stratigraphic, and geological data as well as organic geochemical data for potential source rocks and oils.

The Middle-Upper Jurassic to Early-Late Cretaceous petroleum system of the southern Mesopotamian Basin of Iraq contains several oil-prone source rocks, reservoirs, and local and regional seal rocks resulting in the presence of several giant oil and gas fields, (Ibrahim, 1983; Aqrawi *et al.*, 2010). Most oils of southern Iraq, which are mainly trapped in Lower and Upper Cretaceous sandstone and carbonate reservoirs, were generated mainly from organic matter-rich of the Upper Jurassic to Lower Cretaceous carbonate source rocks (Al-Ameri *et al.*, 2009; Abeed *et al.*, 2012; Al-Khafaji *et al.*, 2021).

4.2. Petroleum System Processes

4.2.1. Petroleum generation

As temperature and pressure increase during burial, organic materials generate oil and gas. In general, this thermal maturation mechanism produces a sequence of gradually smaller hydrocarbon molecules, with increasing volatility and hydrogen content, culminating with methane gas. And, as the kerogen matures thermally, its chemical composition gradually changes, eventually converting it into a carbonaceous residue with a lower H-content (Hood *et al.*, 1975). The pathways of thermal maturation and evolution of kerogen as shown in Figure (4-1), include three main stages according to (Tissot *et al.*, 1974) are; diagenesis stage, catagenesis stage, and metagenesis stage.

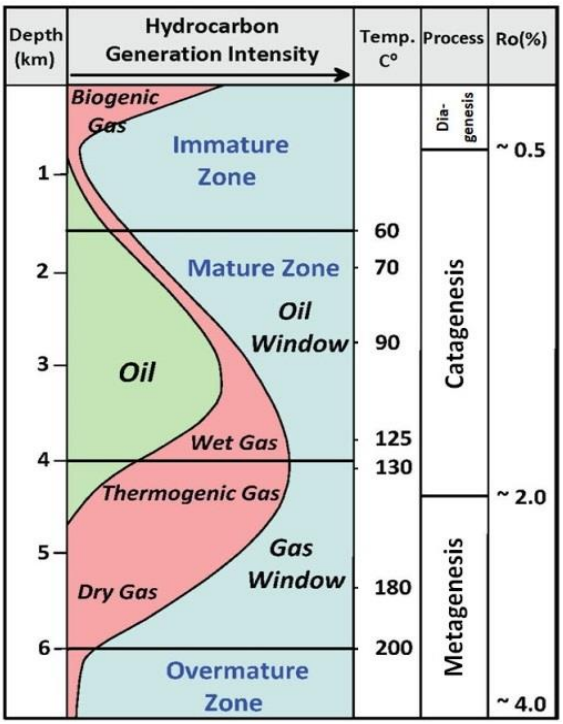

Figure (4-1): Shows the stages of the thermal conversion of kerogen. Modified from (Tissot *et al.*, 1974).

According to the simulation of the rock samples data of the selected formations of Gharraf oil field Well Ga-1 by Petromod software, the transformation ratio parameter refers that the source rocks in Sulaiy, Yamama, Ratawi and Zubair formations in which the organic matter (totally or partially)

began to mature and transform into oil and gas during the geological period represented in the Upper Cretaceous for Sulaiy, Yamama, Ratawi, and lower shale of Zubair formations, and the Paleocene age for the upper shale of Zubair Formation, due to the availability of the appropriate temperature for the maturation of the organic matter in each of these formations during these geological time periods, the expulsion process still not occurs for hydrocarbons from these source rocks formations.

4.2.2. Petroleum expulsion and migration

Where favorable conditions are met, petroleum products produced by thermal cracking at the expense of kerogen can leave the source rock during expulsion during geological periods. Petroleum migration is the stage during which hydrocarbons migrate into and remain trapped in a reservoir during the creation of a petroleum system, see Figure (4-2). Expelling happens on many scales, which makes it harder to grasp than the processing of oil. Petroleum products have to leave solid kerogen particles at the smallest size. Petroleum needs to find its way into the network of pores and micro-fractures at the size of source rock lamina (Burrus, 1998).

Petroleum migrates along the most permeable strata at the scale of beds that will move petroleum to the reservoirs; this marks the end of primary migration and the beginning of secondary migration. The expelling of petroleum does not immediately follow the generation of petroleum, but needs certain requirements to be met. These expelling thresholds are also expressed in the porosity of the source rock as minimum petroleum saturation, or as a critical retention threshold on the organic matter. Both definitions suggest that only when the source rock contains a large enough quantity of petroleum does expel become successful. A distinct-phase transport process is the mechanics of petroleum expelling. This implies that when a hydraulic disequilibrium occurs between the petroleum process present in the source rock and out of the source rock, expelling takes place. This imbalance can be caused by gravity,

which tends to establish pathways of vertical upward migration of petroleum, over-pressure and capillary forces (source rocks are normally tighter than carrier beds, therefore having higher overpressures and higher capillary pressures than carrier beds), which can lead to downward expulsion (Burrus, 1998).

It is commonly accepted that the phase state of petroleum products within mature strata is supercritical. When milder temperatures and pressures are met, liquid and gaseous petroleum breaks along migration pathways towards the surface. An additional expelling process, which primarily affects gas migration, is molecular diffusion. Compared to the composition of petroleum produced in the source rocks, retention processes appear to deplete the expelled petroleum in heavy compounds and aromatics (Burrus, 1998).

4.2.3. Petroleum accumulation

Petroleum accumulation and reserve occur when an impermeable shale or thick layer of rock is encountered by migrating fluids. It's called a trap here. The fluids tend to stratify after accumulation according to their relative densities: gas, oil, and water. They appear to flow to the surface or deposited on the ocean floor if the migrating fluids do not encounter a trap, such as: seepages, natural gas escapes, and bituminous lakes (Zhao *et al.*, 2017).

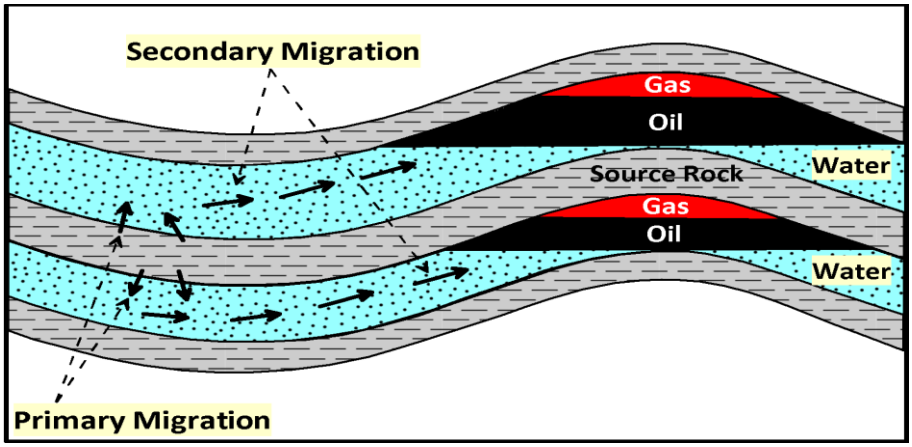

Figure (4-2): Showing primary and secondary migration, and accumulation of hydrocarbons. Modified from (Borazjani *et al.*, 2019).

After the organic matter matured (fully or partially) in the source rocks of the formations: Sulaiy, Yamama, Ratawi, and Zubair due to the availability of the suitable pressure and temperature at the appropriate depths, hydrocarbons (oil and gas) began to flow from the source rocks and moved through the migration paths represented by connected gaps, cracks, faults and fractures. The hydrocarbons moved in all directions according to the nature of the available migration path, until they were collected in the reservoir rocks, either of the same formation as in Yamama Formation and Zubair Formation of Lower Cretaceous, or another formation that possessed only reservoir characteristics, such as Mishrif Formation of Upper Cretaceous.

4.3. Crude Oil Organic Geochemistry

The most important petroleum exploration objectives are determined by combining geochemical knowledge of source rocks with knowledge of generation, migration, and accumulation processes, as well as the geophysical and geological characteristics of the sedimentary basin under evaluation (Martinelli, 2009).

4.3.1. Mishrif oils geochemistry

Geochemical tests were conducted on one sample of crude oil, which was taken from Mishrif reservoir in the Gharraf oil field Well (Ga-1), in order to determine depositional environments, thermal maturity, and age of source rocks which produced these oils depending on the tests results represented by bulk properties and biomarker ratios of the Mishrif reservoir crude oil sample (Table 4-1).

Table (4-1): **(A)** Bulk property values and chemical composition results of the Mishrif crude oil from Ga-1 of Gharraf oil field in the southern Mesopotamian Basin, Southern Iraq, and **(B)** selected biomarker parameters ratios of the Mishrif crude oil.

(A); Bulk Properties														
No.	Oil Wells	Formation	API Gravity	S%	Pr/Ph	Pr/n-C17	Ph/n-C18	C15+ Saturate	C15+ Aromatic	C.V.	Sat%	Aro%	NSO%	Asph%
1	Ga-1	Mishrif	27.2°	4.2	0.79	0.22	0.33	-27.23	-27.53	-3.87	25	56.2	13.2	5.6
(B); Sterane and hopane ratio														
No.	Oilfield	Formation	C22/C21	C24/C23	C26/C25	C29/H	C31R/H	GA/C31R	C35S/C34S	C28%	C29%	C27 Ts/Tm	C29 Ts/Tm	TAS3 (CR)
1	Ga-1	Mishrif	1.04	0.27	0.72	1.6	0.32	0.24	1.11	25.9	39.4	0.18	0.07	0.31

- ✓ API: Gravity degree.
- ✓ S : Sulfur
- ✓ Sat.: Saturated hydrocarbons
- ✓ Aro.: Aromatic hydrocarbons
- ✓ Asph.: Asphaltene.
- ✓ C.V.: Canonical variable.
- ✓ NSO: Nitrogen, Sulfur, and Oxygen compounds.
- ✓ Pr : Pristane.
- ✓ Ph : Phytane
- ✓ Ts: (C27 18α(H)-22,29,30-trisnorneohopane)
- ✓ Tm: (C27 17α(H)-22,29,30-trisnorhopane)
- ✓ C22/C21, C24/C23, and C26/C25: Tricyclic terpanes.
- ✓ C29/H: 30-Norhopane/hopane, also expressed as C29/C30 hopane.
- ✓ C31R/H: C31 regular homohopane/C30 hopane.
- ✓ C29/C30: C29 norhopane/C30 hopane
- ✓ GA/C31R: Gammacerane/C31 22R hopane.
- ✓ C35S/C34S: C35 homohopane/C34 homohopane.

4.3.2. Mishrif oils' source rocks depositional environments

The studied oil sample had a low (resins + asphaltenes) composition is 18.8% for Mishrif sample. The weight percentages of aromatic and saturated hydrocarbon fractions were 56.2%, and 25%, respectively. The results indicated that this oil sample was non-biodegradable, and considered to be aromatic oils, see Figure (4-3).

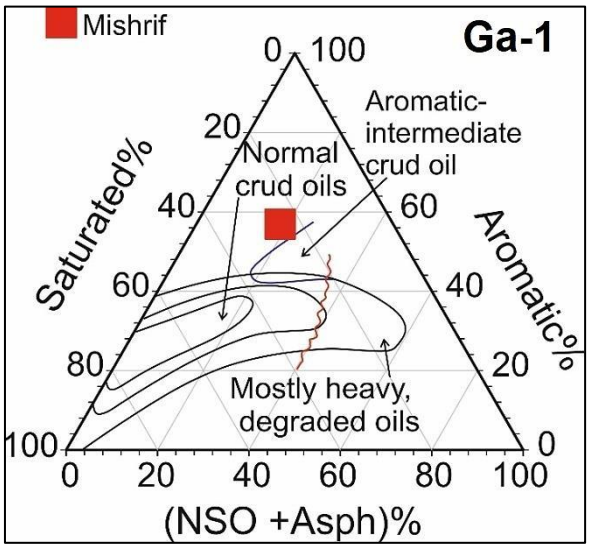

Figure (4-3): Ternary diagram displaying the weight percentage of the gross composition of saturated and aromatic hydrocarbons, resins, and asphaltenes of Mishrif crude oil sample, Well Ga-1. Modified after (Tissot & Welte, 1984).

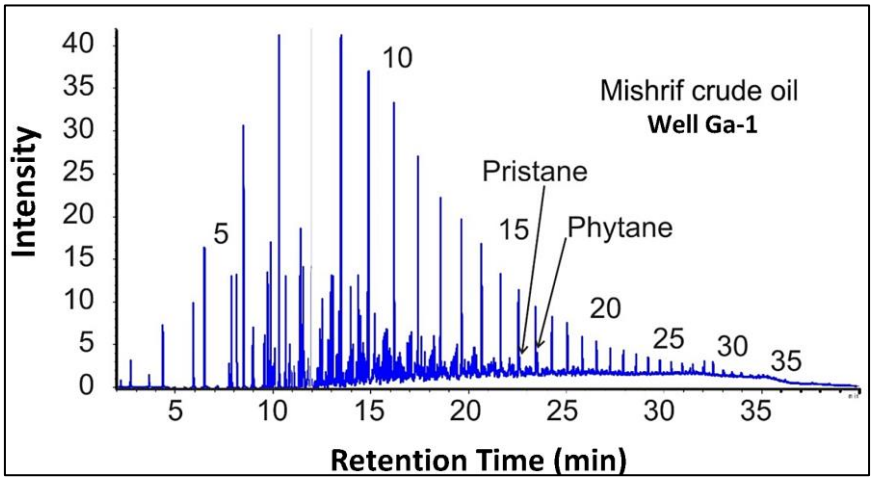

Figure (4-4): The gas chromatogram of the Mishrif crude oil sample, saturated hydrocarbon fraction, Well Ga-1.

The Figure (4-4) shows the gas chromatograms of the examined oil, which is dominated by light n-alkanes or normal alkanes and acyclic isoprenoid biomarkers. This indicates that the oil was not biodegradable, therefore Mishrif oil is aromatic.

The carbon isotope ($\delta^{13}C$) composition of the saturated and aromatic fractions is frequently used to identify marine from terrigenous organic matters input. For the Mishrif sample, the C_{15}+ Saturate and C_{15}+ Aromatic analytical values are -27.23‰, and -27.53‰, respectively. See Figure (4-5). These findings revealed that the organic materials originated in the marine depositional environment (Sofer, 1984).

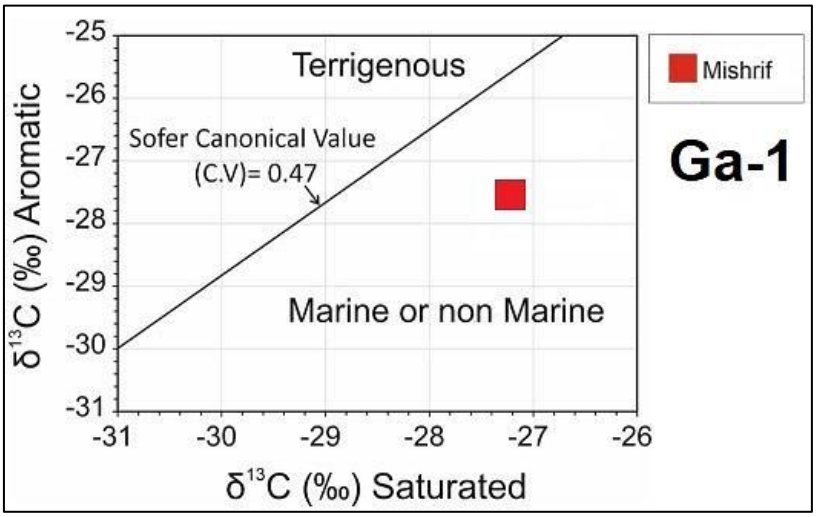

Figure (4-5): Plot of the $\delta^{13}C$ values of aromatic fractions versus of the $\delta^{13}C$ values of saturated fractions for Mishrif analyzed sample, Well Ga-1, after (Sofer, 1984).

The most major acyclic isoprenoid hydrocarbons found in source rocks and oil are pristane and phytane. The acyclic isoprenoid (Pr/Ph) ratio is widely utilized as a redox status indicator (Didyk *et al.*, 1978). The Pr/nC$_{17}$ and Ph/nC$_{18}$ ratios (Figure 4-6) of the Mishrif oils are 0.22 and 0.33 respectively indicated marine type of kerogen (Type II) of the propel source rocks, non-biodegradation oils, and anoxic depositional environment of Mishrif oils in Gharraf oil field, Well Ga-1.

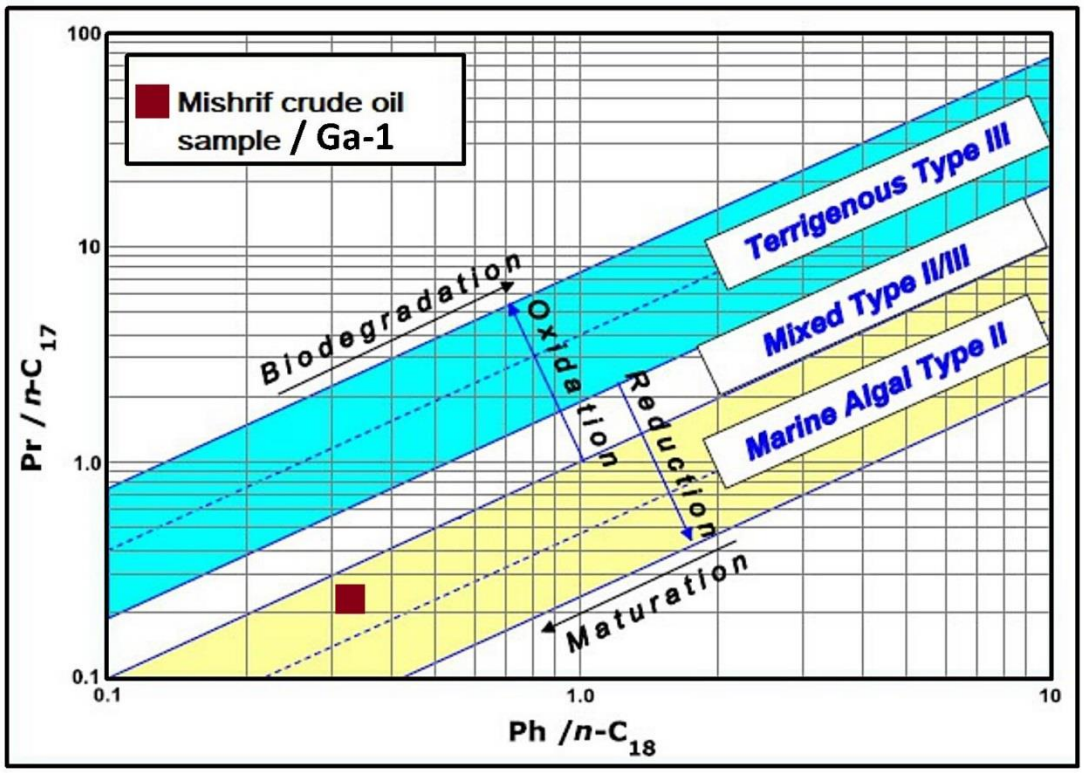

Figure (4-6): A cross plot Pr/nC17 vs. Ph/nC18 showing depositional environment and origin of the organic matter contained in the source rocks generated the Mishrif oils, Well Ga-1. Pr: pristane; Ph: phytane.

Many biomarker parameters can be used to determine the age, the depositional environment of the probable source rocks, and thermal maturity (Peters *et al.*, 2005). High C_{22}/C_{21} is 1.04, low C_{24}/C_{23} tricyclic terpanes is 0.27 (Figure 4-7A), $C_{31}R/H$ is 0.32, C_{26}/C_{25} is 0.72, (Figure 4-7B), $C_{31}R/H$ (C31/C30 Hopane) is 0.32, (Figure 4-7C), $C_{35}S/C_{34}S$ is 1.11, C29/H (C29/C30 Hopane) is 1.6, (Figure 4-7D), for Mishrif respectively, indicated that these oils are carbonate source rocks depositional environment. The high ratio of the $C_{35}S/C_{34}S$ hopane is 1.11 and $GA/C_{31}R$ is 0.24 indicated anoxia conditions and hypersalinity.

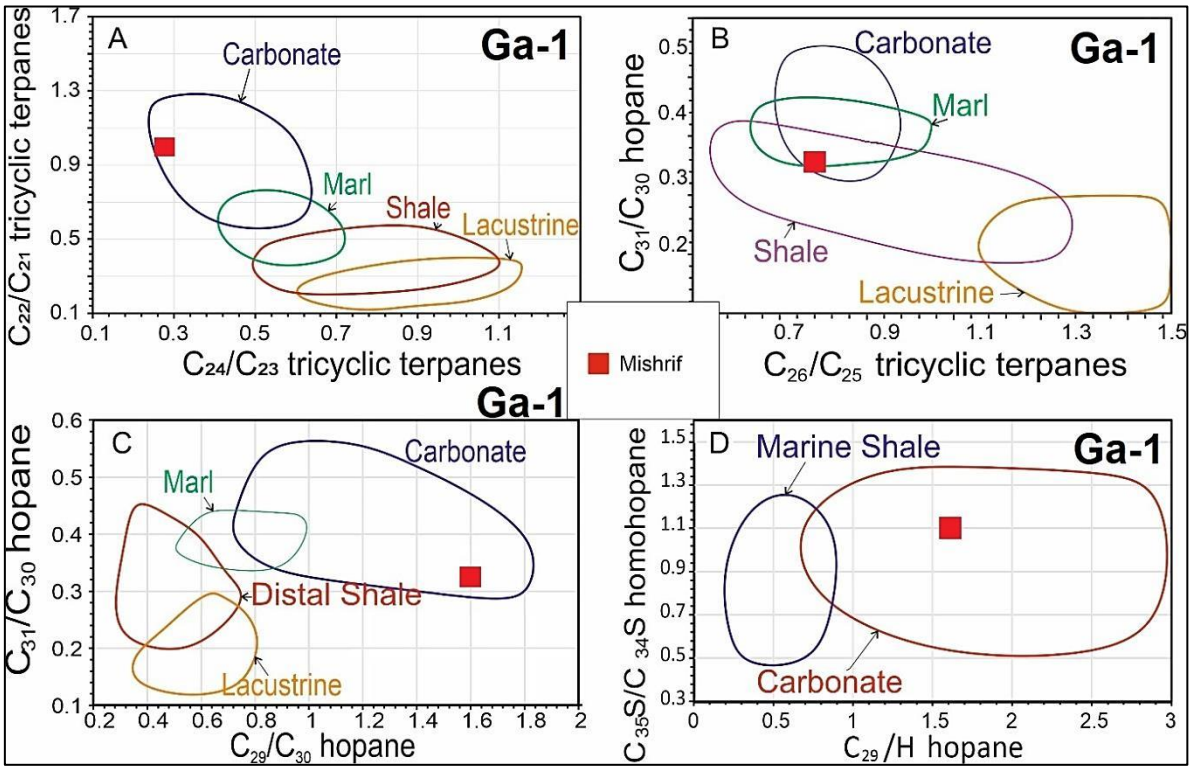

Figure (4-7): Many biomarkers' ratios plots used to predicate source rock and depositional condition of Mishrif crude oil sample, Gharraf oil field, Well Ga-1.

4.3.3. Thermal maturity

Many biomarker maturity ratios used in this study, include C_{27} Ts/Tm is 0.18, TAS3 (CR) is 0.31 as shown in Figure (4-8A), C27 Ts/Tm is 0.18, and C_{29} Ts/Tm is 0.07 as shown in Figure (4-8B), to determine the maturity of Mishrif oil (Peters *et al.*, 2005). These results indicated that the Mishrif oil was early stage thermally mature, in Gharraf oil field, southern Mesopotamian Basin, southern Iraq**.**

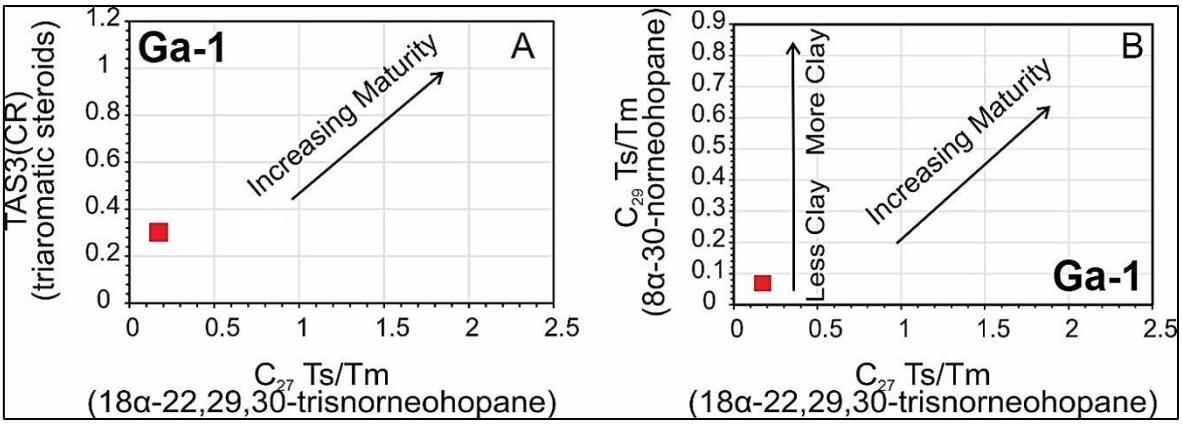

Figure (4-8): Variation biomarker parameters used to assess the thermally mature of the Mishrif crude oil sample, Gharraf oil field, Well Ga-1.

4.3.4. Age

Two biomarker criteria can be used to predict the age of the source rocks that may generate the Mishrif oils. The first is the percentage of C_{28} steranes in comparison to C_{29} steranes. The C_{28}/C_{29} sterane ratio the Mishrif oil is 0.66. The Figure (4-9A) shows that the Mishrif oil originated from Middle and Upper Jurassic. The second criterion is stable carbon isotope values, as shown in Figure (4-9B), the Mishrif oil sample had isotopically heavier (less negative) values which is -27.38‰ (average value) confirmed the previous conclusion.

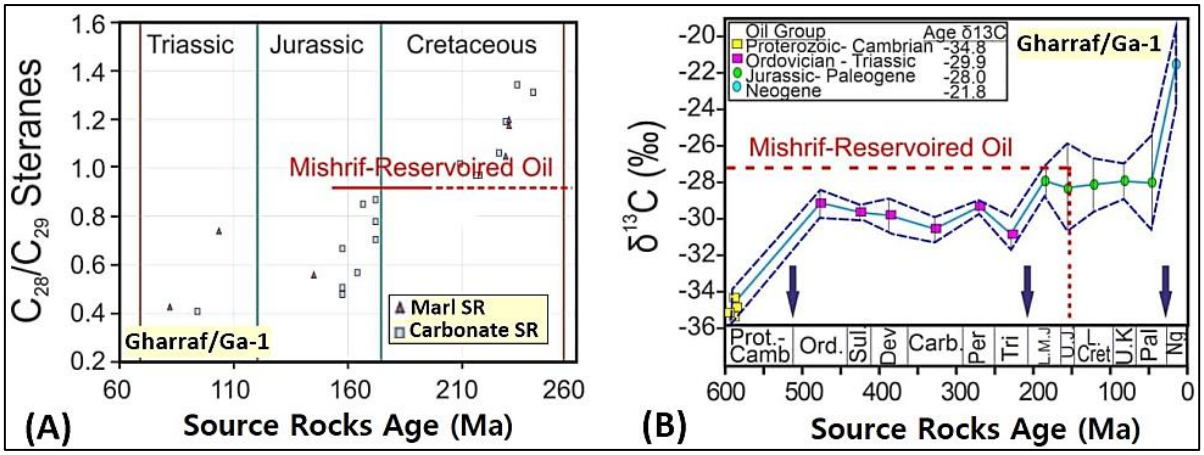

Figure (4-9): (A) Average C_{28}/C_{29} sterane ratio, (Peters *et al.*, 2008). (B) The plot of average stable carbon isotopic ratios, (Sofer, 1984); showed that the Mishrif oil, Well Ga-1 was originated from Middle and Upper Jurassic source rocks.

4.4. Petroleum System Modeling

Petroleum system is a geologic system that contains all of the geological elements and processes which are required for occurrence of a hydrocarbon accumulation, including the hydrocarbon source rocks and all associated oil and gas (Magoon and Dow, 1994). Petroleum system model can be defined as a digital data model represents a petroleum system that allows the interrelated processes and their results to be simulated in order to better understand and predict them. This model is dynamic model which mean that petroleum system modeling provides a complete and unique record of generation, migration, accumulation and loss of oil and gas in petroleum system through geologic time. Petroleum system modeling includes basic assessments such as generation, expulsion, migration, trapping and preservation of hydrocarbons (Hantschel & Kauerauf, 2009). Petroleum System Modeling represents a powerful tool in hydrocarbon exploration which reconstructs and forward simulates deposition and erosion history, as well as the generation, migration,

and accumulation of petroleum (Al-Hajeri *et al.*, 2009). The process of petroleum system modeling covers a wide range of spatial and temporal interval, where a lot of the input parameters are usually highly uncertain, resulting in widely different results. Therefore, understanding the impact of input parameters is critical for exploratory decision making. The use of uncertainty analysis in basin modeling of the petroleum system is becoming more common as computational power allows for the evaluation of multiple models in a reasonable time (Zwach & Carruthers, 1998). Figure (4-10) shows a list of important risk parameters that industry had come up with.

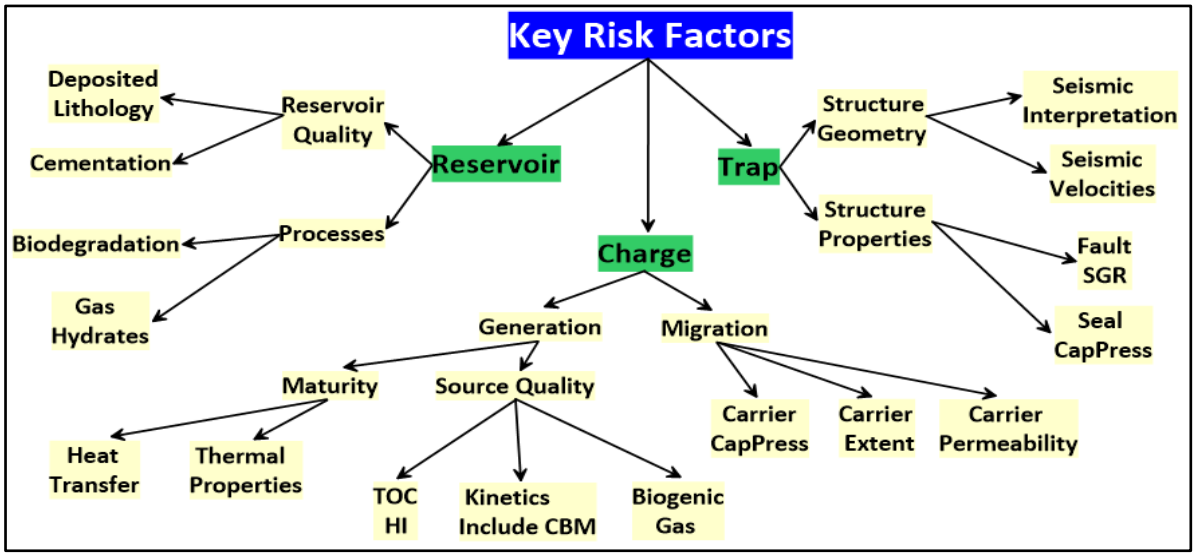

Figure (4-10): Illustrating important risk factors in basin modeling. Modified after (Wygrala, 2008).

Recently, structure model represents the beginning step for compaction analysis. Building of structure models usually depending on picking and interpretation of seismic data constrained by well logs. Process of basin modeling includes solving coupled of nonlinear partial differential equations with moving boundaries. The equations control deformation and flow of fluid in a porous media, coupled with chemical reactions and energy transportation. This coupled system must be solved numerically on spatial grids and discretized

time (Al-Hajeri *et al.*, 2009). The workflow and key input parameters are illustrated in Figure (4-11).

The basin modeling purpose is to numerically simulate the hydrocarbon generation and expulsion history of the organic matter's rich intervals within the probable source rocks of the Jurassic and Cretaceous formations in the southern Mesopotamian Basin. The burial and thermal models were reconstructed at Ga-1 which is located in the Gharraf oil field, using the PetroMod modeling software of Schlumberger.

The Ga-1 is well was selected due to the availability of necessary data for basin modeling, including corrected bottom hole temperature (BHT), measured vitrinite reflectance (%VRo), and geological information, that obtained from reports of OEC. As well as the sedimentary data (rock types, ages of deposition, and erosion) obtained from reports of Oil Exploration Company (OEC) and previously published studies (e.g., Pitman *et al.*, 2004; Abeed *et al.*, 2011; Al-Khafaji *et al.*, 2021). (Table 4-2) were utilized to reconstruct the history of burial and subsidence. The boundary conditions (sediment-water interface temperature (SWIT), paleo-water depth (PWD), the paleo heat flow (mW/m2), heat flow evolution are necessary parameters to build the model of the thermal/burial evolution of sedimentary basins (Welte *et al.*, 2012).

The paleo-heat flow data from Handhal and Mahdi, (2016) and paleo-water depth data from Handhal *et al.*, (2014) of the southern Mesopotamian basin have been used in this study, Figure (4-12). Mean surface temperatures according to the standard model of global mean surface temperature based on Wygrala, (1989) of Arabia region at the latitude of the study area (32˚ N) and PWD used to calculate the sediment-water interface temperature (SWIT), Figure (4-13).

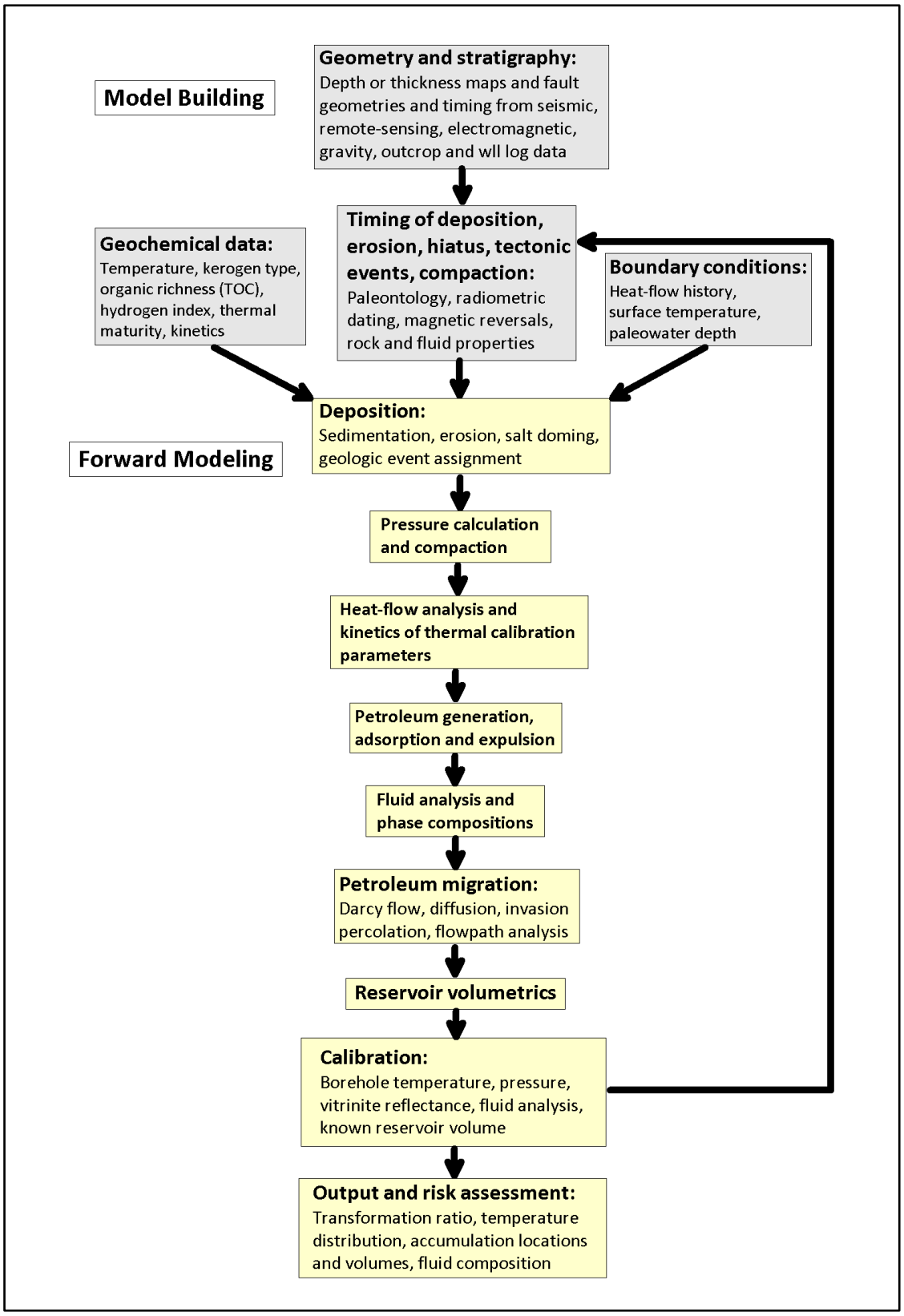

Figure (4-11): The multiple and interrelated steps of basin and petroleum system modeling. Modified from (Al-Hajeri *et al.*, 2009).

4.4.1. PetroMod data inputs

The data that was entered and used in the PetroMod software included:

a. Timing of deposition and erosion, Table (4-2).

b. Geochemical data (temperature, TOC, hydrogen index HI), Table (4-2).

c. Boundary conditions (heat-flow history, surface temperature and paleo-water depth), Figures (4-12) and (4-13).

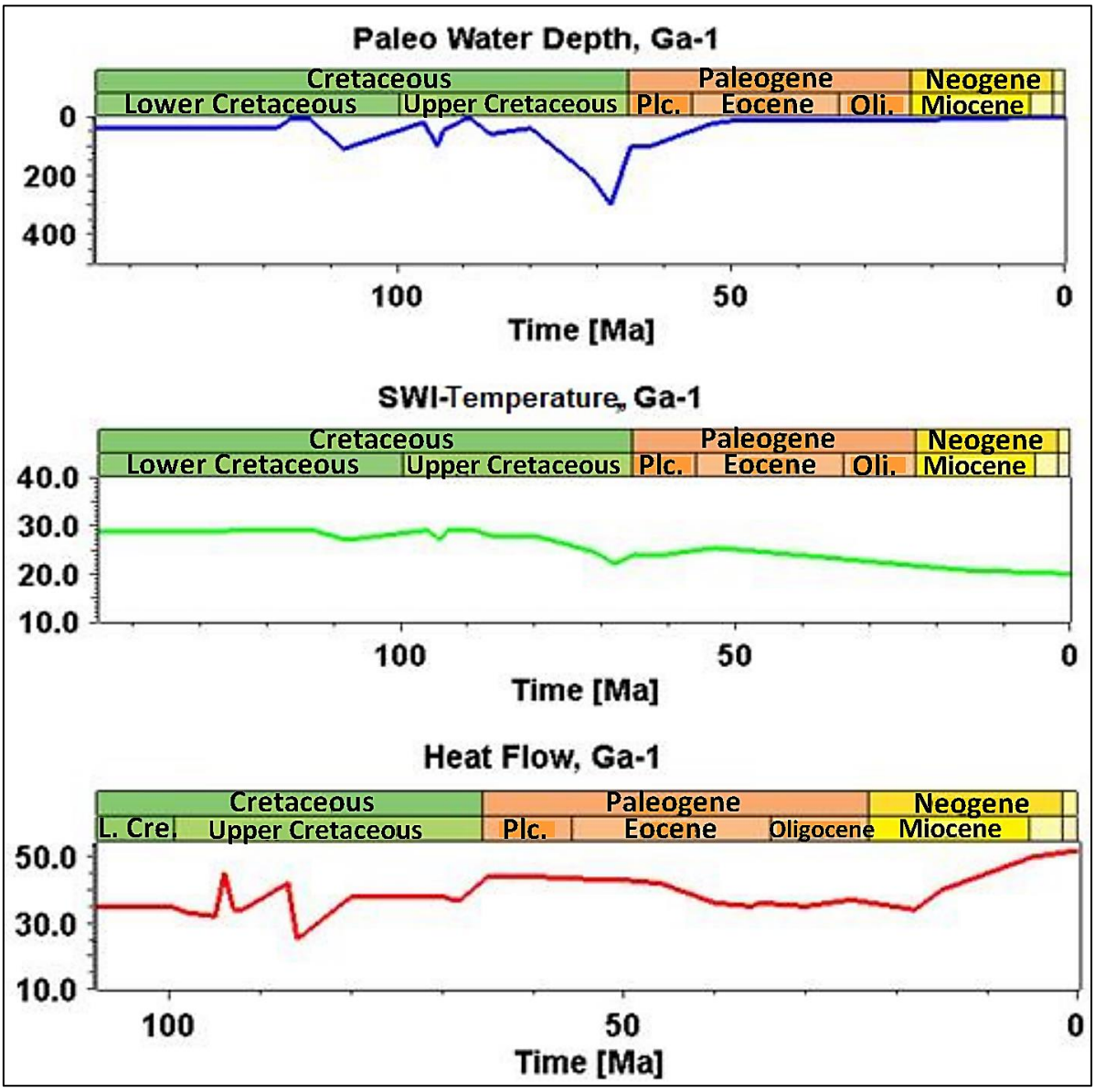

Figure (4-12): Paleo-water depth, surface-water interface temperature and heat-flow history in Well Ga-1 of Gharraf oilfield.

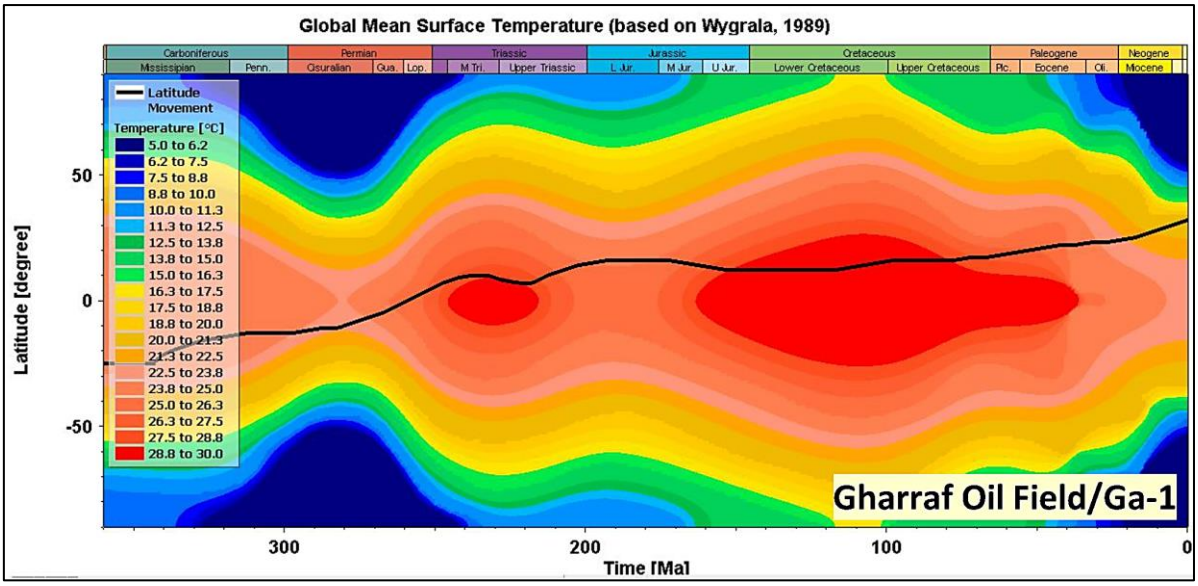

Figure (4-13): Global mean surface temperature based on Wygrala, (1989) of Arabia region at the latitude of Gharraf oil field.

4.4.2. Petroleum generation kinetics

Pitman *et al.*, (2004) referred that the relationship between API gravity and the sulfur content of the produced oils in Iraq is similar to that of oils produced from the Permian Phosphoria Formation, USA. Based on the similarity in these oil compositions, isothermal kinetic parameters for Type-IIS kerogen in the Phosphoria (activation energy = 42.71 kcal/mol; frequency factor = 4.31 x 1023m.y.-1; Lewan and Ruble, 2002) were used as an analog for modeling oil generation in Jurassic source rocks. Using this kinetics as an analog assumes that the atomic mean Sorg/C ratio for Type-IIS kerogen in Jurassic source rocks approximates the atomic Sorg/C ratio for kerogen in the Phosphoria (0.045).

Table (4-2): PetroMod input data for Well Ga-1 in Gharraf oilfield. Source of the data is final reports from Oil Exploration Company (OEC) and previously published studies (e.g., Pitman *et al.*, 2004; Abeed *et al.*, 2011; Al-Khafaji *et al.*, 2021).

Layer	Top (m)	Thick. (m)	Depo from (Ma)	Depo to (Ma)	Eroded from (Ma)	Eroded to (Ma)	Lithology	PSE	TOC %	HI mgHC/gTOC	Comments
Upper Fars	surface		10.8	8.9			SANDcongl	Overburden Rock			Geothermal Gradient=0.0187 c./m.
Lower Fars	669	177	15.3	10.8			LIME&EVAP	Seal Rock			
Bajwan	846	10	24.2	23.9	23.9	15.3	LIMEdolom	Reservoir Rock			
Baba	856	74	24.4	24.2			LIMEdolom	Reservoir Rock			
Tarjil	930	25	26.5	24.4			LIMEdolom	Reservoir Rock			surface temp.=30 c
Palani	955	39	30.8	28.4			LIMEdolom	Reservoir Rock			
Dammam	994	90	36	33.7	33.7	30.8	LIMEdolom	Overburden Rock			BHT=103.3 at 3910 m.
Rus/Umm ErRathuma	1084	303	58	52	52	36	LIME&EVAP	Overburden Rock			
Aaliji	1387	302	62.9	61.1	61.1	58	LIMEmarly	Overburden Rock			Well: Ga-1
Shiranish	1689	142	72.5	69.6	69.6	62.9	LIMEmarly	Source Rock			Field:Gharraf oilfeild
Hartha	1831	144	78.7	72.5			LIMEmarly	Reservoir Rock			
Sadi	1975	166	84.9	80.3	80.3	78.7	LIMESTONE	Reservoir Rock			Note:all tops are from RTKB=18.65 m.
Tanuma	2141	48	85.9	84.9			SHALE	Reservoir Rock			
Khasib	2189	46	91.8	85.9			LIMEmarly	Reservoir Rock			
Mishrif	2235	301	94	92.3	92.3	91.8	LIMESTONE	Reservoir Rock			
Rumaila	2536	40	95.7	94			LIMEshaly	Overburden Rock			X=602200
Ahmadi	2576	12	97.2	95.7			SHALE	Overburden Rock	0.66	182	Y=3514516
Mauddud	2588	202	101.4	99.4	99.4	97.2	LIMESTONE	Reservoir Rock	0.4	173	Kinetics Model: Lewan and Ruble, 2002
Nahr Umr	2790	140	109.6	101.4			SANDshaly	Reservoir Rock	1.4	263.5	
Shuaiba	2930	66	120.7	113.2	113.2	109.6	LIMESTONE	Reservoir Rock	0.2	182.4	
Up.Zb.Sh.	2996	115	123	120.7			SHALEsand	Source Rock	1.37	100	
Mid.Zb.Sst.	3111	174.5	126	123			SANDshaly	Reservoir Rock	1.038	130.2	Rock samples type: cuttings
L.Zb.Sh.	3285.5	155.5	127.4	126			SHALEsand	Source Rock	2.081	179.8	
Ratawi	3441	160	135.9	131	131	127.4	LIMESTONE	Reservoir Rock	0.6	189	
Yamama	3601	269	143.1	135.9			LIMEdolom	Reservoir Rock	1.1	434.5	
Sulaiy	3870	??	148	143.1			LIMEshaly	Source Rock	2.4	367.1	
TD	3873										

4.4.3. Burial history chart

The burial history of a sedimentary basin during geological time is represented by the burial history chart. Subsidence, uplift and erosion are analyzed by utilizing burial history charts, which assume a key part in giving the present-day maximum burial depth. The burial history of basin sediments includes data about preservation of organic material and burial depth, which are related to the temperatures and pressures of the sediments were exposed to and the durations of exposure (Al-Hajeri *et al.*, 2009). The histories of water depth, heat flow and surface temperature complement the burial history. Every one of these components goes into the modeling of a sedimentary basin, and they apply at the boundaries of the basin (Wangen, 2010), Figures (4-12) and (4-13). The sedimentary strata data such as rock types, the time of deposition, and erosion. These data were obtained from the final well report. The data in (Table 4-2) were used to build the burial and subsidence history, (Figure 4-14).

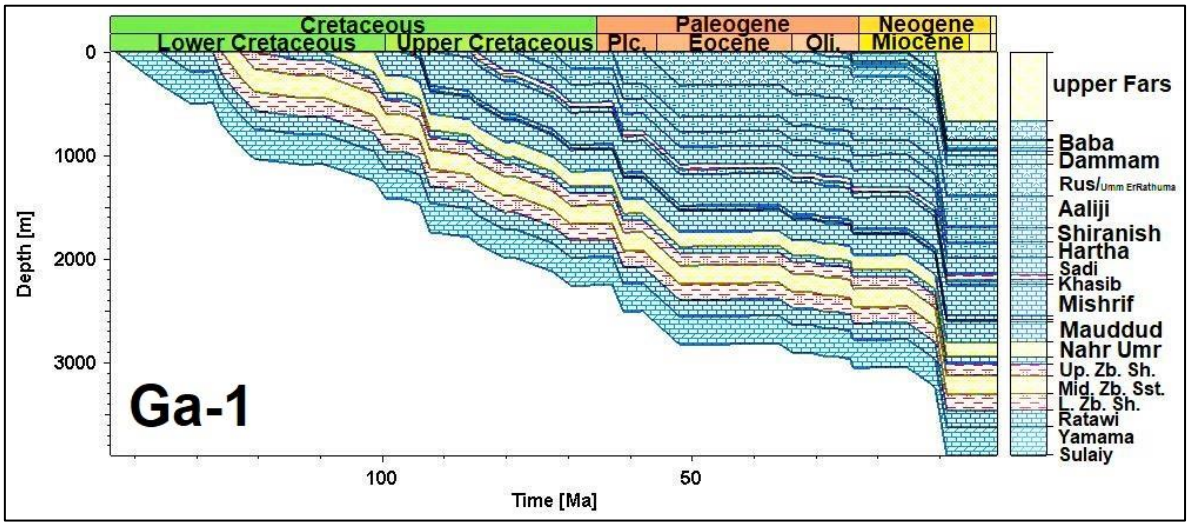

Figure (4-14): Illustrating burial history chart of Cretaceous source rocks in Gharraf oil field Well Ga-1.

4.4.4. Thermal history chart

The thermal history of sedimentary basins can be evaluated depending on the burial history chart and on the heat-flow evolution (Lijmbach, 1975). Burial history and thermal history charts can be utilized to detect the oil and gas potential of a basin and to determine reservoir porosities (Allen & Allen, 2005), Figure (4-14).

The thermal/burial evolution of sedimentary basins, this study based on the necessary parameters to model; the paleo-water depth (PWD), sedimentary-water interface temperature (SWIT), and the paleo heat-flow (mW/m2).

The thermal maturity of source rocks and oil generation history models of the potential source rocks in the Upper Jurassic - Early Cretaceous Sulaiy, was numerically simulated for a Ga-1 well in the Gharraf oilfield, using the PetroMod 1D basin modeling software. According to these models of the burial history chart and thermal maturity history, the Sulaiy Formation was buried of approximately 3780 m, with a maximum temperature of 100–130 °C (Figures 4-14, 4-15, 4-16).

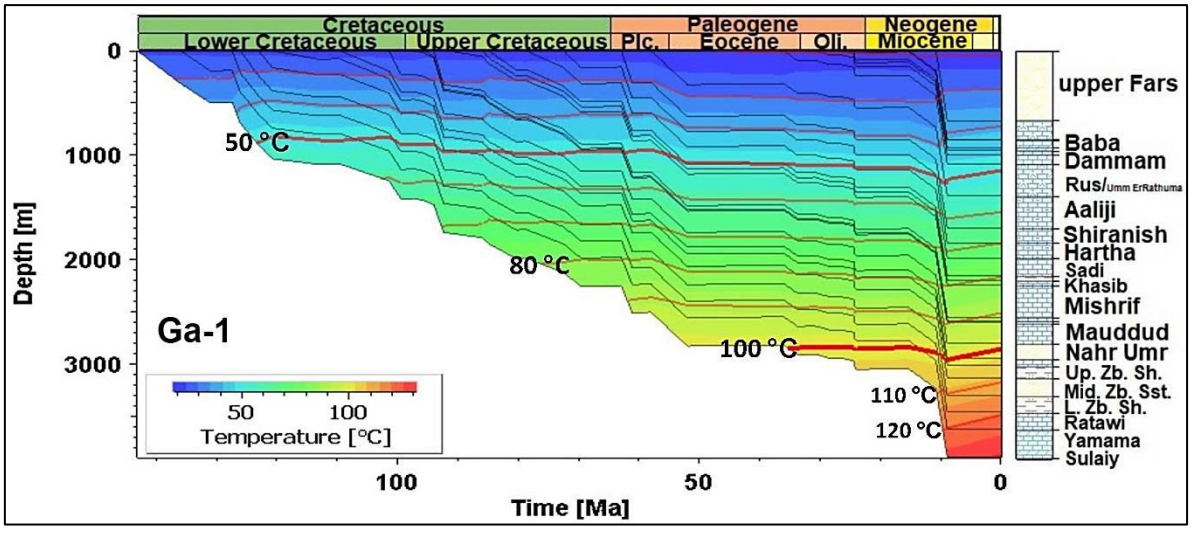

Figure (4-15): Illustrating thermal history chart of Cretaceous source rocks in Gharraf oil field, Well Ga-1.

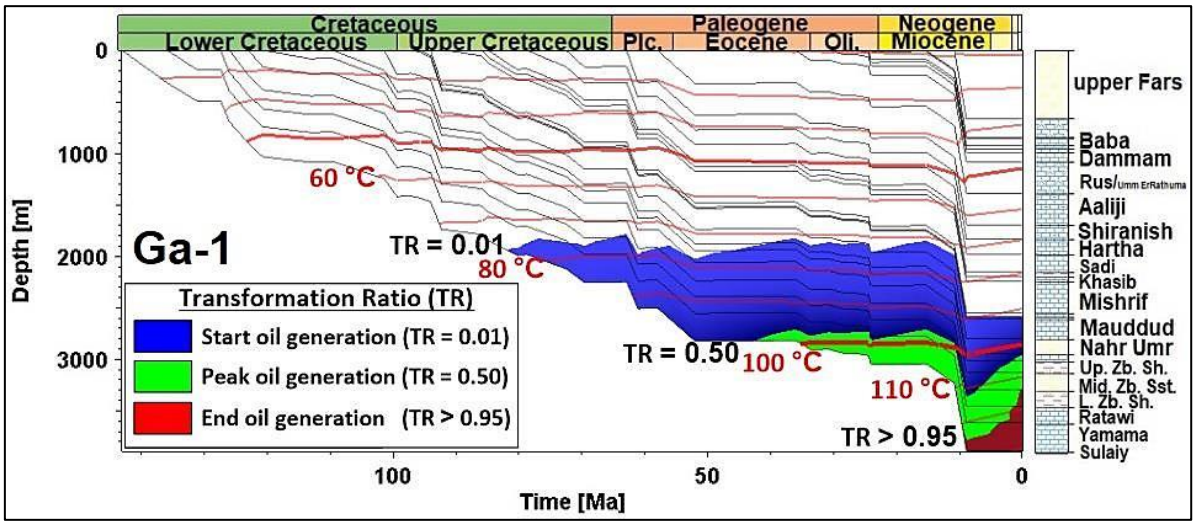

Figure (4-16): Timing and extent of Petroleum Generation of lower Cretaceous source rocks in Gharraf oil field, Well Ga-1.

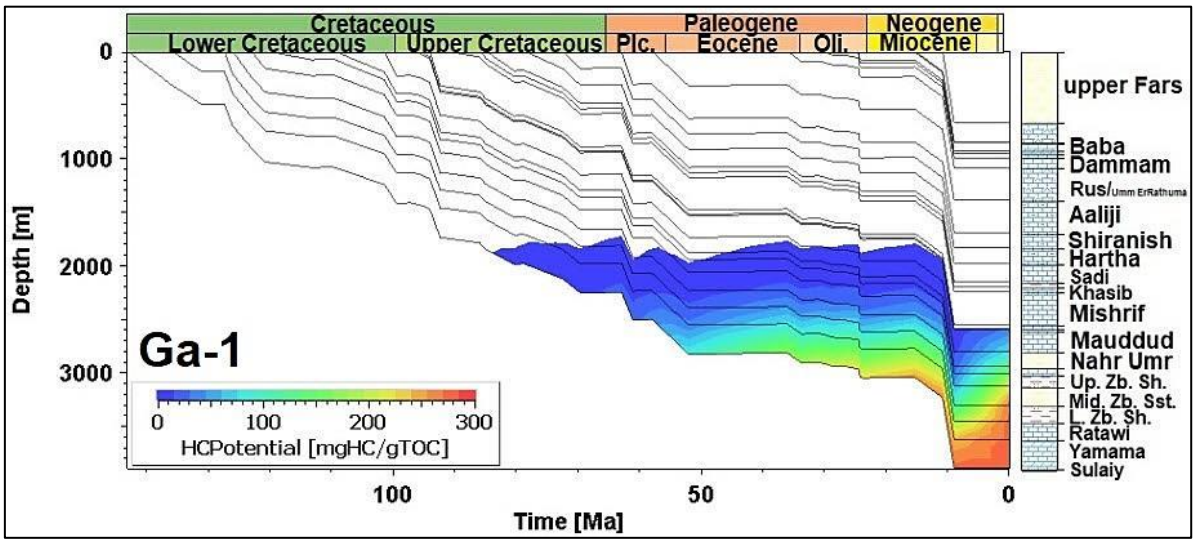

Figure (4-17): Illustrating the burial history with hydrocarbon generation potential of lower Cretaceous source rocks in Gharraf oil field, Well Ga-1.

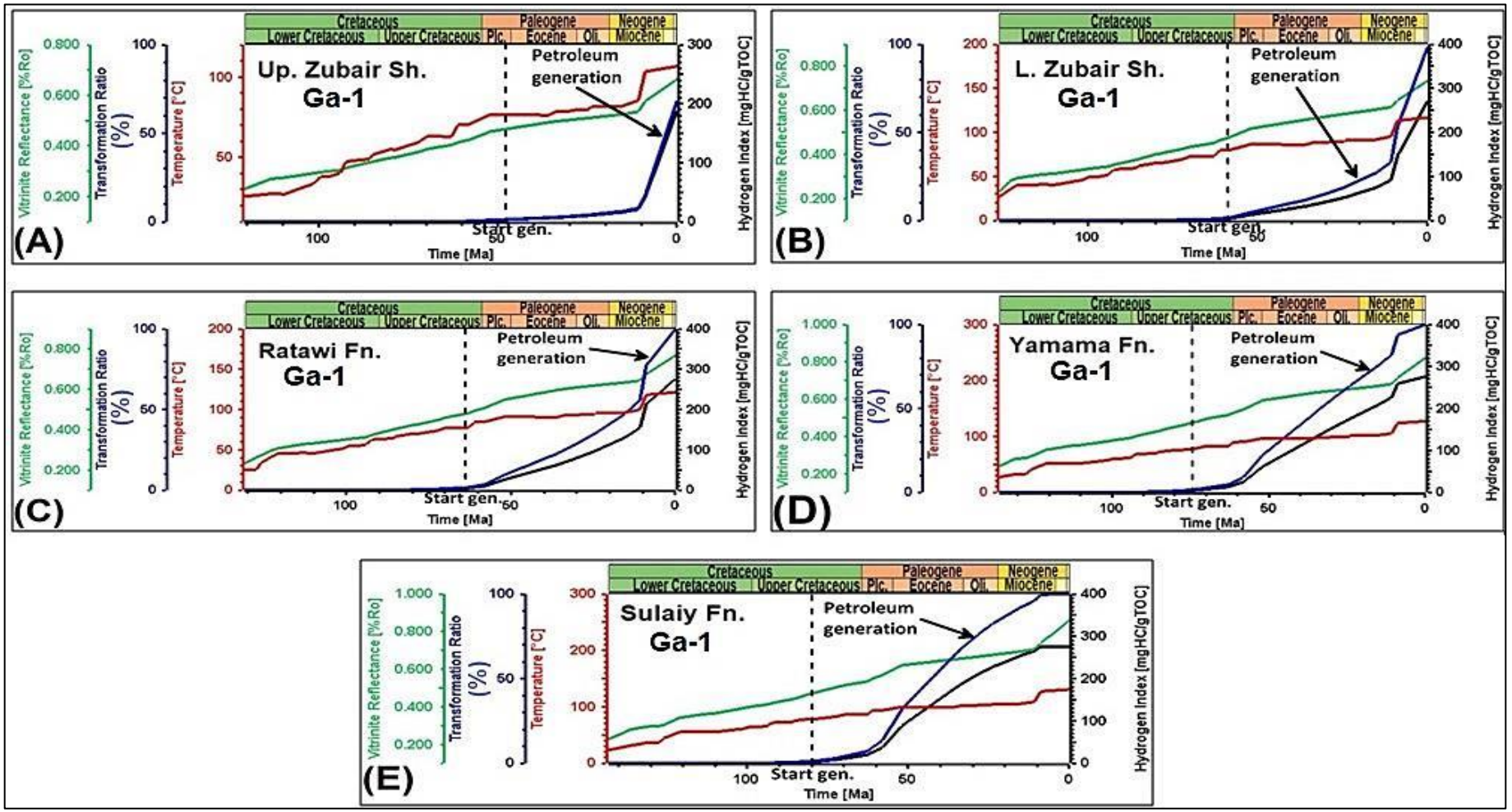

Figure (4-18): Oil and kerogen-gas transformation-ratio (TR) curves and thermal curves depicting timing and temperature of major petroleum-generation events, and extent of petroleum generation of the main lower Cretaceous source rock formations in Ga-1 of the Gharraf oil field; (A) Upper shale of Zubair Formation, (B) Lower shale of the Zubair Formation, (C) Ratawi Formation (D) Yamama Formation, and (E) Sulaiy Formation.

The Zubair Formation (Figure 4-18 A, and B), the Ratawi Formation (Figure 4-18 C), and the Yamama Formation (Figure 4-18 D) was not reaching actually to the peak of oil generation. Although these source rocks are considered at the beginning of their thermal maturity, it is not likely that they have contributed to charging the reservoirs with oil. While the Sulaiy Formation was only reached to the main oil-generation window which equivalent to the peak-mature stage (0.90 EASY %Ro) see the (Figure 4-18 E). Therefore, the organic-rich intervals within the Sulaiy Formation were high mature and genetically linked and are likely the effective source rocks for the oils analyzed in this study.

The beginning of oil generation is often considered to occur when the transformation ratio is about 10%TR then continues with oil generation to the present days, as illustrated by the numerical basin models (Figure 4-18). The Sulaiy source rocks may be reached a high conversion ratio of the TR%, of more than 50% (Figure 4-18 E), results in the expulsion of high amounts of oil.

The timing and extent of oils generation in the Zagros fold belt and Mesopotamain Basin including the studied area of the Gharraf oil field, can be obtained from the transformation ratios TR and temperatures. At Gharraf oil field in the southern Mesopotaminan Basin, the timing of the petroleum generation was began (TR $\geq$ 0.01) in the Late Cretaceous period and ending (TR $\geq$ 0.95) in the Late Paleogene to early Neogene (Figures 4-16; 4-18 E).

4.4.5. Events chart

The events chart illustrates the temporal relationship between essential elements, the rock units, preservation time, processes, and critical moment for each total petroleum system. In order for an evolving total petroleum system (TPS) to trap migrating hydrocarbon fluids effectively, the process of trap origination must happen prior or during the generation migration-accumulation process, Figure (4-19). This simple bar graph quickly shows the order of these

processes, an events chart has the following characteristics (Magoon & Schmoker, 2000):

a. There is usually only one active source rock for each TPS, however, in this assessment, several source rock intervals may be combined (composite TPS).

b. Every reservoir rock needs a seal, no matter how thin.

c. Reservoir rocks are shown that contain, or could contain, petroleum accumulations, shows, or seeps.

d. Eroded overburden rock is shown so that it can be incorporated into the burial depth model.

e. Information for timing of trap formation comes from cross sections through oil and gas fields.

f. The best information for generation-migration-accumulation is from source rock burial modeling and kinetics. From knowing this information, the beginning, peak, and end of generation as well as time of depleting of the active source rock, can be indicated.

g. Preservation time can be defined as that time which has been started directly after the process of generation-migration-accumulation is ended, and preservation time continues till present. There is no preservation time creating if the process of generation-migration-accumulation finishes today or is still going on. Young TPS's usually have no preservation time.

h. The critical moment is the time that best represents the process of generation-migration-accumulation of hydrocarbons in a total petroleum system, and its selection depends on the decision of the investigator.

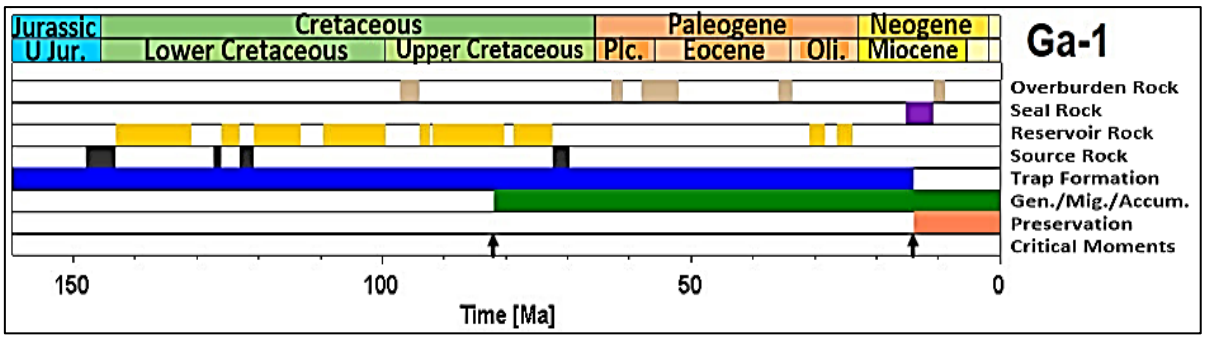

Figure (4-19): Petroleum system events chart summarizing key elements of the petroleum system in the Gharraf oil field Well Ga-1.

The results of the basin model of this study, simultaneously, with the tectonics information of the basin, give the petroleum systems of the studied area and have been proposed by the events chart (Figure 4-19). The events chart shows the major petroleum system elements and critical moments of the petroleum generation and migration history. As shown in the events chart on (Figure 4-19), the Sulaiy Formation was deposited during the Upper Jurassic to Lower Cretaceous. The large quantity of oil has been accumulated in the carbonate intervals of the Early Cretaceous Yamama and Late Cretaceous Mishrif reservoirs formations.

4.4.6. Trap formation

A trap can be defined as a rock structure that is optimum for storing hydrocarbons and is sealed with a relatively impermeable formation that prevents hydrocarbons from migrating. Traps are defined as structural traps that are formed in geological structure such as fault and fold in this type of traps, and as stratigraphic traps originate from transformations in the type of rock (Selley, 1998).

The Gharraf oil field is a longitudinal anticlinal structure extended NW-SE striking, that began forming in the Paleozoic, with continued but more limited growth throughout the Mesozoic and early Cenozoic see Figure (4-19), and it is

a stratigraphic trap in the western side of the field and the eastern side of the field is a structural trap.

Trap-forming mechanisms can be linked to reactivation of deep-seated Precambrian faults and diapiric growth of infra-Cambrian (Hormuz and equivalent) salt. Synorogenic faulting in the Mesozoic, with more restricted movement in the Cenozoic, triggered the growth of infra-Cambrian salt structures, which caused large drape folds to develop over basement fault blocks. Petroleum trapping is mostly within fault-block anticlines overlying evaporites (Pitman *et al.*, 2004).

4.4.7. Oil generation, migration, and accumulation

The 1D modeling by using PetroMod software has been built to determine the burial history, thermal history, hydrocarbon generation potential, and timing of generation of hydrocarbons from the source rock formations in Gharraf oilfield.

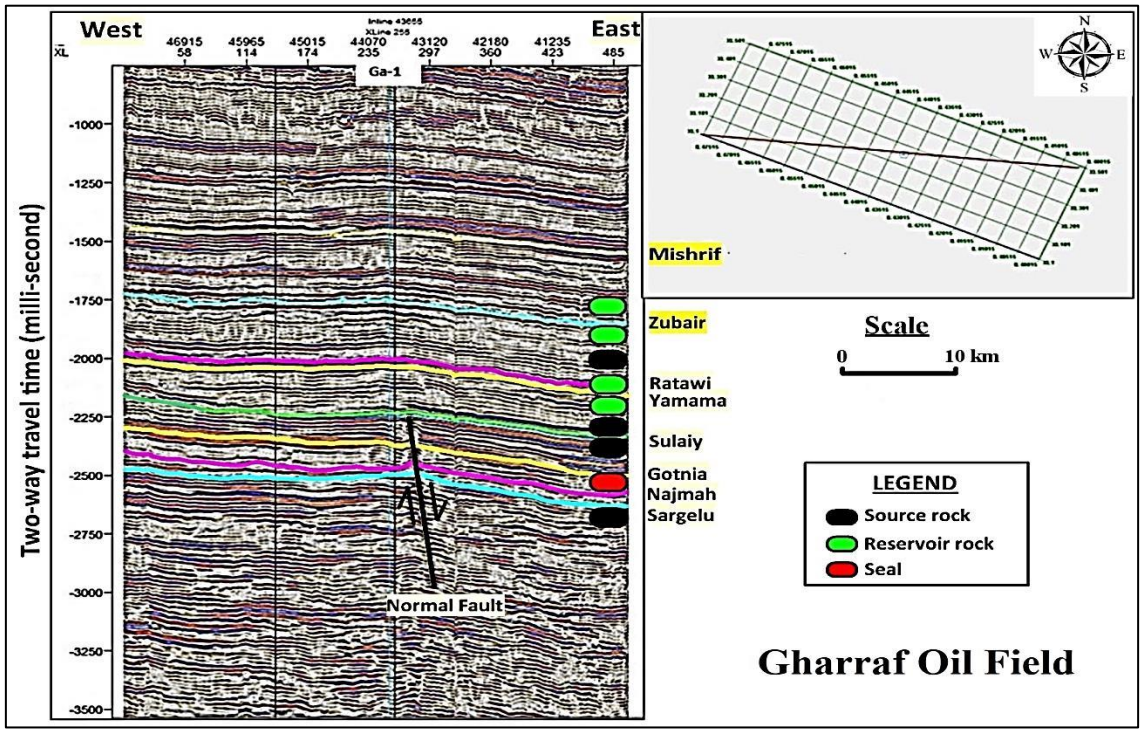

Figure (4-20): Seismic section along the Gharraf oil field showing petroleum system elements. Modified from Oil Exploration Company.

The seismic section in Figure (4-20) extends over a length of 41 km through the Gharraf oil field from east to west. This section shows the petroleum system elements of Gharraf oil field. Because of the small scale of the selected seismic section crossing the Gharraf oil field from E-W, which is provided by Oil Exploration Company, the fault systems extending through the source and reservoir rocks cannot be distinguished clearly, and therefore it is not possible to determine the paths of petroleum migration from the source rocks to the reservoirs. To illustrate this process, a seismic section with large scale was used from a previous study of Al-Khafaji (2015), Figure (4-21). This seismic section extends along the Nasiriyah and Diwan oil fields adjacent to Gharraf oil field. Due to its large scale, the seismic section clearly shows the fault systems extending through the source and reservoir rocks, where the migration paths and accumulation of the generated hydrocarbons were identified.

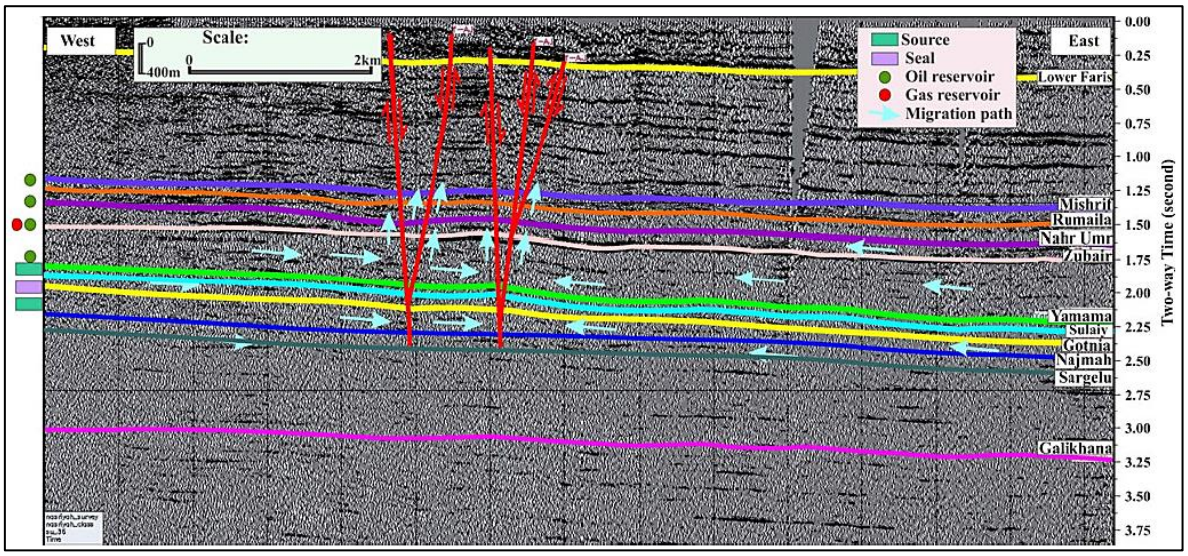

Figure (4-21): Seismic section along Nasiriya- Diwan oilfields showing petroleum system elements and migration paths of generated hydrocarbons and its accumulation sites (Al-Khafaji, 2015).

The vertical upward migration pathways of the hydrocarbons were most common in South Mesopotamian Basin. The large quantities of oil and gas generation caused high pressures and therefore to the expulsion of the oil and

gas from the Sulaiy source rock starting during the end of the Late Cretaceous and continued to the present day (Pitman *et al.*, 2004, Abeed *et al.*, 2013; Al-Khafaji *et al.*, 2021), (Figures 4-18 E; and 4-19). However, these amounts of oil and gas were then secondary migrated upward as vertical migration to the shallow stratigraphic units through the vertical faults as shown in (Figures 4-20; and 4-21), and trapped into the carbonate reservoir intervals of the Mishrif Formation, as shown in the (Figure 4-19). Based on the geological situation of the formation, the oils were very possible that generated oils at enough thermal burial depth then later migrating along with vertical migration through fault up to the reservoir rocks.

There are many researchers like Pitman *et al.* (2004), Najaf, A. A. (2013), and Najaf, A. A. *et al.* (2016) in their previous studies concluded that the Middle Jurassic Sargelu Formation is the main source rocks formation in the Mesopotamian basin and it contributed in generation the most oils of the Cretaceous reservoirs.

4.5. Oil- probable source rocks correlation

Dow (1974) was first introduced the term petroleum system and is based on the concept of oil-source rock correlation. The oil and source rocks-related investigations in the petroleum systems are to define where to explore or to estimate undiscovered commercial quantities of oils and gas using the petroleum system methodology.

The geochemical of oil-probable source rocks correlation using the bulk geochemical, molecular and carbon isotopic characteristics of the oil sample as discussed in the previous subsections, were established. The result of these analyses of Mishrif oils indicated that they were generated from a marine carbonate-rich source rock rich and deposited under an anoxic environment. The moderate sulfur content of the analyzed Mishrif oil sample also suggested that

these oils were derived from sulfur-rich Type II-S kerogen. This corresponds to most of the Iraqi oils in southern Iraq as the previous studies have demonstrated.

For this, the genetic relationship of these oils is consistent with those of the Jurassic to Lower Cretaceous carbonate-rich rocks formations in the southern Mesopotamian Basin, South Iraq. Moreover, the $\delta^{13}C_{sat}$ and $\delta^{13}C_{aro}$ data confirmed that the analyzed oil sample was sourced from Upper Jurassic to Early Cretaceous source rocks. Therefore, the Upper Jurassic - Early Cretaceous Sulaiy is likely potential source rocks for the Mishrif oils. This conclusion is consistent in the fact that the organic matter within the Sulaiy Formation contains a high TOC and sulfur content percentage with high maturity Type II-S kerogen and was deposited under anoxic conditions.

Chapter Five

Conclusions

and

Recommendations

5.1. Conclusions

1. In the determination of the lithology of Mishrif and Yamama formations by using neutron - density cross plot. This proved that the lithology of both Mishrif and Yamama formations consisted mainly of limestone with a small percentage of dolomite.
2. Through the MID and M-N cross plots, it was proved that the Mishrif and Yamamah formations consist of a primary mineral composition, calcite, and secondary mineral dolomite.
3. Mishrif Formation consists of two main units separated by a shale layer, the lower main unit has good reservoir properties and subdivided into nine reservoir units are: M1, M1.2, M2, L1, L1.2, L2, L2.2, L2.3, and L2.4. Units L1.2 and L2 have good petrophysical properties Øeff = 18-22%, Sw = 16-38%, K = 80-343md. They are considered as the best reservoir units for oil. They contain economical quantity of oil reserves 584 million cubic meters. Units M1, M1.2, and M2 have less petrophysical properties and less quantity of oil reserves 229 million cubic meters, while lower units L2.2, L2.3, and L2.4 are almost fully saturated with reservoir water Sw=68-87% with small quantity of oil reserve 125 million cubic meters.
4. Yamama Formation consists of three reservoir units are from upper to lower respectively YA, YB1, and YB2. Unit YA has good petrophysical properties Øeff = 11%, Sw = 26%, K = 119md, and it is considered as the best reservoir unit for oil reserve of Yamama Formation. It contains economical quantity of oil reserve 469 million cubic meters. Units YB1 and YB2 have low petrophysical properties, they contain a large percentage of reservoir water Sw=61-70%.
5. In the hydrocarbon reserves estimation of the main reservoirs of Gharraf oil field, the total reserve of Mishrif Formation is 938 million cubic meters, which is equal to 5900.02 million barrels, while the total reserve of Yamama Formation is 477 million cubic meters, equal to 3000.33 million barrels.

6. The average of the TOC contents present in the Sulaiy Formation in the Gharraf oil field Well Ga-1 is 2.4%, and in the Nasiriyah oil field Well NS-1 is 0.71%, and is 7.33% in the North Rumaila oil field Well R-167. So, it is considered to have the potential to act as efficient petroleum source rocks. The value of Tmax vary for the Sulaiy Formation between 426°C and 432 °C in Gharraf oil field Well Ga-1 and Nasiriyah oil field Well NS-1, indicating that the formation in these fields is ranged between immature to early mature, while Tmax of Sulaiy Formation is between 464-470°C in North Rumaila oil field Well R-167 indicating late stage of maturity. The PI values vary between 0.33 and 0.48 for Sulaiy Formation in the Gharraf oil field Well Ga-1 and Nasiriyah oil field Well NS-1, while PI of Sulaiy Formation is between 0.27 and 0.30 in North Rumaila oil field Well R-167. The high PI values of the formation refer to petroleum generation. The HI values for Sulaiy Formation are moderate in the Gharraf oil field Well Ga-1 is 367.1 mg HC/g TOC, and moderate - high in the Nasiriyah oil field Well NS-1 is between 187 – 379 mg HC/g TOC, indicated immature to early peak oil, while in the North Rumaila oil field Well R-167, HI values of Sulaiy Formation is between 49 and 70 mg HC/g TOC, indicating over-mature stage (gas generation). The kerogen type of Sulaiy Formation in both Gharraf and Nasiriyah oil fields can be classified as Type II-III, and Type II-S kerogen indicated a high petroleum generation potential.

7. The TOC content value for the Yamama Formation is 1.1 % in the Gharraf oil field Well Ga-1, between 0.16-1.55 % in Nasiriyah oil field Well NS-1, and between 2.05-5.90% in North Rumaila oil field Well R-167, it is considered to have the potential to act as good petroleum source rocks. Tmax values of the Yamama Formation in Gharraf oil field Well Ga-1and Nasiriyah oil field Well NS-1 are between 427°C and 433°C, which indicate immature to early peak oil generation. The PI values are range from 0.25 to 0.46 in the Gharraf oil field Well Ga-1 and Nasiriyah oil field Well NS-1 oil

fields. The values over 0.4 may indicate re-migrated hydrocarbons. The S2 values of the Yamama Formation in both Gharraf oil field Well Ga-1 and Nasiriyah oil field Well NS-1 are between 0.39 – 8.73 mg HC/g. HI is 434.5 mg HC/g TOC in the Gharraf oil field Well Ga-1, and between 179-563 mg HC/g TOC in the Nasiriyah oil field Well NS-1. The kerogen type therefore is Type II of Yamama source rocks in both Gharraf Well Ga-1 and Nasiriyah Well NS-1 oil fields, which is considered to be high hydrocarbon generating potential (oil-prone mainly), while in North Rumaila oil field Well R-167 the Yamama source rocks contain kerogen Type III which is mainly gas-prone organic matter.

8. The TOC value of the Ratawi Formation samples in Gharraf oil field Well Ga-1 is 0.6%, and between 0.39-0.81% in Nasiriyah oil field Well NS-1. The T*max* values were between 431°C and 432°C of the formation in both oil fields, indicated immature to early peak oil generation. PI values range from 0.40-0.63, indicating migrated oil. Kerogen type is Type III which is mainly gas-prone organic matter.

9. The TOC values of the Zubair Formation samples in Gharraf oil field Well Ga-1 are between 0.65-1.81%. T*max* values were between 425°C and 433°C, indicated immature to early peak oil generation. PI values range from 0.10 to 0.25 in Gharraf oil field Well Ga-1, indicating non-migrated oil. The kerogen type in the formation source rocks is Type III which is mainly gas-prone organic matter.

10. The geochemical analysis results of the studied oil sample of Mishrif Formation had a low (resins + asphaltenes) composition is 18.8%. The weight percentages of aromatic and saturated hydrocarbon fractions were 56.2%, and 25%, respectively. The results indicated that this oil sample was non-biodegradable, and considered to be aromatic oils. The C_{15}+ Saturate and C_{15}+ Aromatic analytical values are -27.23, and -27.53, respectively. These findings revealed that the organic materials originated in the marine

depositional environment. The Pr/*n*C_{17} and ph/*n*C_{18} ratios of the Mishrif oils are 0.22 and 0.33 respectively indicated marine type of kerogen of the propel source rocks, non-biodegradation oils, and anoxic depositional environment. Biomarker parameters High; C_{22}/C_{21} is 1.04, low C_{24}/C_{23} tricyclic terpanes is 0.27, C_{31}R/H is 0.32 , C_{26}/C_{25} is 0.72, $C_{35}S/C_{34}S$ is 1.11, for Mishrif oils respectively, indicated that these oils are carbonate source rocks depositional environment. The high ratio of the $C_{35}S/C_{34}S$ hopane and GA/C_{31}R which is 0.24 indicated anoxia conditions and hypersalinity. According to biomarker maturity ratios used in this study, include C_{27} Ts/Tm is 0.18, TAS3 (CR) is 0.31, and C_{29} Ts/Tm is 0.07, these results indicated that the Mishrif oil was early stage thermally mature, in southern Gotnia Basin, southern Iraq**.** The C_{28}/C_{29} sterane ratio the Mishrif oil is 0.66 indicated that the Mishrif oil originated from Upper Jurassic to Lower Cretaceous. The stable carbon isotope values of the Mishrif oil sample which is -27.38 confirmed the previous conclusion.

11. According to the models of the burial history chart and thermal maturity history that built by using the PetroMod 1D basin modeling software, The Zubair Formation, the Ratawi Formation, and the Yamama Formation was not reaching to the peak of oil generation. Although these source rocks are considered at the beginning of their thermal maturity, it is not likely that they have contributed to charging the reservoirs with oil. While the Sulaiy Formation was only reached to the main oil-generation window which equivalent to the peak-mature stage 0.90 EASY %Ro. Therefore, the organic-rich intervals within the Sulaiy Formation were high mature and genetically linked and are likely the effective source rocks for the oils analyzed in this study. The Sulaiy source rocks may be reached a high conversion ratio of the TR%, of more than 50% results in the expulsion of high amounts of oil. At Gharraf oil field in the southern Mesopotamian Basin, the timing of the petroleum generation was began TR $\geq$ 0.01 in the

Late Cretaceous period and ending TR ≥ 0.95 in the Late Paleogene to early Neogene.

12. The events chart shows the major petroleum system elements and critical moments of the petroleum generation and migration history. As shown in the events chart, the Sulaiy Formation was deposited during the Upper Jurassic to Lower Cretaceous. The large quantity of oil has been accumulated in the carbonate intervals of the Early Cretaceous Yamama and Late Cretaceous Mishrif reservoirs formations.

13. The large quantities of oil and gas generation caused high pressures and therefore to the expulsion of the oil and gas from the Sulaiy source rock during the Late Cretaceous and continued to the present day, these amounts of oil and gas were then secondary migrated upward as vertical migration to the shallow stratigraphic units through the vertical faults.

14. According to the geochemical of oil-probable source rocks correlation using the bulk geochemical, molecular and carbon isotopic characteristics of the Mishrif oil sample, the result of these analyses indicated that they were generated from a marine carbonate-rich source rock rich and deposited under an anoxic environment. The moderate sulfur content of the analyzed Mishrif oil sample also suggested that these oils were derived from sulfur-rich Type II-S kerogen. For this, the genetic relationship of these oils is consistent with those of the Jurassic to Lower Cretaceous carbonate-rich rocks formations in the southern Mesopotamian Basin, South Iraq. Moreover, the $\delta^{13}C_{sat}$ and $\delta^{13}C_{aro}$ data confirmed that the analyzed oil samples were sourced from Upper Jurassic to Early Cretaceous source rocks. So that, the Upper Jurassic - Early Cretaceous Sulaiy is likely potential source rocks for the Mishrif oils.

5.2. Recommendations

1. Conducting a reservoir study, calculating the petrophysical properties, making three-dimensional geological models for each of the Ratawi and Zubair reservoirs, and calculating the hydrocarbon reserves for each of them when the required data are available.
2. The use of other modern and advanced software in the study, interpretation and representation of the reservoir properties, building of three-dimensional models, and in the calculation of hydrocarbon reserves.
3. Attempting to obtain core samples for the reservoirs of Gharraf oil field and study its petrophysical properties in the laboratory and compare the results with the petrophysical characteristics deduced by well logs to find out the difference between the results to reach more accurate interpretations.
4. Attempting to obtain more core samples of the source rock formations from different wells of Gharraf oil field and conducting the necessary analyzes on them using different analysis methods to more accurately determine the maturity degree of the organic material existed in these core samples, and also determining the type of kerogen and other characteristics.
5. Attempting to obtain more crude oil samples from different wells of Mishrif Formation in Gharraf oil field and conducting the necessary geochemical analyzes on them in order to more accurately determine the type of generated source rocks formations, the maturity degree of the organic material existed in these source rocks, type of kerogen, source rocks age, and other characteristics.
6. Facilitating the necessary procedure followed in the Ministry of Oil and its various departments, and reducing the time it takes in order to obtain the necessary samples (cores, crude oil, cutting), as well as other data in order to achieve different petroleum studies by Iraqi researchers in various Iraqi universities in order to promote the intensification of these researchers and advance this field, due to its great importance to Iraq.

7. The necessity of cooperation between Ministry of Oil and the geology departments in Iraqi universities in order to provide an integrated and common database for all Iraqi fields, whether oil fields or gas fields, for easy access to the information needed for any petroleum study in order to reach a general understanding about the petroleum geology of Iraq and to encourage Iraqi researchers to complete new and advanced studies in this field.
8. The necessity of increasing the Ministry of Education's interest in the field of petroleum geology and providing the necessary laboratories and equipment in all geology departments in Iraqi universities to facilitate the completion of various petroleum studies and to gain experience in dealing with this equipment, whether by researchers or students, also the provision of research centers specialized in this field.

References

- Abeed, Q., Alkhafaji, A., & Littke, R. (2011). Source rock potential of the upper Jurassic–Lower Cretaceous succession in the southern Mesopotamian basin, southern Iraq. Journal of Petroleum Geology, 34(2), 117–134.
- Abeed, Q., Leythaeuser, D., & Littke, R. (2012). Geochemistry, origin and correlation of crude oils in Lower Cretaceous sedimentary sequences of the southern Mesopotamian Basin, southern Iraq. Organic Geochemistry, 46, 113-126.
- Abeed, Q., Littke, R., Strozyk, F., & Uffmann, A. K. (2013). The Upper Jurassic–Cretaceous petroleum system of southern Iraq: a 3-D basin modelling study. GeoArabia, 18(1), 179-200.
- Aboelhassan, N., Tarabees, E., & Alaa, M. (2017). Reservoir evaluation of Bahariya Formation in tut oil field, north Western Desert, Egypt. International Journal, 12(29), 129–203.
- Ahmed, T. (2009). Working guide to reservoir rock properties and fluid flow. Gulf Professional Publishing.
- Al-Ameri, T. K., & Batten, D. J. (1997). Palynomorph and palynofacies indications of age, depositional environments and source potential for hydrocarbons: Lower Cretaceous Zubair Formation, southern Iraq. Cretaceous Research, 18(6), 789–797.
- Al-Ameri, T. K., Al-Khafaji, A. J., & Zumberge, J. (2009). Petroleum system analysis of the Mishrif reservoir in the Ratawi, Zubair, North and South Rumaila oil fields, southern Iraq. GeoArabia, 14(4), 91–108.
- Al-Ameri, T. K. (2013, September). Petroleum Systems of Iraqi Oil Fields. In Second EAGE Workshop on Iraq (pp. cp-355). European Association of Geoscientists & Engineers.
- Al-Ameri, T. K., Najaf, A. A., Al-Khafaji, A. S., Zumberge, J., & Pitman, J. (2014). Hydrocarbon potential of the Sargelu formation, North Iraq. Arabian Journal of Geosciences, 7(3), 987-1000.
- Al-Hajeri, M. M., Al Saeed, M., Derks, J., Fuchs, T., Hantschel, T., Kauerauf, A., Neumaier, M., Schenk, O., Swientek, O., & Tessen, N. (2009). Basin and petroleum system modeling. Oilfield Review, 21(2), 14–29.
- Al-Khafaji, A.J. 2006. Relation of Mishrif reservoir crude oil with the Mishrif Formation and source rocks, using biomarkers and carbon isotopes, Ratawi, South and North Rumaila oilfields, southern Iraq. Master's thesis (unpublished), Baghdad University, Iraq.

- Al-Khafaji, Amer J, Al Najm, F. M., Al Ibrahim, R. N., & Sadooni, F. N. (2019). Geochemical investigation of Yamama crude oils and their inferred source rocks in the Mesopotamian Basin, Southern Iraq. Petroleum Science and Technology.
- Al-Khafaji, Amer Jassim. (2015). The Mishrif, Yamama, and Nahr Umr reservoirs petroleum system analysis, Nasiriya oilfield, Southern Iraq. Arabian Journal of Geosciences, 8(2), 781–798.
- Al-Khafaji, Amer Jassim, Hakimi, M. H., Mohialdeen, I. M. J., Idan, R. M., Afify, W. E., & Lashin, A. A. (2021). Geochemical characteristics of crude oils and basin modelling of the probable source rocks in the Southern Mesopotamian Basin, South Iraq. Journal of Petroleum Science and Engineering, 196, 107641.
- Al-Khirsan, H. and AlSiddiki, A. 1989. Hydrocarbon Exploration in Iraq. 28th International Geological Congress. Washington, D.C. USA July 9-19, 1989. Abstracts Volume 1, p. 28.
- Al-Musawi, A. D. J., & Nasser, M. E. (2019). The Evaluation of Reservoir Quality of Mishrif Formation in South and North Domes of Buzurgan Oil Field. Journal of Petroleum Research & Studies, 25, E89–E106.
- Al-Sakini, J. A. (1992). Summary of petroleum geology of Iraq and the Middle East. Northern Oil Company Press (Naft-Al Shamal Co.) Kirkuk, Iraq (in Arabic).
- Al-Shahwan, M. F. (2002). Thermal maturity patterns of the lower Cretaceous succession, southern Iraq-implication of hydrocarbon potential. PhD dissertation (unpublished), College of Science, Baghdad University, Iraq.
- Al- Yaseri , A. A. A. (2007) Geochemical evaluation of the main potential source rock and Crude oil biomarkers with the Tar-mat identification in reservoir of Mesopotamian Basin, southern Iraq. Unp. Ph. D. Thesis, college of science, Unvi. of Baghdad, 190 P.
- Allen, P. A., & Allen, J. R. (2005). Basin analysis: principles and applications: Malden, Massachusetts. Blackwell Publishing.
- Aqrawi, Adnan A M, Goff, J. C., Horbury, A. D., & Sadooni, F. N. (2010). The petroleum geology of Iraq. Scientific press.
- Archie, G. E. (1942). The electrical resistivity log as an aid in determining some reservoir characteristics. Transactions of the AIME, 146(01), 54-62.
- Asquith, G., & Krygowski, D. (2004). AAPG Methods in Exploration, No. 16, Chapter 2: Spontaneous Potential.

- Bassiouni, Z. (1994). Theory, measurement, and interpretation of well logs (Vol. 4, p. 372). Richardson, TX: Henry L. Doherty Memorial Fund of AIME, Society of Petroleum Engineers.
- Bellen, R. C. Van, Dunnington, H. V., Wetzel, R. and Morton, D., 1959. Lexique Stratigraphique Internal Asie. Iraq. Intern. Geol. Conger. Comm. Stratigr, 3, Fasc. 10a, 333p.
- Borazjani, S., Kulikowski, D., Amrouch, K., & Bedrikovetsky, P. (2019). Composition changes of hydrocarbons during secondary petroleum migration (Case Study in Cooper Basin, Australia). Geosciences, 9(2), 78.
- Bowen, D. G. (2003). Formation evaluation and petrophysics. Core Laboratories, Jakarta, Indonesia, 194.
- Buday, T., 1980. The Regional Geology of Iraq. Vol.1: Stratigraphy and Palaeogeography. Publications of GEOSURV, Baghdad, 445p.
- Burrus, J. (1998). Petroleum: Primary migration (generation and expulsion). In Geochemistry (pp. 500–502). Springer Netherlands. https://doi.org/10.1007/1-4020-4496-8_249
- Darling, T. (2005). Well logging and formation evaluation. Elsevier.
- Dembicki, H. (2016). Practical petroleum geochemistry for exploration and production. Elsevier.
- Didyk, B. M., Simoneit, B. R. T., Brassell, S. C. t, & Eglinton, G. (1978). Organic geochemical indicators of palaeoenvironmental conditions of sedimentation. Nature, 272(5650), 216–222.
- Douban, A. F., & Medhadi, P. (1999). Sequence chronostratigraphy and petroleum systems of the Cretaceous Megasequences, Kuwait. AAPG Inernational Conference and Exhibition, 152–155.
- Dow, W. G. (1974). Application of oil-correlation and source-rock data to exploration in Williston Basin. AAPG bulletin, 58(7), 1253-1262.
- Espitalié, J., Madec, M., Tissot, B., Mennig, J. J., & Leplat, P. (1977, May). Source rock characterization method for petroleum exploration. In Offshore Technology Conference. OnePetro.
- Espitalié, J. (1986). Use of Tmax as a maturation index for different types of organic matter: comparison with vitrinite reflectance. Collection Colloques et Séminaires-Institut Français Du Pétrole, 44, 475–496.
- Espitalié, J., & Bordenave, M. L. (1993). Source rock parameters. Applied Petroleum Geochemistry, 217.
- Espitalie, J, Deroo, G., & Marquis, F. (1985). Rock-Eval pyrolysis and its applications (part one). Oil & Gas Science and Technology-Revue d'IFPEN,

40(5), 563–579.

- Espitalie, Jean, Madec, M., Tissot, B., Mennig, J. J., & Leplat, P. (1977). Source rock characterization method for petroleum exploration. Offshore Technology Conference.
- Ezekwe, N. (2010). Petroleum reservoir engineering practice. Pearson Education.
- Fertl, W. H., & Hammack, G. W. (1971, May). A comparative look at water saturation computations in shaly pay sands. In SPWLA 12th Annual Logging Symposium. OnePetro.
- Fox, J. E., & Ahlbrandt, T. S. (2002). Petroleum geology and total petroleum systems of the Widyan Basin and interior platform of Saudi Arabia and Iraq (Vol. 2202). US Department of the Interior, US Geological Survey.
- Gibson, C. R. (1982). Basic well log analysis for geologists. American Association of Petroleum Geologists.
- Halliburton, A. D. (2001). Basic Petroleum Geology and Log Analysis. Halliburton Company.
- Hamdan, W. K., 2011. Petrel software modeling of the Mishrif Formation in Buzergan field. Unpublished M.Sc. Thesis, Department of Geology, University of Baghdad, 90p.
- Handhal, A. M., Al-Shahwan, M. F., & Al-Yaseri, A. A. (2014). Analysis of burial history for Mesopotamian basin, southern Iraq. Iraqi J Sci, 55(3B), 1292-1311.
- Handhal, A. M., & Mahdi, M. M. (2016). Basin modeling analysis and organic maturation for selected wells from different oil fields, Southern Iraq. Modeling Earth Systems and Environment, 2(4), 1-14.
- Hantschel, T., & Kauerauf, A. I. (2009). Fundamentals of basin and petroleum systems modeling. Springer Science & Business Media.
- Hood, A., Gutjahr, C. C. M., & Heacock, R. L. (1975). Organic metamorphism and the generation of petroleum. AAPG Bulletin, 59(6), 986–996.
- Hsu, C. S., & Robinson, P. R. (2007). Practical advances in petroleum processing (Vol. 1). Springer Science & Business Media.
- IES Integrated Exploration Systems (2009). PetroMod 1D and 3D Basic Tutorials.
- INOC, 1984. Final geological reports, Gharraf oilfield.
- Jafar, M.S.A., 2010. Hydrocarbon source and oil accumulation in Cenomanian–Early Turonian Mishrif Formation reservoir in selected fields,

southeastern Iraq. PhD dissertation (unpublished), University of Baghdad, Iraq. 203 p.

- Jarvie, D. M. (1991). Total organic carbon (TOC) analysis: Chapter 11: Geochemical methods and exploration.
- Jassim, S. Z., & Goff, J. C. (2006). Geology of Iraq. DOLIN, sro, distributed by Geological Society of London.
- Jia, B. (2010). Linking geostatistics with basin and petroleum system modeling: Assessment of spatial uncertainties. STANFORD UNIVERSITY.
- Katz, A. J., & Thompson, A. H. (1986). Quantitative prediction of permeability in porous rock. Physical Review B, 34(11), 8179.
- Kessler, H., Turner, A. K., Culshaw, M., & Royse, K. (2008). Unlocking the potential of digital 3D geological subsurface models for geotechnical engineers.
- Lafargue, E., Marquis, F., & Pillot, D. (1998). Rock-Eval 6 applications in hydrocarbon exploration, production, and soil contamination studies. Revue de l'institut Français Du Pétrole, 53(4), 421–437.
- Lewan, M. D., & Ruble, T. E. (2002). Comparison of petroleum generation kinetics by isothermal hydrous and nonisothermal open-system pyrolysis. Organic Geochemistry, 33(12), 1457-1475.
- Lijmbach, W. M. (1975). SP (1) on the origin of petroleum. 9th World Petroleum Congress.
- Magoon, L B, & Wallace G. Dow.(1994). The petroleum systemfrom source to trap AAPG memoir 60. The American Association of Petroleum Geologists, Tulsa, Oklahoma, U SA.
- Magoon, L B, & Schmoker, J. W. (2000). The total petroleum system–The natural fluid network that constrains the assessment unit. US Geological Survey World Petroleum Assessment, 31.
- Magoon, Leslie B, & Dow, W. G. (1991). The petroleum system-from source to trap. AAPG Bulletin (American Association of Petroleum Geologists);(United States), 75(CONF-910403--).
- Marcus, J., Enaworu, E., Rotimi, O. J., & Seteyeobot, I. (2018). A proposed solution to the determination of water saturation: using a modelled equation. Journal of Petroleum Exploration and Production Technology, 8(4), 1009–1015.
- Martinelli, G. (2009). Petroleum geochemistry. Petroleum Engineering–Upstream. Encyclopedia of Life Support Systems (EOLSS). Developed under the Auspices of the UNESCO, Eolss Publishers, Oxford, 193–216.

- Mayer, C. t. (1980). GLOBAL, a new approach to computer-processed log interpretation. SPE Annual Technical Conference and Exhibition.
- McCarthy, K., Rojas, K., Niemann, M., Palmowski, D., Peters, K., & Stankiewicz, A. (2011). Basic petroleum geochemistry for source rock evaluation. Oilfield Review, 23(2), 32–43.
- Najaf, A. A. (2013, September). Hydrocarbon Potential of the Sargelu Formation, North Iraq. In Second EAGE Workshop on Iraq (pp. cp-355). European Association of Geoscientists & Engineers.
- Najaf, A. A., Al-Dahhan, W. H., & Al Ameri, T. K. (2016). Geochemical correlation of oil and source rocks from selected exploratory wells within Northern Mesopotamian basin, Iraq. Arabian Journal of Geosciences, 9(5), 391.
- Najaf, A. A. (2018). BASIN MODELING OF THE POTENTIAL SOURCED SARGELU FORMATION WITHIN ZAGROS FOLD BELT, NORTH IRAQ. Iraqi Bulletin of Geology and Mining, 14(1), 31-46.
- Noble, R. A. (1991). Geochemical Techniques in Relation to Organic Matter: Chapter 8: GEOCHEMICAL METHODS AND EXPLORATION.
- Nwosu, L. I., & Emujakporue, G. O. (2017). Computer processed interpretation of geophysical logs of an oil field Niger Delta sedimentary basin, onshore, Nigeria. J Geogr Environ Earth Sci Int, 8(4), 1–19.
- Oil Exploration Company (OEC), 1995. An Integrated Geological Evaluation Study of the Garraf Oil Field, (in Arabic), Baghdad, Iraq, 91p., (unbuplished report).
- Perrodon, A. (1983). Dynamics of oil and gas accumulations (Vol. 5). Editions TECHNIP.
- Peters, K. E. (1986). Guidelines for evaluating petroleum source rock using programmed pyrolysis. AAPG Bulletin, 70(3), 318–329.
- Peters, Kenneth E, & Cassa, M. R. (1994). Applied source rock geochemistry: Chapter 5: Part II. Essential elements.
- Peters, K. E., & Fowler, M. G. (2002). Applications of petroleum geochemistry to exploration and reservoir management. Organic Geochemistry, 33(1), 5-36.
- Peters, Kenneth E, Ramos, L. S., Zumberge, J. E., Valin, Z. C., & Bird, K. J. (2008). De-convoluting mixed crude oil in Prudhoe Bay field, North Slope, Alaska. Organic Geochemistry, 39(6), 623–645.
- Peters, Kenneth Eric, Peters, K. E., Walters, C. C., & Moldowan, J. M. (2005). The biomarker guide (Vol. 1). Cambridge University Press.

- Pitman, J. K., Steinshouer, D., & Lewan, M. D. (2004). Petroleum generation and migration in the Mesopotamian Basin and Zagros Fold Belt of Iraq: results from a basin-modeling study. GeoArabia, 9(4), 41–72.
- Poupon, A., & Leveaux, J. A. C. Q. U. E. S. (1971, May). Evaluation of water saturation in shaly formations. In SPWLA 12th Annual logging symposium. OnePetro.
- Powers, R. W. Ramirez, L. F., Redmond, C. D. and Elberg, E. L., 1966. Sedimentary geology of Saudi Arabia. In: The geology of the Arabian Peninsula. USGS Prof. Paper No. 460-D., 177p. Washington.
- Rider, M. H. (1986). The geological interpretation of well logs.
- Roberts, L. N. R., Lewan, M. D., & Finn, T. M. (2005). US Geological Survey Digital Data Series DDS-60-D: Burial History, Thermal Maturity, and Oil and Gas Generation History of Petroleum Systems in the Southwestern Wyoming Province, Wyoming, Colorado and Utah, Chap. 3, Version 1. Denver, Colorado, USA: US Geologic Survey.
- Sadooni, Fadhil N. (1993). Stratigraphie Sequence, Microfacies, and Petroleum Prospects of the Yamama Formation, Lower Cretaceous, Southern Iraq. AAPG Bulletin, 77(11), 1971–1988.
- Schlumberger (1972). Log Interpretation, Vol. I—Principles: New York, Schlumberger Limited, 112 p.
- Schlumberger (1974). Log Interpretation: Applications (Vol. 2). Schlumberger Limited.
- Schlumberger (1991). Log interpretation principles/applications. Schlumberger Educational Services.
- Schlumberger (2005). Log Interpretation Charts. Houston.
- Schlumberger (2007). Petrel Structural Modeling Course. Schlumberger, 105-123p.
- Schlumberger (2008). Seismic- to- Simulation Software, Petrel Introduction Course. Schlumberger, 50-334p.
- Schlumberger (2009). Petrel online help, Petrel Introduction Course. Schlumberger, 560pp.
- Schlumberger (2010a). Petrel Introduction Course. Schlumberger, 13-493p.
- Schlumberger (2010b). Reservoir Engineering Course. Schlumberger, 137-177p.
- Schlumberger (2011). PetroMod Basin and Petroleum Systems Modeling Software: IES GmbH, Ritterstrasser, 23, 52072 Aachen, Germany, accessed on Jan. 2011, at http://www.ies.de

- Schlumberger (2013). Petrel Geology and Modeling, Petrel Introduction Course, 559pp.
- Selley, R. C. (1998). Elements of petroleum geology. Gulf Professional Publishing.
- Serra, O. (1989). Formation microscanner image interpretation: Houston. Texas, Schlumberger Educational Services, 117.
- Simandoux, P. (1963). Dielectric measurements on porous media, application to the measurements of water saturation: study of behavior of argillaceous formations. Revue de L'institut Francais du Petrole, 18(Supplementary Issue), 193-215.
- South Oil Company (S.O.C.), 1987. Final Geological Report, Gharraf oilfield.
- South Oil Company (S.O.C.), 1988. Final Geological Report, Gharraf oilfield.
- South Oil Company (S.O.C.), 2011. Final Geological Report, Gharraf oilfield.
- Sofer, Z. (1984). Stable carbon isotope compositions of crude oils: application to source depositional environments and petroleum alteration. AAPG Bulletin, 68(1), 31–49.
- Tiab, D., & Donaldson, C. (2004). Petrophysics Second Edition–Theory and Practice of Measuring Reservoir Rock and Fluid Transport Properties. Golf professional publishing.
- Tissot, B., Durand, B., Espitalie, J., & Combaz, A. (1974). Influence of nature and diagenesis of organic matter in formation of petroleum. Aapg Bulletin, 58(3), 499–506.
- Tissot, B. P., & Welte, D. H. (1984). Diagenesis, catagenesis and metagenesis of organic matter. In Petroleum formation and occurrence (pp. 69–73). Springer.
- Verma, M. K., Ahlbrandt, T. S., & Al-Gailani, M. (2004). Petroleum reserves and undiscovered resources in the total petroleum systems of Iraq: reserve growth and production implications. GeoArabia, 9(3), 51–74.
- Wangen, M. (2010). Physical principles of sedimentary basin analysis. Cambridge University Press.
- Welte, D. H., Horsfield, B., & Baker, D. R. (Eds.). (2012). Petroleum and basin evolution: insights from petroleum geochemistry, geology and basin modeling. Springer Science & Business Media.
- Wygrala, B. (1989). Integrated study of an oil field in the southern Po basin,

northern Italy (No. FZJ-2014-03033). Publikationen vor 2000.

- Wygrala, B. (2008). Petroleum Systems Modeling: Current and Future Applications. 1 St Annual Meeting, Basin and Petroleum System Modeling, Stanford, USA.
- Wyllie, M. R. J., Gregory, A. R., & Gardner, G. H. F. (1958). An experimental investigation of factors affecting elastic wave velocities in porous media. Geophysics, 23(3), 459–493.
- Zhang, B., & Xu, J. (2016). Methods for the evaluation of water saturation considering TOC in shale reservoirs. Journal of Natural Gas Science and Engineering, 36, 800–810.
- Zhao, J., Cao, Q., Bai, Y., Er, C., Li, J., Wu, W., & Shen, W. (2017). Petroleum accumulation: From the continuous to discontinuous. Petroleum Research, 2(2), 131–145.
- Zwach, C., & Carruthers, D. (1998). Honouring uncertainties in the modelling of migration volumes and trajectories (abs.): IFE Symposium on Advances in Understanding and Modelling Hydrocarbon Migration. Oslo, Norway, December, 7, 37.

Appendix (A)

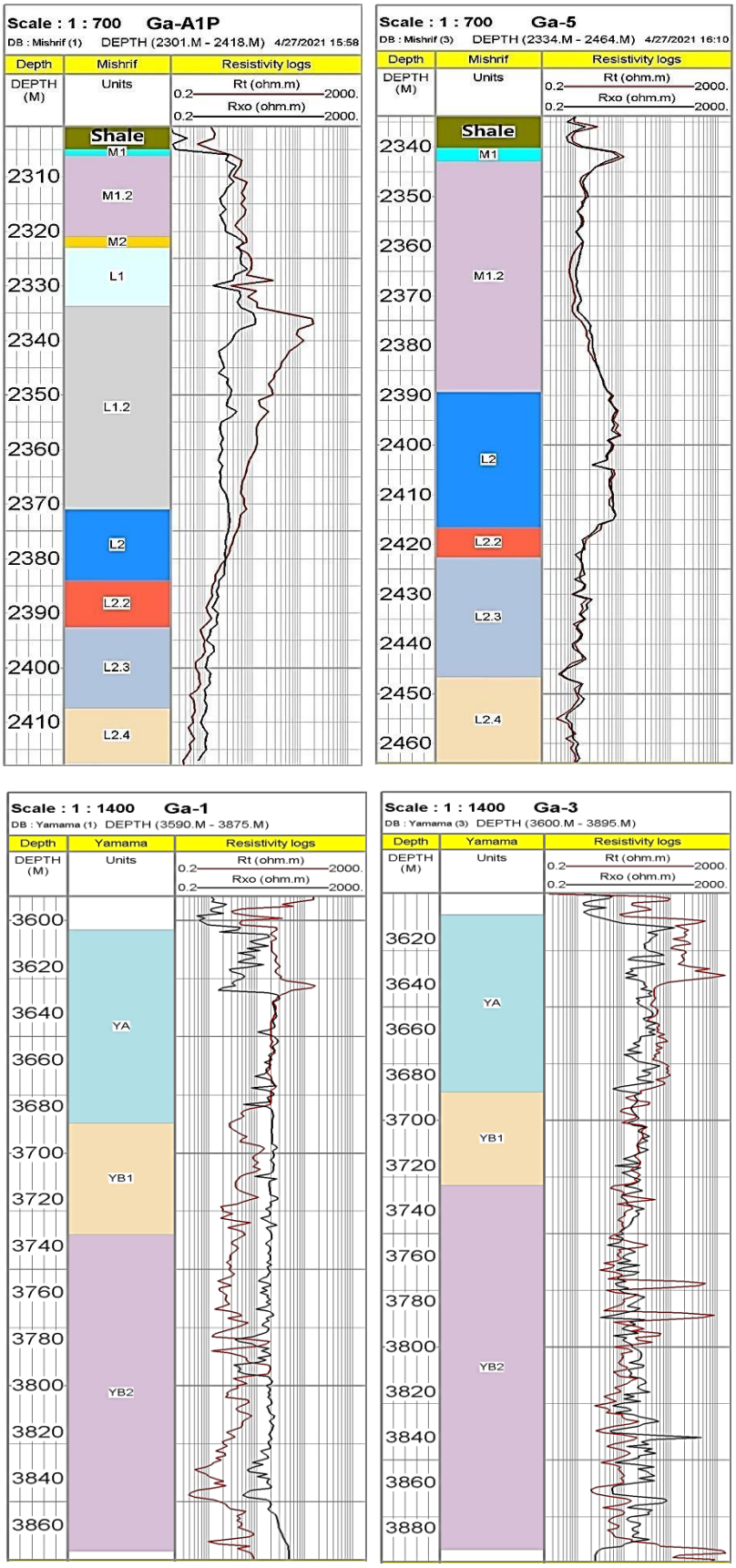

Figure (A-1): Resistivity log plots of the studied wells of Yamama Formation and the lower main unit of Mishrif Formation in Gharraf oil field.

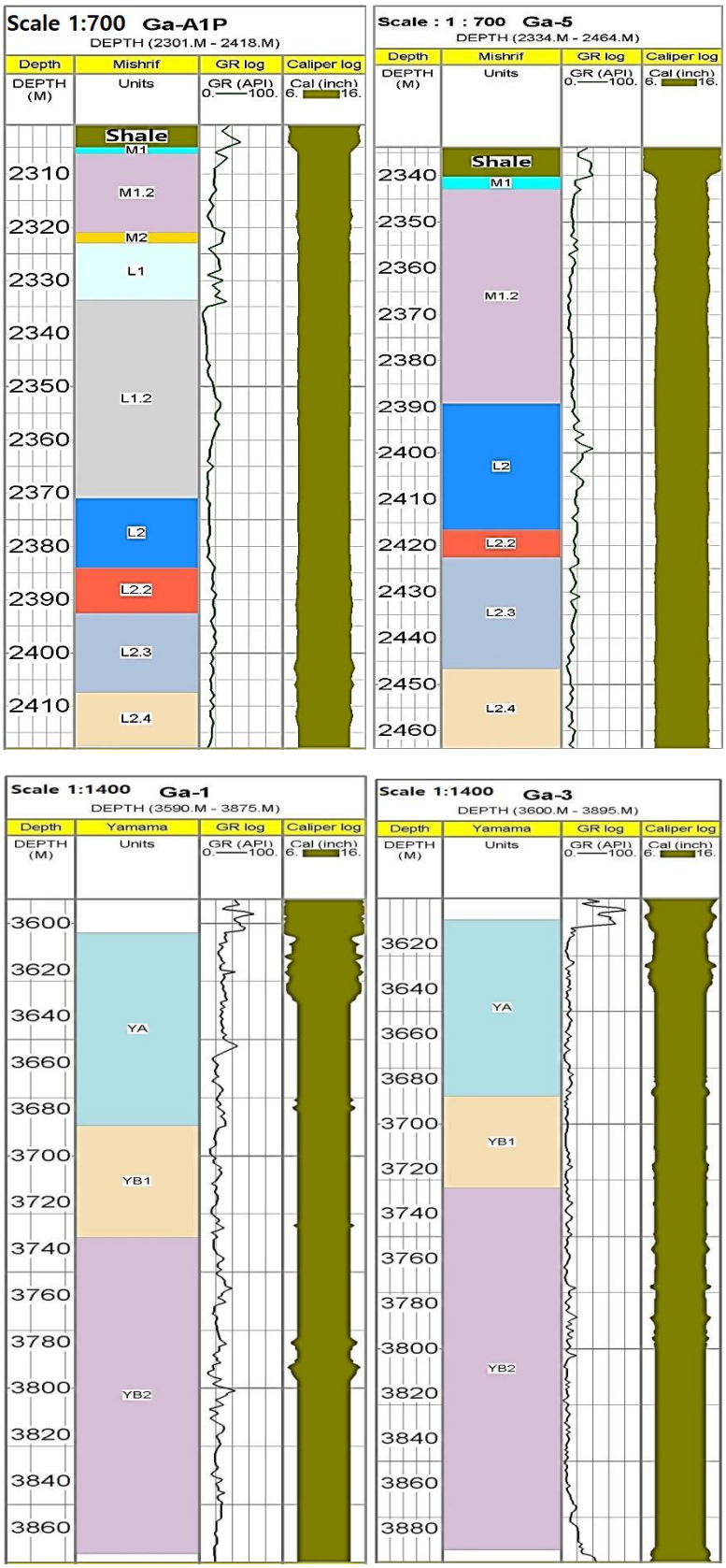

Figure (A-2): Caliper and GammaRay log plots of the studied wells of Yamama Formation and the lower main unit of Mishrif Formation in Gharraf oil field.

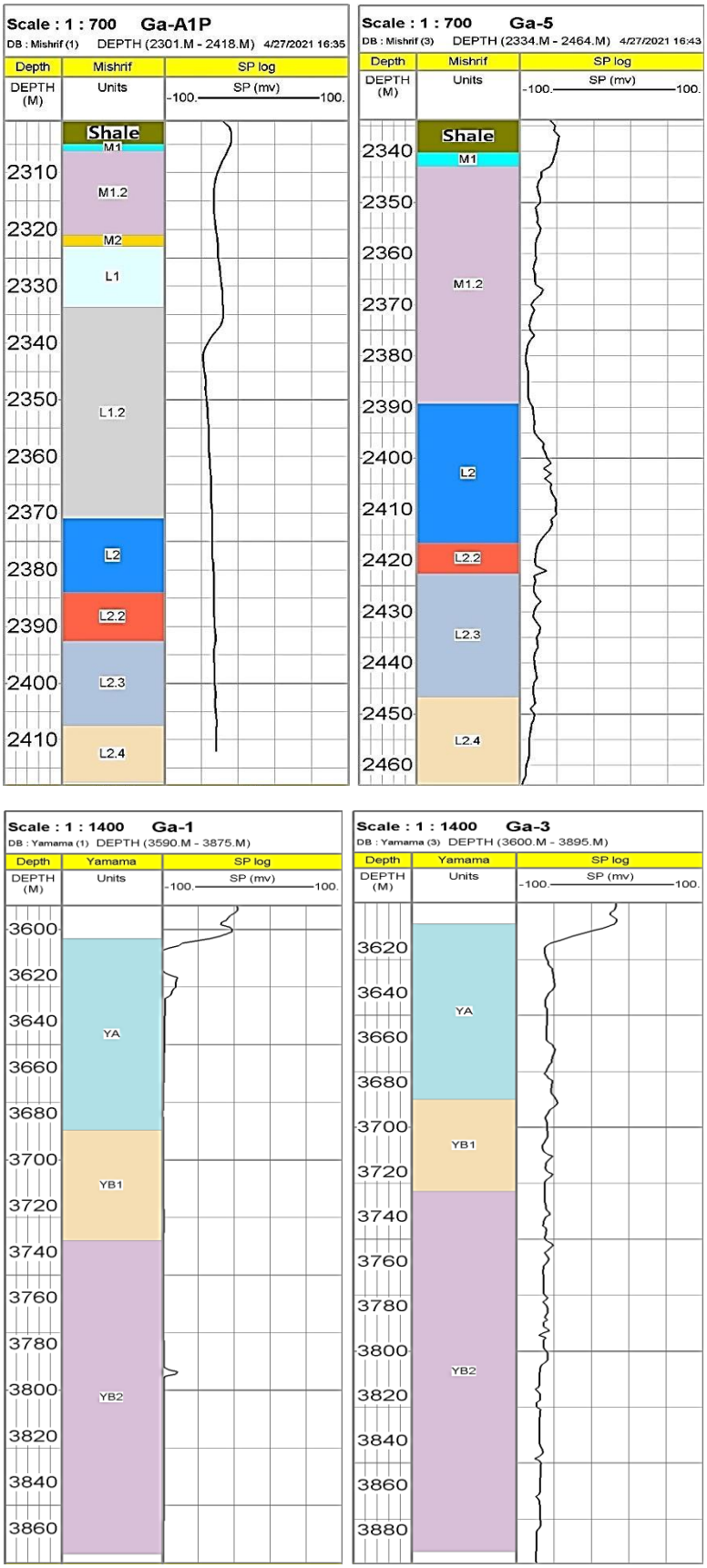

Figure (A-3): SP log plots of the studied wells of Yamama Formation and the lower main unit of Mishrif Formation in Gharraf oil field.

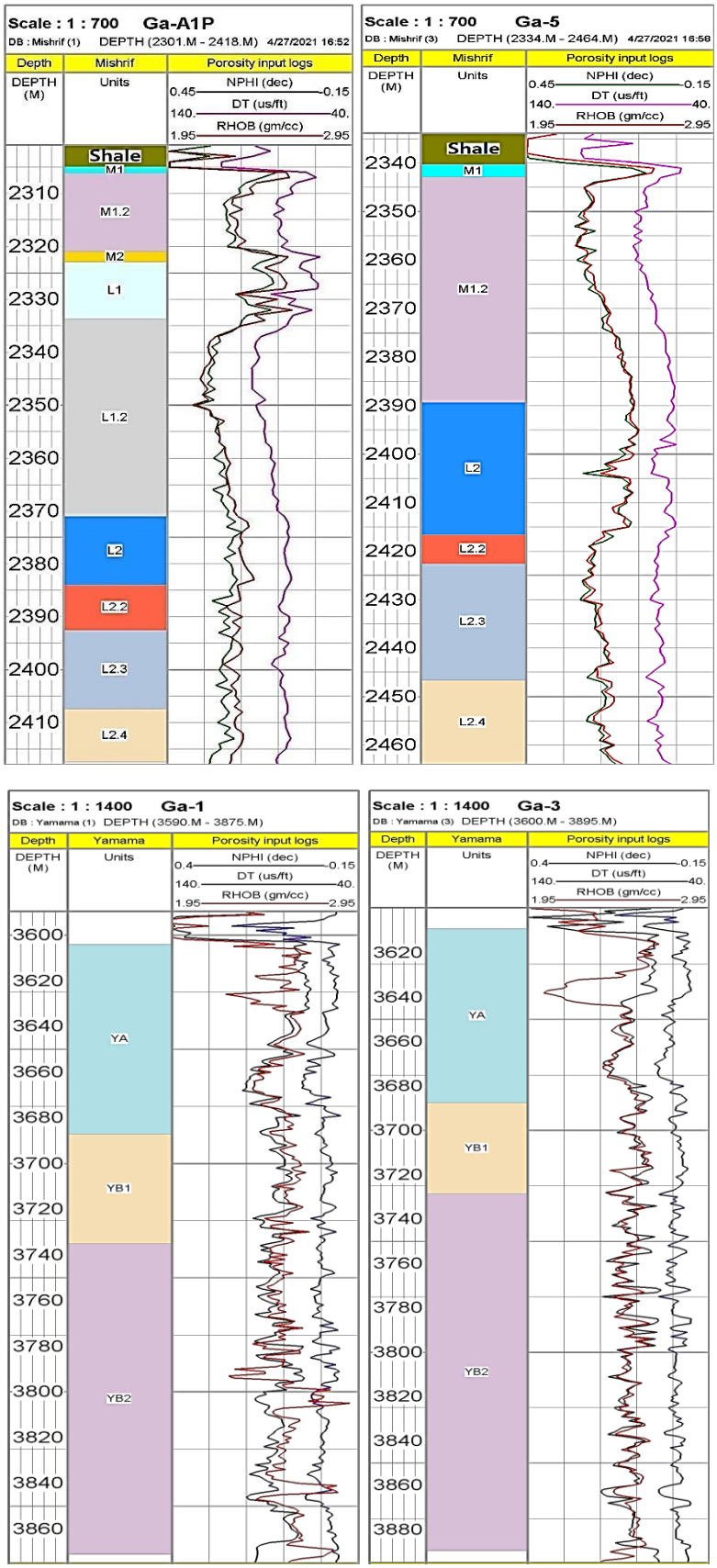

Figure (A-4): Porosity input logs plots of the studied wells of Yamama Formation and the lower main unit of Mishrif Formation in Gharraf oil field.

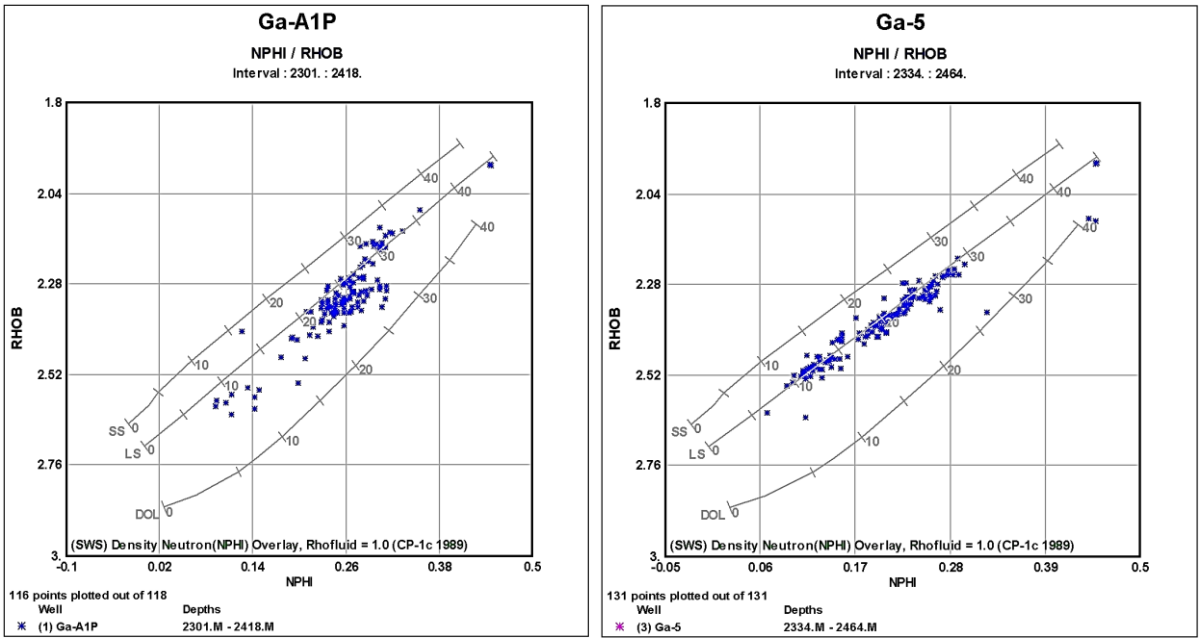

Figure (A-5): Neutron – Density cross plots of Well Ga-A1P and Ga-5 of the lower main unit of Mishrif Formation in Gharraf oil field.

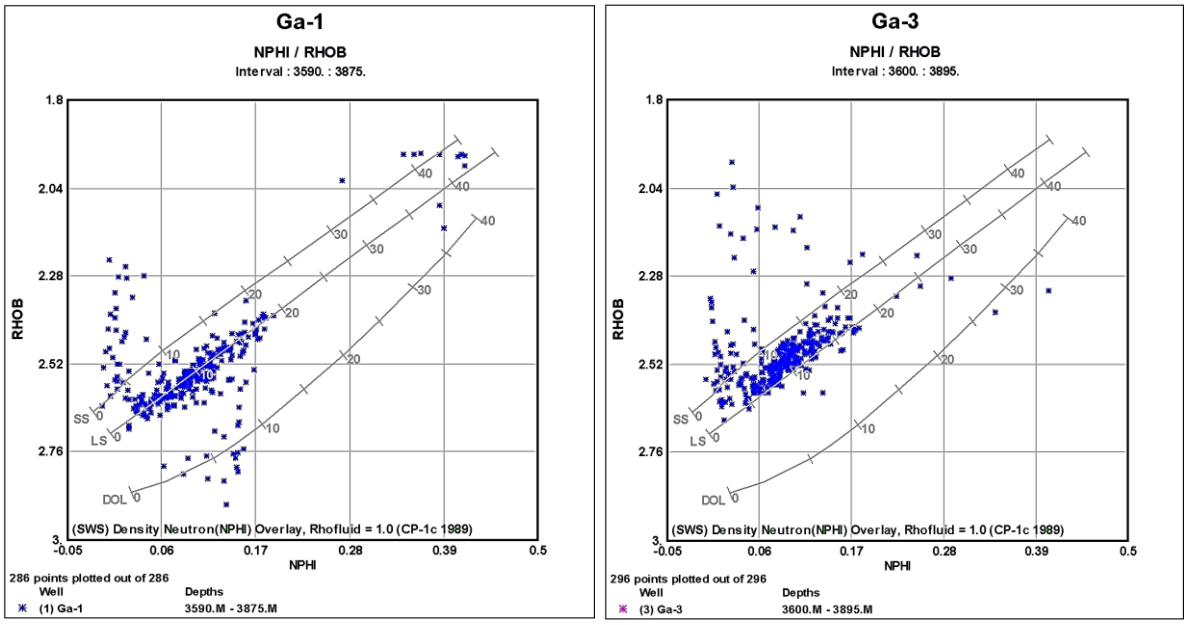

Figure (A-6): Neutron – Density cross plots of Yamama Formation in Well Ga-1 and Ga-3 in Gharraf oil field.

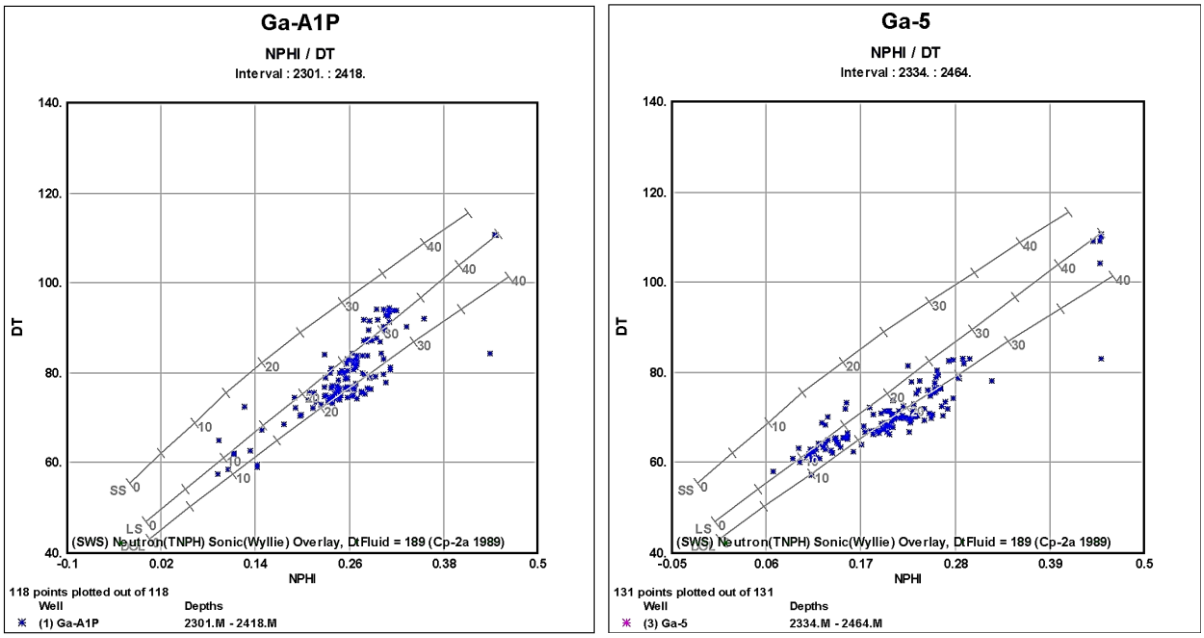

Figure (A-7): Neutron – Sonic cross plots of the lower main unit of Mishrif Formation in Well Ga-A1P and Ga-5 in Gharraf oil field.

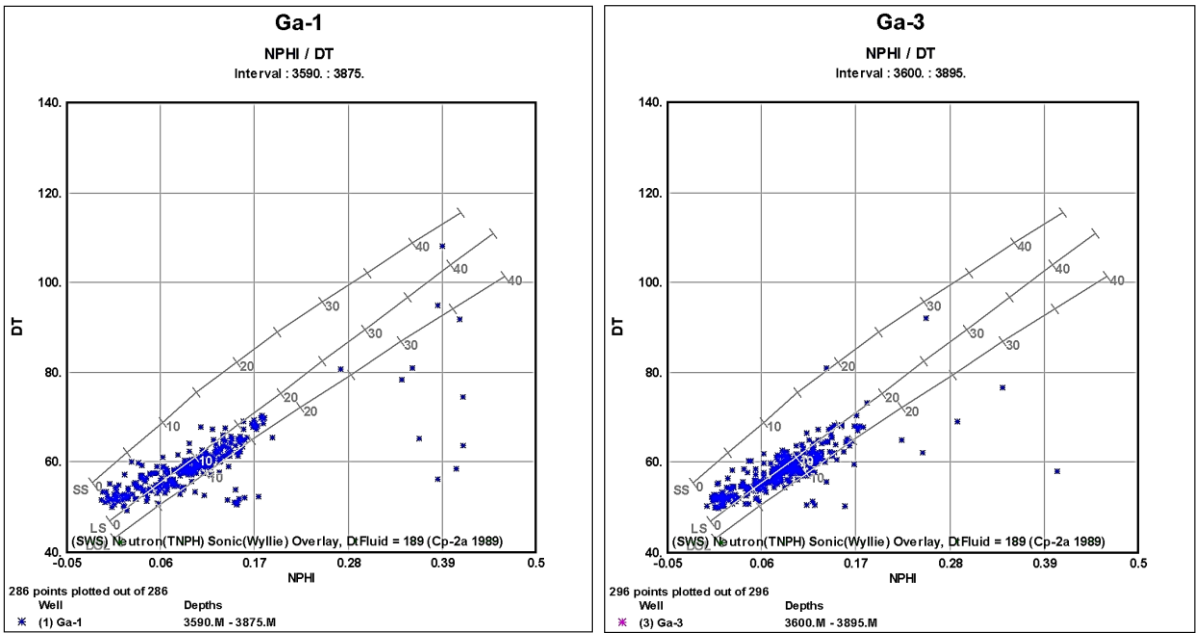

Figure (A-8): Neutron – Sonic cross plots of Yamama Formation in Well Ga-1 and Ga-3 in Gharraf oil field.

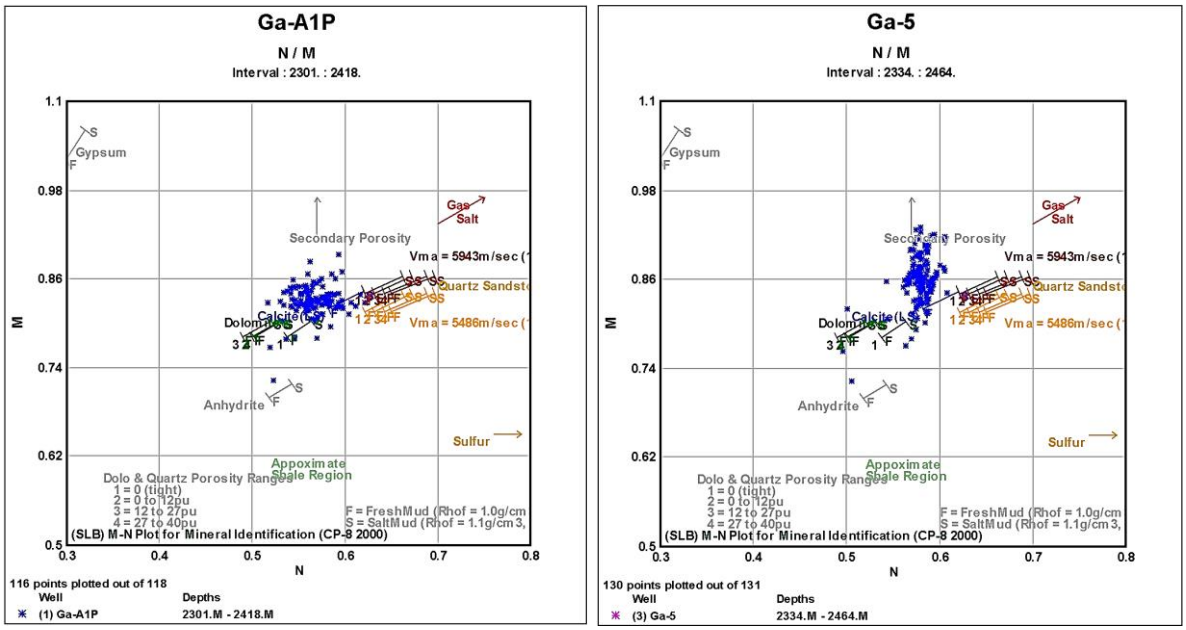

Figure (A-9): M – N cross plots of the lower main unit of Mishrif Formation in Well Ga-A1P and Ga-5 in Gharraf oil field.

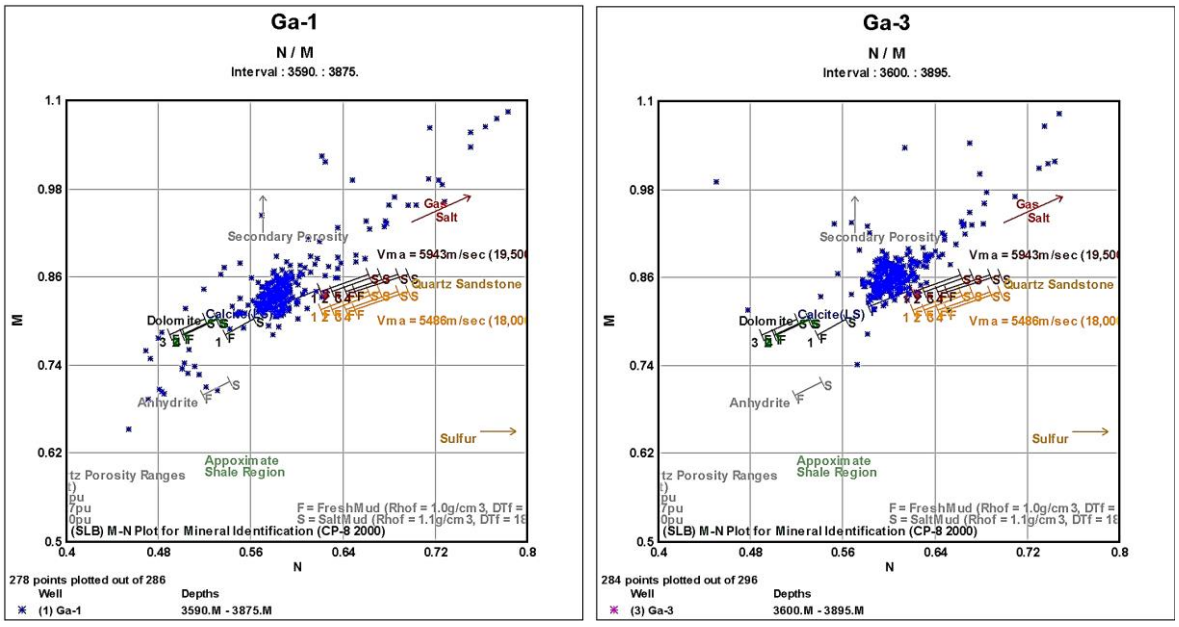

Figure (A-10): M – N cross plots of Yamama Formation in Well Ga-1 and Ga-3 in Gharraf oil field.

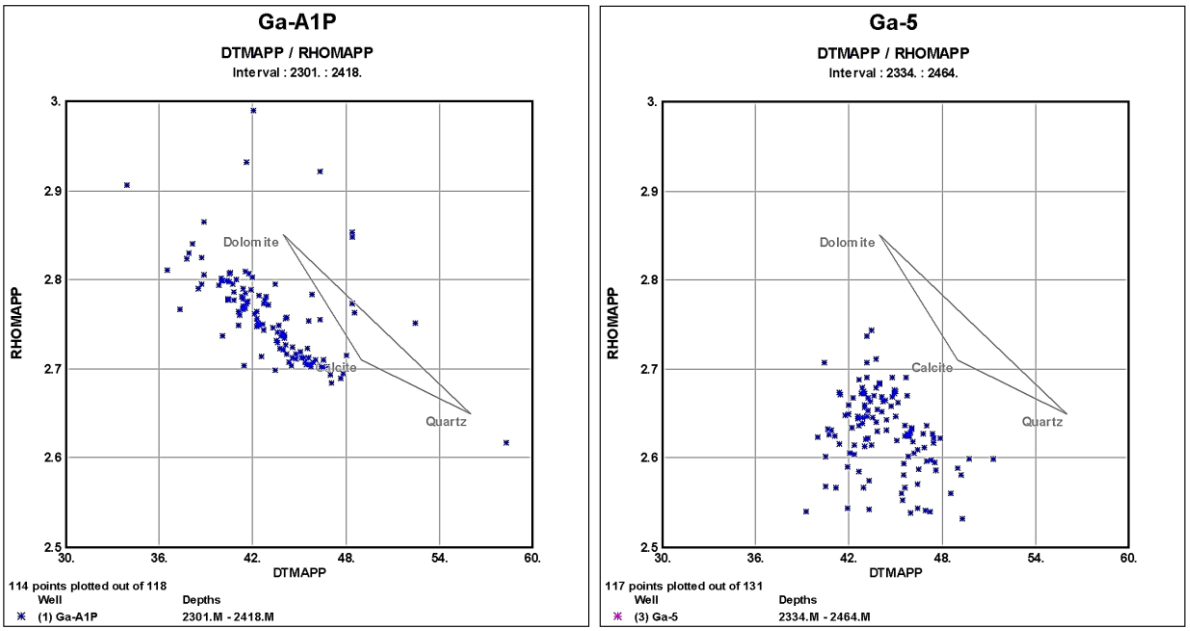

Figure (A-11): MID cross plots of the lower main unit of Mishrif Formation in Well Ga-A1P and Ga-5 in Gharraf oil field.

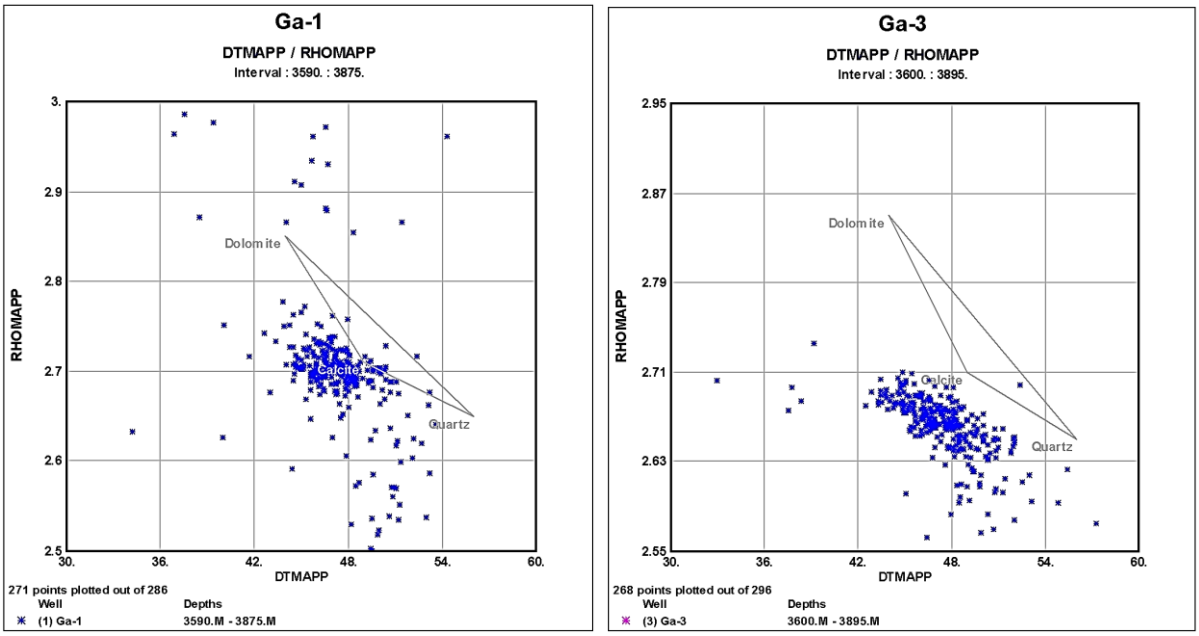

Figure (A-12): MID cross plots of Yamama Formation in Well Ga-1 and Ga-3 in Gharraf oil field.

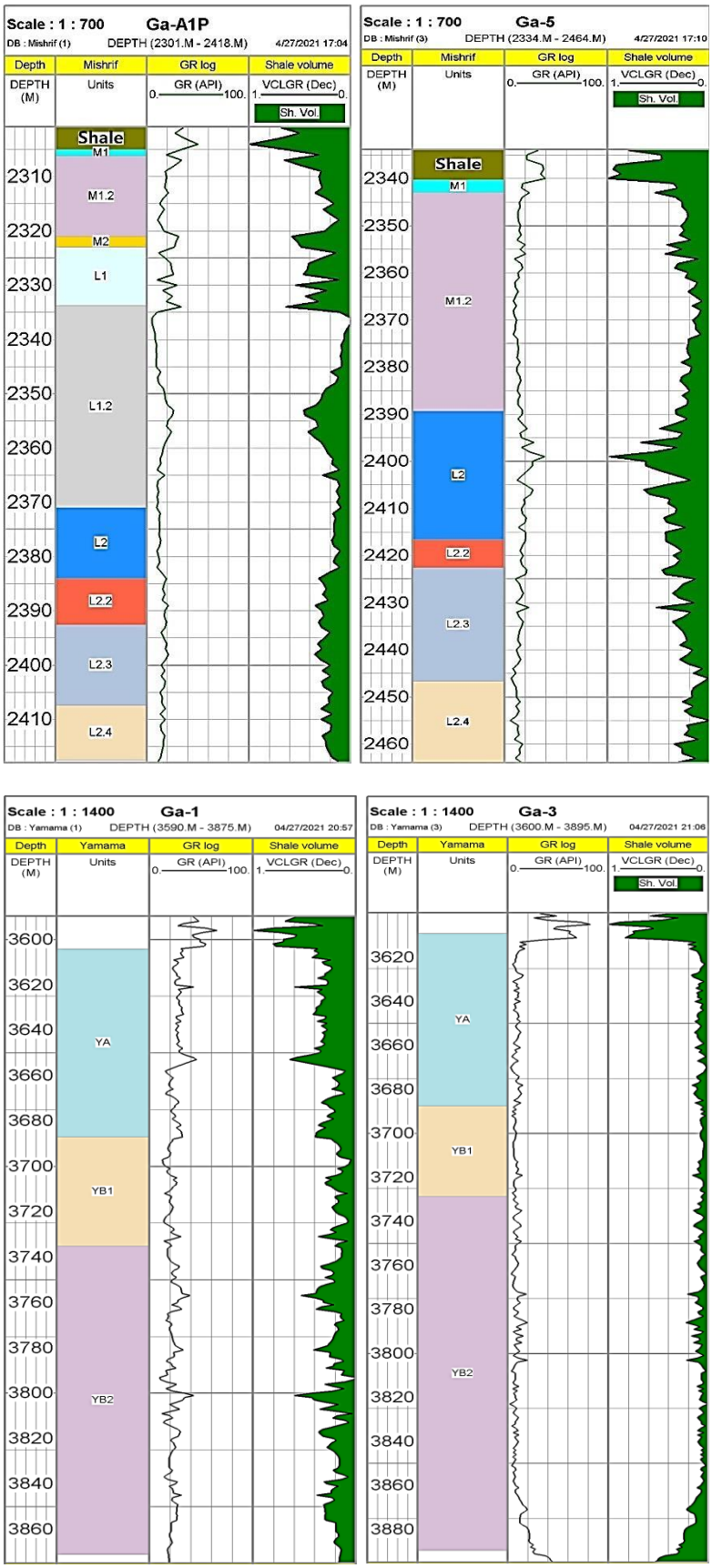

Figure (A-13): Shale volume in the studied wells of Yamama Formation and the lower main unit of Mishrif Formation in Gharraf oil field.

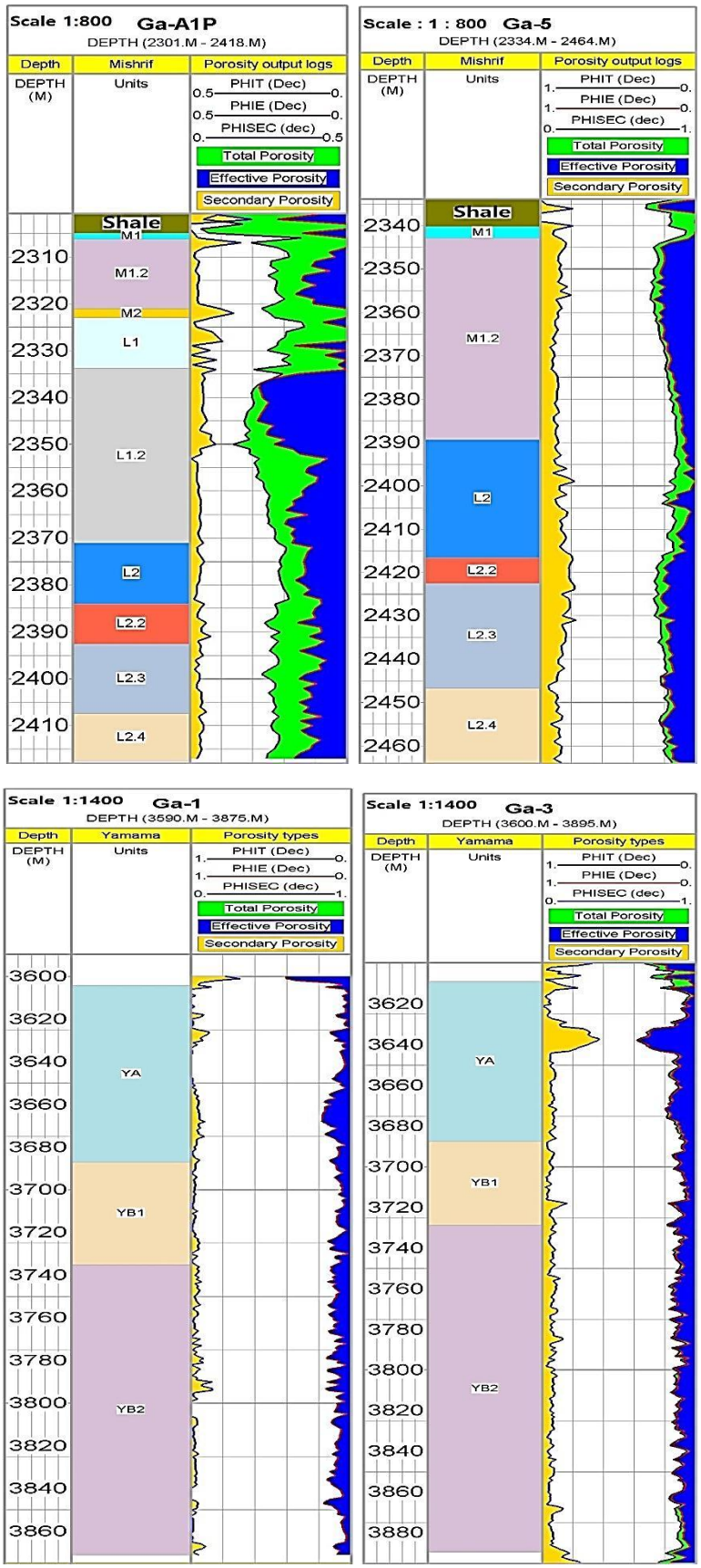

Figure (A-14): Porosity types log plots in the studied wells of Yamama Formation and the lower main unit of Mishrif Formation in Gharraf oil field.

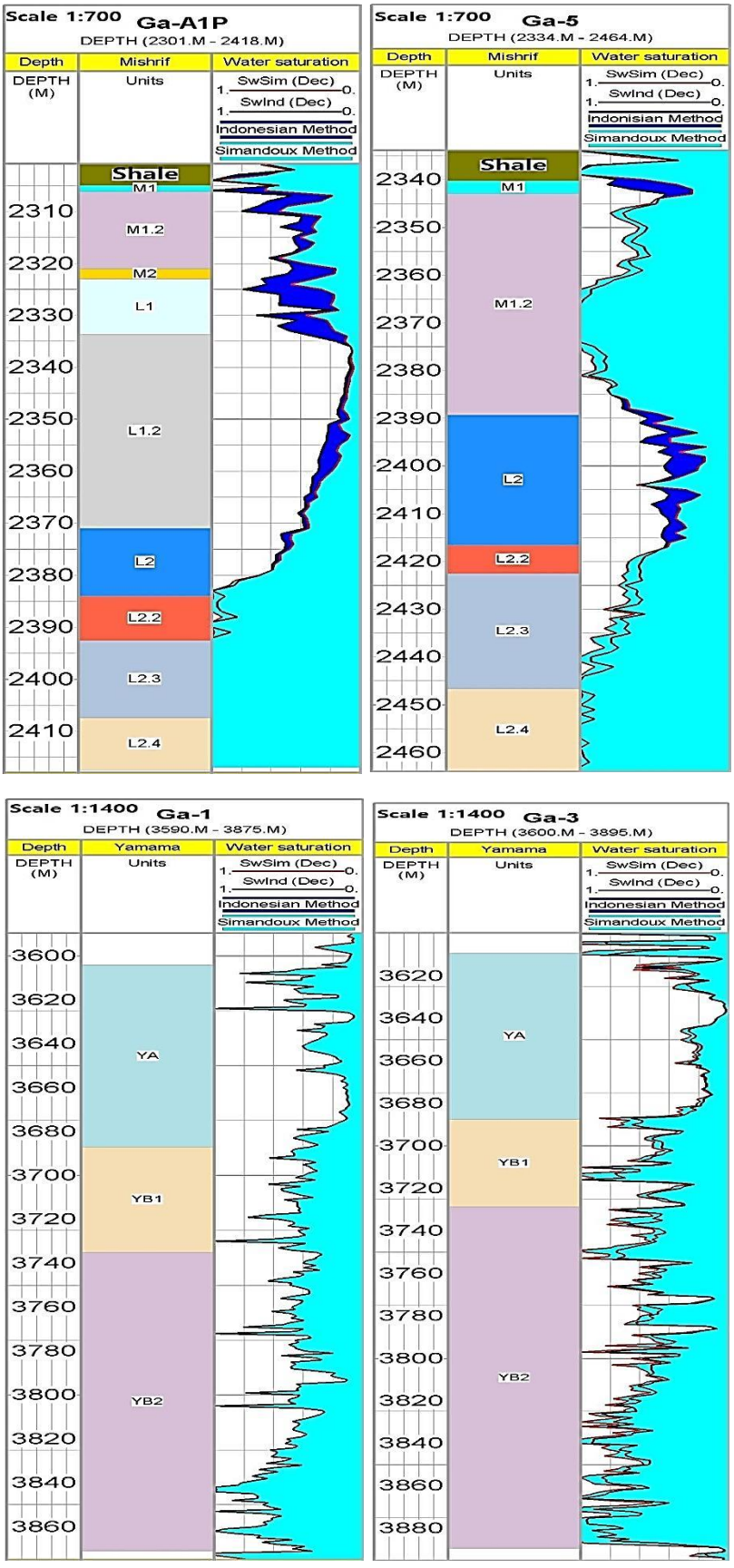

Figure (A-15): Water saturation log plots in the studied wells of Yamama Formation and the lower main unit of Mishrif Formation in Gharraf oil field.

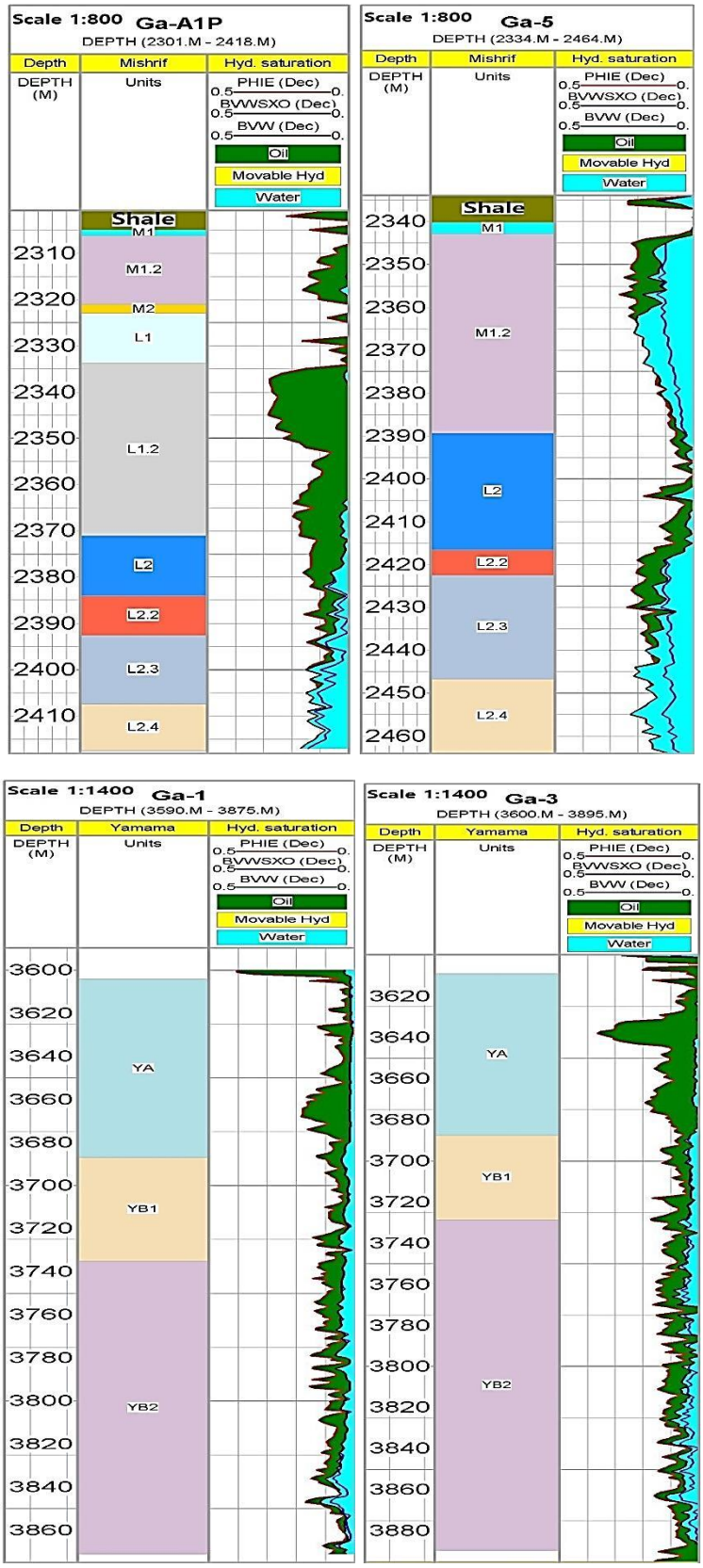

Figure (A-16): Hydrocarbon saturation log plots in the studied wells of Yamama Formation and the lower main unit of Mishrif Formation in Gharraf oil field.

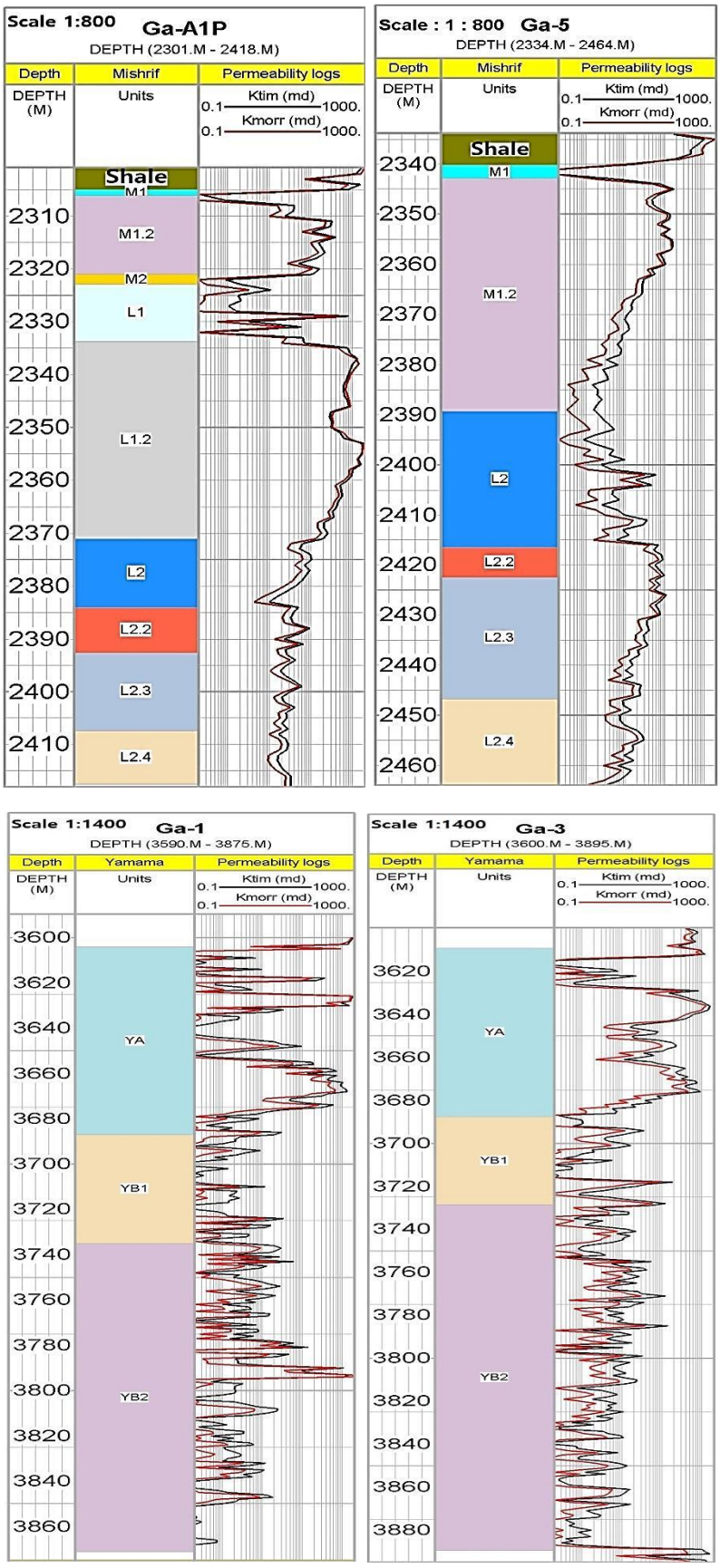

Figure (A-17): Permeability log plots in the studied wells of Yamama Formation and the lower main unit of Mishrif Formation in Gharraf oil field.

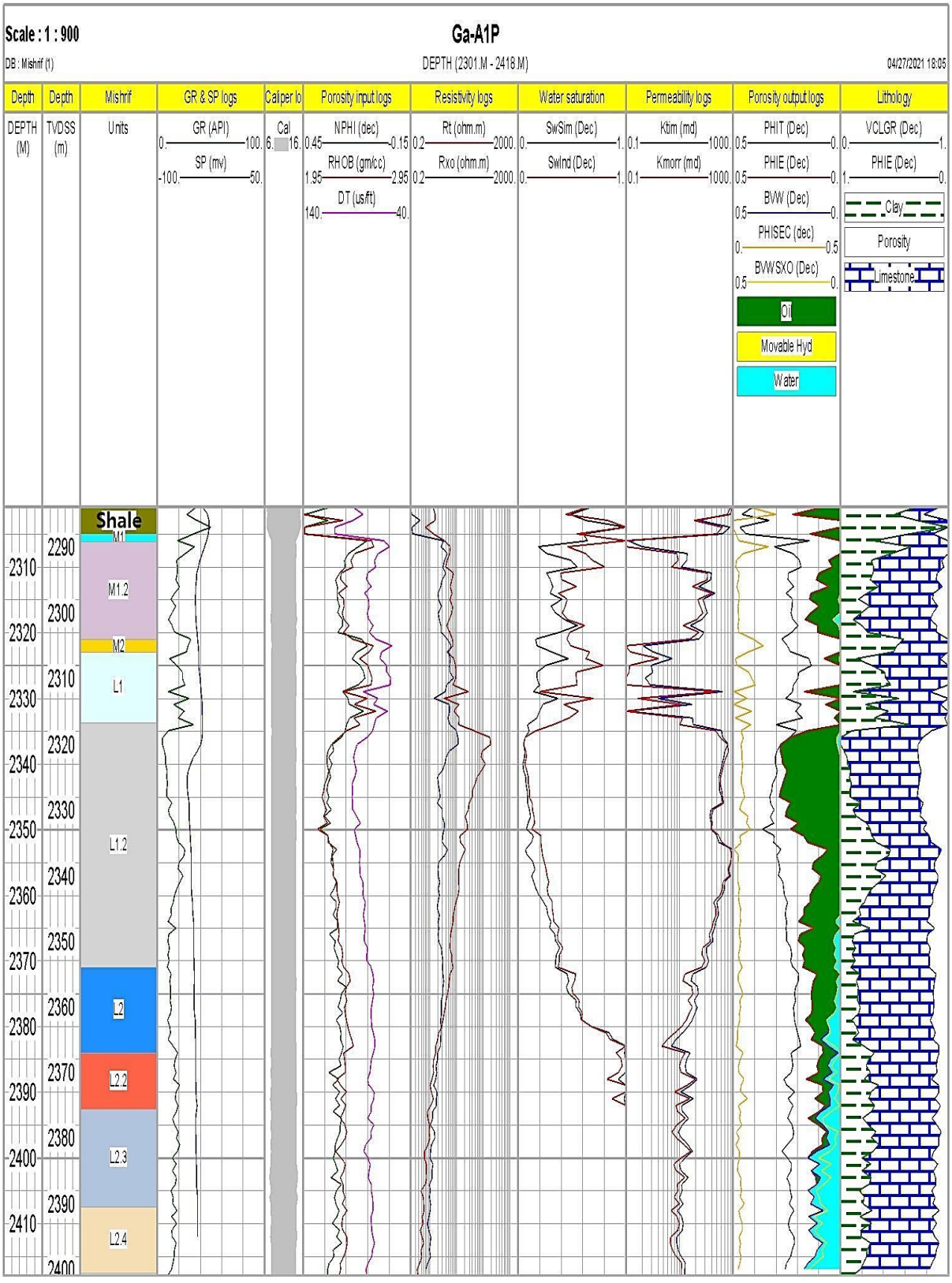

Figure (A-18): Computer Processes Interpretation (CPI) of the lower main unit of Mishrif Formation in Well Ga-A1P.

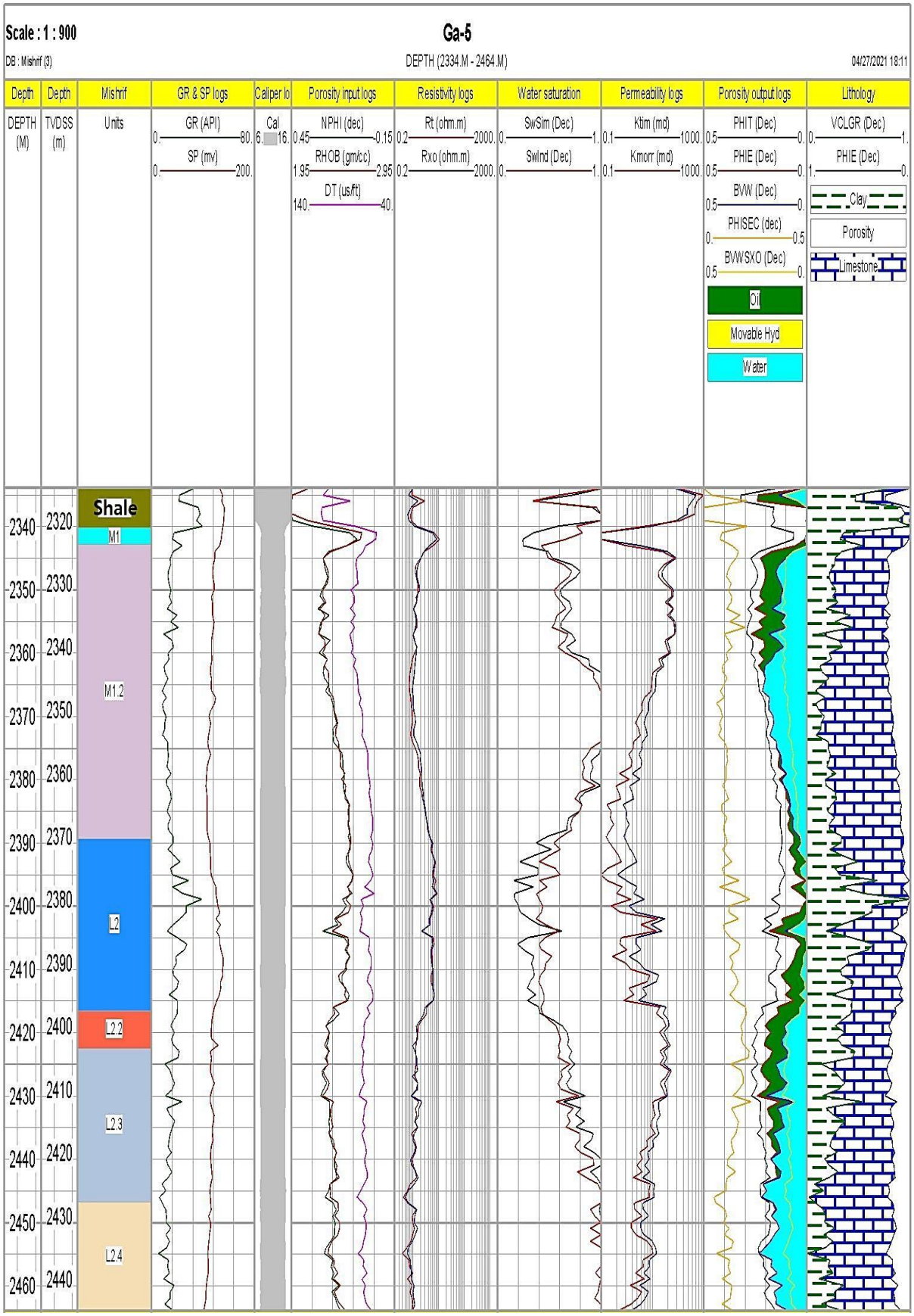

Figure (A-19): Computer Processes Interpretation (CPI) of the lower main unit of Mishrif Formation in Well Ga-5.

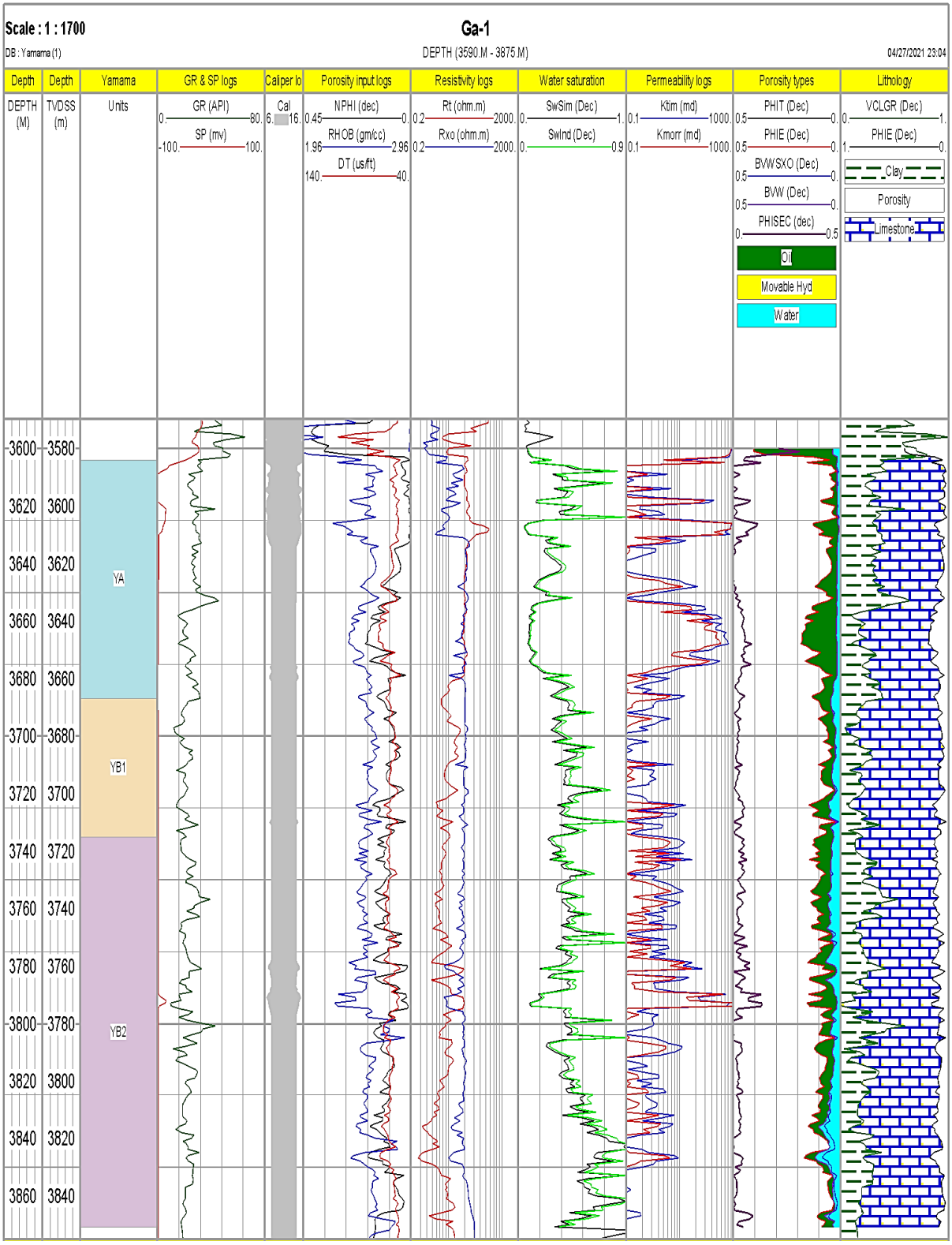

Figure (A-20): Computer Processes Interpretation (CPI) of Yamama Formation in Well Ga-1.

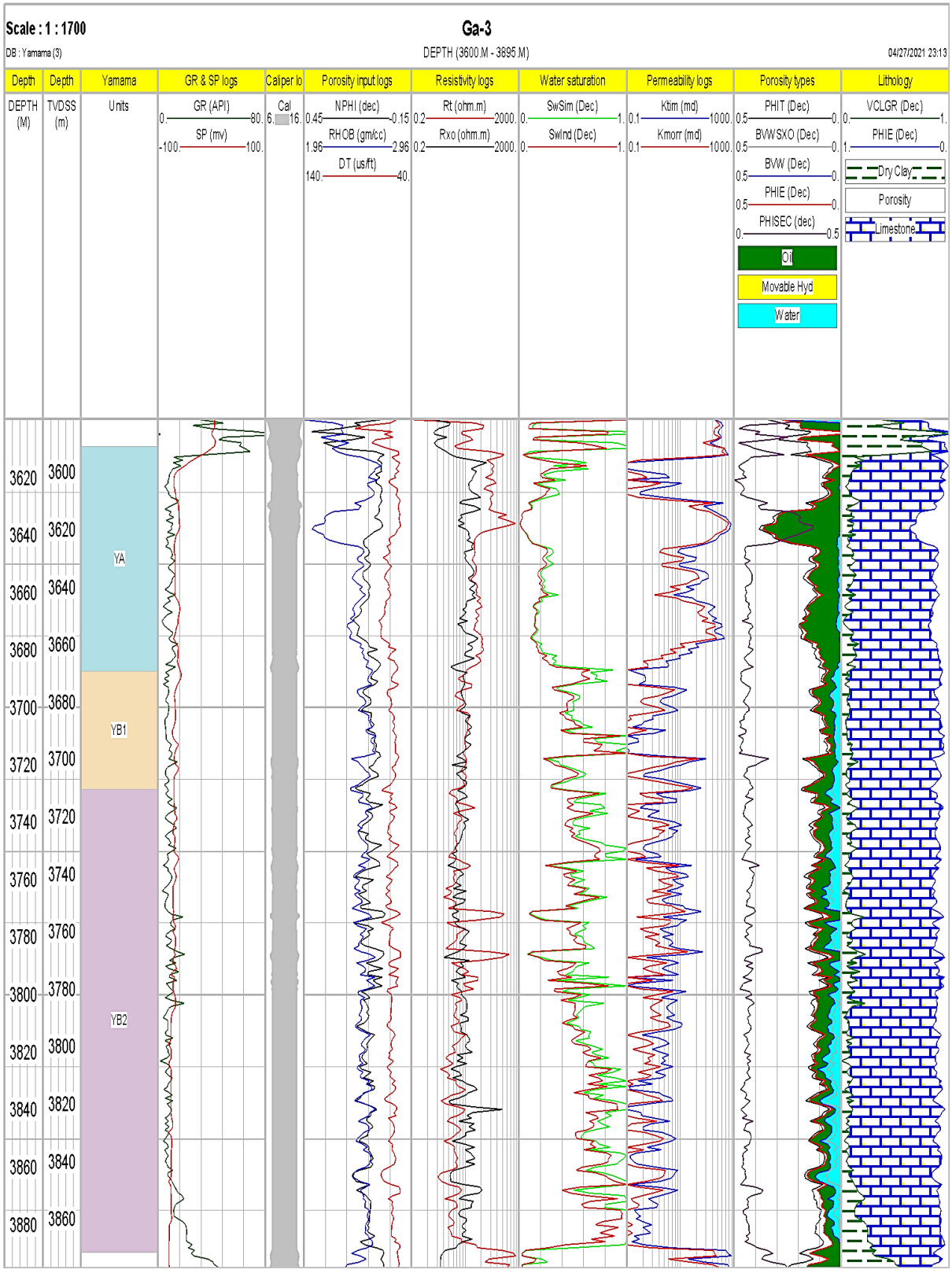

Figure (A-21): Computer Processes Interpretation (CPI) of Yamama Formation in Well Ga-3.

Table (A-1): Net pay and average of the main petrophysical properties of the lower main unit of Mishrif Formation in Well Ga-A1P.

Mishrif Reservoir / Ga-A1P RTKB = 17.07 m											
Units	Top		Bottom		Gross Thick.	Net Thick.	N/G	Av. PHIE%	Av. Sw%	Av. Vcl%	Av. Sh%
	MD	TVDSS	MD	TVDSS							
M1	2305	2287.31	2306.2	2288.51	1.20	0.00	0.00	---	---	---	---
M1.2	2306.2	2288.51	2321	2303.30	14.8	08.00	0.54	12.50	34.90	22.90	65.10
M2	2321	2303.30	2323	2305.29	2.00	0.00	0.00	---	---	---	---
L1	2323	2305.29	2333.71	2316.02	10.71	01.00	0.09	16.80	14.30	11.60	85.70
L1.2	2333.71	2316.02	2371	2353.24	37.29	35.50	0.95	19.50	15.10	18.20	84.90
L2	2371	2353.24	2384	2366.22	13.00	04.50	0.35	13.10	44.60	15.70	55.40
L2.2	2384	2366.22	2392.56	2374.87	8.56	0.00	0.00	---	---	---	---
L2.3	2392.56	2374.87	2407.44	2389.75	14.88	0.00	0.00	---	---	---	---
L2.4	2407.44	2389.75	2417.5	2399.67	10.06	0.00	0.00	---	---	---	---

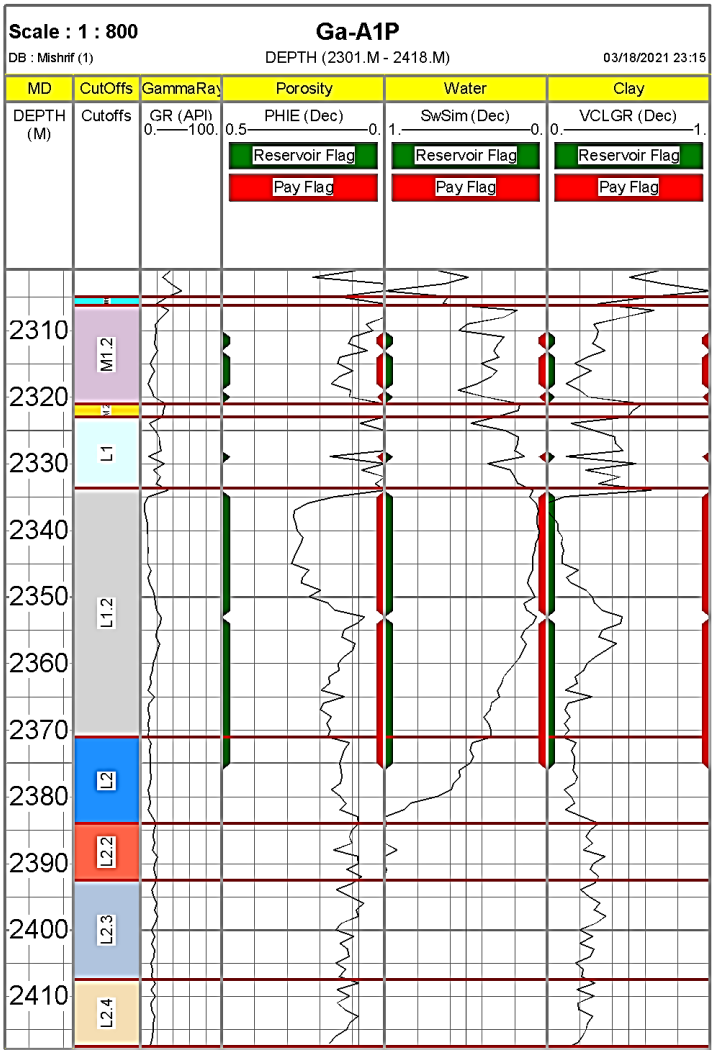

Figure (A-22): Net-pay and reservoir parameters of the lower main unit of Mishrif Formation in Well Ga-A1P.

Table (A-2): Net pay and average of the main petrophysical properties of the lower main unit of Mishrif Formation in Well Ga-5.

Mishrif Reservoir / Ga-5 RTKB = 19.10 m											
Units	Top		Bottom		Gross Thick.	Net Thick.	N/G	Av. PHIE%	Av. Sw%	Av. Vcl%	Av. Sh%
	MD	TVDSS	MD	TVDSS							
M1	2340.21	2320.34	2342.86	2322.99	2.65	0.00	0.00	---	---	---	---
M1.2	2342.86	2322.99	2371.12	2351.23	46.43	1.00	0.02	17.20	48.80	33.80	51.20
L2	2389.29	2369.40	2416.57	2396.66	27.28	7.07	0.26	11.50	35.90	37.50	64.10
L2.2	2416.57	2396.66	2422.53	2402.61	5.96	0.93	0.16	13.60	41.50	43.00	58.50
L2.3	2422.53	2402.61	2446.69	2426.76	24.16	0.00	0.00	---	---	---	---
L2.4	2446.69	2426.76	2464.41	2444.46	17.72	0.00	0.00	---	---	---	---

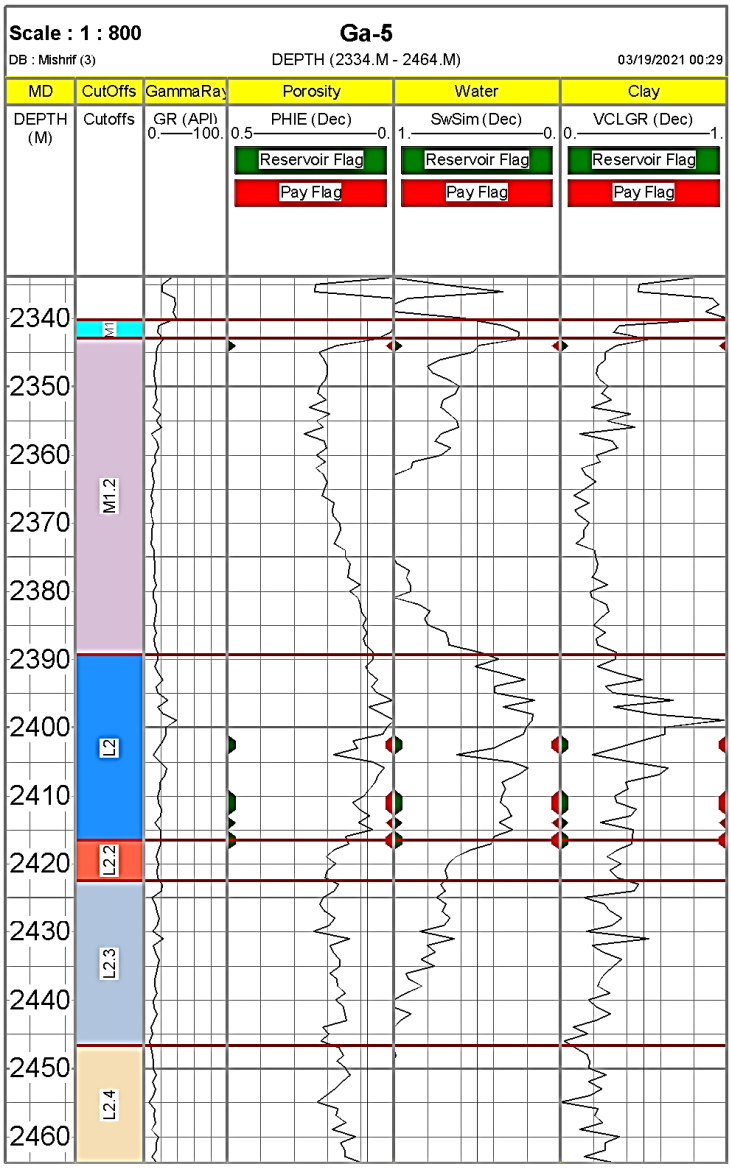

Figure (A-23): Net-pay and reservoir parameters of the lower main unit of Mishrif Formation in Well Ga-5.

Table (A-3): Net pay and average of the main petrophysical properties of Yamama Formation in Well Ga-1.

Yamama Reservoir / Ga-1 RTKB = 20 m											
Units	Top		Bottom		Gross Thick.	Net Thick.	N/G	Av. PHIE%	Av. Sw%	Av. Vcl%	Av. Sh%
	MD	TVDSS	MD	TVDSS							
YA	3604	3584	3687	3667	85.00	15.00	0.18	15.50	11.10	17.50	88.90
YB1	3687	3667	3735	3715	48.00	28.50	0.59	09.20	41.10	16.60	58.90
YB2	3735	3715	3871	3851	136.00	48.00	0.35	10.10	37.40	16.30	62.60

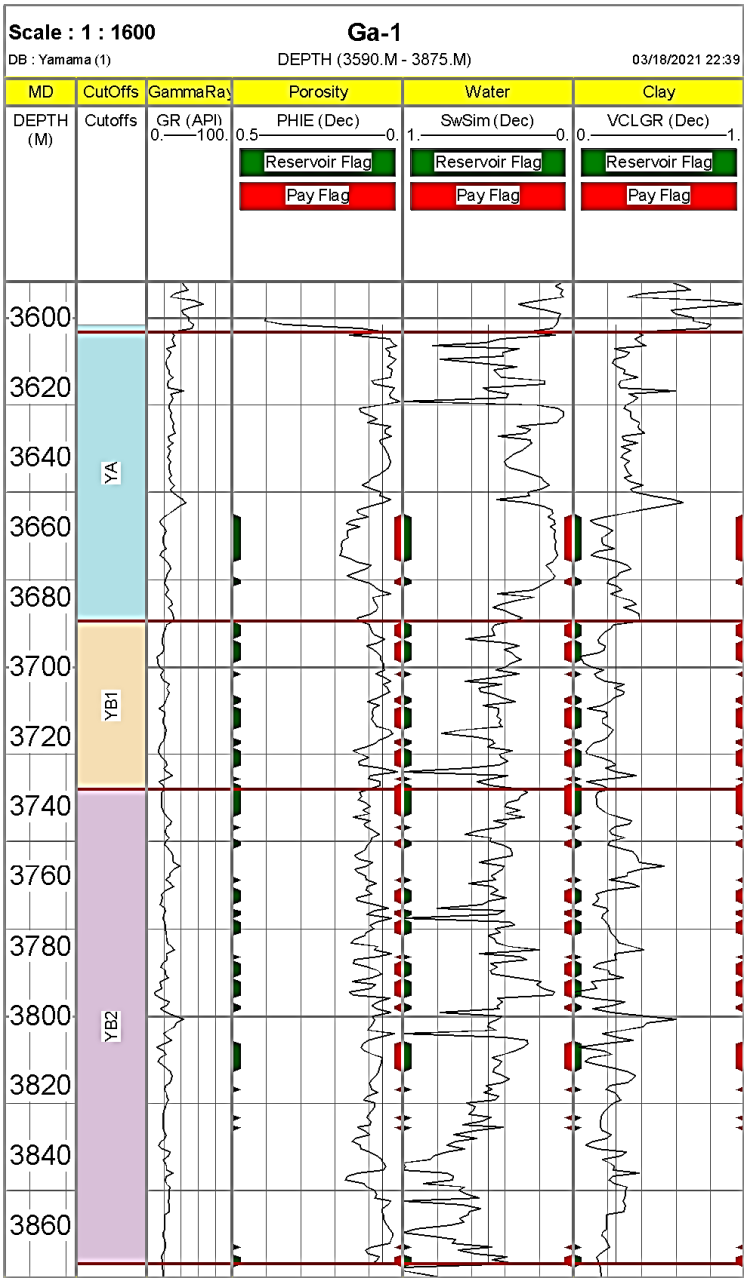

Figure (A-24): Net-pay and reservoir parameters of Yamama Formation in Well Ga-1.

Table (A-4): Net pay and average of the main petrophysical properties of Yamama Formation in Well Ga-3.

Yamama Reservoir / Ga-3 RTKB = 17.54 m											
Units	Top		Bottom		Gross Thick.	Net Thick.	N/G	Av. PHIE%	Av. Sw%	Av. Vcl%	Av. Sh%
	MD	TVDSS	MD	TVDSS							
YA	3609.04	3591.5	3687.54	3670	78.54	67.00	0.85	15.40	15.60	09.40	84.40
YB1	3687.54	3670	3728.54	3711	41.00	16.04	0.39	11.60	39.80	07.40	60.20
YB2	3728.54	3711	3889.54	3872	161.00	17.96	0.11	12.00	38.30	09.30	61.70

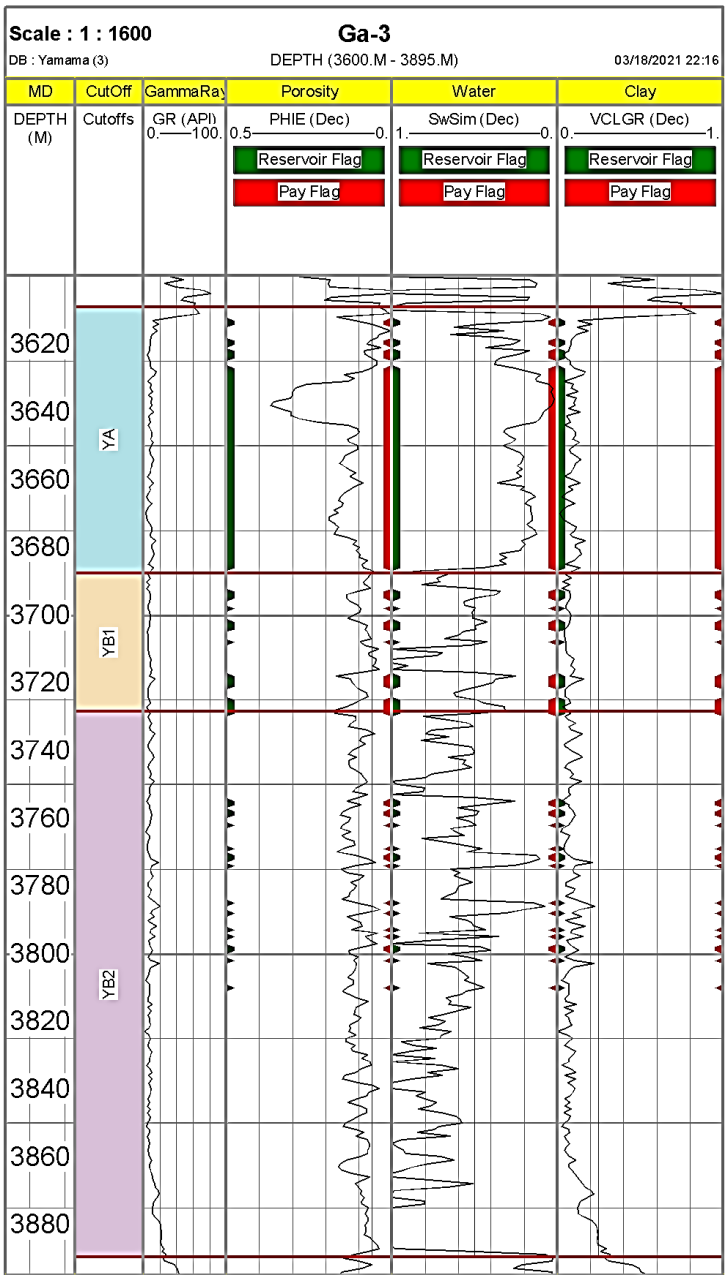

Figure (A-25): Net-pay and reservoir parameters of Yamama Formation in Well Ga-3.

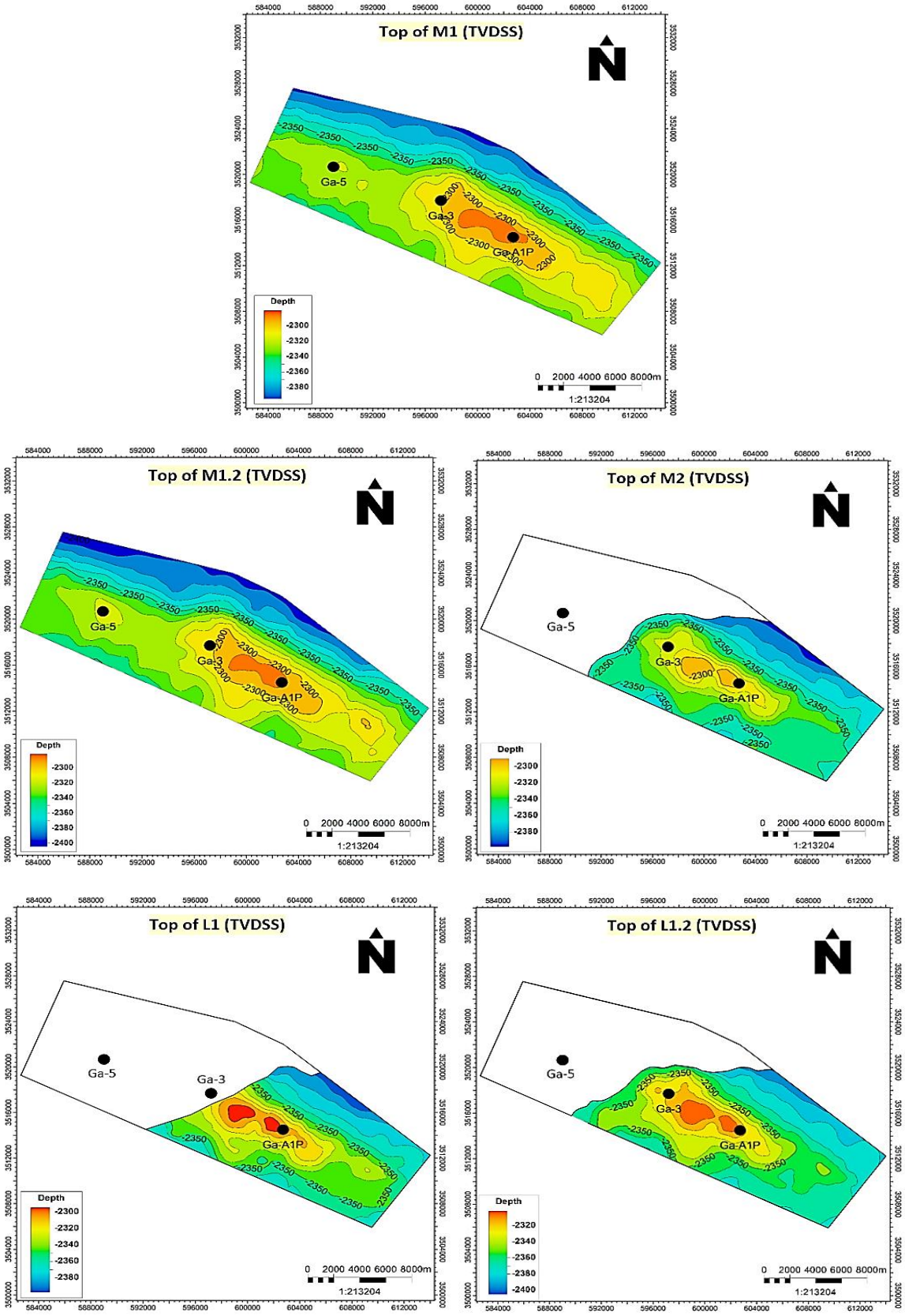

Figure (A-26): Structure contour maps from top of unit M1 to the top of unit L1.2 in the reservoir part of Mishrif Formation in Gharraf oil field.

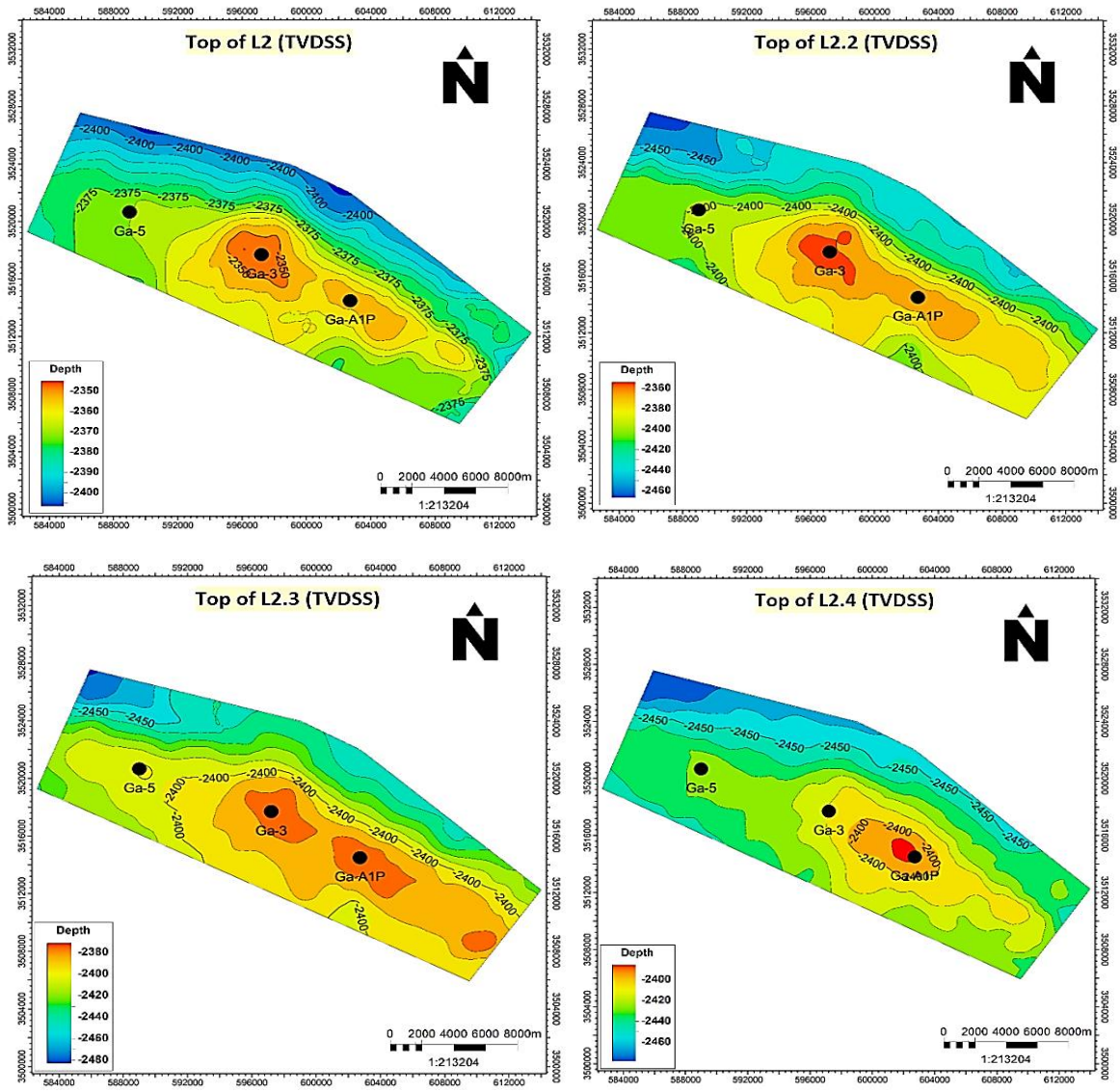

Figure (A-27): Structure contour maps from top of unit L2 to top of unit L2.4 of Mishrif Formation in Gharraf oil field.

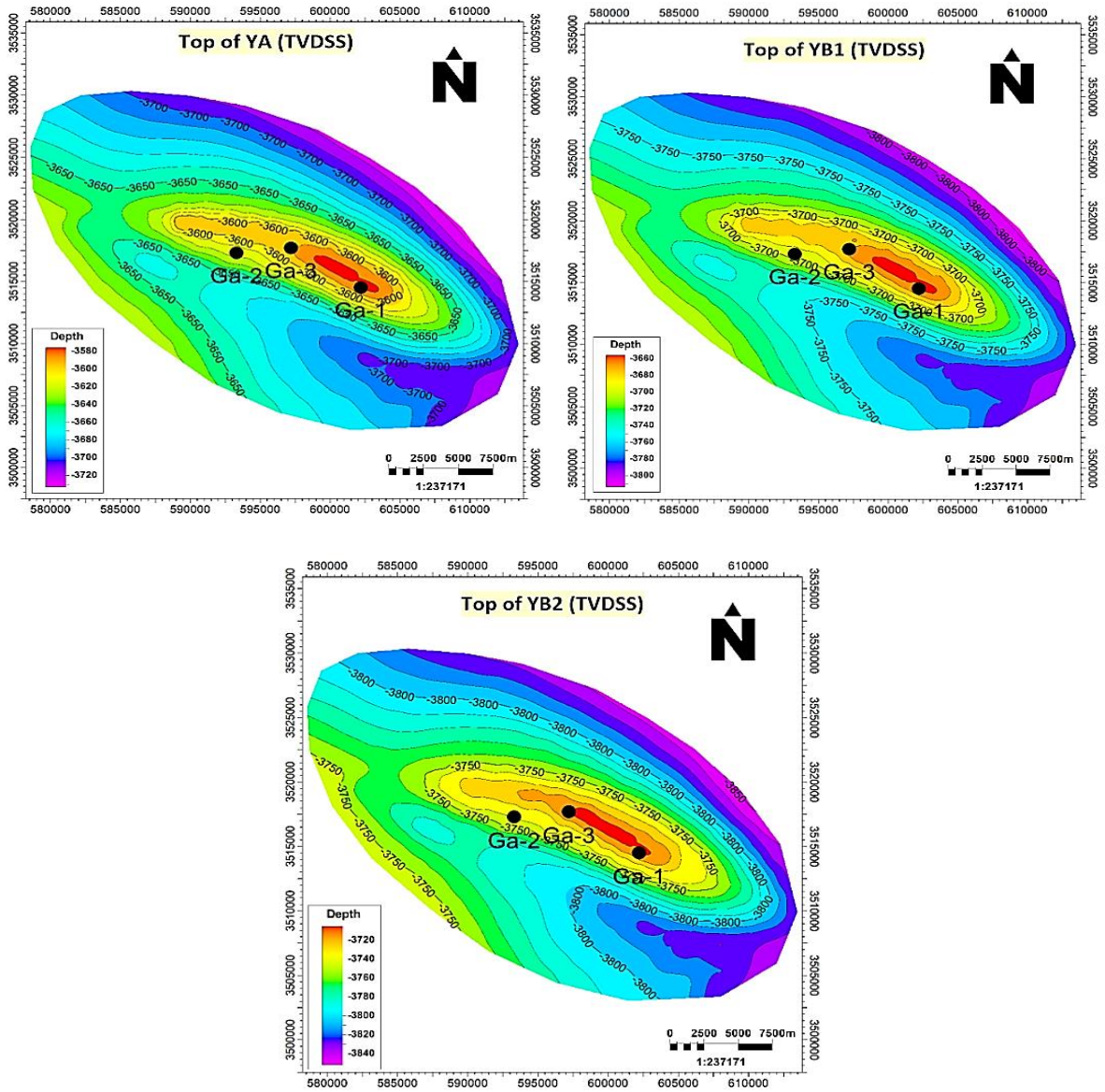

Figure (A-28): Structure contour maps of top of Yamama Formation units (YA, YB1, and YB2) in Gharraf oil field.

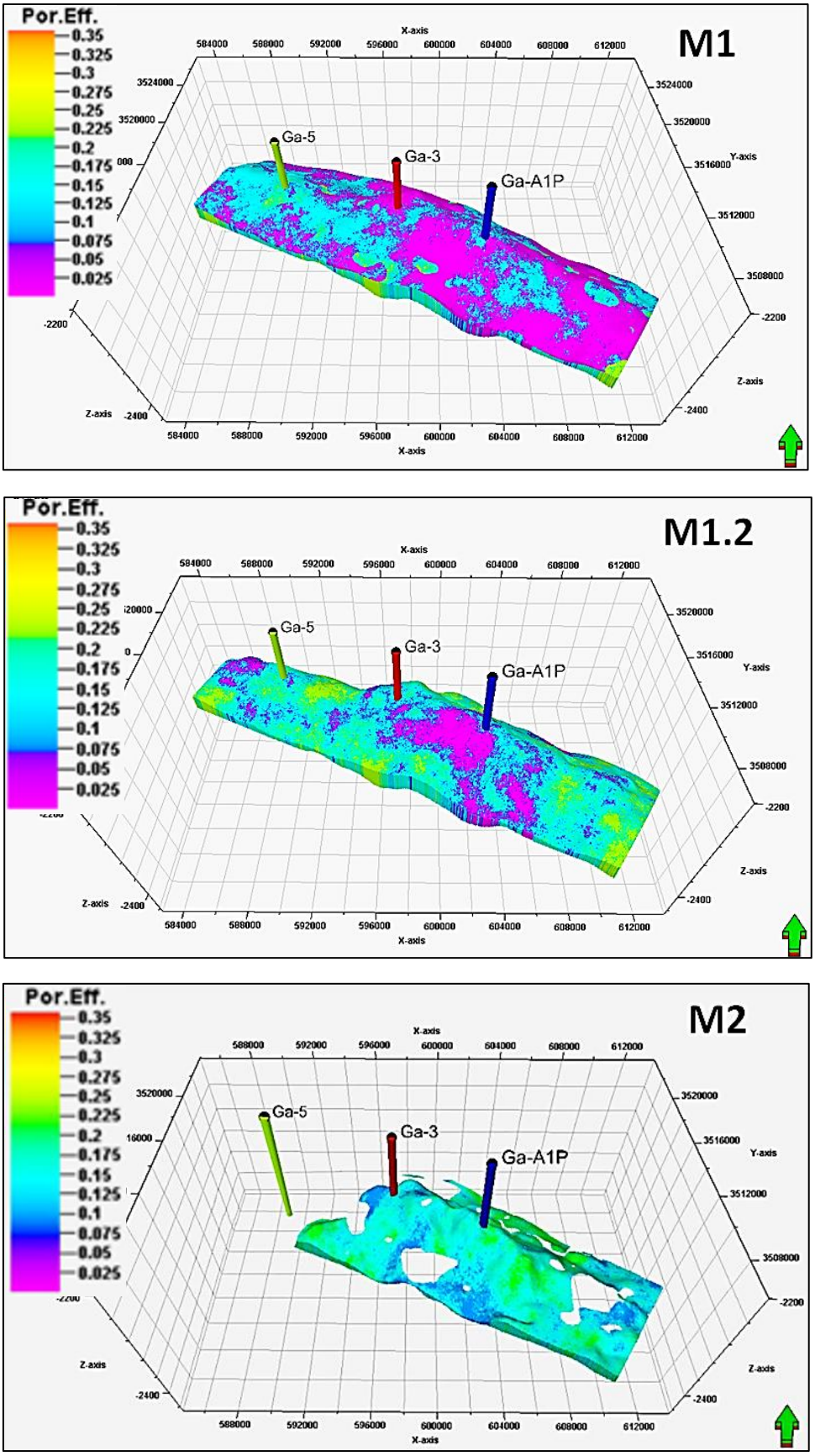

Figure (A-29): Porosity distribution models of the reservoir part units (M1, M1.2, and M2) of Mishrif Formation in Gharraf oil field.

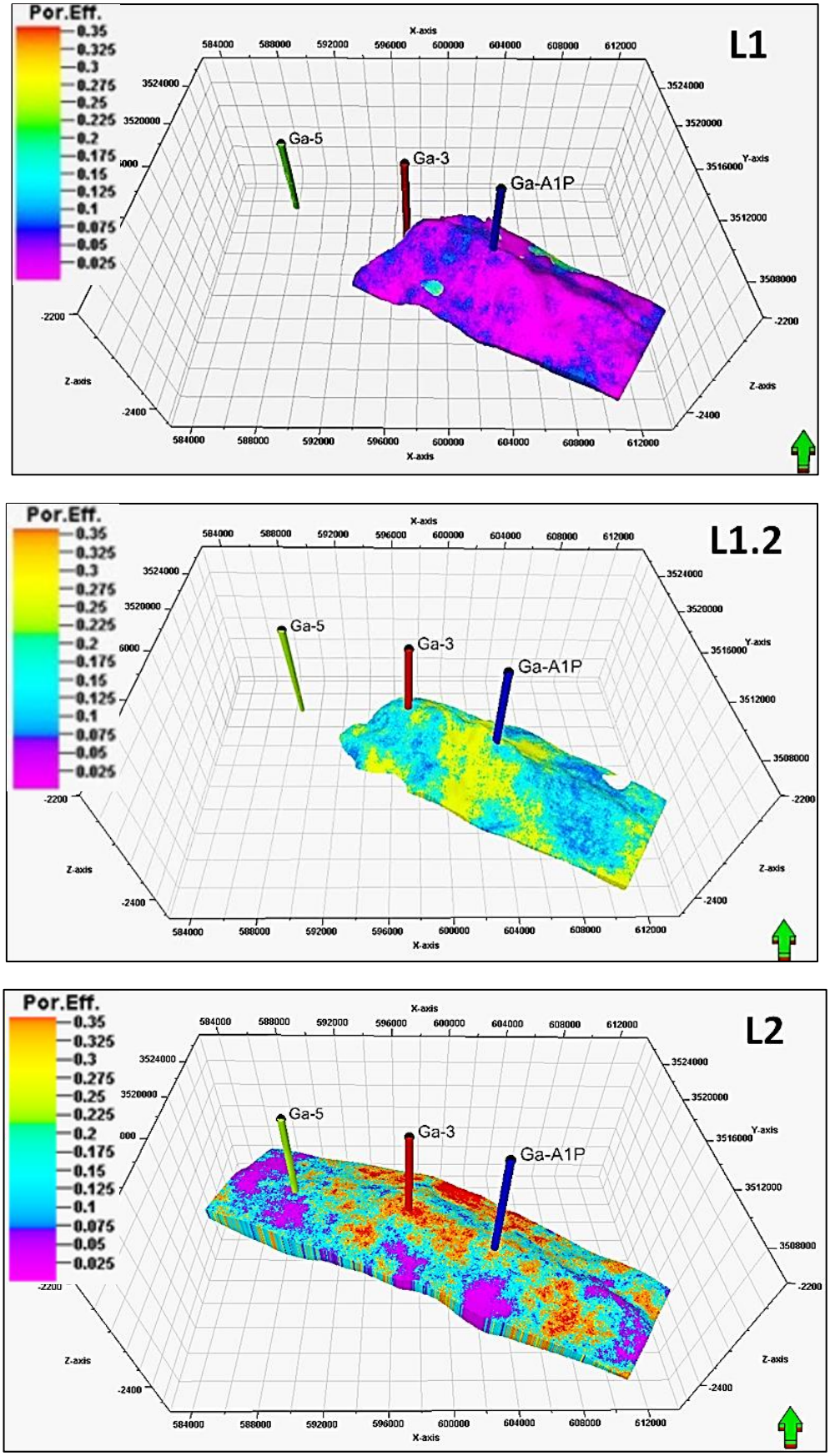

Figure (A-30): Porosity distribution models of the reservoir part units (L1, L1.2, and L2) of Mishrif Formation in Gharraf oil field.

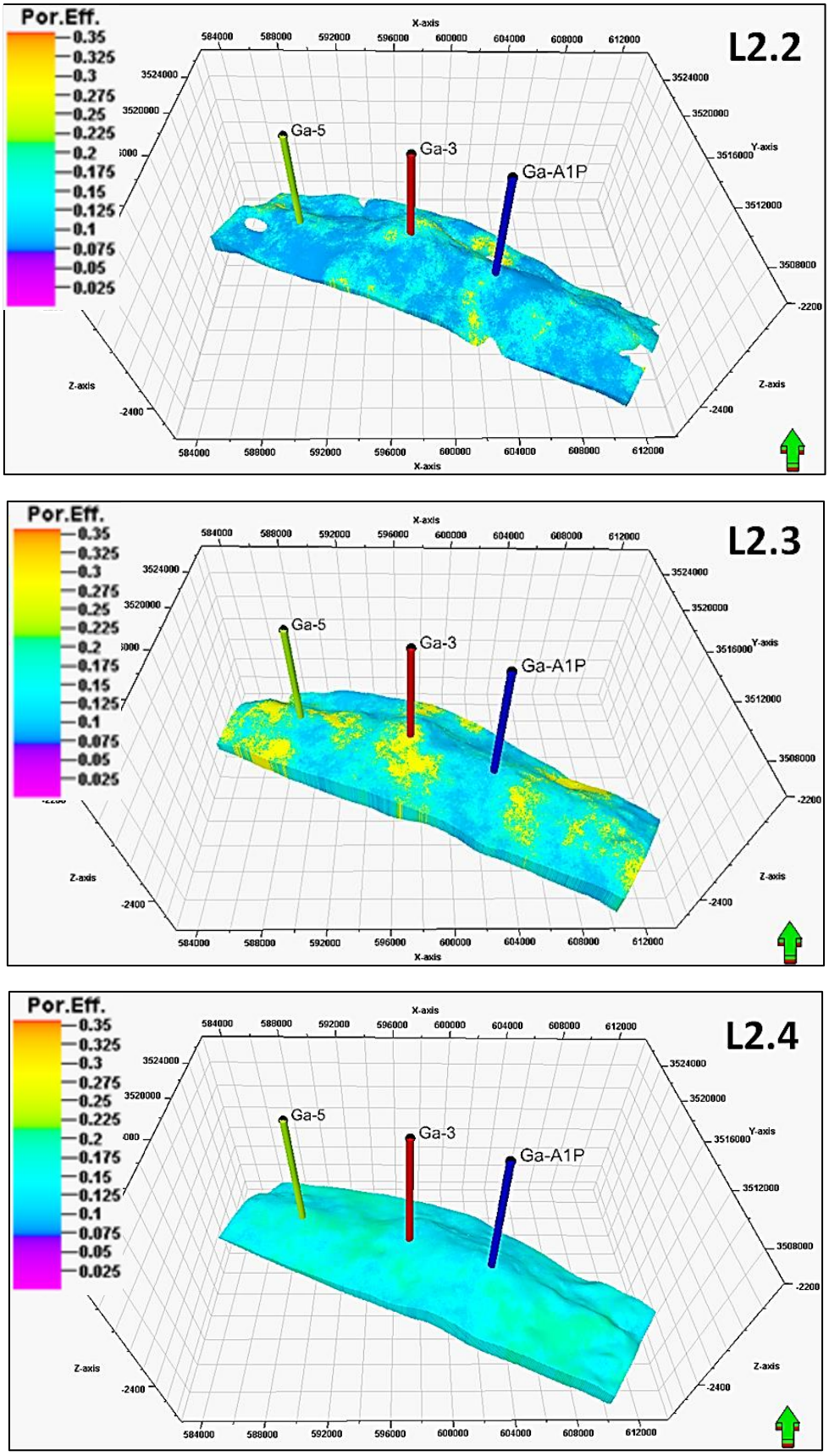

Figure (A-31): Porosity distribution models of the reservoir part units (L2.2, L2.3, and L2.4) of Mishrif Formation in Gharraf oil field.

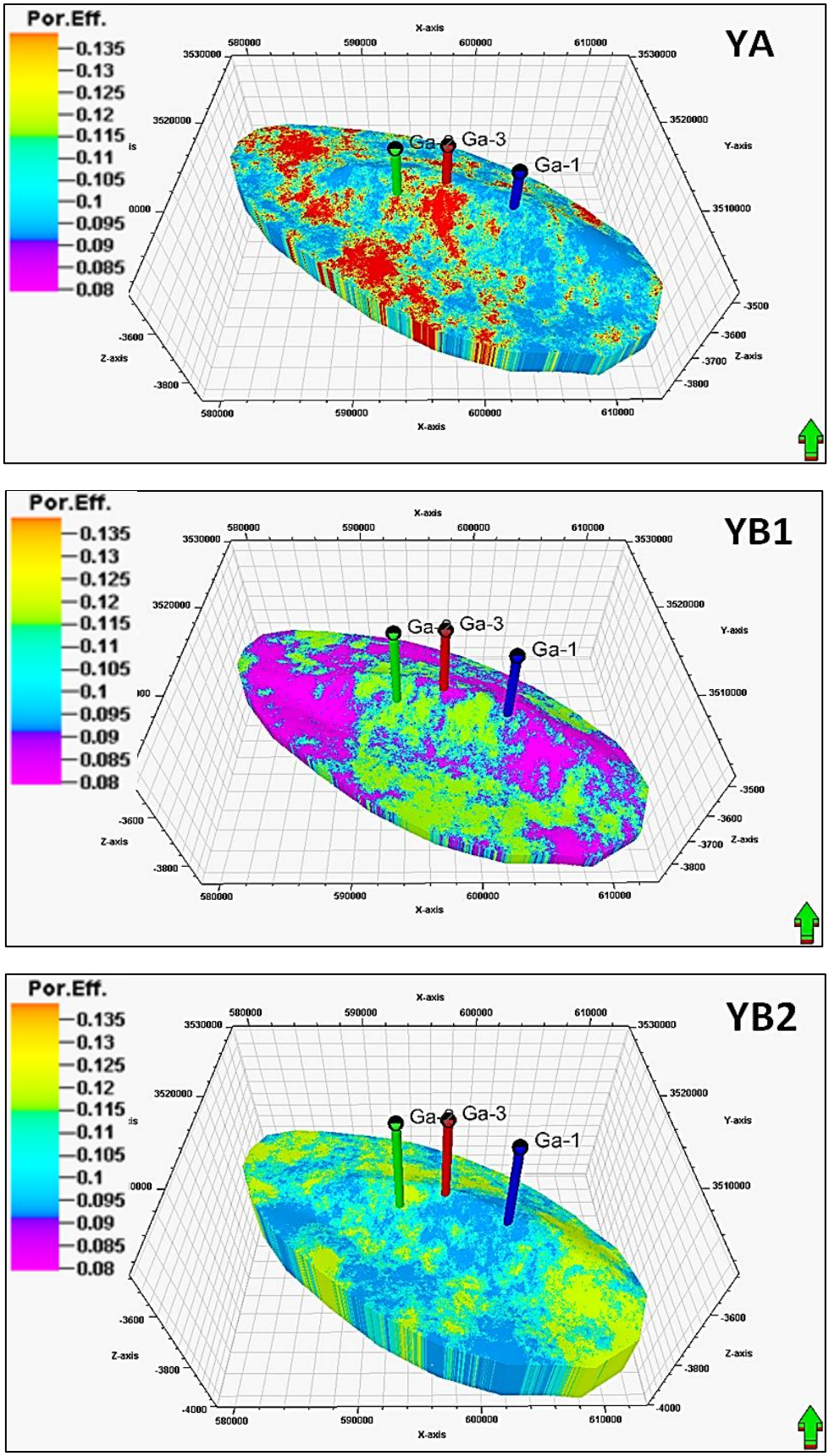

Figure (A-32): Porosity distribution models of Yamama Formation units in Gharraf oil field.

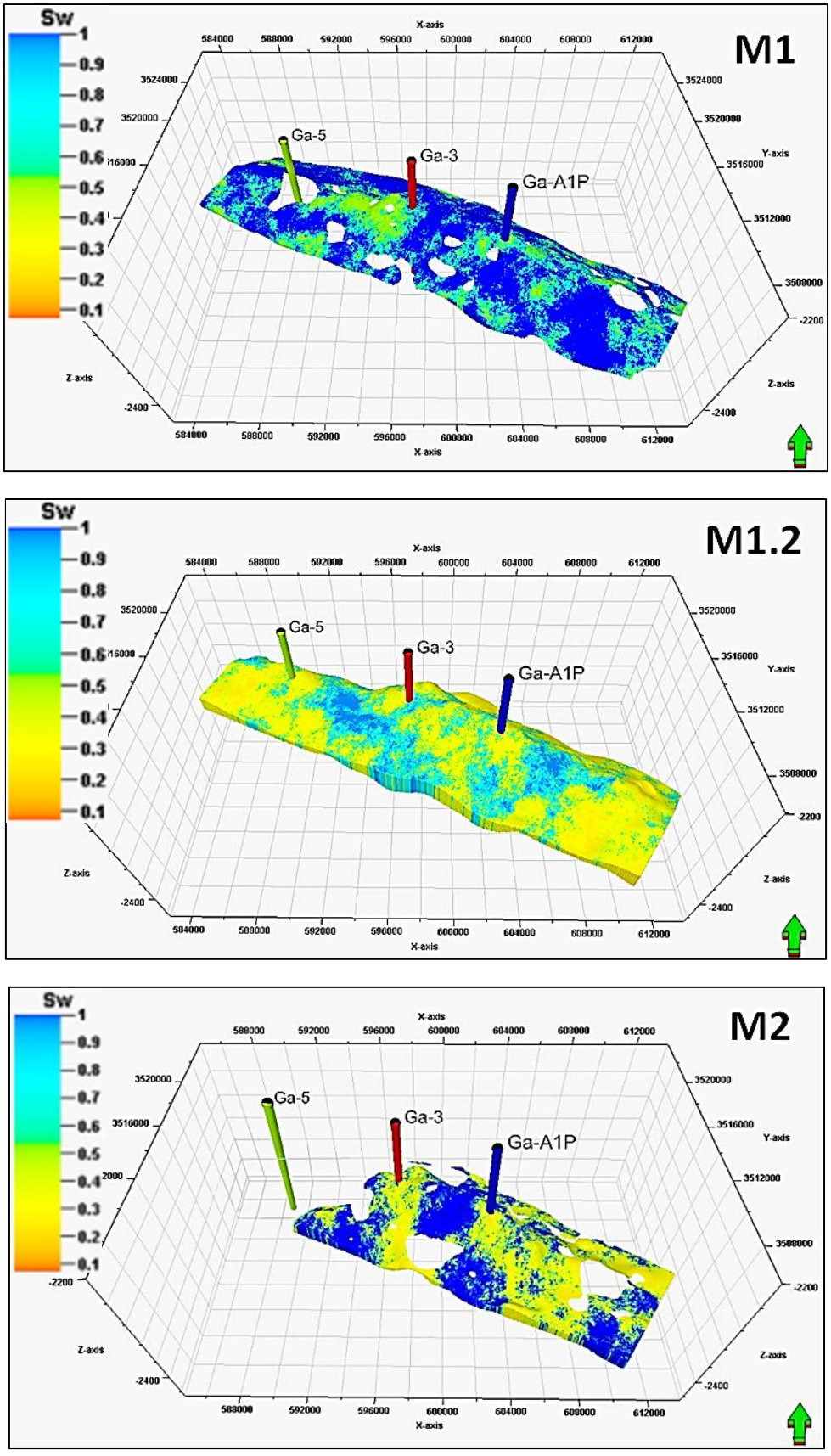

Figure (A-33): Water saturation models of the reservoir part units (M1, M1.2, and M2) of Mishrif Formation in Gharraf oil field.

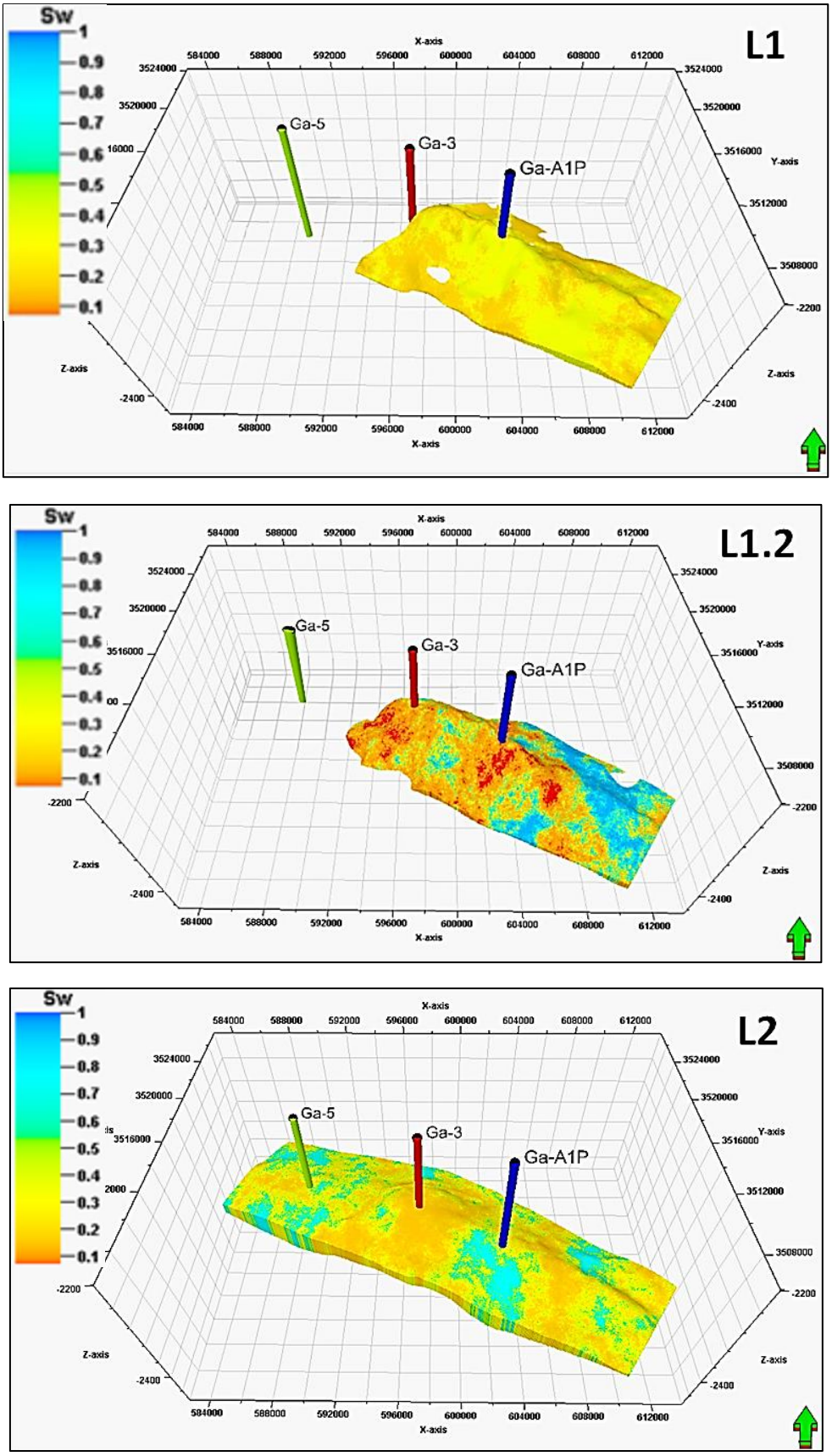

Figure (A-34): Water saturation models of the reservoir part units (L1, L1.2, and L2) of Mishrif Formation in Gharraf oil field.

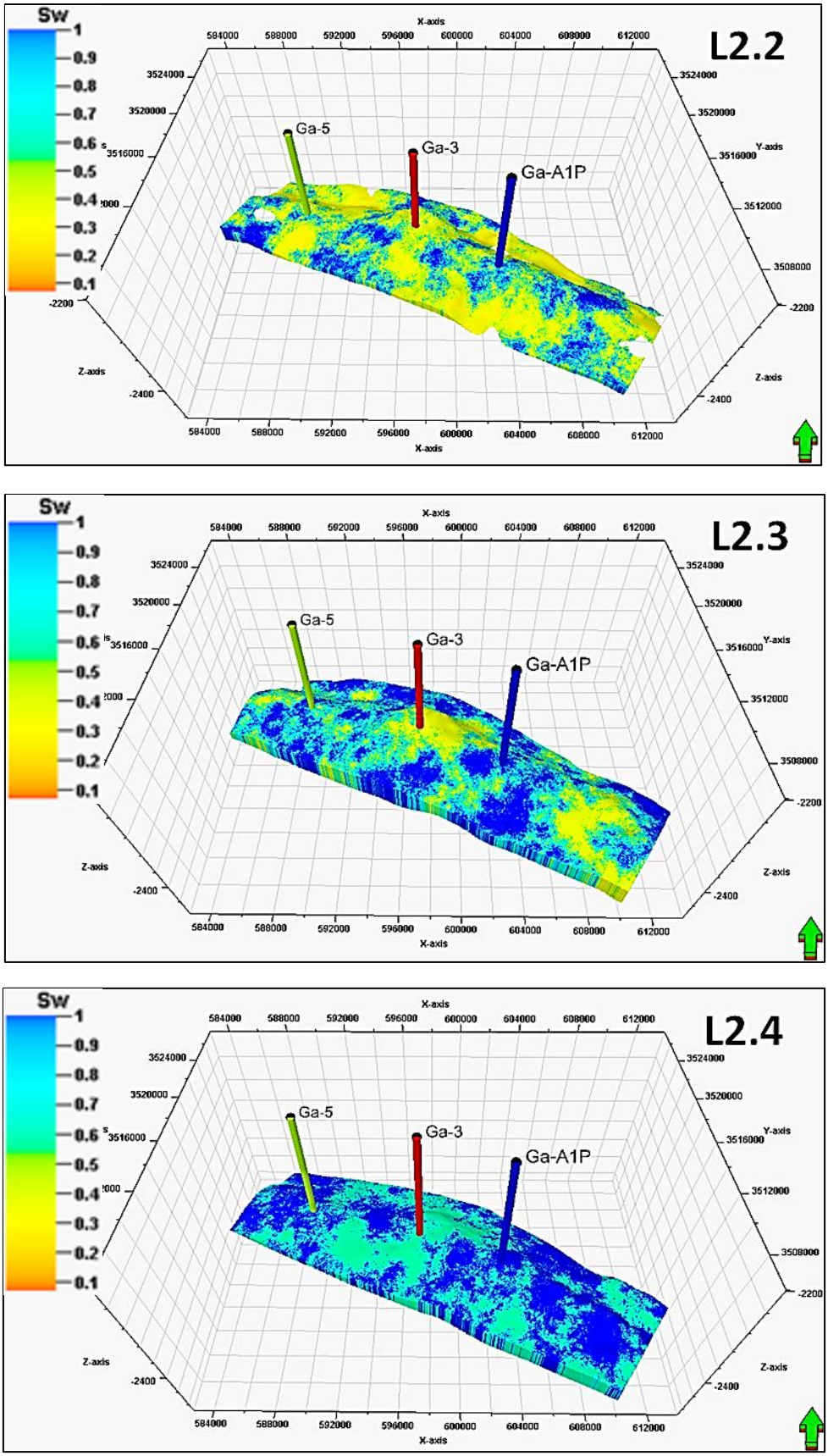

Figure (A-35): Water saturation models of the reservoir part units (L2.2, L2.3, and L2.4) of Mishrif Formation in Gharraf oil field.

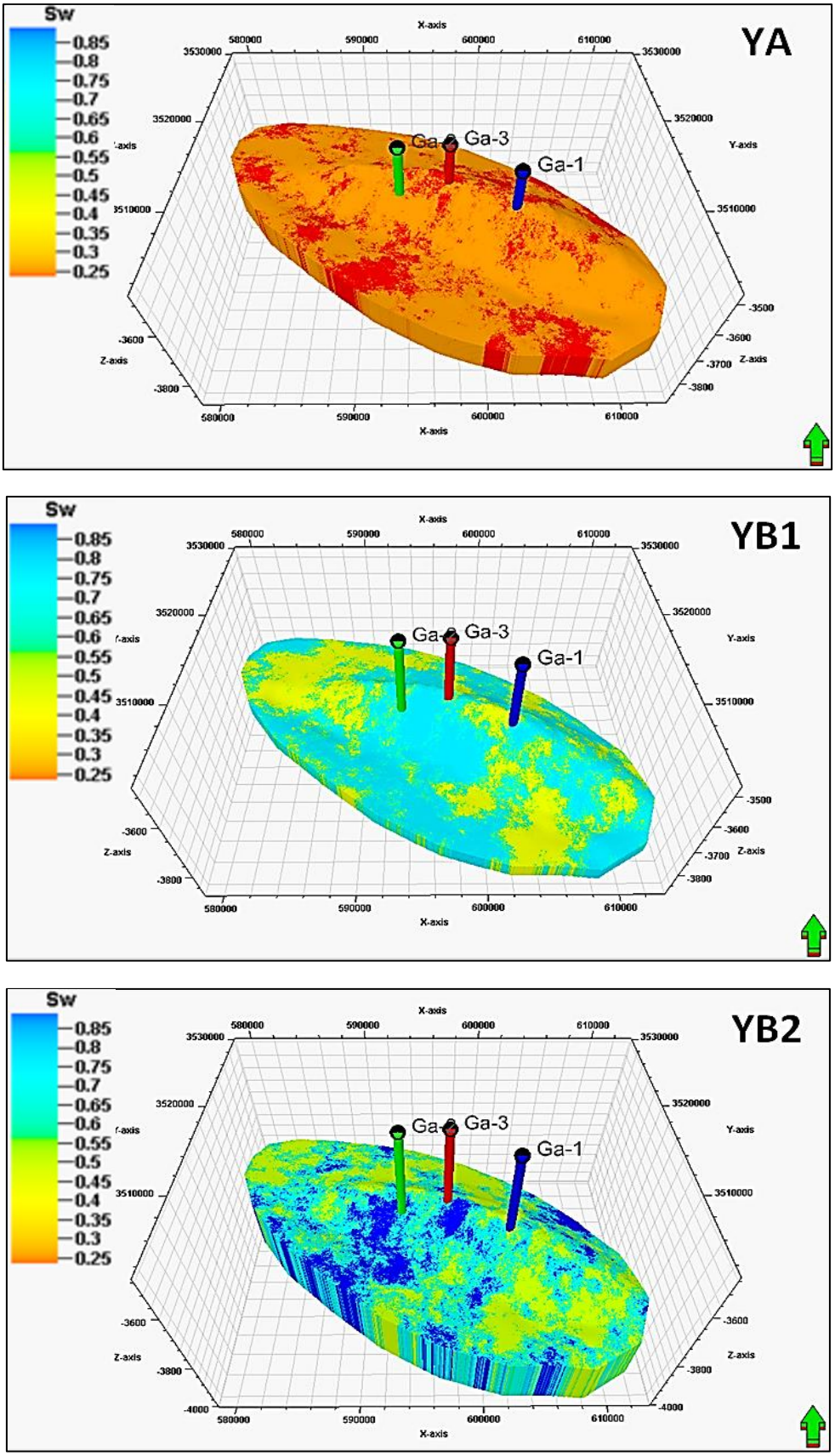

Figure (A-36): Water saturation models of Yamama Formation units in Gharraf oil field.

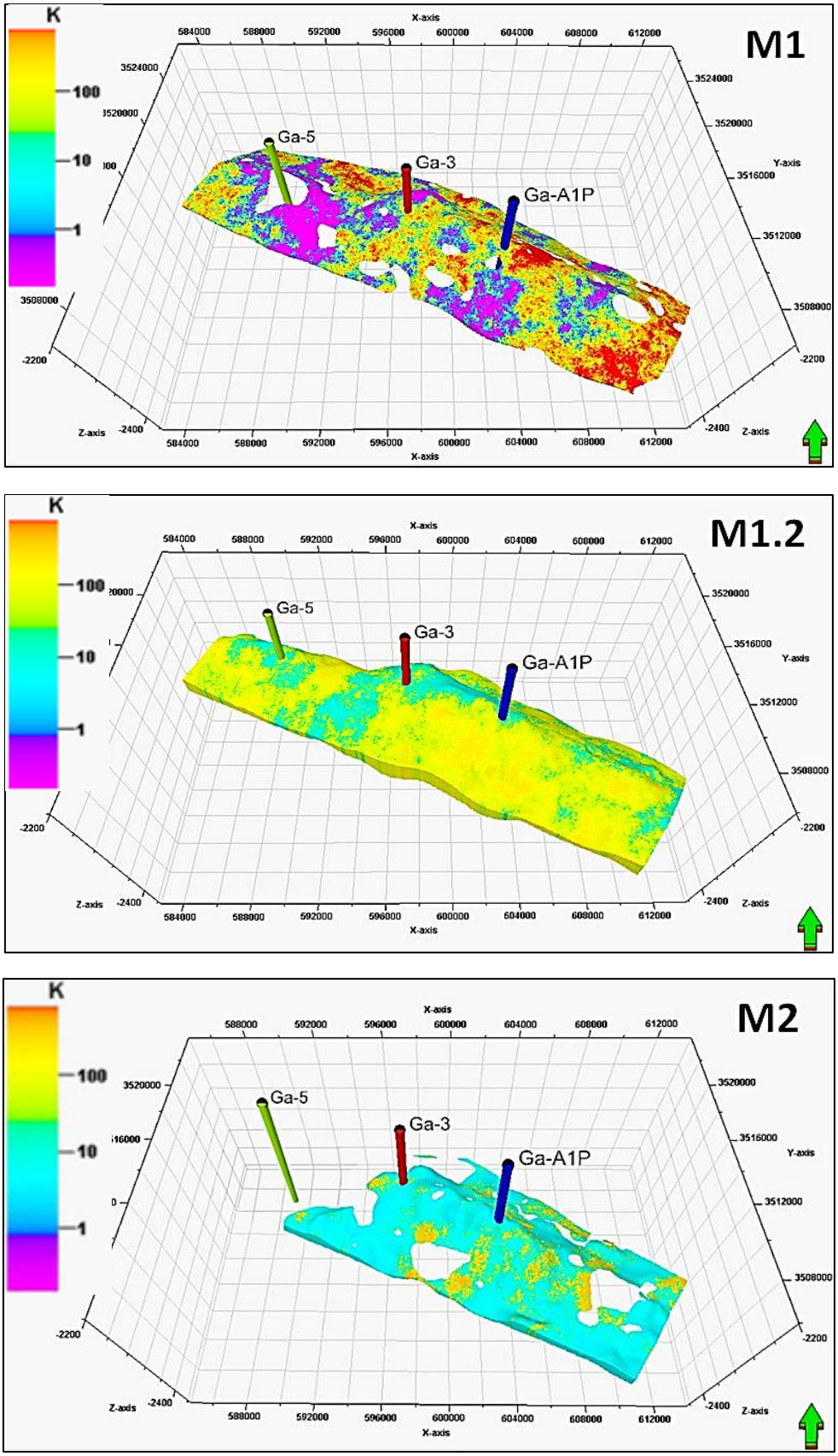

Figure (A-37): Permeability models of the reservoir part units (M1, M1.2, and M2) of Mishrif Formation in Gharraf oil field.

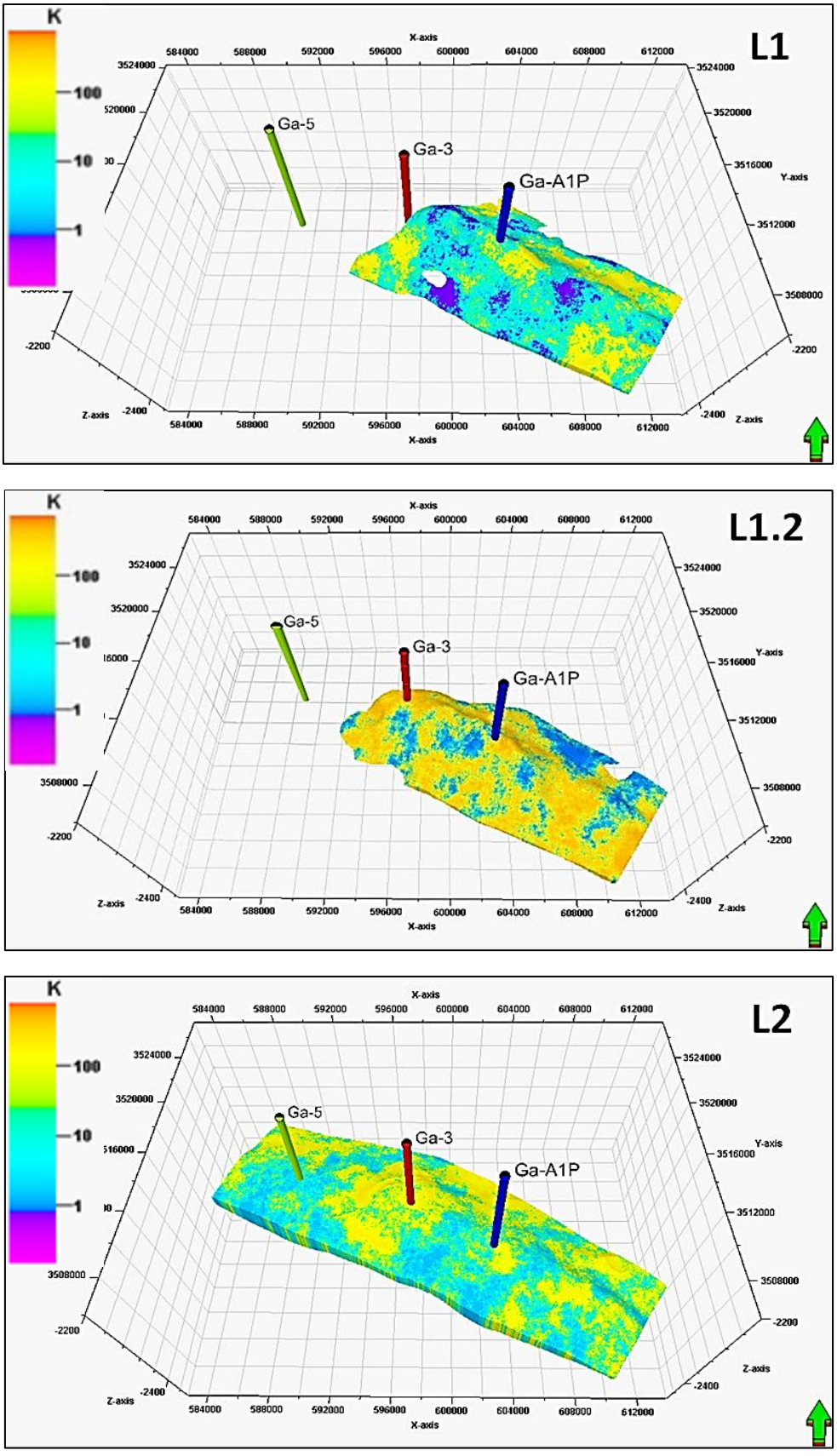

Figure (A-38): Permeability models of the reservoir part units (L1, L1.2, and L2) of Mishrif Formation in Gharraf oil field.

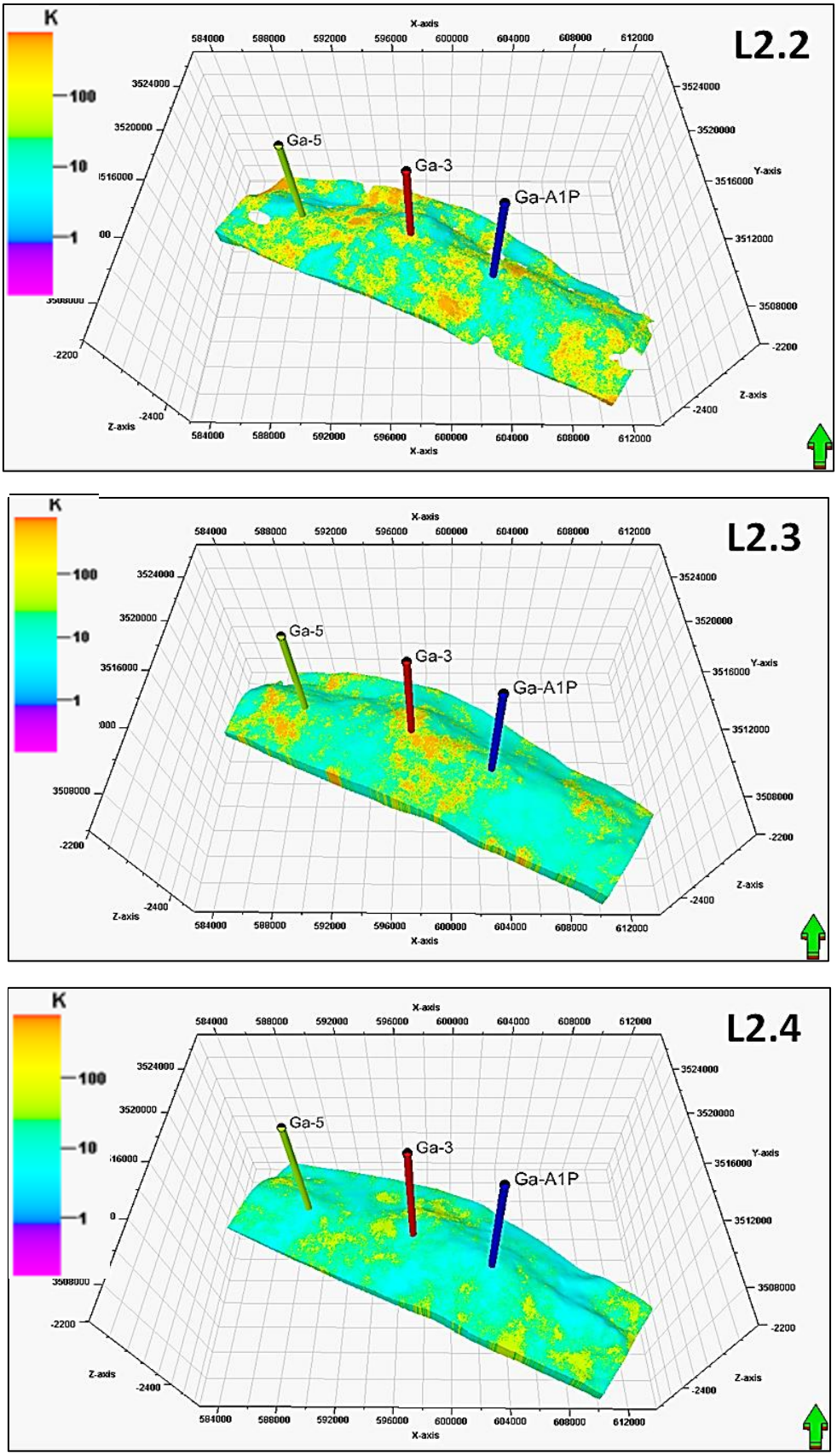

Figure (A-39): Permeability models of the reservoir part units (L2.2, L2.3, and L2.4) of Mishrif Formation in Gharraf oil field.

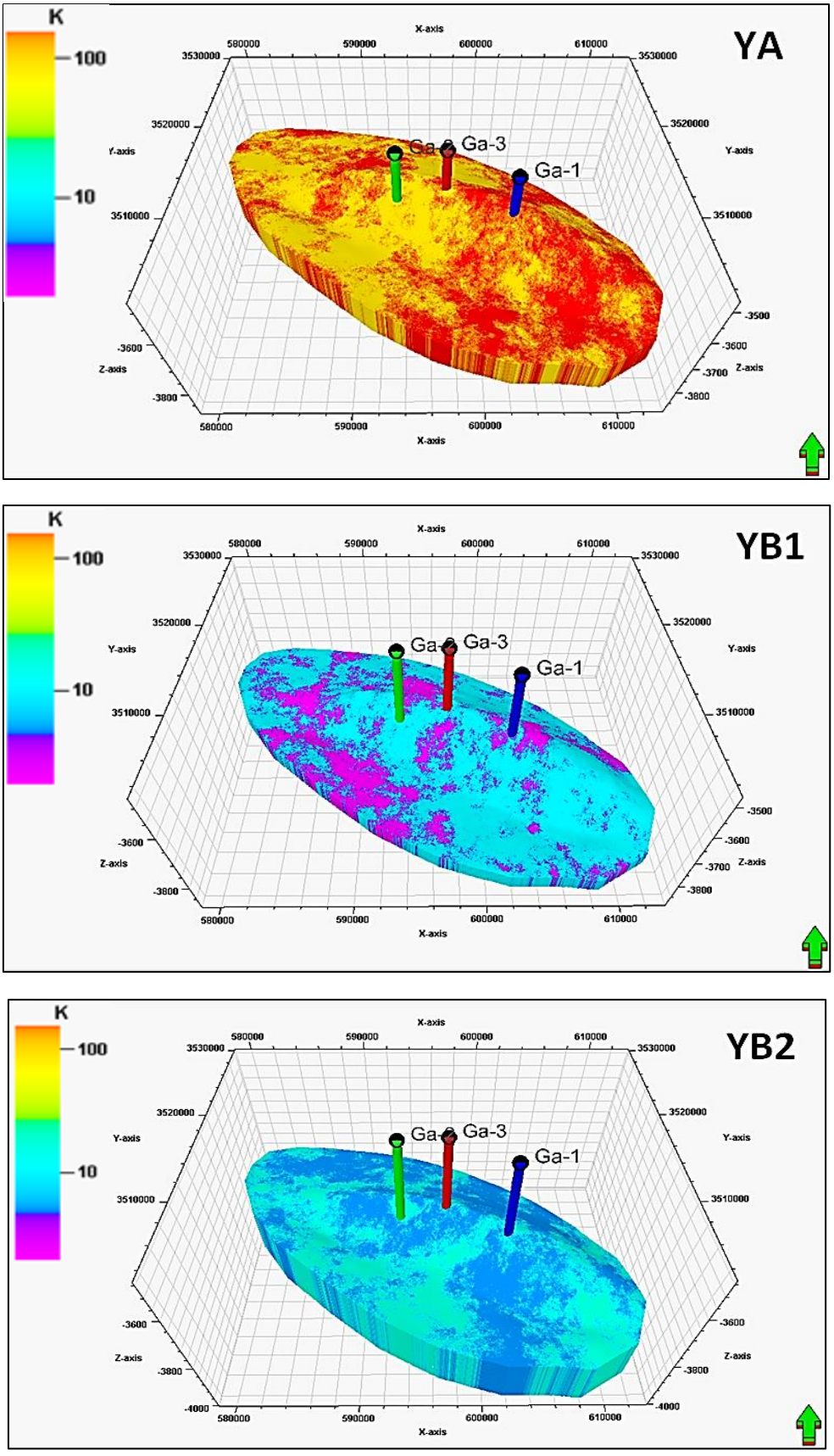

Figure (A-40): Permeability model of Yamama Formation units in Gharraf oil field

المستخلص

تم الحصول على متطلبات الدراسة المتمثلة بالعينات والخرائط ومقطع زلزالي يمر بمنطقة الدراسة وصور لتسجيلات المجسات البئرية اللزمة وغيرها من البيانات من المصادر الرسمية الممثلة في شركة الاستكشافات النفطية (OEC) وقسم المكامن بوزارة النفط ، وكذلك من الدراسات السابقة. تم تثبيت وتهيئة البرامج الضرورية وهي Petrel و IP و Didger و PetroMod من اجل استخدامها للتعامل مع هذه البيانات. تم اختيار خمسة آبار عمودية في هذه الدراسة هي Ga-1 و Ga-2 و Ga-3 و Ga-5 و Ga-A1P. تمت دراسة الخواص البتروفيزيائية مكمني اليمامة والمشرف بناءً على تفسير مجسات الآبار المتاحة باستخدام برنامج Interactive Petrophysics V3.5 ، كما تم بناء نماذج جيولوجية ثلاثية الأبعاد لهم لتحديد توزيع الخواص البتروفيزيائية. (النفاذية والمسامية والتشبع بالماء) في هذين المكمنين. تم تحديد ليثولوجية تكويني المشرف واليمامة على أنها حجر جيري بشكل أساسي مع نسبة ضئيلة من الدولوميت باستخدام عدة علاقات اساسية مثبتة ومعتمدة في تحديد الليثولوجية في برنامج IP. استندت التحليلات الجيوكيميائية لصخور المصدر المحتملة (محتوى الكربون العضوي الكلي والتحلل الحراري) إلى تقارير تم الحصول عليها من شركة الاستكشافات النفطية في بغداد ومن دراسات أخرى منشورة. تم الحصول على بيانات التحليل الجيوكيميائي للنفط لعينة واحدة من مكمن المشرف في حقل الغراف النفطي (الخصائص السائبة ، المؤشرات الحيوية ، ونظائر الكربون) من شركة GeoMark في الولايات المتحدة الأمريكية. أما بالنسبة لدراسة وبناء الموديلات لحوض مابين النهرين في حقل الغراف فقد تمت معالجة البيانات وبناء الموديلات المناسبة باستخدام برنامج PetroMod.

يتكون تكوين المشرف من وحدتين رئيسيتين تفصل بينهما طبقة مارل ، وتتميز الوحدة الرئيسية السفلية بخصائص مكمنية جيدة وتنقسم إلى تسع وحدات مكمنية ثانوية هي: M1، M1.2، M2، L1، L1.2 ، L2، L2.2، 3. L2 و L2.4. الوحدات L1.2 و L2 لها خصائص بتروفيزيائية جيدة Øeff = 18-22%، Sw = 16-38% ، K = 80-343mD. وهي تعتبر أفضل وحدات مكامن للنفط في مكمن المشرف. تحتوي هذه الوحدات على كمية اقتصادية من احتياطي النفط 584 مليون متر مكعب. الوحدات M1 و M1.2 و M2 لها خصائص بتروفيزيائية أقل وكمية أقل من احتياطيات النفط 229 مليون متر مكعب ، بينما الوحدات السفلية L2.2 و L2.3 و L2.4 مشبعة بالكامل تقريبًا بالماء المكمني Sw = 68-87% وتتضمن كمية قليلة من احتياطي النفط 125 مليون متر مكعب. إجمالي الاحتياطي النفطي هو 938 مليون متر مكعب اي مايقابل 5900.02 مليون برميل لخزان المشرف.

يتكون تكوين اليمامة من ثلاث وحدات مكمنية من الأعلى إلى الأسفل على التوالي YA و YB1 و

YB2. تتميز الوحدة YA بخصائص بتروفيزيائية جيدة Øeff = 11%، Sw = 26%، K = 119mD ، وتعتبر أفضل وحدة مكمنية لنفط تكوين اليمامة. تحتوي هذه الوحدة المكمنية على كمية اقتصادية من النفط في الآبار المدروسة Ga-1 و Ga-2 و Ga-3. إجمالي الاحتياطي النفطي هو 477 مليون متر مكعب اي مايقابل 3000.33 مليون برميل لخزان اليمامة.

تشير النتائج الجيوكيميائية لتحليلات نماذج الصخور المصدرية المحتملة في حقل الغراف وحقول نفط الناصرية المجاورة إلى أن تكوين السلي كان جيدة في امكانية توليد الهايروكاربونات، يحتوي على كيروجين من نوع Type II/III والذي يولد نفط بشكل اساسي، وكان ناضجًا. لذلك ، من الممكن أن تكون الصخور المصدرية لتكوين السلي قد أنتجت هيدروكربونات وساهمت في مليء مكامن العصر الطباشيري بالنفط. وان الصخور المصدرية للتكاوين الأخرى وهي اليمامة ، الزبير ، ونهر عمر غير ناضجة، لذلك لم تولد النفط، على الرغم من المؤشرات الجيدة لاحتمالية صخور هذه التكاوين من توليد الهيدروكاربونات وبالتالي فان هذه الصخور المصدرية لم تساهم في مليء مكامن العصر الطباشيري بالهيدروكربونات. تتميز نفوط مكمن المشرف بثقل نوعي يبلغ API = ˚27.2 ومحتوى كبريت عالي بنسبة وزنية تساوي wt.% 4.2 يشير هذا إلى أن نفوط المشرف قد تم إنتاجها من صخور المصدر ذات الكيروجين من النوع Type IIS في مرحلة نضوج مبكرة. تركيز الألكانات الاعتيادية قصيرة السلسلة أعلى من الألكانات الاعتيادية طويلة السلسلة ، بالإضافة إلى نسبة عالية من تربين ثلاثي الحلقات C22 / C21 و C31R / H ونسب منخفضة من C24 / C23 و C26 / C25 تربين ثلاثي الحلقات ، أشارت إلى أنها نشأت من صخور مصدرية غنية بالكربونات البحرية مع القليل من المدخلات الترسيبية القارية. تشتمل نسب نظير الكاربون المستقر على C15 + مشبع -27.23 ‰ وهيدروكربونات عطرية -27.53 C15 + كما تم الإشارة إلى أن نفوط المشرف مشتقة من مادة عضوية بحرية في الغالب. يُظهر تحليل كروماتوغرافيا الغاز(GC) توزيعات الألكان العادية والأيزوبرينويد اللاحلقي. بالإضافة إلى ذلك ، أشارت نسب العلامات الحيوية Pr / n-C17 و Ph / n-C18 و GA / C31R و C35S / C34S إلى أن صخور المصدر ترسبت في ظل ظروف بيئية ناقصة الأكسجين. تشير براميترات النضوج للمؤشرات الحيوية مثل C2920S / R و C27Ts / Tm و C29Ts / Tm و TAS3 CR إلى مرحلة نضج منخفضة لصخور المصدر المحتملة.

في أنظمة البترول (TPS) التي تحتوي على وحدات مصدر كربوناتية ، تشير نسبة الستيران العادية C_{28} / C_{29} البالغة 0.66 ، جنبًا إلى جنب مع ستيرونات الثلاثية المقابلة ($C_{27}R$ / $C_{28}R$) إلى أن نفوط المشرف تم إنتاجها من الجوراسي العلوي (تكوين نجمة) إلى العصر الطباشيري السفلي (تكوين السلي) والتي تمثل صخور مصدرية كاربوناتية. حيث يحتوي الجزء المشبع من النفط الخام الذي تم تحليله على

نسبة من نظير الكاربون المستقر تبلغ -27.23 ‰ ، وهو ما يؤكد ذلك. تظهر نتائج عمل الموديلات احادية البعد للحوض النفطي بواسطة برنامج البترومود أن هذه التكوينات بلغت ذروة نافذة توليد النفط في أوقات مختلفة ، مما أدى إلى إطلاق كميات مختلفة من النفط. منذ أواخر العصر الكريتاسي وحتى الوقت الحاضر، بدأ مصدر النجمة والسلي الغني بالمواد العضوية في تصريف كمية هائلة من النفط ، تعادل نسبة التحول (TR) بنسبة 100% ، وفقًا لنتائج موديلات برنامج البترومود احادية البعد. هاجرت هذه النفوط المتولدة إلى مكامن ضحلة من العصر الطباشيري من خلال المسار الرأسي لانظمة الفوالق المنتشرة في حوض وادي الرافدين.

جمهورية العراق
وزارة التعليم العالي والبحث العلمي
جامعة بابل / كلية العلوم
قسم علم الارض التطبيقي

تحليل النظام النفطي الإجمالي لحوض القطنية / حقل الغراف النفطي للفترة الممتدة من الجوراسي الأعلى الى الكريتاسي الأعلى، جنوب العراق

رسالة مقدمة الى

مجلس كلية العلوم – جامعة بابـــــل

كجزء من متطلبات نيل درجة الماجستير في العلوم / علم الأرض التطبيقي

من قبـــــــــــل

علـــي كريـــم نعمـــــه مشتـــــت

بكالوريوس علـــــوم

٢٠١٢

بإشراف

أ.د. عامر جاسم الخفاجي

أ.د. فاضل نوماس السعدوني

١٤٤٣ هـ ٢٠٢١ م